UNIVERSIDAD DE LAS PALMAS
DE GRAN CANARIA

Biogeochemical cycle of Fe in acidified marine environments

GUILLERMO SAMPERIO RAMOS

LAS PALMAS DE GRAN CANARIA

JULIO 2017

A mi madre y a mi hermano

A mi mujer, Angie.

THESIS PREVIEW

The present PhD thesis has been entitled "***Biogeochemical cycle of iron in acidified marine environments***" and has been performed at the QUIMA group of the Chemistry Department of Universidad de Las Palmas de Gran Canaria. This work gather five different articles framed within the research projects ECOFEMA Project (CTM2010-19517-mar) and EACFeProject (CTM2014-52342-P) of the Ministerio de Economía y Competitividad of Spain. Additionally the PhD has been carried out by the FPI grant with reference number BES-2011-051448 and supervised by Dra Magdalena Santana Casiano and Dr Melchor González Dávila.

Although the thesis has been written in English, in order to comply with the regulations showed in the Official Bulletin (BOULPGC), approved on December 17th, 2012 and modified on September 29th, 2017 by the Governing Council of the Universidad de Las Palmas de Gran Canaria for the Thesis requirements (Article 10, Chapter 1, on November 2008), an Spanish extension of between 5 and 20 pages, which includes the objectives and conclusions have been carried out.

PRESENTACIÓN DE LAS TESIS

La presente tesis doctoral ha sido titulada "Ciclo biogeoquímico del hierro en ambientes marinos acidificados" y ha sido realizada en el grupo QUIMA del Departamento de Química de la Universidad de Las Palmas de Gran Canaria. Este trabajo reúne cinco artículos diferentes enmarcados dentro de los proyectos de investigación: ECOFEMA (CTM2010-19517-mar) y EACFeProject (CTM2014-52342-P) del Ministerio de Economía y Competitividad de España. Adicionalmente el doctorado ha sido realizado por la beca FPI con número de referencia BES-2011-051448 y supervisado por la Dra. Magdalena Santana Casiano y el Dr. Melchor González Dávila.

Aunque la presente Tesis ha sido escrita en inglés, con el fin de dar cumplimiento a lo dispuesto en el BOULPGC, aprobado el 17 de diciembre de 2012 y modificado el 29 de septiembre de 2017 por el Consejo de Gobierno de la Universidad de Las Palmas de Gran Canaria para los requisitos de Tesis (artículo 10, Capítulo 1, en noviembre de 2008), se ha realizado una extensión en castellano de entre 5 y 20 páginas, que incluye los objetivos y conclusiones.

ACKNOWLEDGEMENTS / AGRADECIMIENTOS

Esta Tesis Doctoral ha sido realizada bajo la supervisión de los Doctores J. Magdalena Santana Casiano y Melchor González Dávila. A ellos quería dedicarles mis primeras palabras de agradecimiento ya que desde el momento que decidieron concederme esta gran oportunidad, su apoyo ha sido la base que me han permitido alcanzar los objetivos marcados. Muchas gracias por la motivación y perseverancia inculcadas en el día a día, así como por todo el conocimiento transmitido, que ha sido inestimable. Además, su entusiasmo y dedicación por la investigación y la enseñanza son, sin duda, una gran inspiración para el futuro.

Por supuesto, mi gratitud se extiende al Ministerio de Economía y Competitividad en el año 2011 (BES-2011-051448) por la beca que se me otorgó para el desarrollo de mi Tesis Doctoral.

Esta tesis doctoral viene a continuar el gran trabajo desarrollado por el Doctor Aridane González. A él quería agradecerle su orientación esos primeros meses, cuando al llegar nuevo al laboratorio sus consejos y conocimientos se hicieron tan necesarios. Dentro del Departamento de Química de la Universidad de Las Palmas de Gran son muchas las personas que también me han ayudado en las tareas cotidianas durante la Tesis. Ana, Pedro, Miguel, Milagros, Norma, Patricia, Carolina etc. Pero en especial quería señalar a Rayco, el cual me ayudo infinidad de veces a resolver y solucionar cada uno de los problemas que podían aparecer en el camino. Siempre con la mejor sonrisa, que sólo dedican los buenos amigos. Tampoco me puedo olvidar de todo el personal de administración y servicios de la Universidad de Las Palmas de Gran Canaria, que con una gran profesionalidad me han indicado como superar correctamente todos los procedimientos burocráticos que se debían llevar a cabo durante estos cuatro años.

Gracias al Banco Español de Algas por suministrar las microalgas y cianobacterias con las que se realizó parte de este proyecto. También a todo su personal, con especial mención a la Dra Antera Martel, por sus consejos a la hora de poner en marcha los cultivos y por dejarme hacer uso de sus instalaciones cuando fue requerido.

Durante mi estancia de tres meses en el GEOMAR - Helmholtz Centre for Ocean Research de Kiel (Alemania) estuve bajo la dirección de la Dra. Martha Gledhill y el Dr Eric Achterberg, a quienes quiero agradecer su dedicación durante el periodo que permanecí en su grupo, así como por todos los conocimientos aportados, que fueron muchos y de calidad. Del mismo modo dar las gracias al resto del personal del centro, con especial atención a Lukas por el afecto y amistad demostrados, ya que desde el primer momento me hizo sentir como en casa.

También quiero acordarme de mis familiares y amig@s, del barrio, del colegio, de la universidad, del Master,…etc. Al fin y al cabo soy resultado de todo lo vivido con vosotr@s. Imposible agradecer a mi madre y hermano lo que durante toda una vida me han dado, sin buscar absolutamente nada a cambio. Siempre habéis estado ahí, hasta cuando no lo merecía. A pesar de algunos malos momentos, nunca os habéis apartado de mi lado, alentando y apoyando mis sueños. Gracias por demostrarme que todo es posible., sois los mejores. Finalmente, quería acabar acordándome de mi mujer, mi mejor amiga, mi consejera. Gracias por dedicarme tanto. Ésta tesis, en parte, es tuya. Seguiremos compartiendo alegrías como ésta, seguiremos luchando como hasta ahora, porque aunque ya son 10 años, nuestra historia sólo acaba de comenzar.

The most dangerous worldview is the worldview of those who have not viewed the world.

Alexander von Humboldt (1769 – 1859).

SUMMARY

The oxidation process of Fe(II) has been studied in seawater in presence of high nutrient concentrations and natural organic exudates produced by eukaryote and prokaryote phytoplankton. The oxidation of Fe(II) has been determined under different physical-chemistry conditions, such as pH, temperature and salinity.

The experimental results showed that the nutrient effect was constant over the entire pH range studied. In addition, the enhance of the oxidation rate of Fe(II), by the presence of nutrient, was more intense at the higher temperatures studied, suggesting that the oxidation process of Fe(II) might be increased in the coastal waters due to a synergic effect of eutrophication conditions and the upper ocean warming.

The presence of two organic ligands (hydroxamates and phenolic compounds), under two different iron fertilization scenarios (High-Fe and Low-Fe conditions), was monitored in cultures of *Synechococcus* PCC 7002, during their different growth phases. Iron status conditioned the excretion of these organic ligands by the cyanobacteria. The effect of these exudates, in the Fe-redox chemistry was also evaluated. The organic ligands released under High-Fe conditions produced the retarding of the Fe(II) oxidation rate under the different conditions of pH, temperature and salinity. Nevertheless, in the exudates excreted under Low-Fe conditions a marked acceleration of Fe(II) oxidation rate at pH lower than 7.5 was observed. A pH-dependent photochemical regeneration of Fe(II) was also detected in presence of those exudates. This photolytic reaction modified the reactivity between Fe(II) and the ligands presents in the exudates of *Synechococcus*, increasing the lifetime of Fe(II) in the medium.

The pH-dependence of organic ligand production by *Emiliania huxleyi,* was determined in a series of microcosms by modifying the CO_2 / carbonate system of seawater. The presence of carbohydrates, uronic acids and phenolic compounds in was studied, having in account the different growth stages of the coccolithophorid. The presence of exudates released under the different CO_2 conditions produced the decreasing of Fe(II) oxidation rate in seawater as function of dissolved organic carbon levels. The slowdown of the oxidation process was more intense, when the

exudates of *E.huxleyi* were biosynthesized under the more acid microcosm conditions.

Additionally, and in order to describe the experimental results, a modelling approach was developed for each kinetic study. These models explain the speciation of Fe(II) and the contribution to the overall oxidation rate of the Fe(II) species considered under the different conditions set in the present work. In the studies with phytoplanktonic exudates, the Marcus theory was applied to the oxidation rates, to demonstrate that an outer-sphere electron transfer process controlled the oxygenation of Fe(II) species modelled. Ultimately, from the kinetic model can be extracted that these species plays a key role both speciation and oxidation process of Fe(II).

RESUMEN

El proceso de oxidación del Fe (II) se ha estudiado en agua de mar en presencia de altas concentraciones de nutrientes y exudados orgánicos naturales producidos por fitoplancton eucariota y procariota. La oxidación del Fe(II) se ha determinado en diferentes condiciones físico-químicas, tales como pH, temperatura y salinidad.

Los resultados experimentales mostraron que el efecto de los nutrientes fue constante a lo largo del rango de pH estudiado. Además, el aumento de la tasa de oxidación del Fe(II), por la presencia de nutrientes, se intensificó a las temperaturas más altas estudiadas, lo que sugiere que en un futuro el proceso de oxidación del Fe(II) podría incrementarse en las aguas costeras debido a una efecto sinérgico por el aumento de la eutrofización y el calentamiento de la capa superior del océano.

La presencia de dos ligandos orgánicos (hidroxamatos y compuestos fenólicos), bajo dos diferentes escenarios de fertilización con hierro (High-Fe y Low-Fe), se monitorizó en cultivos de *Synechococcus* PCC 7002, durante sus diferentes fases de crecimiento. La disposición inicial de hierro condicionó la excreción de estos ligandos orgánicos por las cianobacterias. También se evaluó el efecto de estos exudados en la química redox del Fe. Los ligandos orgánicos liberados bajo condiciones de High-Fe disminuyeron la velocidad de oxidación de Fe(II) bajo las diferentes condiciones de pH, temperatura y salinidad. Sin embargo, en los exudados excretados bajo condiciones de Low-Fe se observó una marcada aceleración de la velocidad de oxidación del Fe(II) a pH inferior de 7,5. También, en presencia de dichos exudados, se detectó una regeneración fotoquímica de Fe(II) dependiente del pH Esta reacción fotolítica modificó la reactividad entre Fe(II) y los ligandos presentes en los exudados de *Synechococcus*, aumentando la vida media del Fe(II) en el medio.

La dependencia del pH en la producción de ligando orgánicos por *Emiliania huxleyi*, se determinó en una serie de microcosmos modificando el sistema CO_2 / carbonato de agua de mar. Se estudió la presencia de carbohidratos, ácidos urónicos y compuestos fenólicos, teniendo en cuenta las diferentes etapas de crecimiento del

coccolitóforo. La presencia de exudados, excretados bajo las diferentes condiciones de CO_2, produjo una disminución de la tasa de oxidación de Fe(II) en el agua de mar, como función de los niveles de carbono orgánico disuelto. La ralentización del proceso de oxidación fue más intensa, cuando los exudados de *E.huxleyi* se biosintetizaron bajo las condiciones más acidas del microcosmos.

Además, y con el fin de describir los resultados experimentales, un modelo se desarrolló para cada estudio cinético. Estos modelos explican la especiación de Fe(II) y la contribución a la tasa de oxidación global de las especies de Fe(II) consideradas bajo las diferentes condiciones establecidas en el presente trabajo. En los estudios con exudados fitoplanctónicos, la teoría de Marcus se aplicó a las tasas de oxidación, para demostrar que un proceso de transferencia de electrones de esfera externa controlaba la oxidación de las especies de Fe(II) consideradas. Finalmente, a partir del modelo cinético se puede extraer que estas especies juegan un papel clave tanto la especiación como el proceso de oxidación de Fe(II).

CONTENTS / ÍNDICE

CHAPTER I

General introduction

CHAPTER I

Although iron is the fourth most abundant element on the Earth, in most upper oceanic waters it is a trace element at subnanomolar levels, due to the solubility of Fe is extremely low in contemporary oxygenated seawater (Liu and Millero, 2002). Advances in iron biogeochemistry during the past three decades have transformed our understanding of the oceanic iron cycle. The first vertical profiles of dissolved iron (defined as <0.45 μm filterable iron, including some small colloids), were published in the 1980s (Gordon et al. 1982; Martin and Gordon, 1988; Martin et al. 1989). Since then, multitudes of studies have shown that the vertical distribution of iron in the global ocean (Fig. 1.1) presents a nutrient-like profile indicative of its biological role (Wu and Luther, 1994; de Jong et al. 1998; Boye et al. 2001; Bergquist et al 2007; Kitayama et al. 2009; Tagliabue et al. 2012; Nishioka and Obata, 2017).

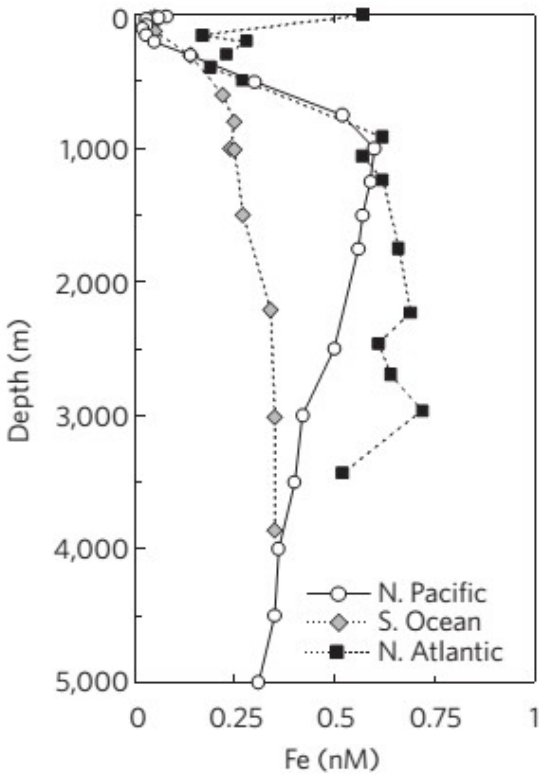

Fig. 1.1 Dissolved iron vertical profiles, for north Atlantic (Bergquist et al. 2007), central Pacific (Kitayama et al. 2009) and Southern (Tagliabue et al. 2012) Oceans respectively, illustrating aspects of supply and removal processes.

CHAPTER I

Iron is a micronutrient necessary in some physiological phytoplankton functions, like nitrogenous assimilation, protein synthesis, or electron transport in respiration and photosynthesis (Stumm and Morgan, 1996; Behrenfeld and Milligan, 2011), therefore iron has been recognized to be important micronutrient in regulating the magnitude and dynamics of ocean primary productivity, making it an integral component of the ocean's biogeochemical cycles (Tagliabue et al. 2017).

On the other hand, the increase in the uptake of anthropogenic CO_2 by the world's oceans and the consequent decrease in surface ocean pH, predicted for the end of this century, represent a change (a decrease in pH of about 0.3-0.5 units) in sea surface chemistry that has not been experienced over at least the past 420,000 years (IPCC, 2014). Nevertheless, ocean acidification has been generally tagged as "the other CO_2 problem" (Doney et al. 2009) and has only been addressed with scientific rigor since the past decade (Gatusso et al. 2015). The physic-chemical mechanisms by which the atmospheric CO_2 is absorbed by the ocean are currently very well established (Zeebe, 2012; IPCC, 2014). Along to the increase in hydrogen ions, carbonate ion concentrations will decrease between 20-30% over this century (Millero et al. 2009), making it more difficult for marine calcifying organisms, such as coccolithophorids, foraminifera, corals, coralline algae, and certain molluscs, to form biogenic calcium carbonate (Kleypas et al. 1999; Riebesell et al. 2000; Orr et al. 2005; Feely et al. 2009; Hoegh-Guldberg et al. 2010; Young et al. 2014) and possibly in many other groups that use $CaCO_3$ as internal or external structural elements, such as crustaceans or sponges (Doney, 2006; Fabry et al. 2008). Several studies have also suggested that the undersaturation of the surface ocean with respect to the calcium carbonate minerals (calcite and aragonite) will affect the amount of carbon that is produced in surface waters and sequestered into the deep oceans (Caldeira and Wickett, 2003; Raven et al. 2005; Hoffmann and Schellnhuber, 2009; IPCC, 2014). However, much less is known about the potential influence of ocean acidification on the biogeochemical cycle of trace metals in the oceans (Millero et al. 2009; Hoffmann et al. 2012; Hutchins and Boyd; 2016).

This work attempts to provide a higher understanding into the effects of ocean acidification on redox behaviour of iron, focusing in its interaction with

nutrients and organic ligands biologically mediated. To help a better insight about the aims of this study, this general introduction has been structured into different sections (i) to identify of the sources of Fe for the upper layers of ocean, (ii) to revise the "iron hypothesis", postulated by John Martin and co-workers, which has demonstrated as the iron is a limiting factor leading to low phytoplankton biomass in the high nutrient low chlorophyll (HNLC) waters, (iii and iv) to explain the main redox mechanisms in seawater and its importance in the Fe-bioavailability, focusing on the key role of biologically produced organic ligands and finally, (v) as the environmental variations in the marine systems, caused by increasing CO_2 atmospheric levels, can affect the biogeochemical behaviour of iron in a future ocean. After this chapter will be examine and discuss the experimental results obtained in the present PhD Thesis.

1.1 Fe inputs to Upper Ocean

The way that iron cycle through atmospheric, terrestrial, oceanic and associated biotic reservoirs can constrain rates of biological production and structures ecosystems in the Upper Ocean.

- ***Aeolian deposition***

From observations and modelling approaches, the atmospheric deposition to the global ocean is approximately 450 Tg yr^{-1}, and assuming a total iron content of 3.5%, the average of Fe-input to the marine systems is approximately 16000 Gg yr^{-1} (Jickells 2005). So that globally, the largest input of Fe into the oceans comes from atmospheric wet/dry deposition (Duce and Tindale, 1991) Atmospheric dust comprises both mineral material, derived from arid and semiarid regions and anthropogenic sourced material, such as products from biomass burning, and industry (Krishnamurthy et al. 2009). However the fractions of the total Fe that can be dissolved in the ocean from atmospheric inputs vary widely depending on source, the dissolution conditions, and the type of deposition (Fan et al. 2006). Additionally,

wet deposition is an important source of organic ligands capable of complexing iron, which allows enhancing the solubility of iron deposited (Kieber et al. 2005).

- ***Riverine inputs***

Estimates of riverine input are derived from the product of global river discharge and the mean concentration of aqueous Fe. The mainly riverine Fe-inputs are located in the mighty rivers, found in the Atlantic basin, such as Amazon, Orinoco, Congo and Paraná. The discharge of particulate Fe from these rivers is around 500 times higher than in dissolved form (Chester, 2009). In addition Dissolved iron (<0.45 μm) is known to behave non-conservatively during passage through an estuarine salinity gradient, since the most of this iron precipitate in the discharge regions (Mahmood et al. 2015), although the capacity of the different river waters to maintain iron in suspension varied greatly. Measurements of the physicochemical speciation of dissolved iron in freshwater indicate that iron transport is associated to humic acids (Batchelli et al 2010). Therefore, lower iron:organic carbon ratios in the riverine waters remarkably increase the transport capacity of iron from rivers to ocean waters (Kritzberg et al. 2014). A fraction of iron deposited in estuarine regions can also be transported to oceanic basins by transport mechanisms through underflows turbidity currents (Meiburg and Kneller, 2010).

- ***Coastal glacial meltwater, sea ice and iceberg sources***

The dissolved iron concentrations measured in the coastal glacial meltwater vary from 2-200 nM (Statham et al. 2008) and 40-4000 μM (Wadham et al. 2013), depending if the input fluxes are oxic or anoxic, respectively. Nevertheless, Wadham et al. (2013) suggest that the anoxic estimates are more realistic than the oxic fluxes since the most of oxic flux may not escape precipitation as iron (oxyhydr)oxides prior to delivery to the open ocean.

Icebergs and sea ice also contain important concentrations of iron, until two orders of magnitude higher than that of the underlying seawater, derived from other

sources, such as atmospheric deposition and coastal glacial debris (Lannuzel et al. 2008, 2011). The most of accumulated Fe, which include variable concentrations of dissolved, colloidal and particulate Fe, is released to surface waters through brine drainage, representing a significant iron flux to promote the onset of a spring phytoplankton bloom (Gerringa et al. 2012).

- ***Fe from marine sediments of continental margins and Upwelling events***

Iron inputs from sediments are an important Fe-source in the continental margins (Bowie, 2002). Diffusion fluxes of Fe(II) produced during diagenetic processes, from organic carbon-rich interstitial water, and the resuspension of sediments, with high content of ferric oxides, control this Fe-input (Rozan et al. 2002; Lam et al. 2012). Nevertheless, Elrod et al. (2004) considered that the iron recycling flux and Fe-rich suspended sediments are efficiently delivered to surface waters only where upwelling occurs at the shelf margin. Occasionally in the coastal margins, submarine magmatic activity and hydrothermal sources can also produce important fertilization events of Fe to the sea surface (Santana-Casiano et al. 2013).

In the surface waters of some HNLC regions, the contribution of upwelled Fe has been also esteemed as a significant source of Fe (Hutchins et al. 2002). For example, in the Southern Ocean the upward flux of Fe is around five times that atmospheric contribution, representing the dominant fraction of iron in the Antarctic upper waters (de Baar et al. 1995). Additionally, the continental margins can be a key Fe-source for the HNLC areas, since iron can be transported at distance over 900 km (Lam and Bishop; 2008).

- ***Biological recycling***

In the Upper Ocean, like other macro- and micronutrients, Fe is biologically regenerated through grazing activities (Barbeau et al. 1996; Tovar-Sánchez et al. 2007), and lysis of cells (Poorvin et al. 2011). Field (Sarthou et al. 2008) and

laboratory experiments (Barbeau et al. 1996) show that the iron bio-recycled is highly availability for the microorganisms, and therefore, in oligotrophic waters with limited Fe-inputs (i.e. Southern Ocean or the Pacific Ocean subtropical gyres) this source of iron may be extremely important for Fe-limited phytoplankton communities.

1.2 "Iron Hypothesis"

In the late 1980's, when trace metal clean techniques became available, one concept provided a new focus on iron biogeochemistry. This view, denominates the "Iron Hypothesys" and formulated by John Martin and co-workers (Martin and Fritzwater 1988; Martin et al 1991), recognised that iron could limit phytoplankton productivity in the ocean, which in turn affect the biogeochemical cycles of carbon, nitrogen, silicon, and sulphur and ultimately influence the Earth climate system (Martin, 1990). Ship-board iron-addition bottle experiments clearly showed that iron is an essential micronutrient for the growth of marine phytoplankton in surface waters and, in some regions of the open ocean, the low bioavailability of iron limits their photosynthesis activity (Fig. 1.2) (de Baar et al. 1990; Buma et al. 1991).

Nevertheless the appearance of other key factors during the experiments, such as light limitation and grazing, made the interpretation of the results more complex. After rigorous discussion, the execution of mesoscale Lagrangian-type oceanic experiments, allowed for investigate the influence of iron additions on primary productivity, and study the consequences for ecosystem dynamics and carbon export into deeper waters (de Baar et al. 2005; Boyd et al. 2007). However, the artificial experiments have indicated a limited efficiency of biological carbon export into deeper water regarding to natural Fe fertilization (Boyd et al. 2004; Chever et al. 2010). These differences may be partly due to the immediate loss of added Fe during artificial fertilisations (de Baar et al. 2008).

In summary, the artificial iron experiments have showed that iron limits primary production and has impact on phytoplankton species composition and bloom dynamics in tropical as well as in polar HNLC waters (Fig 1.2). However, from a

marine trace-metal research perspective, both laboratory and field fertilization studies priority should be specifically designed to address clearly defined research questions of iron chemistry that have not yet been resolved (Breitbarth et al. 2010).

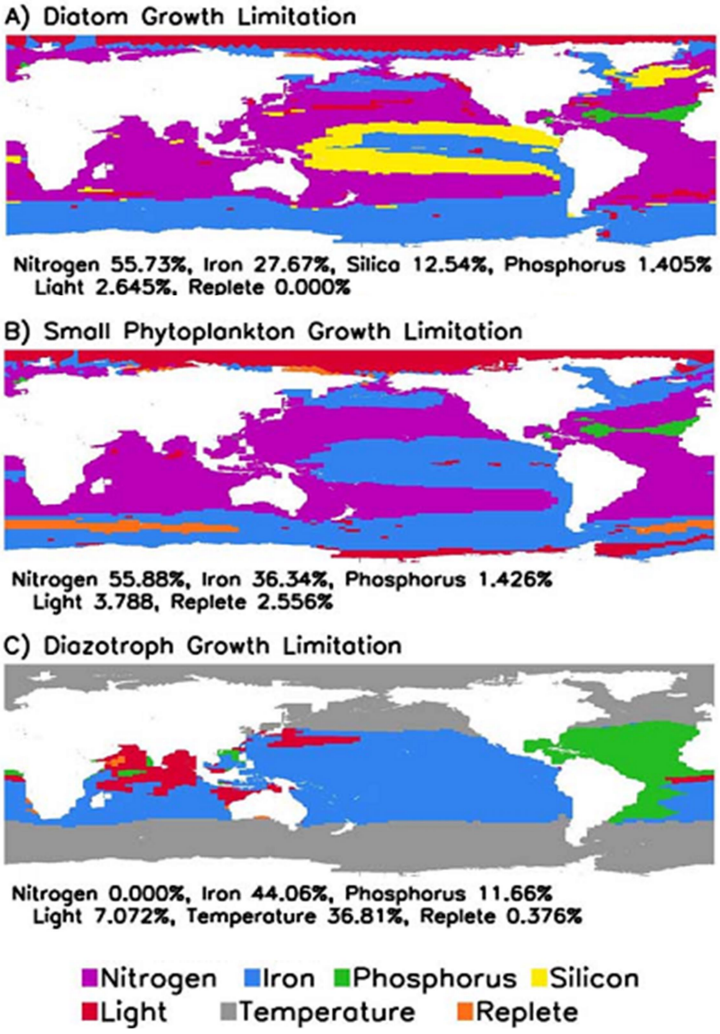

Fig. 1.2 Factors most limiting the development for each phytoplankton group during summer months in the Global Ocean. (From Moore et al. 2004).

1.3 Speciation and redox behaviour of iron in seawater

The speciation of Fe in natural waters is controlled by its redox state (Fe(II) or Fe(III)). Fe(III) is the more thermodynamically stable form in well oxygenated sea surface waters (Miller et al. 1995; Santana-Casiano et al. 2005), since Fe(II), exhibits a half-life from seconds or minutes, depending on the physical-chemistry

properties of the media (Millero et al. 1987; King et al. 1995; Rose and Waite, 2002; González-Dávila et al. 2006; González et al. 2010). The inorganic Fe(III) products are extremely insoluble and precipitate as stable minerals or through scavenging onto sinking particles (Kuma et al. 1996; Liu and Millero 2002; Boyd and Ellwood 2010). Nevertheless, since its first use (Gledhill and van den Berg, 1994), the competitive ligand exchange-adsorptive cathodic stripping voltammetry (CLE-AdCSV) technique has revealed that >99% of Fe(III) is complexed with natural organic ligands (Boye et al. 2001, 2006, 2010), allowing also to determine the stability constants and concentration of Fe-ligand complexes (Croot and Johansson, 2000; Laglera et al. 2011). These organic ligands have been categorized in two types (L_1 and L_2), according to their binding affinities for iron (Boyd and Tagliabue, 2015). Although the analytical overlapping range suggests that there may be additional weaker ligand classes (L_3 and L_4) present in the marine systems (Gledhill and Buck, 2012; Bundy et al. 2014).

However, due to the observation of unusual Fe(II) concentrations (> 0.4 nM) which have been measured in surface seawater for some places in the ocean (Hong and Kester, 1986; O'Sullivan et al. 1991; Roy et al. 2008; Shaked, 2008; Breitbarth et al. 2009), including mesoscale Fe addition experiments (Croot et al. 2005; Boyd et al. 2007), it has been suggested that either Fe(II) is continuously produced, or kinetically stabilized by the presence of organic ligands (Fan, 2008; Gledhill and Buck, 2012). Thus, due to important redox reactivity of iron in the marine system are strongly subject to the presence of organic matter (Croot and Heller, 2012), different studies have been reported as some organic substrates modify the Fe(II)/Fe(III) redox balance, such as humic/fulvic compounds (Lis et al. 2015), exopolymeric substances (Hassler et al. 2011), and siderophores (Barbeau et al. 2001).

1.3.1 Oxidation of Fe(II) in seawater

The Fe(II) oxidation behaviour exhibits differences between micromolar levels and nanomolar concentrations. When Fe(II) is presented in solution at

micromolar concentrations, the oxidation by O_2 and H_2O_2 presents a 4:1 and 2: stoichiometry, respectively (Millero et al.1987; King and Farlow, 2000), while the Fe(II) oxidation at nanomolar levels shows a 2:1 stoichiometry for both oxidants species (González-Dávila et al. 2005). This results is due to key role played by the reaction intermediates ($O_2^{\cdot-}$ and $OH^{\cdot}$), which are not effective at micromolar concentrations (Santana-Casiano et al. 2005). Nonetheless, at micromolar and nanomolar levels, the most broadly accepted oxidation mechanism is the Haber–Weiss sequence (Haber and Weiss, 1932).

$$Fe(II) + O_2 \rightarrow Fe(III) + O_2^{\cdot-} \quad (1)$$

$$Fe(II) + O_2^{\cdot-} + 2H^+ \rightarrow Fe(III) + H_2O_2 \quad (2)$$

$$Fe(II) + H_2O_2 \rightarrow Fe(III) + OH^{\cdot} + OH^- \quad (3)$$

$$Fe(II) + OH^{\cdot} \rightarrow Fe(III) + OH^- \quad (4)$$

In addition, this mechanism can be completed by considering both the hydrolysis-formation of colloidal Fe(III) and the competitive reaction between reactive oxygen species (O_2^- and H_2O_2) with other redox active metals such as copper (Rose and Waite, 2002; González-Dávila et al. 2009; González et al. 2016).

$$Fe(III) + 3OH^- \rightarrow Fe(OH)_{3(s)} \quad (5)$$

$$Cu(II) + O_2^{\cdot-} \rightarrow Cu(I) + O_2 \quad (6)$$

$$Cu(I) + O_2^{\cdot-} + 2H^+ \rightarrow Cu(II) + H_2O \quad (7)$$

Additionally, the interaction of Fe(II) with the major inorganic anions change the oxidation rate of the metal. For example, the oxidation process has a significant dependence with the carbonate levels present in the medium, since the species Fe(II)-carbonate strongly contribute to the overall rate, both with O_2 and H_2O_2 (King, 1998; King and Farlow, 2000).

Important redox processes, which are subject to the presence of organic matter, affect to Fe(II)/Fe(III) balance directly or indirectly in the marine system (Croot and Heller, 2012). The photooxidation of organic matter produces reactive oxygen species (Rose and Waite 2003; Steigenberger et al 2010), which can

condition the Haber-Weiss mechanism (eq 2-3), especially in coastal waters (Cooper and Zika, 1983; Miller et al. 2012).

$$Org + h\upsilon \rightarrow Org^{*} + e^{-} \quad (8)$$

$$4e^{-} + O_2 + 2H^{+} \rightarrow 2H_2O \quad (9)$$

$$2e^{-} + O_2 + 2H^{+} \rightarrow H_2O_2 \quad (10)$$

$$2e^{-} + H_2O_2 + 2H^{+} \rightarrow H_2O \quad (11)$$

$$e^{-} + O_2 \rightarrow O_2^{\cdot -} \quad (12)$$

$$O_2^{\cdot -} + 2H^{+} \rightarrow H_2O_2 + O_2 \quad (13)$$

The majority of the studies of complexation of iron in seawater have been carried out for Fe(III) and therefore, there is relatively little knowledge about the reactivity of the organic compounds present in seawater and their effects on the Fe(II) oxidation rate. However, some studies have shown that organic ligands can retard, increase or not affect oxidation process of Fe(II) in seawater (Santana-Casino et al. 2000; Rose and Waite, 2003; Roy and Wells, 2008; 2011). For example, the complexation of Fe(II) by the phenolic functional groups of the humic substances drags out the oxidation process, keeping to Fe(II) in the system longer (Catrouillet et al. 2014). While the organic buffer EDTA (ethylenediaminetetraacetic acid), used in many research studies as metals chelating agent, increases the oxidation of Fe(II), the role of cysteine, an relevant organic compound in seawater, in the oxidation of Fe(II) is a function of the cysteine:Fe(II) ratio (Santana-Casiano et al. 2000). Recently, the effect of exudates of diatom *Phaeodactylum tricornutum* and green alga *Dunaliella tertiolecta* have been studied, showing that the organic compound excreted by these eukaryote phytoplankton can form complexes with Fe(II) that inhibit its oxidation (Gonzalez et al. 2012; 2014). Therefore, the formation and consequent oxidation of organic complexed ferrous iron (eq 14) can strongly affect to the generation of reactive oxygen species presented in the reactions 1-4 (Miller et al. 2012).

$$Fe(II) - L + O_2 \rightarrow Fe(III) - L \quad (14)$$

Accordingly, there are research experiments that considered individual organic ligands and their interaction with Fe(II), but it is also necessary to characterize the effect of organic ligands released by marine microorganisms on the overall oxidation rate in seawater.

1.3.2 Reduction of Fe(III) in seawater

The equation 14 shows the inorganic mechanism assumed for the photo-regeneration of Fe(II), from (oxyhydr)oxides of Fe(III), in the aquatic media (King et al. 1993). While $Fe(OH)^{2+}$ has been identified as the specie dominant in the reaction, the more highly hydrolysed Fe(III)-species (Fe(OH)x, x=2-4) are photochemically less reactive (Millero, 1998). Therefore this pH-dependent mechanism is not a significant source of Fe(II) in natural waters with a pH > 6.5.(King et al 1995).

$$Fe(OH)^{2+} + h\upsilon \rightarrow Fe-(OH)^{*} \rightarrow Fe^{2+} + OH^{-} \qquad (15)$$

Different laboratory studies have detected a direct light absorbance at the ligand to metal charge transfer (LMCT) band of the surface bound organic (Kuma et al. 1992; Miller et al. 1995; Barbeau et al. 2001; Weller et al. 2013). Therefore, photolytic mechanisms, organically complexed Fe(III), are considered the dominant pathways to regenerate Fe(II) in ocean upper layers (Rijkenberg et al. 2008). Another important reduction mechanisms are carried out by extracellular reactive oxygen species, either biological-mediated (Rose, 2012) as produced by photooxidation of organic matter (Steigenberger et al. 2010), by photo-independent redox mechanism through dissolved organic ligands (Santana-Casiano et al. 2010; 2014), by phytoplankton cell surface enzymatic activity (Maldonado and Price, 2001; Salmon et al. 2006) and by thermal regeneration (Hansard et al. 2009).

It is important to review that Fe(III) bound to organic ligands may undergo one of two reduction processes, non-dissociative (eq 16) reduction and dissociative (eq 17) reduction (Garg et al. 2007; 2007b). During non-dissociative reduction mechanism, Fe(III) is transformed to Fe(II) but the ligand is remains chemically intact, so the Fe-ligand complex does not dissociate (Salmon et al. 2006; Harrington and Crumbliss, 2009). However, during dissociative reduction the Fe(III) is reduced

to Fe(II) and the ligand undergo an oxidation, resulting a dissociation, which forms inorganic Fe(II) and a ligand with different binding capacities (Vraspin and Butler, 2009; Butler and Theisen, 2010; Santana-Casiano et al. 2010).

$$Fe(III) - L \rightarrow Fe(II) - L \quad (16)$$

$$Fe(III) - L \rightarrow Fe(II) + L^{*} \quad (17)$$

Carboxylic, thiolic and alchololic moities are shown to be the mainly organic fucntional groups that, when they coordinate to Fe(III), are able to regenerate Fe(II) (Cunningham et al. 1985; Kuma et al. 1995; Barbeau et al. 2006; Santana-Casiano et al. 2014). Therefore, Fe redox berhaviour in the marine envioments are strongly influenced by the presence of organic ligands, and accordingly, it is important to determine the stability and reactivity of the complexes formed during the different regimens of the biogeochemical Fe-cycle, since the redox speciation of Fe influences in the iron acquisition by microorganisms.

1.4 Fe-bioavailability for phytoplankton

Within the framework of ocean sciences, the bioavailable of iron is the part of the Fe-pool which is biologically accessible to phytoplankton and can sustain their development (Shaked and Lis, 2012). Therefore, Fe-bioavailability controls the photosynthetic microorganism biomass and their growth, as well as, the diversity of the phytoplankton assemblage, thereby affecting in turn the community food web (Lis et al. 2015). Nevertheless, Fe-requirement and uptake strategies of phytoplanktonic species differ considerably.

Inorganic Fe, specially Fe(II) species, is the most easily assimilated species by phytoplankton, although as the Figure 1.3 shows, the organically complexed Fe can also be assimilated directly or by phytoplankton via redox and ligand interchange processes (Hutchins et al. 1999; Maldonado and Price, 2001; Shaked et al. 2005; Morel et al. 2008; Hassler and Schoemann, 2009; Hassler et al. 2011; Sunda, 2012). Due to Fe(II) bind more weakly to ligands, organic ferrous complexes may favour dissociation of free Fe(II) and increase bioavailability. However, if Fe(II) remains

complexed, its oxidation may be stalled/accelerated compared to inorganic Fe(II), conditioning Fe-bioavailability (Roy and Wells 2008, 2011; González et al. 2014; Norman et al. 2015). In addition, Fe(III)-chelates can also carry out a reduction reactions through photolytic, chemical or biological processes, as well as, slow down Fe(III) hydrolysis and precipitation, enhancing the availability of iron (Voelker and Sedlak, 1995; Barbeau et al. 2001; Kustka et al. 2005; Hassler et al. 2012; Santana-Casiano et al, 2014).

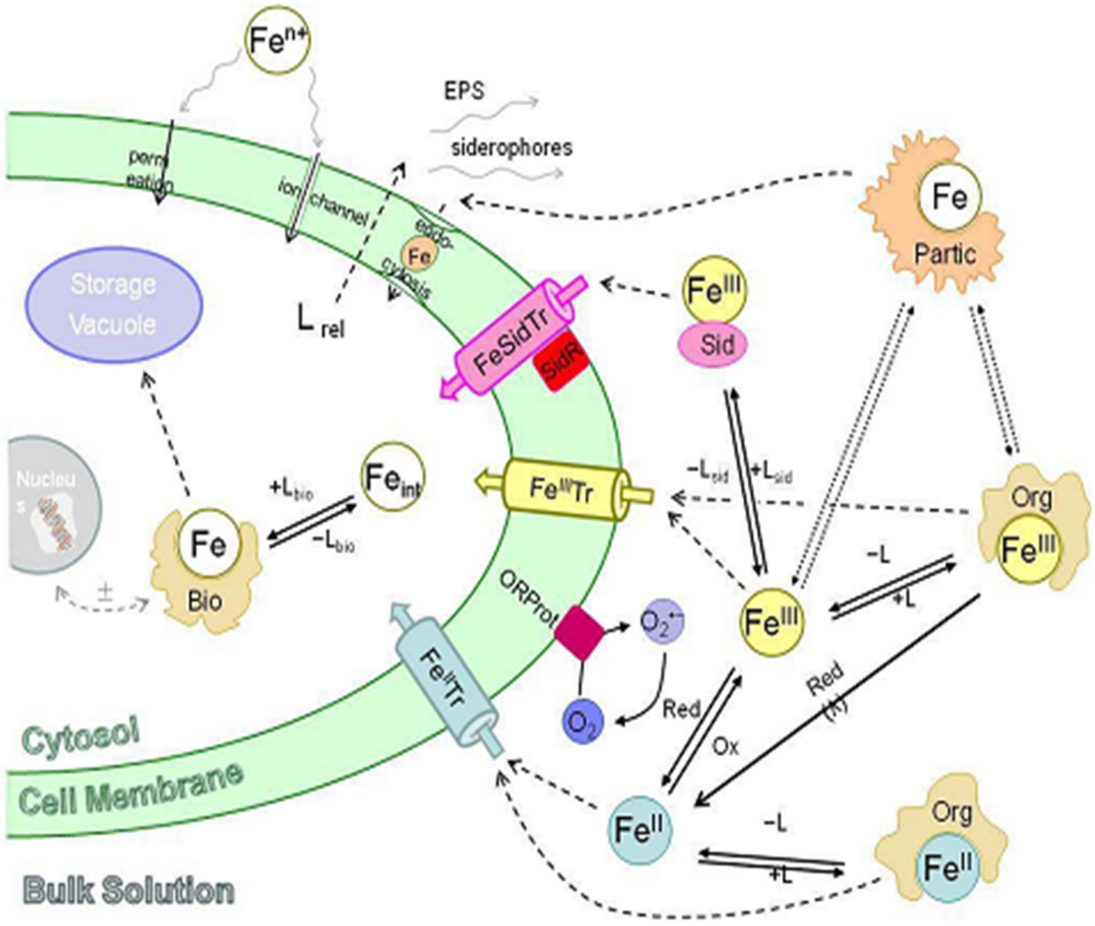

Fig. 1.3. Schematic of the complex interplay between iron (Fe) chemistry and biology, defining its bioavailability to marine microorganisms. In surface water, Fe is mainly associated with particles (Partic), and with dissolved or colloidal organic ligands (Org). Both biology (via surface reductase protein, ORProt) and light (λ) favour Fe reduction and subsequent transport with Fe(II) or Fe(III) transporters (FeTr). Highly specific transporter uptake strategy, is represented separately (FeSidTr).. Once inside the microorganism, Fe (Fe_{int}) reacts with intracellular biological ligands (L_{bio}, e.g Chlorophyll-a), is stored (e.g. vacuole, ferritin) or is involved in cellular homeostasis via gene regulation. (From Hassler et al. 2012).

While the transport of both inorganic and organic iron with membrane transporters are commonly development by eukaryotic phytoplankton (Morrissey et al. 2012), the Fe(III)-L uptake strategies through highly specific proteins present on the cell surface are chiefly carried out by bacterioplankton (Kranzler et al. 2014). The Figure 1.3 also shows other non-specific uptake pathways, such as ion channels endocytosis and direct permeation (Hassler et al. 2012). In addition, release of Fe organic ligands, biologically mediated, can exert a feedback in the control of both Fe redox chemistry and bioavailability (Hassler et al. 2011b, 2015; Norman et al. 2015). Barbeau et al. (2001) have demonstrated that the presence siderophores –highly affinity iron ligands excreted by some prokaryote microorganisms under Fe-limited conditions- produce a photochemical reaction, which facilities iron acquisition. Gonzalez et al. (2014) have showed that the presence of exudates of eukaryote phytoplankton retard the Fe(II) oxidation rate and can act as an important Fe(II) supplier to microalgae. And recently, Hassler et al. (2015) have indicated that when iron binds the rich-saccharides exopolymeric substances, produced by photosynthetic microorganisms, is highly bioavailable.

In summary, bioavailability of iron many factors such as, ligand strength, metal to ligand ratios, and photolability should be taken into consideration. Nevertheless, the environmental perturbations of extracellular media, such ocean warming or acidification, can also indirectly influence in Fe-bioavailability, increasing the Fe stress of phytoplanktonic populations in some areas of the ocean (Hoffmann et al. 2012; Hutchins and Boyd, 2016).

1.5 Iron and changing ocean

Rising atmospheric CO_2 concentrations affect the oceanic environment directly via the uptake of CO_2 that acidifies the seawater and indirectly via global temperature enhance that also results in sea-surface warming (IPCC, 2014). Thereby diverse processes of Fe-cycle, including external/internal supply modes, chemical speciation, reactivity, bioavailability and the removal of Fe with sinking particles, may be alter by the changing ocean. However, there are only a few studies/articles

that have considered the impacts of rising atmospheric CO_2 on iron biogeochemistry in the marine systems (Byrne, 2002; Sunda and Huntsman, 2003; Millero et al. 2009; Boyd et al. 2010; Breitbarth et al. 2010; Shi et al. 2010; Hoffmann et al. 2012; Hoppe et al. 2013; Xu et al. 2014; Gledhill et al. 2015; Hutchins and Boyd; 2016).

1.5.1 Impact of climate change

Global models reveal alterations in the inputs of Fe to Upper Ocean, due to aftermaths produced by the changing climate, such as increasing stratification that results in reduced upwelling and wind-driven mixing (Doney 2006; IPCC, 2014), changing wind patterns (Tokinaga et al. 2012), expansion of the areal extent of oxygen minimum zones (Gruber 2011), and changes in the thermohaline circulation (Rahmstorf and Ganopolski 1999, Boyd and Doney 2003). Global warming will potentially influence global dust into the ocean, but the projections of the likelihood of future modifications get an important uncertainty than for other supply modes, as for example the melting of sea-ice, which is increasing the sources of Fe in high latitudes (Boyd and Ellwood, 2010). Modelling simulations also suggest a future enhance in the atmospheric water vapour levels as well as, an increase in the precipitation regimens, but with large geographical differences (Meehl et al. 2005). In addition a direct contribution of gases, such as carbon dioxide, sulphur dioxide, and nitrogen oxide, to decrease the pH of cloud water may double the bioavailable of atmospheric Fe supplied, via increasing its dissolution conditions and solubility (Desbouefs et al. 2001).

Because high latitudes are more sensitive areas to ocean warming, in principle, these processes may increase the marine productivity in Arctic and Antarctic ecosystems, since temperature and higher Fe inputs have shown a synergistic effect on growth rates in cold diatom community (Rose et al. 2009; Xu et al, 2014; Boyd et al. 2016; Zhu et al. 2016). At the same time, solubility and chemical speciation of Fe in seawater are key parameters for Fe-bioavailability (Hutchins et al. 1999; Lis et al. 2015) and while the rise of sea surface temperature will diminish the Fe-inorganic solubility, the fraction of dissolved Fe(III), complexed

by organic ligands, will not significantly vary (Lui and Millero; 2002). The Fe-redox behavior is also strongly affected by temperature (Table 1). For example, in presence of diatom exudates, an increase of 5º C diminish the half-life of more bioavailable Fe(II) until 45% (Gonzalez et al. 2014), as has been observed in the Gulf of Aquaba (Shaked, 2008), which might imply that warming will favor to microrganisms that more efficiently leverage their existing cellular Fe pools to support growth (Sunda and Huntsman, 2011), or those that get Fe(III) through highly specific transporter uptake strategies (Hassler et al. 2012). Contrary to these, Boyd et al. (2008) suggest that an increase mean light intensities in the surface mixed layers of Southern Ocean, due to the intensification of surface stratification, would enhance photochemical Fe(III) reduction and will lead to a larger pool of Fe(II) in surface waters, since Kuma et al. (1992, 1995) have demonstrated that the regeneration of Fe(II), induced by light in laboratory experiments with seawater as well as diatom exudates, enhances linearly with increasing light intensity and is independent of temperature (Table 1).

Table 1. Overview of potential ocean warming and acidification effects on Fe-chemistry.

Parameters	**Factors**	
	↑ SST	**↓ pH**
Inorganic-Fe	↓ Solubility[1] ↑ Complexation[2] ↑ Fe(II) oxidation[3] ↓ Fe(III) reduction[4]	↑ Solubility[2] ≈ Fe(III)[2]; ↓ Fe(II)[3] complexation ↓ Fe(II) oxidation[3] ↑ Fe(III) reduction[4]
Organic-Fe	≈ Solubility[1] ≈ Complexation[1] ↑ Fe(II) oxidation[5] ≈ Fe(III) reduction[6]	≈ Solubility[1] ↓? Fe(III)[7]; ↑? Fe(II)[8] complexation ↓ Fe(II) oxidation[5] ? Fe(III) reduction

Legend: ↑ increase; ↓ decrease; ≈ without significant changes; ? unknown or not clear effect

[1]Liu and Millero 2002; [2]Millero et al. 1995; [3]Santana-Casiano et al. 2005; [4]King et al. 1993; [5]González et al. 2014; [6]Kuma et al. 1995; [7]Gledhill et al. 2015; [8]Breithbarth et al. 2010.

Both the Fe-binding ligands production and release by phytoplankton might also be influenced by the increasing sea surface temperature (Thornton, 2014). In this way, an experimental study with mesoscosms, conducted by Engel et al (2011), showed that rising temperature result in an earlier, faster and higher accumulation of total combined carbohydrates, which could control the growth of planktonic microorganisms increasing the Fe-bioavailability (Hassler et al. 2011b, 2012) and therefore, affecting the bottom-up control of the microbial loop in cold seas in the future.

1.5.1 Impact of Ocean Acidification

Trace metal biogeochemistry is strongly influenced by their chemical speciation, which in turn is conditioned by presence of other ions with which it may interact (Morel and Price, 2003; Hofmann et al. 2012; Hutchins and Boyd, 2016). Therefore, the chemical form of iron in seawater is affected by the presence both carbonate ion and hydrogen ion concentrations (Liu and Millero, 2002). Consequently, a decrease in surface ocean pH, due to Ocean Acidification, can alter the inorganic speciation of iron (Table 1). A drop in pH increases the fraction of free ionic forms (specially Fe^{2+}) and diminishes the complexes with OH^- and CO_3^{2-} ions, since these anions are expected to fall in surface waters by 20% and 30% by the year 2100, respectively (Millero et al. 2009).

The role of Ocean acidification in the organic Fe-complexation is less clear (Table 1). In a recent work, Gledhill and coworkers (2015) have suggested a slightly decrease in Fe(III) binding by organic matter at lower pH, although the authors indicate that a variation of the levels of dissolved organic ligands, might have a greater impact on iron speciation in seawater, than projected variability in pH resulting from increases in atmospheric CO_2. In addition the response of organic complexation to pH lower, both for Fe (III) and Fe(II), can vary depending on the nature of the binding site (acidic or basic) (Gonzalez et al. 2014; Gledhill et al. 2015).

These changes in seawater pH will also increase the thermodynamic and kinetic reactivity of iron (Millero et al. 2009). The oxidation of inorganic Fe(II) as function of pH has widely been studied (Millero et al. 1987; Millero and Sotolongo 1989; King et al. 1993, 1995; King, 1998; King and Farlow, 2000; Santana-Casiano et al. 2005; Gonzalez-Dávila, 2005, 2006). The results support a longer lifetime for Fe(II) in oxic waters at lower pH. Gonzalez et al. (2014) have also shown that the interaction between Fe(II) and natural ligands produced by phytoplankton species is also pH-dependent. Nevertheless, the effect of pH on Fe(II) regeneration is still unknown (Table 1).

The production of organic ligands by phytoplankton is a key factor to be considered when studying the effects of a lower ocean pH on iron speciation, Fe-redox behavior and Fe-bioavailability. For example, Ocean Acidification might enhance the biosynthesis and release of some organic ligands, such as uronic acids or phenolic compounds (Lidbury et al. 2012; Jin et al. 2015) which, can form organic complex with iron (Gyurcsik and Nagy, 2000; Elhabiri et al. 2007) and constituting a part of organic ligand pool in the ocean and phytoplanktonic exudates (Hung et al. 2001; Rico et al. 2013; Borchard and Engel 2015; Heller et al. 2016), as well as, increasing the Fe-bioavailability of iron in phytoplankton communities (Maldonado et al. 2005; Hassler et al. 2015).

These changes in ocean chemistry could also cause strong impacts in Fe-bioavailability. For example, a laboratory study (Shi et al. 2010) has suggested that the availability of dissolved Fe to marine phytoplankton may decline consequence of pH-linked changes in iron chemistry. Nevertheless recently, during a mesocosm experiment carried out in Southern Ocean with natural phytoplankton communities, the results have shown that Fe-bioavailability slightly enhance with increasing pCO_2 (Hoppe et al. 2013).

Definitely, it is necessary to study and recognize the effects the organic compounds excreted by microorganisms on the marine iron chemistry, due to the biogeochemical cycle of iron are strongly linked with potential future changes in carbon regulation of ocean productivity and, accordingly, climate (Sunda, 2010).

1.6 Outline and aims

As explained in the general introduction, currently, the need to carry out a kinetic study of Fe-redox chemistry in presence of exudates biologically mediated is because phytoplankton is the main source of organic ligands for iron in the open ocean, which condition the Fe-bioavailability in HNLC areas. Therefore, from marine trace-metal research perspective, characterizing the effect of different physic-chemical conditions, such as temperature and pH, on Fe(II)/Fe(III) balance in presence of natural organic exudates arouses great interest, in order to know how affect the changing ocean to biogeochemical cycle of iron.

Therefore, the main objective of present PhD research is to assess "***the biogeochemical cycle of iron in acidified marine environments"***. To achieve this goal was characterize the effect of Ocean Acidification on redox behavior of iron, focusing both on its interaction with nutrient and its organic complexation with ligands produced by two phytoplankton species, the cyanobacteria *Synechococcus* PCC 7002 and the coccolithophorid *Emiliania huxleyi*. The first one specie was selected due to great plasticity to growth under different iron regimens, as well as the capacity of this cyanobacterium to modify the composition of the organic exudates as function of Fe-bioavailability. *E.huxleyi* was chosen because representing a key phytoplankton group in ocean carbon cycle, since are responsible for a significant part of carbonate production in the surface ocean and therefore, they are especially sensitive to Ocean Acidification. In addition, both species present an especial heeded due to their wide oceanographic distribution and for the awaken interest by their organic compounds excreted, in the trace metal complexation.

As previous step, the kinetics studies with Fe(II) were carried out in seawater at high nutrient concentration. These conditions are usually used as medium for microalgae culture. In addition during last decades human activities have increased in the fluxes of nutrients to ocean, enhancing the rates of eutrophication in many coastal regions and favoring periodic proliferation of harmful algae blooms. Thus, in this work has been studied the interactive effect between eutrophication conditions, ocean warming and acidification, on the Fe(II) oxidation process.

The overall objective has been structured into five specific aims, which correspond to five chapters included in the present PhD Thesis.

- **Aim 1: To examine the effect of ocean warming and acidification on the Fe(II) oxidation rate in oligotrophic and eutrophic waters.**

A number of kinetic studies have to be performed to elucidate the oxidation of Fe(II) at nanomolar levels seawater, considering the synergistic effect of ocean acidification, global warming and coastal eutrophication. This goal implies the study of the oxidation process, varying the physical-chemistry parameters of pH and temperature, both in presence and absence of nutrients. To avoid organic interferences, the natural seawater has to be pre-treated with UV radiation, comparing the results achieved in it with those obtained in artificial seawater.

A kinetic model has been developed to describe the experimental results obtained and to help to understand the interaction between Fe(II) and nutrients under different environmental conditions and thus recognize the factors that produce greater changes in the oxidation process observed during the experiments, as well as the Fe(II)-redox species that lead them. The development of this aim constitutes Chapter II.

- **Aim 2: To characterize the production of Fe organic ligands, by *Synechococcus* PCC 7002, under two different iron fertilization scenarios.**

In order to reach this aim, it was necessary to determine the development of *Synechococcus* PCC 7002 under the two experimental Fe-scenarios. Once the growth is characterized, organic assays have to be carried out in order to determine the dissolved organic carbon, hydroxamates moieties and phenolic compounds in the cultures during the different growth stages, and so it has been possible statically evaluate the variability of ligand production by the cyanobacteria, between both fertilization scenarios considered. This study is presented in Chapter III.

- **Aim 3: To study the impact on the Fe-redox cycling of organic ligands released by *Synechococcus* PCC 7002, under two different iron fertilization scenarios.**

To determine the interaction between Fe(II) and the organic exudates from *Synechococcus* PCC 7002, released under two different Fe-scenarios, the kinetic study should be done at different pH, temperature and salinity. Then, the capacity of these exudate to photo-regenerate Fe(II) and the possible pH-dependence of this process has been evaluated, as well as, its effect on the re-oxidation of Fe(II).

A kinetic model has been developed which explain the experimental results obtained in order to detail the Fe(II) speciation and the fractional contribution of each Fe(II) species to the overall oxidation rate. The model describe both Fe-scenarios, as well as the interaction of organic ligands with Fe(II) and Fe(III), monitored in aim 2. The photolytic mechanism also has been considered in the modelling approach. The equilibrium constant and kinetic rates have been fitted from the model. These results are presented in Chapter IV.

- **Aim 4: To evaluate the release of organic ligands by *Emiliania huxleyi*, under simulated ocean acidification conditions.**

In order to reach this aim, the growth of *E.huxleyi* has been tested in an acidification microcosm set-up, considered the projections of Intergovernmental Panel on Climate Change (IPCC, 2014) for Ocean Acidification.

Then, the effect of pCO_2 in the exudation of *E.huxleyi*, has been carried out. In this way, the levels of dissolved organic carbon, phenolic compounds, carbohydrates and uronic acids have been monitored in each growth stage. Finally, a statistical treatment of experimental results has been also performed. These results are presented and discussed in the Chapter V.

- **Aim 5: To determine the effect of organic Fe-ligands, released by *Emiliania huxleyi* on Fe(II) oxidation rate, under simulated Ocean Acidification conditions.**

In order to reach this aim, the experimental studies about oxidation of Fe(II) has been performed under the acidification conditions obtained in the experimental microcosms, for the different growth stages of *E.huxleyi*.

Finally, a kinetic model has been carried out according to the experimental results collected, considering the levels of organic ligands previously analyzed and which are capable to bind Fe(II). The kinetic model allow to account the contribution the most important Fe(II) species to the overall rate. The development of this aim is presented Chapter VI.

1.6 Esquema y Objetivos

En la actualidad, como se explica en la introducción general, la necesidad de llevar a cabo un estudio cinético de la química redox del Fe, en presencia de exudados biológicamente mediados, debido a que el fitoplancton es la principal fuente de ligandos orgánicos para el hierro en el océano abierto, los cuales a su vez condicionan su biodisponibilidad en las zonas HNLC. Por lo tanto, desde una perspectiva de la investigación marina de metales traza, caracterizar el efecto en el balance Fe(II)/Fe(III) de diferente condiciones físico-químicas, como pH y temperatura, y en presencia de exudados orgánicos naturales, despierta un gran interés para conocer cómo podría afectar el futuro cambio del océano al ciclo biogeoquímico del hierro.

De este modo, el principal objetivo de esta investigación de doctorado es evaluar ***"el ciclo biogeoquímico del hierro en ambientes marinos acidificados".*** Para lograr este objetivo se caracterizó el efecto de la Acidificación Oceánica en el comportamiento redox del hierro, enfocándose tanto en su interacción con los

nutrientes como en su complejación orgánica con ligandos producidos por dos especies de fitoplancton, la cianobacteria *Synechococcus* PCC 7002 y el cocolitofórido *Emiliania huxleyi.* La primera especie fue seleccionada debido a su gran plasticidad para crecer en diferentes regímenes de hierro, así como por la capacidad para modificar la composición de sus exudados orgánicos en función de la biodisponibilidad de hierro.

Como paso previo, los estudios cinéticos con Fe (II) se realizaron en agua de mar con alta concentración de nutrientes. Estas condiciones se usan normalmente como medio cultivo para microalgas. Además durante las últimas décadas las actividades humanas han aumentado en los flujos de nutrientes al océano, aumentando las tasas de eutrofización en muchas regiones costeras y favoreciendo la proliferación periódica de algas dañinas. Por ello, en este trabajo se ha estudiado la interacción entre las condiciones de eutrofización, el calentamiento de los océanos y la acidificación, sobre el proceso de oxidación del Fe (II).

El objetivo general se ha dividido en cinco objetivos específicos, que corresponden a cinco capítulos incluidos en la presente tesis doctoral.

- **Objetivo 1: Examinar el efecto del calentamiento de los océanos y la acidificación sobre la tasa de oxidación de Fe (II) en aguas oligotróficas y eutróficas.**

Se deben realizar varios estudios cinéticos para dilucidar la oxidación del Fe (II) a niveles nanomolares de agua de mar, considerando el efecto sinérgico de la acidificación de los océanos, el calentamiento global y la eutrofización costera. Este objetivo implica el estudio del proceso de oxidación, variando los parámetros físico-químicos de pH y temperatura, tanto en presencia como en ausencia de nutrientes. Para evitar interferencias orgánicas, el agua de mar natural debe ser pretratada con radiación UV y comparar los resultados con los obtenidos en agua de mar artificial.

Se ha desarrollado un modelo cinético para describir los resultados experimentales obtenidos y ayudar a comprender la interacción entre Fe(II) y nutrientes bajo diferentes condiciones ambientales y reconocer así los factores que

producen mayores cambios en el proceso de oxidación observados durante los experimentos, así como las especies redox de Fe(II) que llevan a cabo estos cambios. El desarrollo de este objetivo constituye el Capítulo II.

- **Objetivo 2: Caracterizar la producción de ligandos orgánicos de Fe, por *Synechococcus* PCC 7002, bajo diferentes escenarios de fertilización con hierro.**

Para alcanzar este objetivo, fue necesario determinar el desarrollo de *Synechococcus* PCC 7002 bajo los dos escenarios Fe experimentales. Una vez que se caracteriza el crecimiento, se deben realizar ensayos orgánicos para determinar el carbono orgánico disuelto, los restos de hidroxamatos y los compuestos fenólicos en los cultivos durante las diferentes etapas de crecimiento. De esta manera, se ha podido evaluar estadísticamente la variabilidad de la producción de ligandos en los exudados de las cianobacterias, entre ambos escenarios de fertilización considerados. Este estudio se presenta en el Capítulo III.

- **Objetivo 3: Estudiar el impacto en el ciclo Fe-redox, de los ligandos orgánicos liberados por *Synechococcus* PCC 7002, bajo dos diferentes escenarios de fertilización con hierro.**

Para determinar la interacción entre Fe(II) y los exudados orgánicos de *Synechococcus* PCC 7002, liberados bajo dos diferentes escenarios de Fe, el estudio cinético debe realizarse a diferentes pH, temperatura y salinidad. A continuación, se ha evaluado la capacidad de estos exudados para regenerar el Fe(II) y la posible dependencia del pH de este proceso, así como su efecto sobre reoxidación.

Finalmente, se ha desarrollado un modelo cinético de acuerdo a los resultados experimentales obtenidos, para explicar la especiación de Fe(II) y la contribución

fraccional de cada especie de Fe(II) a la tasa de oxidación global. El modelo describe ambos escenarios de Fe, así como la interacción de ligandos orgánicos con Fe(II) y Fe(III), monitoreados en el objetivo 2. El mecanismo fotolítico también se ha considerado en el enfoque de modelado. La constante de equilibrio y las tasas cinéticas se han ajustado desde el modelo. Estos resultados se presentan en el Capítulo IV.

- **Objetivo 4: Evaluar la liberación de ligandos orgánicos por *Emiliania huxleyi*, bajo condiciones simuladas de acidificación oceánica.**

Con el fin de alcanzar este objetivo, el crecimiento de *E. huxleyi* se ha probado en un microcosmos de acidificación, considerando las proyecciones del Panel Intergubernamental sobre el Cambio Climático. A continuación, se ha probado el efecto de pCO_2 en la exudación de E. huxleyi. De esta manera, los niveles de carbono orgánico disuelto, compuestos fenólicos, hidratos de carbono y ácidos urónicos han sido monitoreados en cada etapa de crecimiento. Finalmente, se ha realizado un análisis estadístico de los resultados experimentales. Estos resultados son presentados y discutidos en el Capítulo V.

- **Objetivo 5: Determinar el efecto de los ligandos orgánicos de Fe, liberados por *Emiliania huxleyi,* sobre la tasa de oxidación de Fe (II), bajo condiciones simuladas de Acidificación del Océano.**

Para alcanzar este objetivo, los estudios experimentales sobre la oxidación del Fe(II) se han realizado manteniendo las condiciones de acidificación obtenidas en los microcosmos, para los diferentes estadios de crecimiento de *E. huxleyi.*

Finalmente, se ha realizado un modelo cinético según los resultados experimentales recogidos, considerando los niveles de ligandos orgánicos

previamente analizados y capaces de fijar Fe(II). El modelo cinético permite considerar la contribución de las especies Fe(II) más importantes a la tasa global. El desarrollo de este objetivo se presenta en el Capítulo VI.

CHAPTER II

Effect of ocean warming and acidification on the Fe(II) oxidation rate in oligotrophic and eutrophic natural waters

Samperio-Ramos, G., Santana-Casiano, J.M. and González-Dávila, M.: Effect of ocean warming and acidification on the Fe(II) oxidation rate in oligotrophic and eutrophic natural waters. *Biogeochemistry*, 128 (1), 19-34, 2016. doi:10.1007/s10533-016-0192-x.

CHAPTER II

Abstract

The oxidation rates (k_{app}) of nanomolar levels of Fe(II) were studied in seawater enriched with nutrients (SWEN) in air saturated conditions. The nutrient effect (nitrate, phosphate and silicate), on the oxidation of Fe(II), was evaluated as a function of pH (7.2-8.2), temperature (5-35 ºC) and salinity (10-37.09). The oxidation of Fe(II) was faster in the presence of nutrient with the change in the Fe(II) oxidation rates ($\Delta \log k_{app}$) more intensive at higher temperatures over the entire pH range studied.

A kinetic model that considers the interactions of Fe(II) with the major ions in seawater, including phosphate and silicate, was applied to the experimental results in order to describe the effect of ocean warming and acidification in the speciation of Fe(II) and to compute the fractional contribution of each Fe(II)-specie to the overall oxidation rate. The inorganic speciation of Fe(II) was controlled largely by pH, either in SW or in SWEN. A greater presence of Fe-nutrient reactive species ($FeH_3SiO_4^+$ and $FePO_4^-$) in SWEN at higher temperatures explained the changes in the oxidation process. The individual oxidation rates by oxygen, for the Fe(II) most kinetically active species (Fe^{2+}, $FeOH^+$, $Fe(OH)_2$, $FeCO_3(OH)^-$, $FeCO_3$, $Fe(CO_3)_2^{2-}$, $FeH_3SiO_3^+$, $FePO_4^-$), were fitted as a function of the temperature.

CHAPTER II

CHAPTER II

2.1 Introduction

The iron oxidation rate in seawater has a strong dependence on pH, temperature and media composition (Millero et al. 1987; Gonzalez-Dávila et al. 2006; González et al. 2014). Changes in pH and temperature affect photochemical processes such as production and consume of O_2^- and H_2O_2 (Millero 2009; Kieber et al. 2014). For example, the Haber-Weiss mechanism (eq 1-4) is affected by changes in pH, which modify the lifetime of reactive oxygen species and the production of H_2O_2, since the overall rate for the dismutation reaction of the superoxide molecule and the disproportonation of HO_2 radical, to form hydrogen peroxide, are functions of pH (Millero 1987). The thermal dependence, of individual oxidation rates by H_2O_2, for the Fe(II) most kinetically active species, also have been determined (González-Davila et al. 2005). Accordingly, ocean warming and acidification may have a significant impact on the kinetics behavior of iron in seawater (Millero 2009; Hoffmann et al. 2012; Hutchins and Boyd, 2016).

The observed upper ocean warming (about 0.2 ºC per decade) is expected to increase in coming decades, since human activities to intensify the release of CO_2 into the atmosphere (Rogelj et al. 2012; IPCC 2014). Owing to the rise of sea surface temperature (SST) the reactivity of Fe(II) species should increase, reducing the half-life for Fe(II) (Santana-Casiano et al. 2005). Similarly, the kinetic behavior of Fe(II) also should be conditioned by the latitudinal variation of SST. In addition, due to the equilibration of rising atmospheric CO_2 with the ocean, Earth System Models project a global increase in ocean acidification for all Representative Concentration Pathway (RPC) scenarios over this century (IPCC 2014). As a result, the pH of the surface seawater may decrease from its current value of 8.1 to 7.8 by the end of the 21st century (IPCC 2014). A reduction in the pH should result in a lower reactivity of Fe(II), due to a decrease in the concentrations both of Fe(II)-hydroxides and Fe(II)-carbonates, thus increasing the residence time of Fe(II) in seawater (King and Farlow, 2000; King, 1998). On the other hand, the natural variability in seawater carbonate chemistry can occur at rates even higher than the decline of pH due to anthropogenic contribution (Byrne et al. 2010). Therefore, the pH-dependence of

Fe(II) speciation entail that the dynamics of specific CO_2 systems on local scales (Hofmann et al. 2011) and the substantial temporal variability of oceanic carbon cycle (Santana-Casiano et al. 2007; Dore et al. 2009) should be considered, inasmuch as may produce events of acidification with important impacts in the iron redox chemistry. In addition, carbon and iron cycles are strongly interrelated to with other major biogeochemical cycles, such as those of P and Si (Dutkiewicz et al. 2005; Ragueneau et al. 2006; Baron et al. 2013). For example, in the presence of high nutrient concentrations iron chemical speciation may be modified (Öztürk et al. 2003). Moreover, different mesoscale Fe addition experiments showed that iron supply exerts controls on the dynamics of phytoplankton blooms, which in turn condition the biogeochemical behaviour of carbon and nutrients, and ultimately influence the climate system (Boyd et al. 2007).

Over the past several decades researches have revealed anthropogenic disturbance of the Si cycle in rivers, estuaries, and coastal zones. The alteration of rock weathering rates due to the rapid agricultural expansion, and the construction of dams, which currently retain a third of the global sediment discharge, has modified the river input of silica to the ocean, causing a variation of the dissolved Si concentrations in coastal waters (Laruelle et al. 2009; Struyf and Conley 2012). In addition, more changes in the silica cycle related to conversion of forests to farmland, additional damming and global warming are expected in the near future (Laruelle et al. 2009; Tréguer and De La Rocha 2013). Moreover, human activities have promoted an increase in the global fluxes of nitrogen and phosphorus, accelerating the rates of eutrophication in many coastal regions and favoring periodic proliferation and dominance of harmful algae blooms (HAB's) (Conley et al. 2009; Paerl and Paul 2012). Groundwater discharge may also be a significant factor in the eutrophication of coastal waters, as nutrient levels in submarine groundwater may reach several orders of magnitude greater than surface water of coastal systems (Moore 2010). Some studies have linked the nutrients inputs by submarine estuaries to HAB's (Hu et al. 2006; Lee et al. 2010). Accordingly variations in the concentrations of Si, P and Fe have significantly influenced the outcome in the structure and abundance of phytoplankton communities under eutrophication conditions (Garmendia et al. 2011; Guenther et al. 2015). Thus the possible

interactive effects produced by ocean warming and acidification, on the nutrient biogeochemical cycles, need to be carefully considered in designing and interpreting experiments and eutrophication models (Rabalais et al. 2009). Likewise, recent studies have analyzed the combined effect between ocean acidification and coastal eutrophication processes (Feely et al. 2010; Wallace et al. 2014). For example, in future scenarios with higher atmospheric CO_2, Cai et al. (2011) have predicted important increases in acidification of coastal waters, due to the decomposition of organic material produced during eutrophication processes.

Recent kinetic models have shown the significance of nutrients both, in the speciation of Fe(II), and in the fractional contribution to the overall oxidation rate in natural waters at 25 ºC (González et al. 2010; Mao et al. 2011). No studies have considered the effect of temperature on both of these processes. Due to the Fe(II)-nutrient interactions, especially with silicate and phosphate, the oxidation process appears to be intensified (González et al. 2010; Mao et al. 2011). For example, in aerobic conditions, Fe(II)-phosphate species have a strong tendency to be oxidize, with subsequent possible formation and precipitation of stable mineral vivianite (Wang et al. 2012). However, to date there have been no kinetic models developed to evaluate the redox behavior of Fe(II) to consider the synergistic effect of ocean acidification, global warming and coastal eutrophication.

In the present study, and for the first time, we examine the oxidation of Fe(II) at nanomolar levels in seawater and seawater enriched with nutrients, changing the chemical and physical conditions (pH, temperature and salinity). The speciation of inorganic Fe(II) species as a function of the pH and temperature have been modeled in order to elucidate the inorganic Fe(II) redox behavior over a wide range of scenarios of acidification and global warming of the upper ocean, as well as, changes due to natural ambient fluctuations of pH and temperature. In addition, a kinetic modeling approach has been carried out to elucidate the fractional contribution of most kinetically active Fe(II) species to the overall oxidation rate to improve our future and present knowledge with respect to redox iron chemistry in the marine systems.

2.2 Material and methods

2.2.1 Reagents and medium

All chemicals used in this study were trace analytical grade. Stock solutions of Fe(II) (400 μM) were prepared using ferrous ammonium sulfate hexahydrate (Sigma), acidified until pH = 2 with suprapure HCl (Panreac). Nutrient stocks solutions were made ready in a saline matrix, using sodium chloride (Sigma) (0.7 M), sodium nitrate (Sigma) (850 mM), potassium hydrogen phosphate (Sigma) (25 mM) and sodium silicate (Sigma) (140 mM). All dilutions were carried out with ion exchange Mili-Q water (18 MΩ).

The seawater used for this study was obtained at 250 m off-shore of the east coast of Gran Canaria (The Canary islands) at 10 m depth and was filtered (0.22 μm) through a membrane system (PCI Membranes, Inc.). Dissolved organic matter was removed from the SW via photo-oxidation with UV radiation, for 4 h, via a mercury lamp. Later, the seawater was filtered (0.1 μm in vacuum). Both the 20 L polyethylene containers and the second filtration system were cleaned according to a standard protocol (Achterberg et al. 2001).

The residual concentration of the total dissolved organic carbon (DOC) was measured with a TOC continuous flow analyzer (TOC-V Shimadzu), previously calibrated with potassium hydrogen phthalate standard (Sigma-Aldrich) (Arístegui et al. 2014). Then the filtered UV treated seawater was stored in the dark (> 1 month) to allow the complete decay of any Fe(II) and other reactive oxygen species present in the radiated seawater collected (Borer et al. 2009; Garg et al. 2011). The practical salinity was determined using a salinometer (Portasal, 8410A) and, for the salinity studies, dilutions were made with Milli-Q water. The final values were adjusted and measured using the salinometer, in each case. The total carbonate concentrations adjusted to the initial value (2.05 μmol kg^{-1}) in order to remove carbonate effects on the salinity (Santana-Casiano et al. 2004).

2.2.2 Experimental conditions

The nutrient effect on the Fe(II) oxidation was studied for seawater solutions at initial Fe(II) concentrations of 25 nM as a function of pH (7.2-8.2), temperature (5-35 ºC) and salinity (10-37). In recent studies carried out in seawater (González et al. 2010), at different pH values but at a constant temperature of 25 ºC, González et al. fitted the behavior of the log k_{app} to an exponential function, where the Fe(II) oxidation rate reached a maximum and remained unchanged when the [$NaNO_3$] > 750 μM, [K_2HPO_4] > 15 μM and [$Si(OH)_4$] > 120 μM. In the present study, two extreme Fe(II) oxidation scenarios were considered depending on nutrient concentrations: oligotrophic and extremely eutrophic waters, labeled as SW and SWEN respectively. The studies carried out with seawater enriched with nutrients (SWEN: [NO^{3-}] = 850 μM, [HPO_4^{2-}] = 25 μM and [$Si(OH)_4$] = 140 μM) were compared with studies carried out in SW, which was considered to be the reference value. The seawater (SW) used in the present study was superficial oligotrophic North Atlantic Seawater, and although nutrients have not be previously determined, earlier analysis (Haroun 1994; Pérez et al. 2001; González-Dávila et al. 2003; González-Dávila et al. 2006a) indicated that the nutrient concentrations in superficial seawater of Canary basin did not exceed 1.5 μM, 0.5 μM and 2.0 μM for nitrate, phosphate and silicate respectively.

The kinetic experiments were carried out, in a 250 ml thermostated glass reaction cell, with oxygen saturated conditions, by bubbling pure air through the solution for one hour. The temperature was set with an error of ± 0.02 ºC in a NesLab circulating bath. The pH was adjusted automatically with small additions of HCl (1 M) using a titrator system (Tritino 719S, Methrom). The pH was measured potentiometrically, on the free hydrogen ion scale (pH_F = -log[H^+]) with an Orion pH-meter. Tris-(hydroximethyl)aminomethane(tris)-artificial seawater buffer (0.005 mol kg^{-1} Tris and Tris-HCl in artificial seawater) was used to calibrate the combination electrode (Ross Combination, glass body). Over all the studies the effect of temperature and salinity on the pK^* of the Tris-buffers was considered (Millero 1986). The concentration of O_2 were determined from the theoretical solubility equations (Benson and Krause 1984).

Fe(II) concentrations were measured spectrophotometrically using the modified ferrozine method (Viollier et al. 2000). A blank, with seawater and reagents, was carried out for each experiment. The addition of Fe(II) to the reaction cell corresponded to time zero. At selected times 10 ml of seawater was added to the 25 ml glass flask that contained the reagents. In this method, the sample reacted with ferrozine (50 μL, 0.01 M) in a acetate buffer solution (2 ml, pH = 5.5) to produce a Fe(II)-ferrozine complex, that absorb at 562 nm. Absorbance measurements were normalized to a non-absorbing wavelength (700 nm) in order to compensate for turbidity and instrument drift. Fe(II) measurements were always carried out between 1 min and 5 min after addition of seawater in the 25 ml glass flask that contained the reagents, minimising the "background" iron reduction (Waterbury et al. 1997). Furthermore, NaF was added as reagent to avoid, to a large degree, the interferences by the formation of Fe(III)-ferrozine complex (Hansen 1999; González-Davila et al. 2005).

A 5 m long waveguide capillary flow cell (World precision instrument^{TM}) connected to the UV detector S2000 (Ocean Optics^{TM}) was used to measure Fe(II) concentrations at nano-molar levels. In accordance with the Beer-Lambert law, the response in the calibration method was linear over 2 orders of magnitude ([Fe(II)] (nM) = 0.06 + 82.69 Abs; $r^2 = 0.999$) with a molar absorptivity (ε) = 2.5 (±0.3) $\cdot 10^4$ M^{-1} cm^{-1}, close to that obtained by other authors (Waterbury et al. 1997; Santana-Casiano et al. 2005).

2.2.3 Numerical model

CHEAQS PRO (Verveij 2013) was used to calculate the chemical equilibria in aquatic systems and nutrient equilibria constants to be used in the kinetic model.

The Gepasi Version 3.30 software system was used to model the chemical kinetics for all reagents. The overall and individual rate constants k_i were obtained by adjusting experimental Fe(II) concentrations/time pairs of data to the model output as indicated elsewhere (Mendes 1997). In accordance with the experimental data obtained in this article, the kinetic model (Santana-Casiano et al. 2006) was

broadened to include both Fe(II)-phosphate and Fe(II)-silicate species and it was applied as a function of pH and temperature for both seawater and seawater enriched with nutrients (SWEN), considering all dissociation and equilibrium constants for the reaction of Fe(II) species with the major inorganic species in seawater under different experimental conditions (Table 2.1).

Table 2.1 New stability constants of complexes considered for the kinetic model developed by Gonzalez-Dávila et al. (2006) and Santana-Casiano et al. (2005), at different temperatures.

REACTIONS	I = 0.7 M				*Ref.*
	35 ºC	**25 ºC**	**15 ºC**	**5 ºC**	
$H_2SiO_4^{2-} + 2H^+ \leftrightarrow Si(OH)_4$	21.66	22.29	23.12	24.00	*3*
$H_2SiO_4^{2-} + H^+ \leftrightarrow Si(OH)_3O^-$	12.26	12.72	13.28	13.9	*3*
$Fe^{3+} + H_2SiO_4^{2-} + H^+ \leftrightarrow FeSi(OH)_3O^{2+}$	21.66	21.66	21.66	21.66	*4*
$Fe^{2+} + H_2SiO_4^{2-} + H^+ \leftrightarrow FeSi(OH)_3O^+$	**14.38**	**14.26**	**14.11**	**13.96**	***This study***
$Ca^{2+} + H_2SiO_4^{2-} + H^+ \leftrightarrow CaSi(OH)_3O^+$	13.18	13.18	13.18	13.18	*4*
$Mg^{2+} + H_2SiO_4^{2-} + H^+ \leftrightarrow MgSi(OH)_3O^+$	13.48	13.48	13.48	13.48	*4*
$PO_4^{3-} + H^+ \leftrightarrow HPO_4^{2-}$	11.52	11.63	11.80	11.96	*3*
$PO_4^{3-} + 2H^+ \leftrightarrow H_2PO_4^-$	18.33	18.37	18.45	18.59	*3*
$PO_4^{3-} + 3H^+ \leftrightarrow H_3PO_4$	20.73	20.28	19.88	19.51	*3*
$Fe^{3+} + PO_4^{3-} + H^+ \leftrightarrow FeHPO_4^+$	22.29	22.29	22.29	22.29	*3*
$Fe^{2+} + PO_4^{3-} \leftrightarrow FePO_4^-$	5.76	5.76	5.76	5.76	*5*
$Fe^{2+} + PO_4^{3-} + H^+ \leftrightarrow FeHPO_4$	13.75	13.75	13.75	13.75	*5*
$Fe^{2+} + PO_4^{3-} + 2H^+ \leftrightarrow FeH_2PO_4$	19.58	19.58	19.58	19.58	*5*
$Ca^{2+} + PO_4^{3-} \leftrightarrow CaPO_4^-$	6.46	6.46	6.46	6.46	*6*
$Ca^{2+} + PO_4^{3-} + H^+ \leftrightarrow CaHPO_4$	15.03	15.03	15.03	15.03	*3*
$Ca^{2+} + PO_4^{3-} + 2H^+ \leftrightarrow CaH_2PO_4$	20.92	20.92	20.92	20.92	*3*
$Mg^{2+} + PO_4^{3-} \leftrightarrow MgPO_4^-$	4.85	4.85	4.85	4.85	*6*
$Mg^{2+} + PO_4^{3-} + H^+ \leftrightarrow MgHPO_4$	15.17	15.17	15.17	15.17	*3*
$Mg^{2+} + PO_4^{3-} + 2H^+ \leftrightarrow MgH_2PO_4$	19.19	19.19	19.19	19.19	*3*

[3]Verweij, 2013; [4]Smith and Martell, 1991; [5]Mao et al. 2011; [6]Turner, 1981

The package Seacarb (Lavigne et al. 2011) was used to corroborate, together with the model, the theoretical silicate and phosphate concentrations under the different experimental conditions. R (R Development Core Team, 2008) was used for statistical computing and graphics.

2.3 Results and discussions

The rates of oxidation of Fe(II) with O_2 have been expressed as an apparent oxidation rate (k_{app}), independent of the mechanism describing the process.

$$d[Fe(II)]/dt = - k_{app} [Fe(II)] [O_2] \quad (18)$$

where k_{app} (M^{-1} min^{-1}) is a second-order rate for oxidation by O_2. When the studies are performed with excess O_2, the reaction becomes a pseudo-first order reaction (Millero et al. 1987).

$$d[Fe(II)]/dt = - k' [Fe(II)] \quad (19)$$

where $k' = k_{app} [O_2]$

In a first series of measurements, the Fe(II) oxidation rate constants in Artificial Seawater (ASW, S = 35.5) and UV-treated Seawater (SW) were determined. The observed differences were slight (Fig 2.1) ($\Delta \log k_{app} \leq 0.02$ M^{-1} min^{-1}) and could be explained as a result of the differences in the salinities between solutions and the presence of reactive oxygen species (ROSs) produced under the seawater treatment for removing organic matter with UV irradiation. However, we stored the UV-treated seawater in the dark (> 1 month), in order to minimize the influence of most of those ROSs (Garg et al. 2011).

When the Fe(II) oxidation rates were obtained within the first half-life ($t_{1/2}$) these always followed pseudo-first order behavior (with a correlation coefficient over 0.98), under the experimental conditions used in the present work. Beyond the first half-life time, the oxidation process was slowed, probably because of reduction Fe(III) with O_2^- and scavenging of O_2^- by reactive species (Voelker and Sedlak 1995). Some studies, with SWEN and SW, were carried out in the dark in order to ensure that the photochemical production of Fe(II) did not occur under different experimental conditions. The oxidation rates in the dark were within the same experimental error as those carried out in the light (Fig 2.1), confirming that the rate of photo-reduction of inorganic Fe(III) species was very slow above a pH of 7 (King et al. 1995; Miller et al. 1995)

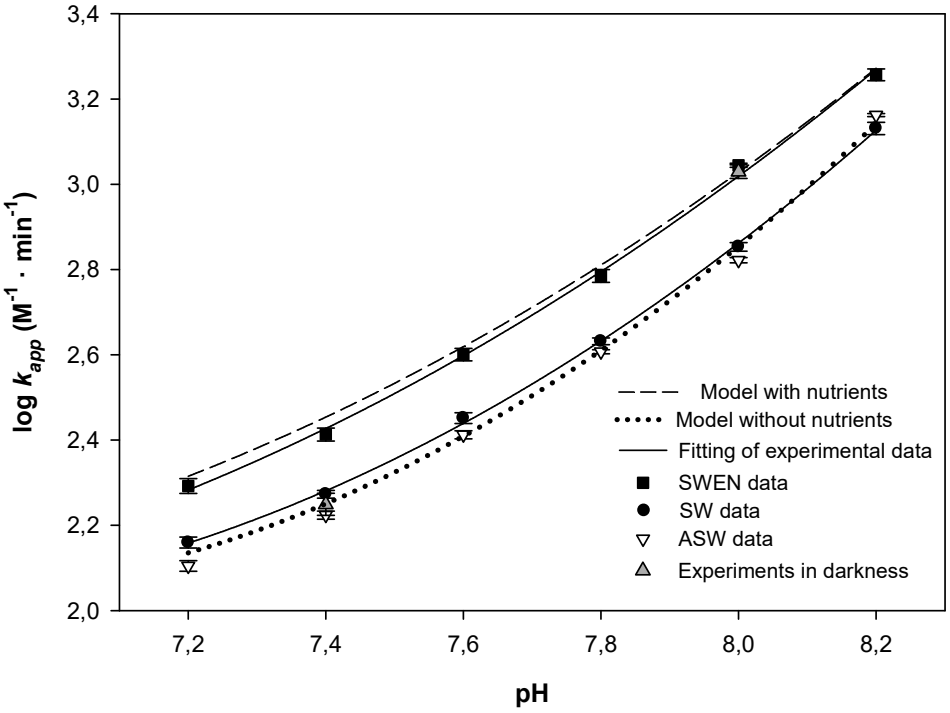

Fig 2.1 Polynomial fitting of log k_{app} (M^{-1} min^{-1}) data (solid lines) and model predictions (dashed lines), in seawater (S ‰ = 37.09) with absence and presence of nutrients -Nitrate (850 μM), Phosphate (25 μM) and Silicate (140 μM)- and artificial seawater (S ‰ = 35.5) over pH range 7.2 – 8.2 at 25 ºC. $[Fe(II)]_0$ = 25 nM. Symbols represent the mean and the bars are the standard error of the mean from triplicate experiments.

2.3.1 Effect of pH

The Fe(II) oxidation rates as a function of pH, for each temperature, were studied in the range 7.2-8.2 in SW and SWEN (Table 2.2). The results were fitted to second-order polynomial equations for all cases (Table 2.3). The oxidation rates in SWEN were always higher than in SW. The highest values in the apparent oxidation constants, were at pH = 8.2 (log $k_{app,SWEN}$ = 3.84 ± 0.01 M^{-1} min^{-1} and log $k_{app,SW}$ = 3.71 ± 0.01 M^{-1} min^{-1} at 35 ºC), while the minimum oxidation rates (log $k_{app,SWEN}$ = 1.26 ± 0.01 M^{-1} min^{-1} and log $k_{app,SW}$ = 1.32 ± 0.01 M^{-1} min^{-1}, at 5 ºC and pH =7.4, and 15 ºC and pH = 7.2, respectively) were given at the lower values of pH of the study (Table 2.2).

Table 2.2 Log k_{app} and half-life times ($t_{1/2}$) for Fe(II) oxidation in SW and SWEN -Nitrate (850 µM), Phosphate (25 µM) and Silicate (140 µM)- at different pH and temperatures (S‰ = 37.09).

T[a] (°C)	pH	SW			SWEN		
		log k_{app} (M^{-1} min^{-1})	Standard Error	$t_{1/2}$ (min)	log k_{app} (M^{-1} min^{-1})	Standard Error	$t_{1/2}$ (min)
35	**8.2**	3.71	0.01	0.7	3.84	0.01	0.5
	8.0	3.43	0.02	1.4	3.61	0.01	0.9
	7.8	3.21	0.02	2.4	3.42	0.01	1.5
	7.6	2.99	0.01	3.9	3.23	0.01	2.3
	7.4	2.85	0.01	5.4	3.08	0.01	3.2
	7.2	2.75	0.01	6.8	2.95	0.02	4.3
25	**8.2**	3.13	0.01	2.4	3.26	0.01	1.8
	8.0	2.85	0.01	4.6	3.03	0.01	3.1
	7.8	2.63	0.01	7.6	2.78	0.02	5.4
	7.6	2.45	0.01	11.6	2.6	0.01	8.2
	7.4	2.27	0.01	17.4	2.41	0.02	12.6
	7.2	2.16	0.01	22.6	2.29	0.02	16.7
15	**8.2**	2.53	0.02	8.1	2.6	0.02	6.8
	8.0	2.3	0.01	13.8	2.41	0.02	10.6
	7.8	2.08	0.03	22.8	2.2	0.01	17.4
	7.6	1.88	0.02	36.4	2.03	0.01	25.8
	7.4	1.73	0.01	50.5	1.88	0.01	36.5
	7.2	1.65	0.01	61.5	1.76	0.02	47.8
5	**8.2**	2.02	0.01	21.2	2.11	0.01	17.3
	8.0	1.79	0.01	35.9	1.91	0.01	27.0
	7.8	1.6	0.02	55.9	1.71	0.01	43.0
	7.6	1.39	0.03	89.6	1.49	0.01	71.0
	7.4	1.26	0.01	120.9	1.32	0.02	104.5

Table 2.3 pH-dependence of Fe(II) oxidation rate (log k_{app}, M^{-1} min^{-1}) in SW and SWEN (Nitrate (850µM), Phosphate (25 µM) and Silicate (140 µM) at different temperatures.

Media	T[a] (ºC)	Log k_{app} (M^{-1} min^{-1})[a]	r^2	± Standard Error
SW	35	27.25 (± 2.66) – 7.24 (± 0.69) pH + 0.53 (± 0.04) pH^2	0.999	0.01
	25	23.83 (± 2.50) – 6.86 (± 0.65) pH + 0.44 (± 0.04) pH^2	0.999	0.01
	15	22.26 (± 3.79) – 6.16 (± 0.99) pH + 0.46 (± 0.06) pH^2	0.998	0.02
	5[b]	13.85 (± 6.80) – 4.11 (± 1.73) pH + 0.32 (± 0.11) pH^2	0.997	0.02
SWEN	35	15.09 (± 1.05) – 3.96 (± 0.27) pH + 0.31 (± 0.02) pH^2	0.999	0.01
	25	14.08 (± 4.87) – 3.93 (± 0.92) pH + 0.32 (± 0.06) pH^2	0.998	0.01
	15	12.10 (± 3.07) – 3.45 (± 0.80) pH + 0.28 (± 0.05) pH^2	0.998	0.01
	5[b]	2.24 (± 5.62) – 1.47 (± 1.05) pH + 0.15 (± 0.09) pH^2	0.998	0.01

[a] pH range 7.2-8.2. [b] pH range 7.4-8.2

At each temperature, the difference between SWEN and SW was constant over the pH range studied, therefore the nutrient effect can be considered dominant over the entire pH range. Nevertheless the difference between SWEN and SW was not constant over the whole temperature range (Fig 2.2). One common feature of all the conditions of this study, was that the nutrient effect on the Fe(II) oxidation rate became more pronounced as temperature increased. The Δlog k_{app} increased accordingly to 5 ºC (Δlog k_{app} = 0.09 ± 0.01) < 15 ºC (Δlog k_{app} = 0.12 ± 0.01) < 25 ºC (Δlog k_{app} = 0.15 ± 0.01) < 35 ºC (Δlog k_{app} = 0.20 ± 0.02). This variation of Δlog k_{app} with temperature can be linked to the presence of nutrient reactive species, $H_3SiO_4^-$, $H_2PO_4^-$ HPO_4^{2-} and PO_4^{3-}.

In addition the log $k_{app,SW}$, at pH = 8.0 and 25 ºC (2.85 M^{-1} min^{-1}), was compared with other studies. Gulf Stream waters (log k_{app} = 3.06 M^{-1} min^{-1} (Santana--Casiano et al. 2005), Pacific Subarctic waters (log k_{app} = 2.66 M^{-1} min^{-1} (Roy et al. 2008) and Gran Canaria off-shore waters (log k_{app} = 2.77 M^{-1} min^{-1}(González et al. 2010) offered similar values to those obtained in this study. The slight variations in the Fe(II) oxidation rate constants are related to the different organic matter content of the seawater samples (Millero 2006).

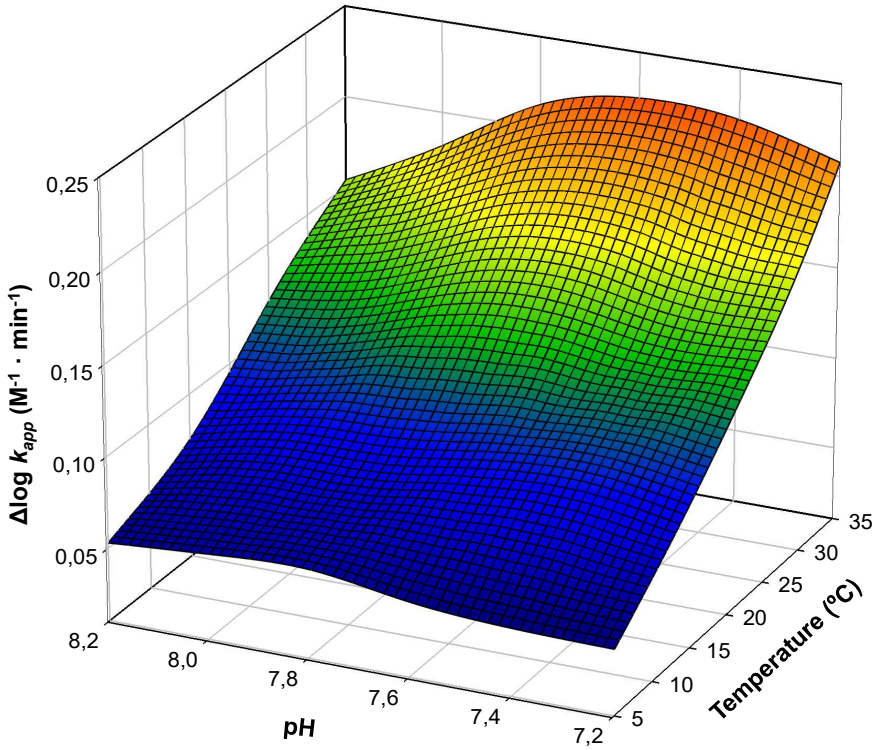

Fig 2.2 Maximum increase for Fe(II) oxidation rate constant in seawater ($\Delta\log k_{app} = \log k_{app\text{-}SWEN} - \log k_{app\text{-}SW}$) by nutrient presence (Nitrate, Phosphate and Silicate) at different pH and temperatures. Salinity = 37.09.

The half-life was reduced 1 order of magnitude (Table 2.2) over the whole pH range, both in SW and SWEN. For example at 25 ºC, the $t_{1/2}$ decreased from 16.7 min (pH = 7.2) to 1.8 min (pH = 8.2) in SWEN and from 22.6 min (pH = 7.2) to 2.4 min (pH = 8.2) in SW. A pH decrease in natural waters should, therefore, increase the concentration of dissolved inorganic Fe(II). Breitbarth et al. (2010), using a CO_2 mesocosm experiment, showed changes in Fe(II) oxidation rates that agree with the results of this study. The authors considered that, the acidification experiments had influence on inorganic Fe(II) speciation, and so that the low pH treatments slowed down the oxidation process of Fe(II) significantly. In addition, they also suggested that the organic iron chelation might affect the Fe(II) half-life in the low pH treatments, either because the Fe(III) organic complexes were the major pool of Fe(II) by photoreduction of Fe(III), or retarding the Fe(II) oxidation rate due to the direct effect of the biologically mediated Fe-ligands. Likewise, ocean acidification might affect the redox kinetics of Fe(II), yielding a change in the fraction of Fe that could be highly bioavailable (Shaked et al. 2005; Hoffmann et al. 2012).

Nevertheless, the ongoing acidification of seawater also might increase the Fe stress in some phytoplankton species (i.e. coccolithophores and diatoms) and one such effect could produce a decrease in the Fe-bioavailability (Shi et al. 2010).

2.3.2 Effect of temperature

The strong temperature dependence on the Fe(II) oxidation process was tested, since the nutrient effect on reaction rates is not only important because climate change leads to upper ocean warming, but also because the latitudinal temperature range found in the coastal waters is wide. Table 2.2 shows that the oxidation rates decreased when the temperature was reduced from 35 to 5 ºC, both in the presence and in the absence of nutrients. The pseudo-first order oxidation rate was a linear function of 1/T ($^{o}K^{-1}$) over the entire temperature range (Table 2.4). The slopes, which might be considered as coefficients of thermal dependency, were lower when the nutrients were not present in the solution, decreasing when the pH decreased. Nevertheless, in seawater enriched with nutrients, the slopes were constant over the pH range studied. Therefore, the presence of nutrients dominated the oxidation process, over the pH range studied. The temperature influence on the speciation of phosphoric and silicilic acids were studied in SWEN by applying the Seacarb program (Lavigne et al. 2011) and showing the correlation between the temperature and the presence of reactive nutrient species. Therefore, in SWEN at high temperatures, a greater presence of these reactive nutrient species seems to intensify the oxidative process.

The half-life time of Fe(II) decreased with the increase in temperature for each pH treatment (Table 2.2). Therefore the high temperatures increased the Fe(II) reactivity both in SW and SWEN. An increase in the superficial seawater temperature, as a result of ocean warming, would decrease the Fe(II) concentrations in many oceanic regions due to higher oxidation rates. This decline would probably be more pronounced in coastal areas, due to a higher concentration of nutrients, as observed recently in the Red Sea (Shaked 2008).

Table 2.4 Temperature dependence of log k_{app} (M^{-1} min^{-1}) in SW and SWEN -Nitrate (850 µM), Phosphate (25 µM) and Silicate (140 µM)- under different pH conditions (Salinity = 37.09). E_a is the Energy of Activation (kJ mol^{-1}). ± SE denotes the standard error of the esteem.

Media	pH	Log k_{app} (M^{-1} min^{-1})	r^2	± SE	E_a ± SE (KJ mol^{-1})
SW	8.2	19.45 (± 0.73) - 4858 (± 213) / T	0.996	0.06	92.98 ± 4.09
	8	18.63 (± 0.68) - 4692 (± 198) / T	0.996	0.05	89.83 ± 3.80
	7.8	18.14 (± 0.80) - 4614 (± 235) / T	0.995	0.06	88.39 ± 4.46
	7.6	17.96 (± 0.64) - 4607 (± 186) / T	0.997	0.05	88.13 ± 3.65
	7.4	17.52 (± 0.79) - 4534 (± 230) / T	0.995	0.06	86.67 ± 4.47
	7.2	17.31 (± 0.82) - 4501 (± 241) / T	0.994	0.06	86.17 ± 4.61
SWEN	8.2	20.12 (± 0.93) - 5022 (± 272) / T	0.994	0.07	96.13 ± 5.21
	8	19.48 (± 0.82) - 4896 (± 239) / T	0.996	0.06	93.99 ± 4.48
	7.8	19.20 (± 1.04) - 4878 (± 304) / T	0.992	0.08	93.37 ± 5.82
	7.6	19.14 (± 0.82) - 4948 (± 240) / T	0.996	0.06	94.68 ±4.53
	7.4	19.11 (± 0.93) - 4955 (± 271) / T	0.994	0.07	94.84 ± 5.19
	7.2	18.88 (± 0.92) - 4922 (± 270) / T	0.994	0.07	94.23 ± 5.17

The minimum energy required to carry of the chemical oxidation process, which is defined as energy of activation (E_a) by the Arrhenius equation (Arrhenius 1889), was similar over all the ranges of pH (Table 2.4). At pH = 8.0, the E_a was 89.83 ± 3.80 KJ mol^{-1} and 93.99 ± 4.48 KJ mol^{-1} in SW and SWEN respectively The results were close to those obtained in other studies with Gulf Stream waters (Santana-Casiano et al. 2005), sub-Artic Pacific seawaters (Roy et al. 2008) and Gran Canaria off-shore waters (González et al. 2010). Despite this fact, a slight increase of E_a, was observed together with a more intense oxidative process. The E_a increased from 86.17 ± 4.61 KJ mol^{-1} (pH = 7.2) to 92.98 ± 4.09 KJ mol^{-1} (pH = 8.2) in SW, whereas in SWEN, the energy of activation remained constant (94.54 ± 0.94 KJ mol^{-1}), indicating that the presence of nutrients contributed steadily to the Fe(II) oxidation rate over the pH range studied. Therefore, these results indicate that the chemical and physical conditions of the media, such as nutrient content and pH, affected the speciation and controlled the E_a that is required to carry out the Fe(II) oxidation process.

2.3.3 Effect of salinity

The effect of salinity on the Fe(II) oxidation rate, for the samples, was carried out by dilution with Milli-Q water, keeping the nutrient concentrations constant in the solutions. The range of salinity studied was from 10 to 37.1 with pH (8.0) and temperature (25 ºC) constants. The amount of HCO_3^- was corrected after dilutions (Santana-Casiano et al. 2005) and fitted to 2.05 mM. The Fe(II) oxidation process was swifter for SWEN over the whole range salinity range (Table 2.5).

Table 2.5 Log k_{app} and half-life times ($t_{1/2}$) for Fe(II) oxidation in SW and SWEN (Nitrate (850 µM), Phosphate (25 µM) and Silicate (140 µM) at different salinities (pH = 8.0; T^a = 25 ºC).

Salinity	SW			SWEN		
	log k_{app} (M^{-1} min^{-1})	Standard Error	$t_{1/2}$ (min)	log k_{app} (M^{-1} min^{-1})	Standard Error	$t_{1/2}$ (min)
30	2.90	0.02	3.9	3.11	0.02	2.4
20	3.02	0.03	3.0	3.22	0.01	1.8
10	3.16	0.02	1.9	3.38	0.01	1.2

The dependence of experimental results was fitted to quadratic equations, respectively (eqs 20-21), where S is salinity. r^2 was 0.998 and 0.993 respectively; the standard error of estimation for both equations was 0.01. The difference in log k_{app} for both media remained constant at 0.20 ± 0.01 M^{-1} min^{-1}

$$\text{Log } k_{app\text{-}SW} = 3.36 - 0.02\ S - 2\cdot10^{-4}\ S^2 \quad (20)$$

$$\text{Log } k_{app\text{-}SWEN} = 3.54 - 0.02\ S - 1\cdot10^{-4}\ S^2 \quad (21)$$

. The apparent rate constant (M^{-1} min^{-1}) can be fitted under experimental conditions of pH (free scale), temperature ($ºK^{-1}$) and salinity, in SW (eq 22) and SWEN media (eq 23),

$$\text{Log } k_{app\text{-}SW} = 38.87 - 6.19\ pH - 0.46\ pH^2 - 4633.28\ T^{-1} - 0.02\ S - 3\cdot10^{-4}\ S^2 \quad (22)$$

$$\text{Log } k_{app\text{-}SWEN} = 29.97 - 3.55\ pH - 0.29\ pH^2 - 4938.96\ T^{-1} - 0.02\ S - 1\cdot10^{-4}\ S^2 \quad (23)$$

The standard error of estimation was 0.05 and 0.06. The r^2 was 0.995 and 0.994 for SW and SWEN respectively. These equations can be used and applied in the environment, under the experimental conditions used.

2.3.4 The kinetic modelling approach

In line with previous experimental results, we have considered that the Fe(II) oxidation process in seawater enriched with nutrients (SWEN) is controlled by both silicate and phosphate effects (González et al. 2010; Mao et al. 2011). In seawater at pH = 8.2, both HPO_4^{2-} as PO_4^{3-} (79.2% and 20.4% respectively) and $Si(OH)_4$ as $H_3SiO_4^-$ (95.6% and 4.3% for each species) are the predominant forms of phosphate and silicate (Millero 2006; Paytan and McLaughlin 2007).

The oxidation of Fe(II) with oxygen (eq 1) is a process with a series of parallel reactions where the individual Fe(II) species react at different rates. The oxidation kinetics of Fe(II) with O_2 can be expressed as a function of the apparent oxidation rate (k_{app}), in terms of the weighted sum of oxidation rates of individual Fe(II) species (Santana-Casiano et al. 2005).

$$k_{app} = k_{Fe^{2+}}\alpha_{Fe^{2+}} + k_{FeOH^+}\alpha_{FeOH^+} + k_{Fe(OH)_2}\alpha_{Fe(OH)_2} + k_{FeHCO_3^+}\alpha_{FeHCO_3^+} + k_{FeCO_3}\alpha_{FeCO_3} + k_{Fe(CO_3)_2}\alpha_{Fe(CO_3)_2} + k_{Fe(CO_3)OH^-}\alpha_{Fe(CO_3)OH^-} + k_{FeCl^+}\alpha_{FeCl^+} + k_{FeSO_4}\alpha_{FeSO_4} + \boldsymbol{k_{FeH_3SiO_4^+}\alpha_{FeH_3SiO_4^+}} + k_{FePO_4^-}\alpha_{FePO_4^-} + k_{FeHPO_4}\alpha_{FeHPO_4} + k_{FeH_2PO_4^+}\alpha_{FeH_2PO_4^+} \quad (24)$$

The brackets denote the total molar concentration, $\alpha_i = [FeX_i] / [Fe(II)]_T$ is the molar fraction of each Fe(II) species in the solution, and k_i are the individual rate constant for the Fe(II) species.

In order to determine the individual rate constants and distribution of the nutrient-Fe(II) species over the range of experimental conditions, the kinetic model defined in this study is based on all pertinent dissociations, complex formations, ion-pair formation and oxidation constants, for all the inorganic species involved in the oxidation process for seawater, to which reference is made in the model of Santana-Casiano et al. (2006). We have included the contribution of other authors as further validation of the consistency of the results of this study (King et al. 1995; Voelker

and Sedlak 1995; King 1998; King and Farlow 2000; Rose and Waite 2002). The model also have been extended with the oxidation rates of the Fe(II)-phosphate species (Mao et al. 2011). Due to the role played by H_2O_2 and O_2^- in the chemistry of iron, the individual oxidation rates for the oxidation of Fe(II) with hydrogen peroxide and superoxide in seawater are also considered in the model (González-Davila et al. 2005; Santana-Casiano et al. 2005). The effect of temperature on the hydrolysis constants, and carbonate stability constants with Fe(II) and major ions were obtained following González-Davila et al. (2005). The thermodynamic effect on the PO_4^{3-} and $H_2SiO_4^{2-}$ protonation constants and phosphate and silicate ion-pair constants with Fe(II) and/or with major ions are given from elsewhere references (Table 2.1), whereas the corresponding enthalpies of processes are considered constant over the temperature range studied.

The individual oxidation rates by oxygen, of the Fe(II) most kinetically active species (Fe^{2+}, $FeOH^+$, $Fe(OH)_2$, $FeCO_3(OH)^-$, $FeCO_3$, $Fe(CO_3)_2^{2-}$, $FeH_3SiO_3^+$, $FePO_4^-$) were reckoned, over the range of temperature studied, using the kinetic model. The individual Fe(II) oxidation rates constants included in this study are presented in Table 2.6.

Table 2.6 Individual Fe(II) oxidation rates* (log k_i, M^{-1} min^{-1}) with oxygen in seawater and seawater enriched with nutrients (Nitrate, Phosphate and Silicate) at different temperatures, obtained from kinetic model and valid for pH range 7 to 8.5.

Species	35 ºC	25 ºC	15 ºC	5 ºC
Fe^{2+}	1.15	0.53	-0.10	-0.60
$FeCO_3$	1.30	0.64	0.04	-0.52
$Fe(CO_3)_2^{2-}$	4.24	3.60	2.94	2.24
$Fe(CO_3)(OH)^-$	1.95	1.85	1.74	1.63
$FeOH^+$	2.49	2.30	2.10	1.95
$Fe(OH)_2$	6.10	5.90	5.68	5.46
$FeH_3SiO_4^+$	4.83	4.79	4.74	4.70
$FePO_4^-$	2.80	2.75	2.71	2.67

* **The $FeCl^+$, $FeSO_4$, $FeHPO_4$ and $FeH_2PO_4^+$ species are considerate inactive in all cases (Santana-Casiano et al. 2005; Mao et al. 2011).**

As well as the ion-pair formation constant, for the specie $FeH_3SiO_4^+$ was estimated, considering that divalent cations such as Ca^{2+}, Mg^{2+} and Fe^{2+} reveal a similar tendency to form inorganic complexes with ligands with tetrahedral structures (Millero 2006). In order to get the values for all individual rate constants for the oxidation of Fe(II), the kinetic model was applied to the experimental results at different pH and temperatures. The application of this methodology, as it is shown in Figure 2.3 the model outputs, for log k_{app} (M^{-1} min^{-1}) versus pH, are consistent with experimental polynomial fitting over the whole range of conditions studied.

To gain insight into the role played by the nutrients, the inorganic Fe(II) speciation in seawater and seawater enriched with nutrients at different temperatures was modeled (Fig 2.4). In SW the speciation of Fe(II) is dominated by Fe^{2+}, $FeCO_3$, $FeCl^+$, $FeSO_4$ and $Fe(CO_3)(OH)^-$, over the whole temperature range. In SWEN, considering silicate and phosphate concentrations as reference values for coastal systems with high nutrient levels (Newton and Mudge 2005; Santos et al. 2008; Maier et al. 2009; Guenther et al. 2015), the Fe(II) species followed a similar distribution. Both in SW and SWEN, the Fe^{2+} is the dominant species from pH 7 (57%-62% between 35 ºC and 5 ºC) to 8.2 (36-40% between 35 ºC and 5ºC), while the concentration of $FeCO_3$ increases drastically with increasing pH to dominate the speciation between pH 8.2 and pH 8.5 (43-44% in all temperature range). The results of the model have shown that the temperature is not a factor to modify significantly the inorganic speciation of dominant Fe(II) species at equilibrium, either in SW or in SWEN (Fig 2.4).

In seawater enriched with nutrients, the mole fraction of Fe(II)-nutrient species ($FeH_3SiO_4^+$, $FePO_4^-$, $FeHPO_4$ $FeH_2PO_4^+$) was minor, under the different experimental conditions, compared to species that dominated the speciation of inorganic Fe(II) in seawater (Fig 2.5). The presence of nutrients was insignificant for the speciation of Fe^{2+}, $FeCO_3$, $FeCl^+$ or $FeSO_4$. The model shows that, the concentration of $FeH_3SiO_4^+$ and $FePO_4^-$ increased as pH increased, whereas the levels of $FeHPO_4$ and $FeH_2PO_4^+$ were reduced with an increase in pH range studied; meanwhile $FeH_3SiO_4^+$ experienced a severe increase in orders of magnitude in concentration, from 5 ºC (< 0.001%) to 35 ºC (0.5%).

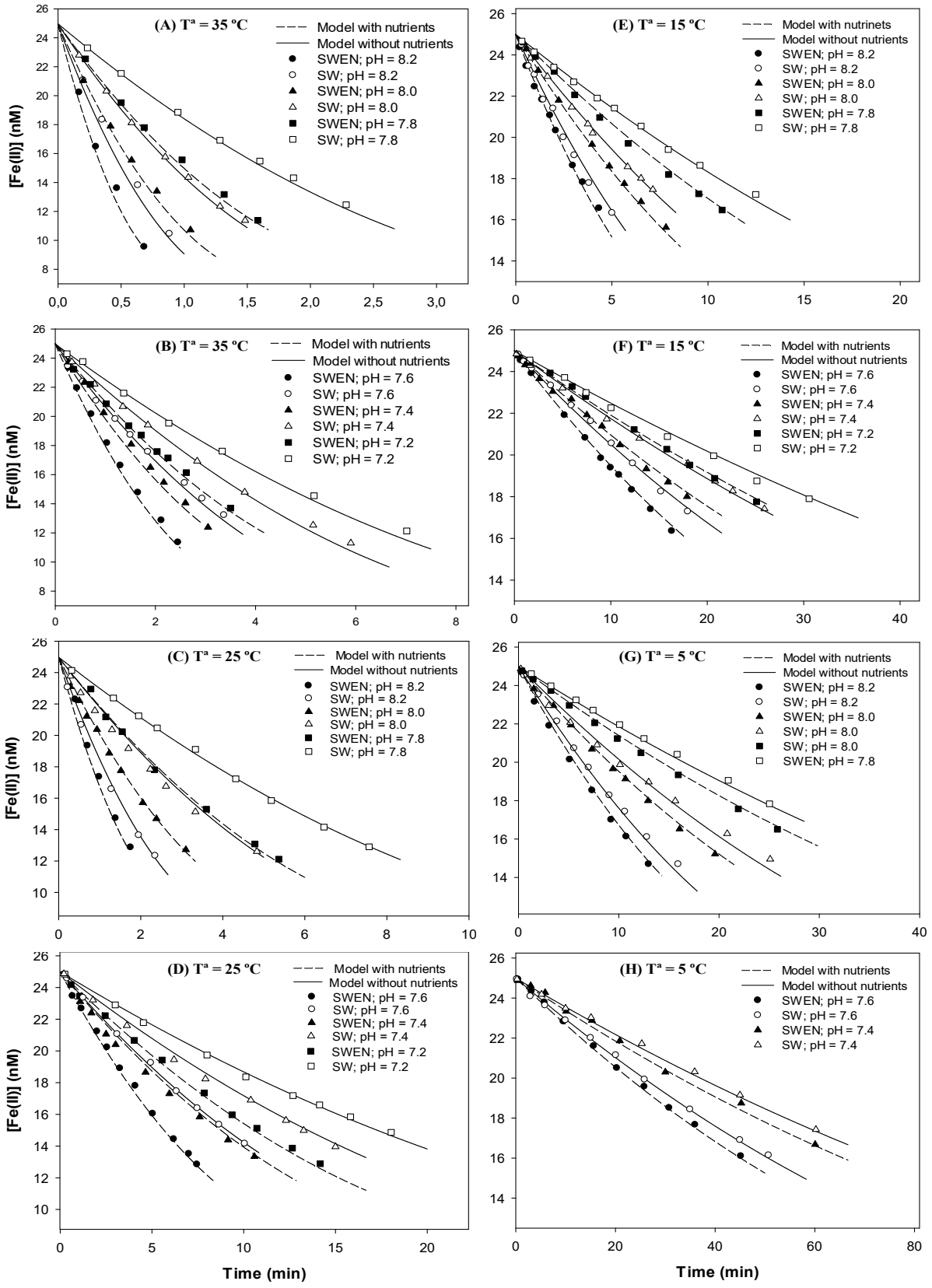

Fig 2.3 Experimental data (symbols) and modeled (lines) Fe(II) concentrations as a function of time in SW and SWEN at different pH and temperatures.

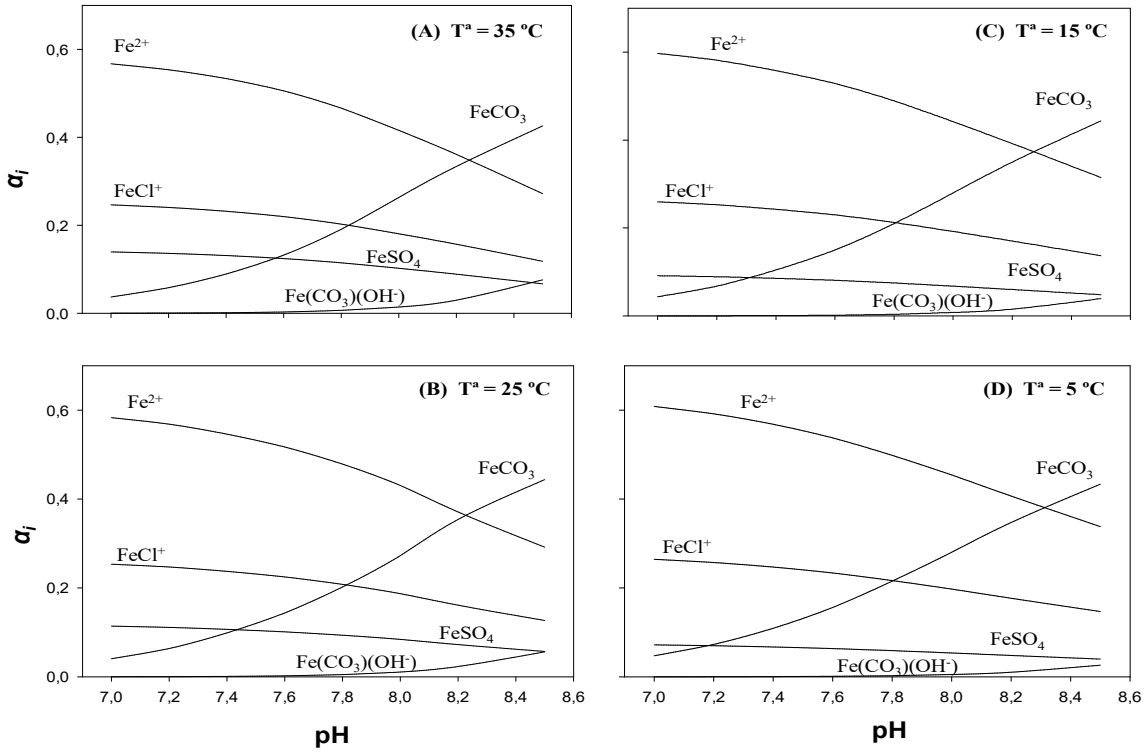

Fig 2.4. Speciation of dominant Fe(II) species in SW and SWEN at different temperature.

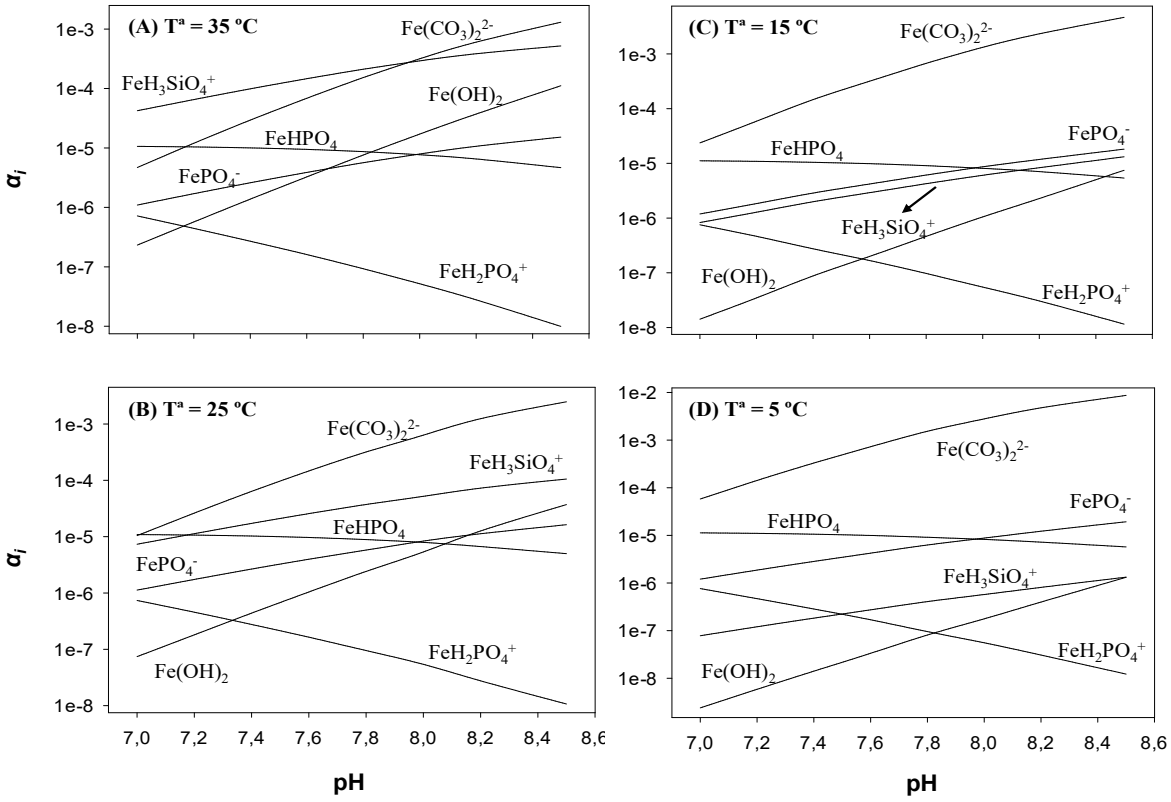

Fig. 2.5 Speciation of minor Fe(II) species in SWEN at different temperatures

In coastal systems, where silicate and phosphate can be found at high concentrations ([$Si(OH)_4$] > 120 μM and [H_3PO_4] > 15 μM), $FeH_3SiO_4^+$ should be considered the most important Fe(II)-nutrient species when the temperature is over 25 ºC, while Fe-phosphate species should control the Fe(II)-nutrient speciation when the temperatures are below 25 ºC.

The contribution of individual species to the overall Fe(II) oxidation rate was computed from the results of the kinetic model (Table 2.6) and the speciation of Fe(II). The results were strongly influenced by pH, temperature and presence of nutrients. In absence of nutrients (Fig 2.6) and at all the temperatures studied, second-order dependence with pH was determined, which was consistent with previous reported data (Santana-Casiano et al. 2005). When the temperature was ≥ 25 ºC, the second hydrolysis product of Fe(II), $Fe(OH)_2$, was the species that dominated the Fe(II) oxidation process, while the contribution in the k_{app} was controlled by $Fe(CO_3)_2^{2-}$ when the temperature was ≤ 15 ºC. In contrast, when nutrients were present in the solution (Fig 2.7), $FeH_3SiO_4^+$ became the most contributor to the overall rate between pH 7.4 and 8.0 at 35 ºC (over 35%) and between 7.6 and 7.8 at 25 ºC (over 20%). However, $FePO_4^-$ is presented as the most reactive iron phosphate species, although its impact on the oxidation rate is less than 1%. This contribution to the overall Fe(II) oxidation rate of Fe-phosphate species is significantly lower compared to previous studies carried out in NaCl solutions (0.1M) (Mao et al. 2011). At circum-neutral pH, when the phosphates were present in solution at milimolar levels, Mao et al. (2011) showed $FePO_4^-$ to be the major Fe(II) species contributing to the overall rate of Fe(II) oxygenation. Nevertheless, our model evaluates the role of phosphates at micromolar concentrations, which covers levels common in phytoplankton cultures, coastal groundwater or eutrophication coastal processes (Guillard 1975; Cloern 2001; Kucuksezgin et al. 2006; Maier et al. 2009; Guenther et al. 2015). In addition, our model includes interactions of the phosphate species with other major ions present in seawater, such as Ca^{2+} and Mg^{2+}, besides taking into account the silicate interaction with Fe(II). These differences may explain the variations as observed in the Fe-phosphate contributions to the overall Fe(II) oxidation rate.

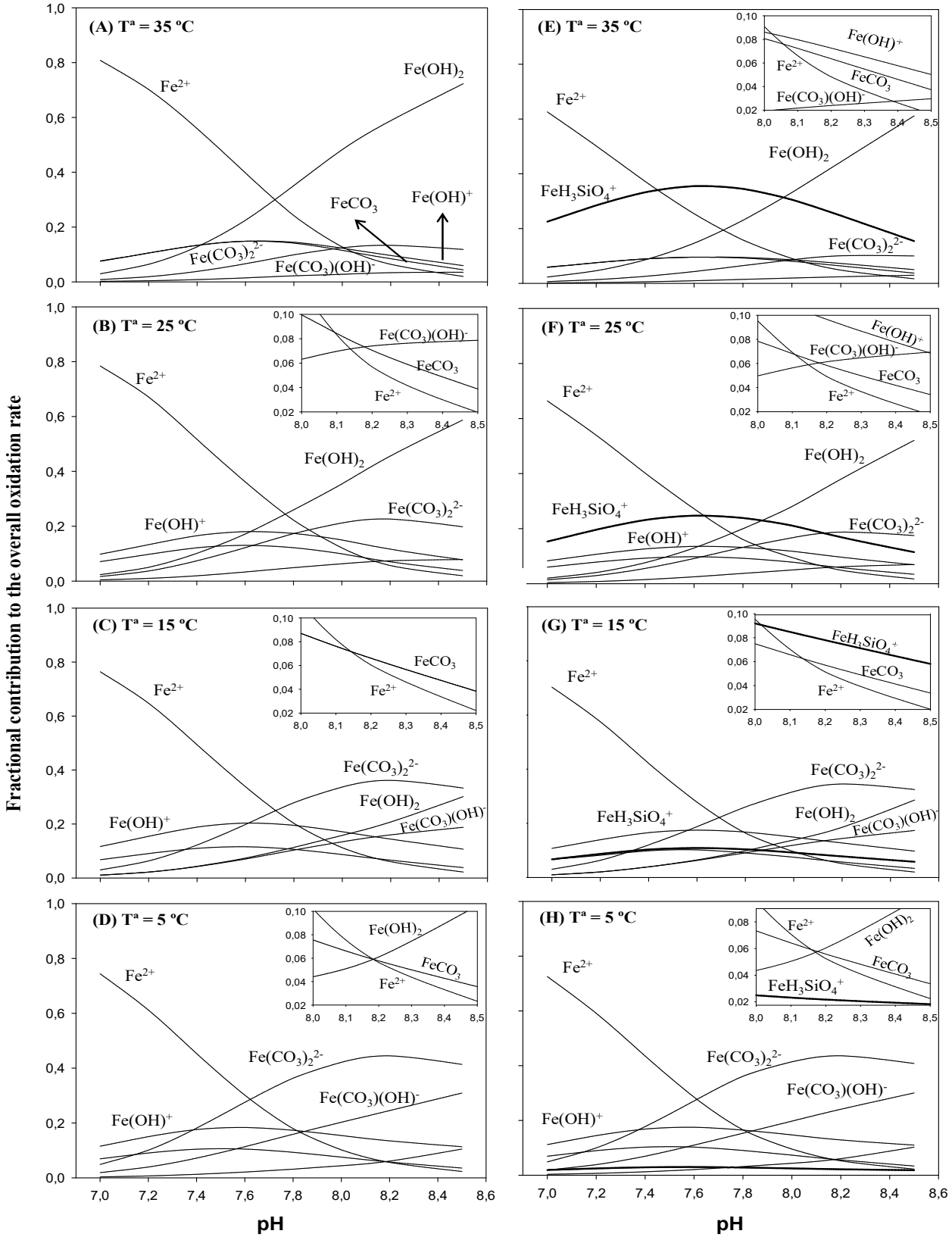

Fig. 2.6 Contribution of each individual species on the overall rate constant for Fe(II) oxidation, in SW (A, B, C, D) and SWEN (E, F, G, H), at different temperatures.

The effects of temperature on the individual rate constant (ln k_i) for the most kinetically reactive species in SW and SWEN have been determined as an inverse function of temperature (Table 2.7 and Fig 2.7). The E_a ranged from 6.90 ± 0.35 KJ mol^{-1} to 109.16 ± 0.99 KJ mol^{-1}, respectively for $FePO_4^-$ and $Fe(CO_3)_2^{2-}$, and therefore, were similar to the results computed for González-Dávila et al. (2005) in the oxidation of Fe(II) by H_2O_2. Enthalpies obtained by the activated complex theory (Eyring 1935), followed a similar pattern to those for the E_a.

Table 2.7 The effect of temperature on the individual oxidation rate constant and thermodynamic parameters (E_a and ΔH^o) computed for Fe(II) species in SW and SWEN. Temperature range: 5-35 ºC. Salinity 37.09. ±SE denotes the standard error of the estimate.

Species	Ln k_i (M^{-1} min^{-1})	r^2	± SE	E_a ± SE (KJ mol^{-1})	ΔH^o ± SE (KJ mol^{-1})
Fe^{2+}	40.02 (± 2.16) – 11545 (± 632) 1/T	0.994	0.17	95.98 ± 5.25	94.56 ± 5.34
$FeCO_3$	41.67 (± 1.92) – 11946 (± 562) 1/T	0.996	0.15	99.32 ± 4.67	97.89 ± 4.65
$Fe(CO_3)_2^{2-}$	52.37 (± 0.41) – 13130 (± 118) 1/T	0.999	0.03	109.16 ± 0.99	107.73 ± 0.97
$Fe(CO_3)(OH)^-$	11.22 (± 0.13) – 2074 (± 37) 1/T	0.999	0.01	17.24 ± 0.30	15.81 ± 0.43
$FeOH^+$	17.25 (± 0.85) – 3558 (± 25) 1/T	0.991	0.06	29.58 ± 2.07	27.15 ± 2.04
$Fe(OH)_2$	27.61 (± 0.16) – 4182 (± 46) 1/T	0.999	0.01	34.77 ± 0.38	32.34 ± 0.36
$FeH_3SiO_4^+$	13.93 (± 0.09) – 866 (± 27) 1/T	0.998	0.01	7.20 ± 0.22	5.77 ± 0.53
$FePO_4^-$	9.13 (± 0.15) – 830 (± 42) 1/T	0.995	0.01	6.90 ± 0.35	5.47 ± 0.42

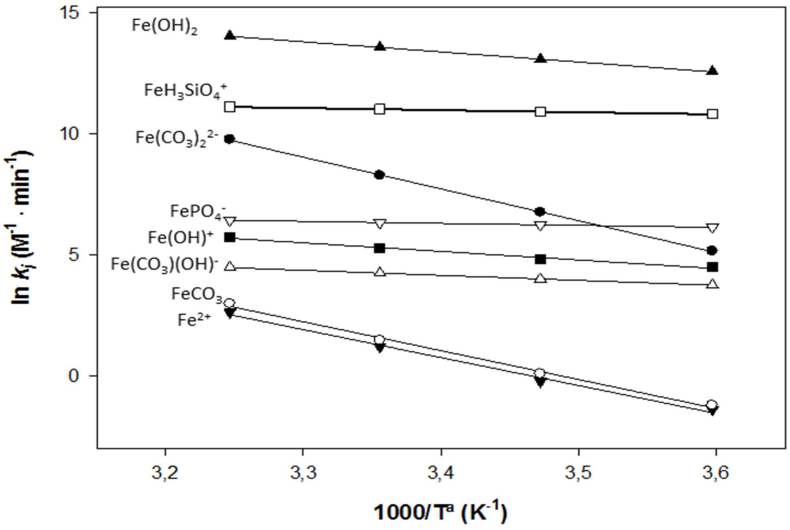

Fig 2.7 The effect of temperature for the most reactive Fe(II) species on the oxidation rate constants (ln k_i) by O_2 in seawater and seawater enriched with nutrients. Salinity = 37.09.

The ion-pair constant, for each temperature, for the formation of $FeH_3SiO_4^+$ species was estimated using the kinetic model (Fig 2.8). The model assumed that the silicate ion (SiO_3^{2-}), in aqueous solution, formed the reactive species $H_2SiO_4^{2-}$, which quickly converted to $H_3SiO_4^-$ by consuming a proton (eq 24). At circum-neutral pH, most of the $H_3SiO_4^-$ further transformed to H_4SiO_4 consuming another proton (eq 25). The global equilibrium formation constant for the $FeH_3SiO_4^+$ species, independent of pH (eq 26), can be determined as;

$$Fe^{2+} + H_2Si\ {}_4^{2-} + H^+ \leftrightarrow FeH_3SiO_4^+ \quad (24)$$

$$H_3SiO_3^- \leftrightarrow H_2SiO_4^{2-} + H^+ \quad (25)$$

$$\boldsymbol{Fe^{2+} + H_3Si\ {}_3^- \leftrightarrow Fe\ {}_3SiO_4^+} \quad (26)$$

The ion paring model has been used by a number of workers (Byrne et al. 1988; Millero and Pierrot 1998) in order to estimate the speciation of ions in natural water. Considering the ionic interactions of the major ions, the model developed by Millero and Pierrot (1998) fitted different equations, for the thermodynamic association constant in the ion pairs formations, with the general form,

$$pK_{FeH3SiO4}^+ = A + B / T + C\ T \quad (27)$$

where A, B and C are the theoretical coefficients for the formation of ion pairs in natural waters and T is the temperature (ºC). In this work, the $FeH_3SiO_4^+$ ion pair constants can be described (Fig 2.8) by a similar equation (eq 28).

$$\boldsymbol{pK_{FeH3SiO4}^+ = -0.004\ (\pm 0.149) + 1.287 / T\ (\pm 0.736) - 0.062\ (\pm 0.005)\ T} \quad (28)$$

The standard error of estimation is 0.047 and the r^2 is 0.997. This equation can be used and applied in the environment, under the experimental conditions used in this work.

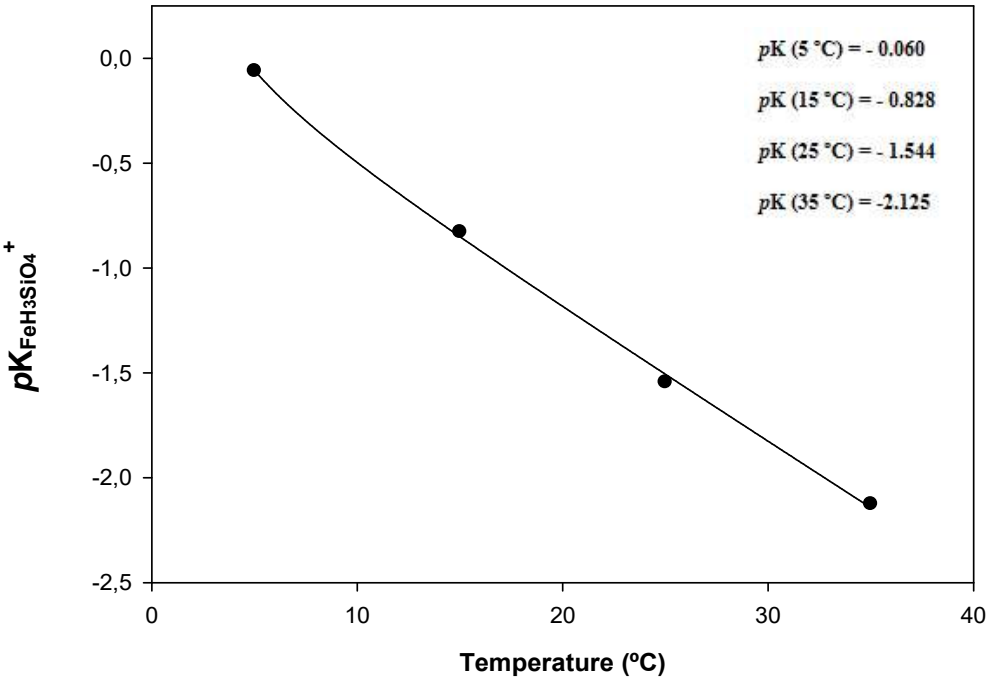

Fig 2.8 Thermodynamic dependence (eq 19) for ion-pair constant of Fe-Silicate specie ($FeH_3SiO_4^+$) ued in the model. S = 37.09.

2.4 Environmental implications

This study confirms that environmental factors, such as the presence of nutrients, (especially silicates), temperature and pH may play an important role in kinetic processes of iron in coastal waters. We suggest that the combination of anthropogenic nutrient loading and raising of seawater surface temperature may intensify the oxidation of Fe(II), making it less available for biologically mediated processes in coastal systems (Shaked et al. 2005). Likewise, ocean acidification may decrease inorganic complexation as well as possibly leading to enhance the concentration of a form of Fe that may be highly bioavailable. Inasmuch as the phytoplankton responses to eutrophication processes are complex and depend upon multiple biotic and abiotic interactions (Guenther et al. 2015), this work can be used in field observations and environmental models to characterize the effects of increased nutrients delivered to the coastal zone and their impact on carbonate chemistry as well as the changes that may result in the biogeochemical iron cycle.

CHAPTER II

CHAPTER III

Variability in the production of Fe organic ligands, by Synechococcus PCC 7002, under different iron scenarios

Samperio-Ramos, G., Santana-Casiano, J.M. and González-Dávila, M.: Variability in the production of Fe organic ligands, by *Synechococcus* PCC 7002, under different iron scenarios. *Journal of Oceanography*. Submitted.

CHAPTER III

Abstract

Marine *Synechococcus* are one of the most diverse and widespread cyanobacteria, and iron is an essential micronutrient that limits their growth in many areas of the ocean. Several Fe-uptake mechanisms strongly suggest the importance of the presence of organic matter, since some organic ligands facilitates the acquisition of iron. Here, it has been studied how coastal *Synechococcus* (strain PCC 7002) acclimates to Fe bioavailability, comparing the growth and organic exudation under two different Fe regimes. These cyanobacteria were incubated in UV-treated sea water supplemented only with major nutrients (N, Si and P) and two different iron scenarios without chelating agents in order to analyze the Fe organic ligands production. Nanomolar levels of two ligands with iron-chelation properties (hydroxamic acids and dihydroxyphenolic moieties) were detected. The response in both cyanobacteria growth and organic release was statically analyzed considering Fe-scenarios and different development stages.

We observed *Synechococcus* compensated growth-limiting levels of iron availability by decreasing its maximum growth rate and changing the type of organic ligand excreted. The concentration of dissolved organic carbon (DOC) increased, over time of culture, from 15.84 to 127.13 μmol C L^{-1} and from 15.76 to 150.51 μmol C L^{-1} when *Synechococcus* grew under Low-Fe and High-Fe conditions respectively. The results have shown that no-significant variations were found in individual production of DOC, among related growth phases and regarding to iron availability. The production of Fe-specific hydroxamate ligands is inhibited during high-iron growth. The study has also shown that higher levels of iron in the medium result in a significant decrease in individual exudation of phenolic ligands. Our study demonstrates that iron availability and the growth stages might be key parameters in regulating the release performance of extracellular Fe-specific organic ligands by cyanobacteria.

CHAPTER III

CHAPTER III

3.1 Introduction

Marine cyanobacteria play a fundamental biogeochemical role in the world's oceans, contributing substantially to carbon fixation in marine systems (Schaum et al. 2013), accounting for 25% of global ocean net primary productivity (Uitz et al. 2010). The underlying keys, which governing cyanobacterial development in the marine systems, are multiple and strongly affected by the complex environmental factors (Armbrecht et al. 2015; Cadier et al. 2017). Iron has been suggested to be the main factor in limiting phytoplankton growth, in high nutrients low chlorophyll areas of the oceans (Martin and Fitzwater, 1988), as Fe-availability can influence, for example the biological productivity and microorganism community composition of the ocean (Sunda, 2012). However, marine cyanobacteria have shown dynamic and multitier adaptive response, to the different iron bioavailability regimes found in the ocean, by the excretion of iron chelating compounds (Ito and Butler, 2005) or the biosynthesis of iron transport systems (Jiang et al. 2014; Kranzler et al. 2014; Morrissey and Bowler, 2012). Additionally, in open ocean, the spatial and temporal dynamics of most of natural organic ligands, denote they have been biosynthesized in situ (Boyd and Tagliabue, 2015; Boye et al. 2005; Roy and Wells, 2011). Important accumulations of dissolved organic matter (DOM), have been observed to take place toward the end of phytoplankton blooms (Carlson and Hansell, 2015). Levels of up to 80 μmol C kg^{-1} have been measured in tropical and subtropical environments (40°N to 40°S), when superficial stratification of seawater column has favoured the accumulation of this dissolved organic carbon (DOC) (Hansell et al. 2009). Emerging tools in analytical chemistry and microbiology enhance knowledge about the composition and reactivity of dissolved products excreted by ocean microbiome (Moran et al. 2016). For example, natural organic exudates have been reported to modify the potential availability of Fe and to promote the growth of photosynthetic microorganisms (Vasconcelos and Leal, 2008).

Siderophores are iron chelating agents with low molecular weight that are generated by some prokaryote organism, as an Fe acquisition strategy in response to iron stress conditions (Hider and Kong, 2010). The high binding capacity of

siderophores is usually attributed to their oxygen containing functional groups (hydroxamates, carboxylic acids and catecholates) (Vraspir and Butler, 2009). Over the past decade, several marine bacterial siderophores have been isolated and structurally characterized (Butler and Theisen, 2010); nevertheless there is much less knowledge about cyanobacterial iron chelators. The first report on a cyanobacterial siderophore was schizokinen from the freshwater *Anabaena* PCC 7120 (Simpson and Neilands, 1976). Schizokinen is a citrate derivative of which two carboxylate groups are amidated with an acetyl hydroxamic amine. While Armstrong and Van Baalen (Armstrong and Van Baalen, 1979) isolated the first hydroxamate-type siderophore from an axenic culture of the marine cyanobacterium *Synechococcus* PCC 7002, Ito and Butler (Ito and Butler, 2005) chemically characterized this siderophore, synechobactin, which can be considered as an amphiphilic derivate of schizokinen, where one of the hydroxamic acids is appended to one long fatty acid. The authors reported three different synechobactin structures (A-C) depending on the length of the fatty acid. Recently, Boiteau et al. (2013) have tuned up a method to detect low concentrations of organic Fe ligands using reverse-phase high-performance liquid chromatography. In exudates of *Synechococcus* PCC 7002, this technique has allowed identifying three new members of the synechobactin suite with different side chain lengths of carbons (Boiteau and Repeta, 2015). Besides, it has been suggested that this amphiphilic structure of marine siderophores helps to anchor them into the membrane of microorganisms and thus prevents the loss of ligand by dilution in oceanic environments (Sandy and Butler, 2009).

Some polyphenolic compounds can also form strong complex with Fe(III) due to the presence of hydroxyl groups (Elhabiri et al. 2007), although their affinity for Fe(III) is noticeably lower than hexadentated siderophores, such as enterobactin or bacillibactin (Butler and Theisen, 2010). Phenols are considered to be one of the principal groups present in humic substances (Stubbins et al. 2008), acting as their major electron donating moiety (Aeschbacher et al. 2012). Phenolic compound are naturally present in marine systems, since humic substances reach between 10-50% of DOC in estuaries and coastal waters (Laglera et al. 2007). Moreover, phenolic compounds are excreted by a wide range of marine macroalgae as secondary metabolites (Celis-Plá et al. 2016; López-Alarcón and Denicola, 2013; Pereira et al.

2015). Phytoplankton also excretes phenols to be adapted to the environmental conditions (Stengel et al. 2011). For example, Jin et al. (2015) have shown that ocean acidification alter the metabolic pathways of phytoplankton, as the Krebs cycle and mitochondrial respiration, by enhancing in the production of phenolic compounds. Beside recently, differences in the phenolic profiles have been measured in exudates of marine microalga when those microorganism grow under metallic stress conditions (López et al. 2015; Rico et al. 2013), so that, in some oceanic regions phytoplankton could be a significant source of phenolic compounds (Heller et al. 2016).

Due to variability in the Fe-ligands production showed by *Synechococcus* PCC 7002 under different iron conditions (Li et al. 2007; Trick and Wilhelm, 1995), the aim of this research has been to study the effect of two extreme high and low iron concentrations in the dissolved organic carbon and Fe-ligands exudation (hydroxamic and phenolic compounds). In the study, we have carried out a statistical analysis for production rate of DOC and two specific types of Fe-ligands, with reactivity very differentiated, having into account two Fe-scenarios and the growth stages of this cyanobacteria

3.2 Material and methods

3.2.1 Culture media and organic exudates enrichment

Both UV-treatment and characteristics of sampled seawater used for this study, as well as the nutrient enrichment, to which has been subjected, are described in the point 2.2.1 of chapter 2. Additionally, iron was added (50 nM and 500 µM) from a stock solution (1 mM) of ferric chloride (Sigma), The final concentration of dissolved inorganic ferric species in the medium, (expressed as pFe = -log[Fe^{3+}]), was determined with CHEAQS-Next (free-software for calculating Chemical Equilibria in AQuatic Systems, design by Wilko Verweij, 2013). Although in the

free-organic medium the most of the iron added precipitated, two different Fe-scenarios were generated (High-Fe with *p*Fe = 15 and Low-Fe with *p*Fe = 19).

The axenic culture of *Synechococcus* PCC 7002 was supplied in ASP-12 culture media (Guillard, 1975), from the National Algae Bank (BNA) collection, in Gran Canaria. All cultures were kept in autoclaved erlenmeyer flasks (Tuttnauer 2540), acid-washed using cleaning methods (Achterberg et al. 2001). The stock and experimental cultures were kept with aeration and stored in a clean culture chamber (Friocell FC11) at constant temperature (25 ºC), and illumination (complete photoperiod of 24 h and 200 µmol photons m^{-2} of light intensity). Stock cultures were tested weekly for contamination and cell densities using a hematocytometer (Microbiotest, Inc.) and microscopy.

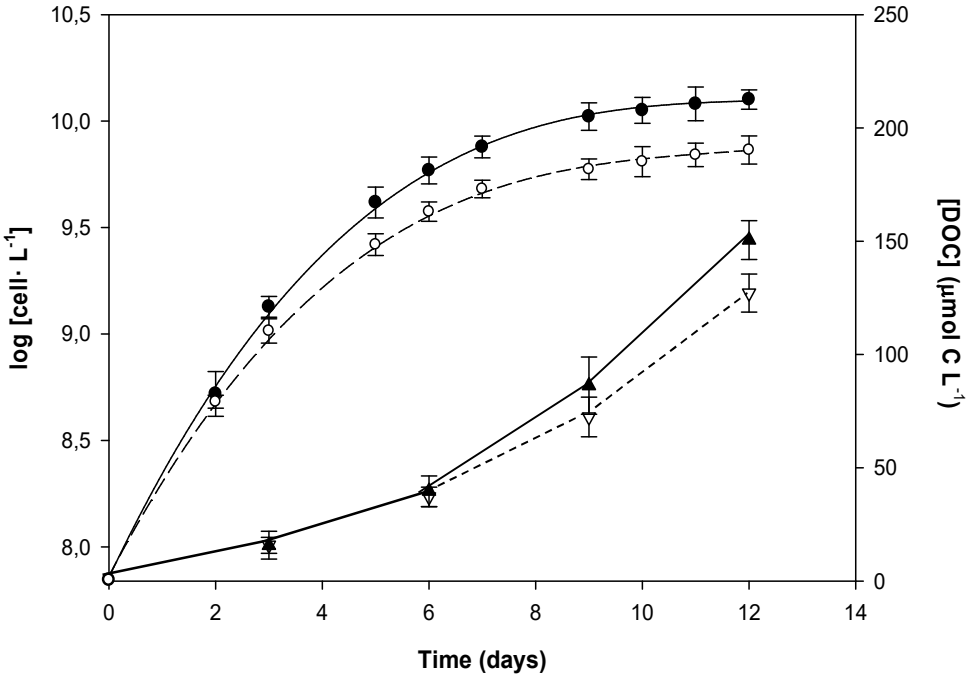

Fig. 3.1 The experimental growth (cell L^{-1}, denoted with circles) and evolution in the levels of dissolved organic carbon (µmol C · L^{-1}, denoted with triangles) present in cultures of *Synechococcus* PCC 7002 obtained in seawater enriched with nutrients, under High-Fe conditions ($[Fe(III)]_0$ = 500 µM, represented with filled figures) and Low-Fe condition ($[Fe(III)]_0$ = 50 nM, represented with white figures). The cultures were illuminated for 24 hours at 25ºC. Bars denote the error standard of the esteem.

Hemacytometer counts of cell density were found to be directly correlated to absorbance at 750 nm (r^2 = 0.984) (Ito and Butler, 2005; Wilhelm et al. 1996). Cell densities were estimated spectrophotometrically (S4000, Ocean Optics^{TM}) every 24 h. To avoid interferences in the chemical assays and interactions with iron in the kinetic experiments, by introducing of chemicals from ASP-12 medium to experimental cultures, the selected aliquots from *Synechococcus* stock cultures were centrifuged (4000 rpm) 3 times with UV treated seawater. The initial cell concentrations in the experimental cultures were always $7 \cdot 10^7$ cell/L, reaching the stationary phase the 12th day ($7.3 \cdot 10^9$ cell L^{-1} and $1.2 \cdot 10^{10}$ cell L^{-1} for Fe-deficient and Fe-replete conditions respectively; Fig 3.1). Homogenous distribution of the cells was achieved through injection of sterile, filtered air.

In this study, the exudates were always produced at natural seawater pH and at 25 ºC. Cyanobacterial culture medium was rendered cell-free by centrifugation (4000 rpm) for 15 min and then supernatant was filtered (0.1 μm). This seawater enriched with organic exudates was used to carry out the determination of dissolved organic carbon and extracellular iron chelates

3.2.2 Dissolved organic carbon

Samples for the analysis of DOC were collected after filtration and stored at 2–4 ºC until analysis (Sharp et al. 2002). DOC concentration in samples (both in UV treated seawater and in the seawater enriched with *Synechococcus* natural exudates) was monitored using a Total Organic Carbon analyzer (Shimadzu TOC-V) previously calibrated from standard curves (10 to 200 μmol C L^{-1}) with potassium hydrogen phthalate standard (Sigma-Aldrich) (Arístegui et al. 2014). DOC reference material (D. Hansell; Univerity of Miami) was analyzed to check for the accuracy and precision of instrument. The method had an uncertainty of 3% and a detection limit of 1.3 μmol C L^{-1}.

3.2.3 Chrome Azurol Sulphonate

The CAS assay is a universal method for the detection of strong iron-binding compounds (e.g. siderophores), based on the affinity of chromeazurol sulphonate per Fe^{3+}. Anhydrous piperazine (PIPES), hexadecyltrimethylammonium bromide (HDTMA, chromeazurol S and $FeCl_3$ were purchased from Sigma to prepared CAS assay solution, according to Schwyn and Neilands (1987). Exudates were filtered with PVDF 0.1 μm Syringe Driven Filter Units (Millipore Corporation). Qualitative estimation was done with the addition of equal volumes (0.5 ml) of 1 μM of CAS reagent solution to the samples and was allowed to equilibrate at room temperature and in dark for 5 hours. The colour change of samples was detected by monitoring the absorbance at 630 nm, using a UV-VIS spectrophotometer (S4000, Ocean Optics^{TM}). The percent of the reduction of CAS activity was calculated following the general equation (Payne, 1994),

$$Reduction_{CAS-Activi} \quad (\%) = \left(\frac{Abs_r - Abs_s}{Abs_r}\right) \cdot 100 \qquad (29)$$

where, Abs_r and Abs_s are the absorbance of reference (UV treated seawater) and sample, at 630 nm, respectively.

3.2.4 Csaky test

The principle of Csaky test, with slight amendment (Gillam et al. 1981), was used for the specific detection of hydroxamic functional groups, features of some high-affinity Fe(III)-coordinating ligands, as hydroxamate-type siderophores. The principle of the assay involved the acid hydrolysis of the sample (2 ml filtered by 0.1 μm), with sulfuric acid (Sigma-Aldrich) at 100ºC for 4 h, in order to release hydroxylamine from the hydroxamic groups, quantitatively, under acetate buffered conditions (pH = 3.5). The solution was read spectrophotometrically (S4000, Ocean Optics^{TM}) at 545 nm and the detection limit of the method, using a 5 m long waveguide capillary flow cell (World precision instruments^{TM}), was 2 μgr eq hydroxylamine· L^{-1}. The standard used for the assay was hydroxylamine hydrochloride (Sigma) and UV treated seawater was used as blank.

3.2.5 Arnow test

The Arnow test (Arnow, 1937) enabled the selective detection of dihydroxyphenolic compounds in the sample (5 ml) by addition of hydrochloric acid (5 ml; 0.5 M), followed by addition of 5 ml (0.5 M) of sodium molybdate (Sigma-Aldrich) and 5 ml (0.5 M) sodium nitrite (Sigma). Then, sodium hydroxide (Sigma) is added in excess (5 ml; 1 M). Maximum absorbance was measured at 510 nm using UV-VIS spectrophotometer (S4000, Ocean Optics^{TM}), that connected to a 5 m long waveguide capillary flow cell (World precision instruments^{TM}), allowing to reach a detection limit of 4 µgr eq catechol L^{-1}. The standard used for the assay was catechol (Sigma-Aldrich) and UV treated seawater was used as blank.

3.2.6 Data analysis

. The relative growth rates (µ) were calculated as the slopes of linear regressions of ln (cell concentration) versus day number for individual cultures over the range of linearity.

In the present work, the statistical analysis for the measurements of concentrations, as well as, the determination of organic extracellular release rates have been analyzed distinguishing 4 stages in the growth curves of *Synechococcus* PCC 7002 (Fig 3.1): initial phase (IP, until 3th day), exponential stage, differentiating in turn between an early exponential (EEP, from 4th to 6th day), late exponential phase (LEP, from 7th to 9th day) and finally stationary phase (SP, from 9th day to 12th day).

R (R Development Core Team, 2008) was used for statistical computing. One-way analysis of variance (ANOVA) was used to test for significant effects of different growth stages on the production normalized of DOC and hydroxamate-type ligands present in the *Synechococcus* exudates. Tukey's HSD test was carried out to do a multiple comparison procedure (post-hoc analysis) to find means that are significantly different. To test the difference in the variable monitored between the Fe-treatments (growth rates and release rates of DOC and phenolic compounds in the

exudates), a two-sample t-test was used. The assumptions of normality and homoscedasticity were verified using the Shapiro-Wilk and Barlett tests respectively. For all statistical analyses, a probability level of $\alpha = 0.05$ was considered.

3.3 Results and discussion

3.3.1 Growth rates

The growth of *Synechococcus*, achieved in the two different iron regimes, is shown in Fig 3.1. High-Fe conditions supported a higher phytoplankton biomass, maintaining a growth rate of 0.56 ± 0.01 day^{-1}, which was significantly higher (two sample t-test: t=-33.34, df=16.00, p-value <0.001) than when *Synechococcus* grew under Low-Fe conditions ($\mu = 0.49 \pm 0.01$ day^{-1}). The reduction of the growth rate between these two Fe-scenarios indicates that iron limit the growth of *Synechococcus* PCC 7002. These results were comparable to those obtained by other authors (Liu et al. 2012; Liu and Qiu, 2012; Wilhelm et al. 1996). A decrease in the availability of iron in the medium culture, typically, leads to an important reduction in the growth rate in cyanobacteria, due to they have an exceptionally large iron requirement to carry out the photosynthetic activity (Jiang et al. 2014). Nevertheless, the growth of *Synechococcus* PCC 7002 might be less affected by Fe-limitation, due to the ability of these cyanobacteria to synthetize siderophores, under Fe-stress conditions, in combination with high-affinity transport systems consisted in a Fe-specific receptor protein (Kranzler et al. 2014; Morrissey and Bowler, 2012).

3.3.2 DOC dynamics

The DOC levels in the experimental cultures increased concurrently with the cell density, reaching at 12th day of growth 153.70 ± 7.75 μmol C · L^{-1} and 127.13 ± 16.76 μmol C · L^{-1} under High-Fe and Low-Fe conditions, respectively (Fig 3.1). Therefore our results were in accordance with those obtained by Biddanda and Benner (1997) and Flynn et al. (2008), with different *Synechococcus* strains, where

the period with higher DOC levels in the cultures also occurred during the stationary phase. High-Fe cultures led higher levels of DOC during exponential and stationary growth phases than Low-Fe cultures, although no-statistical differences were observed (Table 3.1). Meon and Kirchman (2001) using mesoscosms enriched with nitrate, phosphate and silicate shown higher accumulation of DOC when the inorganic nutrients were presented. Nevertheless, as in this study, their findings were supported by increased phytoplankton biomass when nutrients were added. The production of DOC, standardized as a release rate (µmol C $cell^{-1}$ day^{-1}) was greater when the supply of iron was lower (Fig 3.2), even though no-significant variations were found (Table 3.1). Our experimental data, align well with the results of Becker et al. (2014) for different cyanobacteria species. The extracellular release rate of DOC was higher during the stationary phase; however no-statistical differences (Table 3.2) were found between growth stages due to highly variability in the measures.

Table 3.1 Results from two sample t-test for levels (µmol C L^{-1}) and production (µmol C $cell^{-1}$ day^{-1}) of DOC, between Fe-treatments (Low-Fe and High-Fe conditions) for different growth stages analysed.

Variable	Factor		*T*	*df*	*p-value*
Levels of DOC (µmol C L^{-1})	***Initial Fe in cultures***	***IP***	-0.0104	6	0.9920
		EEP	0.2713	6	0.7953
		LEP	0.8106	4	0.4631
		SP	1.2414	6	0.2608
Release rate of DOC (µmol C $cell^{-1}$ day^{-1})	***Initial Fe in cultures***	***IP***	-0.037	6	0.9717
		EEP	-0.7897	6	0.4598
		LEP	-0.7727	4	0.4828
		SP*	-1.0135	3.518	0.3754

*With the values of extracellular release of DOC during *SP* was carried out a Welch two sample t-test.

Extracellular release rate of DOC has been partially kept among related growth phases and regarding to iron bioavailability, implicating that individual organic exudation of *Synechococcus* PCC 7002 may be considered as a factor fairly constant. Nevertheless, growth phase and iron availability may affect chemical composition of dissolved organic material released by phytoplankton (Barofsky et al. 2009; Ito and Butler, 2005; Rico et al. 2013).

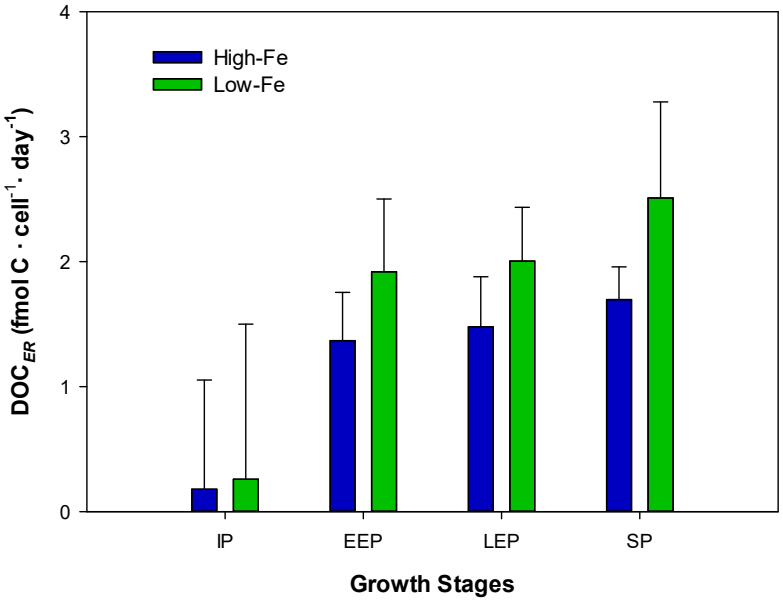

Fig 3.2 Extracellular release of dissolved organic carbon (DOC_{ER}; fmol C· cell^{-1} day^{-1}) during the different growth stages (denoted as: IP = Initial Phase, EEP = Early Exponential Phase, LEP = Late Exponential Phase and SP = Stationary Phase), both under High-Fe and Low-Fe conditions. Bars indicate standard error (n=4).

Table 3.2 Results of one-way analysis of variance (ANOVA), for production (µmol C cell^{-1}) of DOC under Low-Fe and High-Fe conditions, as function (factor) of different growth stages.

Variable		Factor	MS	*df*	F	*p-value*
Release rate of DOC (µmol C · cell^{-1} · day^{-1})	***High-Fe***	*Growth stages*	16.43	3	1.565	0.253
		Error	10.50	11		
	Low-Fe	*Growth stages*	34.05	3	0.687	0.578
		Error	49.55	11		

3.3.3 CAS activity

The chemical assays were used to indicate presence or absence in solution of organic iron-complexing ligands. A reduction of CAS activity is indicative of the production of strong Fe-binding compound. The maximum discoloration was reached during the SP for both Fe-treatments, although clearly, Low-Fe cultures showed lower CAS activity than cultures with High-Fe conditions (Fig 3.3),

indicating a greater presence of strong Fe-binding ligands when iron is limited. The development of assays is comparable to that obtained by Ito and Butler (2005) and suggest that the exudation of organic ligands with strong Fe-binding capacity is stimulated more neatly under low Fe-regimes (Adly et al. 2015; Gledhill et al. 2004). The CAS assay indicates the presence of Fe strong ligands in the exudates, but does not distinguish between functional Fe-binding groups.

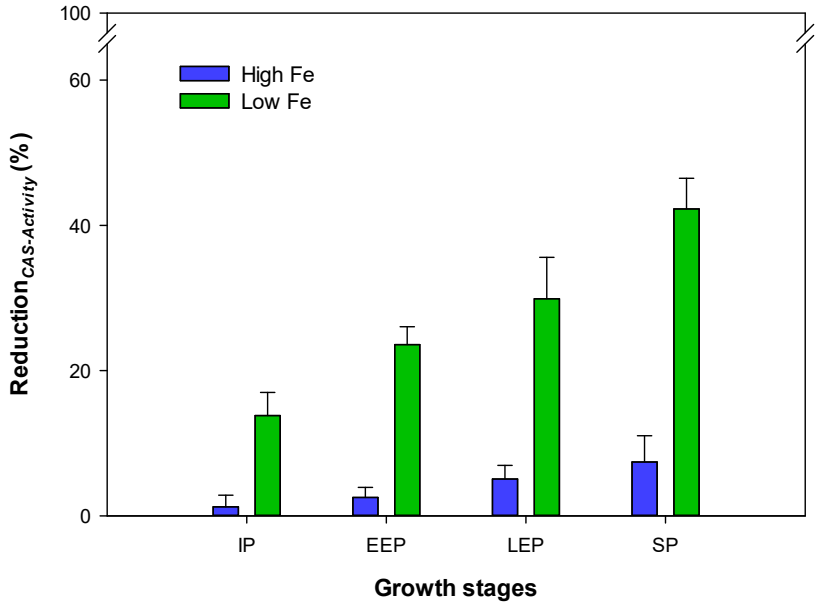

Fig 3.3 Time course CAS activity reduction in exudates of *Synechococcus* PCC 7002 produced under High-Fe and Low-Fe conditions, during the different growth stages (denoted as: IP = Initial Phase, EEP = Early Exponential Phase, LEP = Late Exponential Phase and SP = Stationary Phase). Bars indicate standard error. $[Fe\text{-}CAS]_0 = 1\ \mu M$).

3.3.4 Hydroxamic and phenolic ligands

Figures 3.4 and 3.5 depict the levels of detectable hydroxamic-type and phenolic-type ligands, expressed semi-quantitatively as hydroxylamine equivalent (Csaky test) and catechol equivalent (Arnow test), respectively.

The cultures with High-Fe conditions were negative in the Csaky assay for hydroxamic moieties; however the assay confirmed that the exudates of *Synechococcus* PCC 7002 obtained from Low-Fe cultures, contained type-

hydroxamate groups. The levels of hydroxamates (µgr equivalent L^{-1}) increased an order of magnitude in the days that lasted the cultures (Fig 3.4). Ito and Butler (Ito and Butler, 2005) isolated an amphiphilic hydroxamate siderophore, synechobactin, when *Synechococcus* PCC 7002 grew under iron-limited conditions, which would suggest the presence of synechobactin, in the exudates excreted by *Synechococcus* in the present study, since the presence of extracellular hydroxamato-type ligands was totally dependent on the initial iron concentration in the medium.

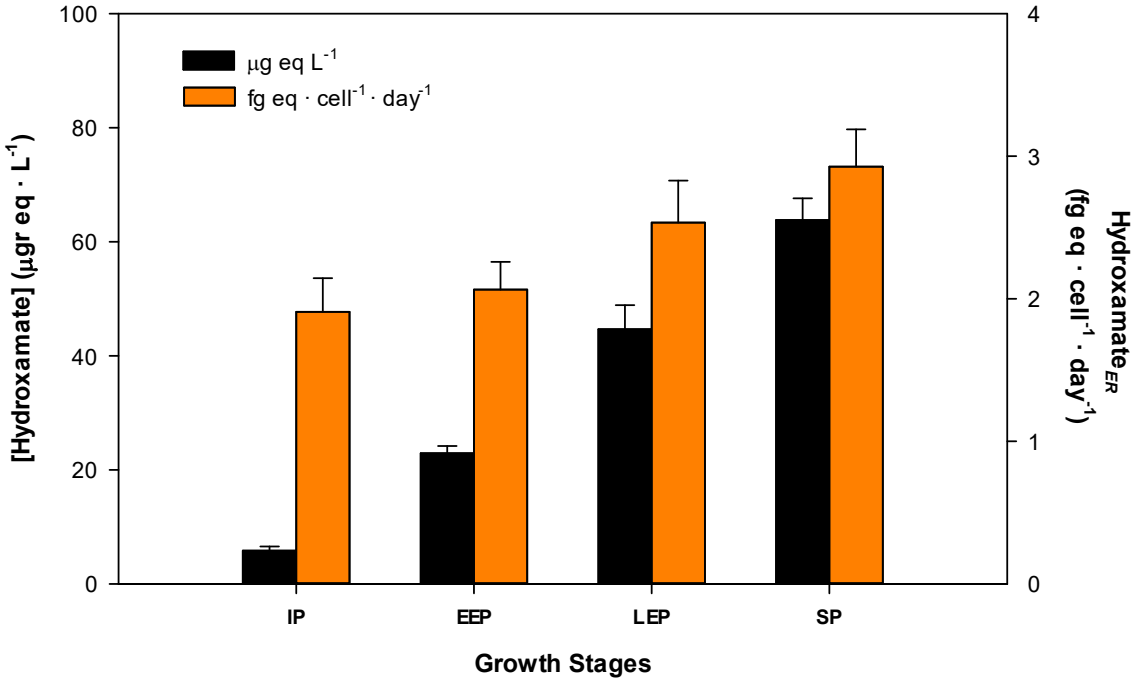

Fig 3.4 Results of Csaky assay. Changes in levels (µg hydroxilamine equivalent L^{-1}) and extracellular release (ER) of hydroxamic ligands (fg hydroxylamine equivalent $cell^{-1}day^{-1}$) in seawater enriched with exudates from the cultures of *Synechococcus* PCC 7002, under Low-Fe conditions, during the different growth stages (denoted as: IP = Initial Phase, EEP = Early Exponential Phase, LEP = Late Exponential Phase and SP = Stationary Phase). Bars indicate standard error. (n=4 for IP, n=3 for LEP and n=6 for EEP and SP).

The results showed the hydroxamate-type ligands release rate (fg $equivalent^{-1}$ $cell^{-1}$ day^{-1}) by *Synechococcus* also increased significantly with the growth stages (Table 3.3). In addition, while the extracellular release rate was fairly constant during the earlier stages of development (i.e IP and EEP), a nonlinearity in the excretion rate of hydroxamic moieties were esteemed during the final phase of growth (Fig 3.4),

where extracellular release rate during SP (2.93 ± 0.26 fg eq $cell^{-1}day^{-1}$) was significantly higher than during the IP (1.91 ± 0.24 fg eq $cell^{-1}$ day^{-1}; Tukey contrast: t-value = 3.174, $p<0.05$) and during the EEP (2.06 ± 0.17 fg eq $cell^{-1}$ day^{-1}; Tukey contrast: t-value = 2.847, $p<0.1$). *Synechococcus* PCC 7002 adaptation to low-iron bioavailability includes diminish the intracellular iron requirements (Wilhelm et al. 1996), and the excretion of specific iron ligands (Ito and Butler, 2005) as part of a highly specific iron uptake mechanism via receptor system (Morrissey and Bowler, 2012). Proteomic analysis with *Synechococcus* PCC 7002 have shown that multiple siderophore biosynthesis and Fe transporter proteins are just expressed during growth under Fe-limited and oxic conditions (Swanner et al. 2015). Therefore our results demonstrated that the hydroxamate-type ligands release rate is highly conditioned by the Fe-bioavailability conditions.

Table 3.3 Results from one-way analysis of variance (ANOVA) for production (µg eq $cell^{-1}$) of hydroxamate-type ligand in exudates produced under Low-Fe conditions for different growth stages considerate (factor) in the cultures of *Synechococcus* PCC 7002.

Variable	Factor	MS	*Df*	F	*p-value*
Extracellular release rate of hydroxamate-type ligands (fg eq · $cell^{-1}$ · day^{-1})	***Growth stages***	$9.842*10^{-19}$	3	4.293	< 0.05
	Error	$2.293*10^{-19}$	13		

Arnow assay showed a negative response in both Fe-treatments (Fig 3.5) in IP and early exponential phase (EEP). However during the later exponential phase (LEP) and the steady phase (SP) the exudates of *Synechococcus* PCC 7002 showed positive response to the presence of phenolic compounds in both iron treatments. When Ito and Butler (Ito and Butler, 2005) cultured *Synechococcus* sp. PCC 7002, under iron-deficient conditions, the HPLC analysis of supernatant did not detect trace of catechol siderophore production. In contrast, recently it has been measured nanomolar levels of phenolic compounds in exudates of *Phaeodactylum tricornutum* and *Dunaliella tertiolecta* (López et al. 2015; Rico et al. 2013) under high and low iron concentrations. Therefore, the response obtained in our study, through the

Arnow test, could be due to the presence of polyphenolic compounds, and not by the presence of catecholate-type siderophores.

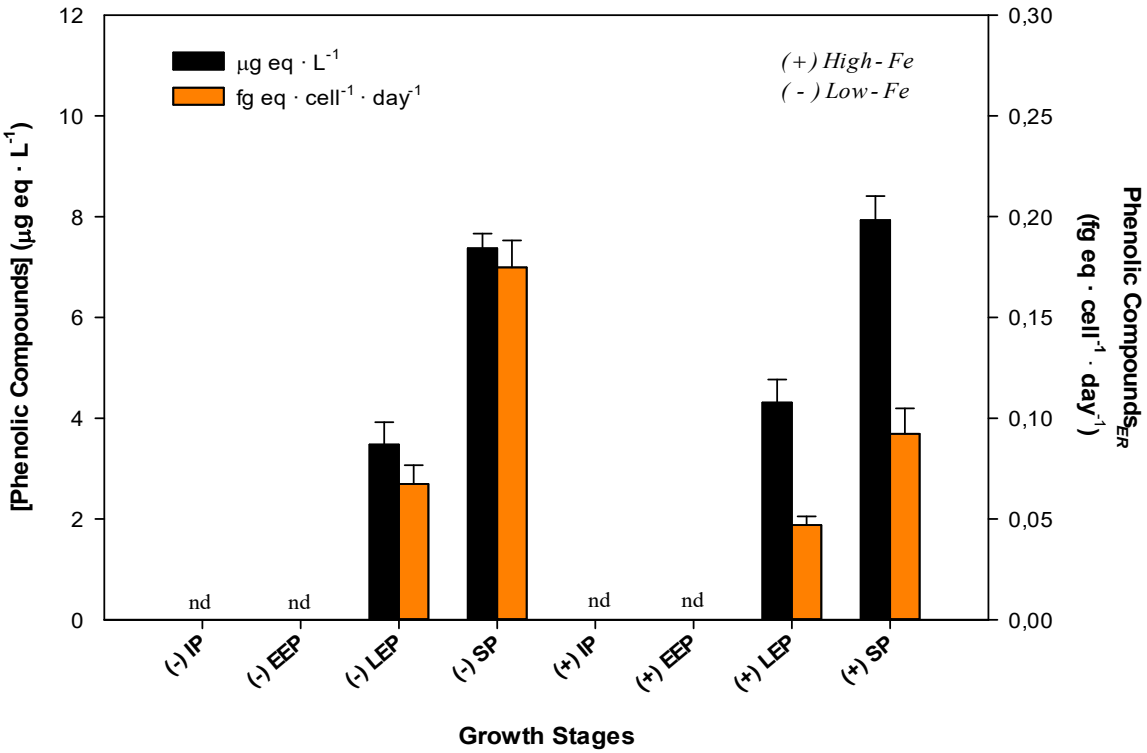

Fig 3.5 Results of Arnow test. Changes in levels (µg catechol equivalent L^{-1}) and extracellular release (*ER*) rate of phenolic compounds (fg catechol equivalent $cell^{-1}day^{-1}$) in seawater enriched with exudates from the cultures of *Synechococcus* PCC 7002, during the different growth stages (denoted as: IP = Initial Phase, EEP = Early Exponential Phase, LEP = Late Exponential Phase and SP = Stationary Phase), both under High-Fe (denoted as +) and Low-Fe (denoted as -) conditions. Annotation *nd* means *not detected*. Bars indicate standard error (n= 5 for LEP and n=9 for SP).

During the LEP and SP the concentration of phenolic compounds did not obtain significant differences (two sample t-test; t=-1.8033, df=8, p-value=0.190 and t=-0.4691, df=17, p-value=0.645 for LEP and SP respectively) between Fe-treatments. Nevertheless, the phenolic release rate, expressed as fg eq $cell^{-1}$ day^{-1} was significantly higher (two sample t-test; t=-2.1128, df=8, p-value<0.1 and t=-7.0129, df=16, p-value<0.0001; for the LEP and SP respectively) in the cultures with Low-Fe conditions in both growth stages. Additionally, the extracellular release rate of phenolic compounds increased significantly during the growth under Low-Fe conditions (two sample t-test; t=-3.6421, df=12, p-value<0.01), but nevertheless it

remained almost constant under High-Fe conditions (t=-1.5103, df=12, p-value=0.1568).

The quantification of phenolic compounds in the seawater enriched with exudates of *P. tricornutum* and *D. tertiolecta* (López et al. 2015; Rico et al. 2013), from the iron enrichment cultures, showed that the amount excreted per cell of single phenolic compounds, as catechin or epicatechin, declined dramatically as compared to the control. Our results also align well with the study carried out by Wells et al. (2005), where a synergistic link between the release rate of the iron complexing ligand domoic acid and the limitation by iron in toxigenic diatoms *Pseudo-nitzschia* spp was observed. Therefore the experimental behavior of *Synechococcus* PCC 7002 suggested that the cyanobacteria metabolically increased the production and release of exudates capable of complexing the iron in the solution, as the bioavailability conditions decreased.

3.4 Environmental implications

Different authors have demonstrated that inorganic Fe is highly available for acquisition by phytoplankton but that organic chelated Fe is necessary in order to explain the total uptake system (Hassler et al. 2011; Kustka et al. 2015). The decline in the extracellular release both of phenolic and hydroxamate type-ligands during the Fe-replete treatments may have its explanation in the higher levels of iron in the medium, which reduce the metabolic effort (synthesis of Fe-ligands) needed to iron uptake. In addition, within ligand-bound pool released by bacterioplankton, the excretion of siderophores and phenolic compounds may represent a differentiating strategy to access iron under deficient conditions.

Cyanobacteria exudates can also influence the fate and composition of iron in Upper Ocean via their role in the Fe redox cycle (Swanner et al. 2017). Thus, the presence or absence of hydroxamic and phenolic moieties might have a key influence on the redox behavior of iron, since can simultaneously act as Fe-chelates and

Fe(III)-reducing agents (Barbeau et al. 2001; Santana-Casiano et al. 2014), and therefore, influencing in the iron acquisition by photosynthetic microorganisms (Lis et al. 2015; Shaked and Lis, 2012).

CHAPTER IV

Impact on the Fe-redox cycling of organic ligands released by Synechococcus PCC 7002, under two Fe-fertilization scenarios. Modelling approach

Samperio-Ramos, G., González-Dávila, M. and Santana-Casiano, J.M.: Impact on the Fe redox cycling of organic ligands released by *Synechococcus* PCC 7002, under different iron fertilization scenarios. Modelling approach. *Journal of Marine Systems*. In revision.

CHAPTER IV

➢ Abstract

The kinetics of Fe redox transformations are of crucial importance in determining the bioavailability of iron, due to inorganic Fe(II) and Fe weakly organic complexed forms are the most easily assimilated species by phytoplankton. The role played by the natural organic ligands excreted by the cyanobacteria *Synecococcus* PCC 7002 on the Fe(II) oxidation rate was studied at different stages of growth, considering changes in the organic exudation of the cyanobacteria, associated with growth at two different scenarios of iron availability. The oxidation processes of Fe(II) was studied at nanomolar levels and under different physicochemical conditions of pH (7.2−8.2), temperature (5−35°C) and salinity (10−37).

A pH-dependent Fe(III) reduction processes was detected, produced under light-induced conditions in the presence of exudates excreted in Fe-limited conditions. Photolytic reaction also modified the reactivity of those exudates with respect to Fe(II), increasing its lifetime in seawater. Without light mediated processes, organic ligands excreted under iron deficient conditions intensified the Fe(II) oxidation at the low pH < 7.5. In the presence of organic exudates produced under Fe-replete conditions the experimental rate always decreased with respect to control seawater.

A kinetic modelling approach to describe the speciation and the contribution of each Fe(II) species to the overall oxidation rate constant was applied, considering the experimental data and delimiting the equilibrium and redox constants between iron and major ligands present in solution. Two organic type ligands for the exudates of *Synechococcus* PCC 7002 with different iron-chelation properties (hydroxamic acids and phenolic compounds) were considered in the model. The individual Fe(II) oxidation rate constants for the organic ligands fitted in the model were analyzed in the context of Marcus theory. The half potential for reduction (E^0_{FeL})of Fe−siderophore type complex (Syn) and its photoproduct (^{PP}Syn) ranged between -0.082 and -0.335 V, whilst, the E^0 of Fe-phenolic complex (E^0_{Fe-Ph}) varied from 0.245 V to 0.380 V. The Fe(II) complexing constants were log $K_{Fe(II)\text{-}Syn}$ = 3.45 ± 0.29, log $K_{Fe(II)\text{-}SynPP}$ = 4.16 ± 0.34 and log $K_{Fe(II)\text{-}PPH}$ = 9.42 ± 0.81, and their

corresponding computed oxidation rates (log k_{app}) were 7.46 ± 0.41, 6.71 ± 0.27 and 1.42 ± 0.38 M^{-1} min^{-1}, respectively. The Fe(III)-binding strength fitted in the model for the siderophore type complex (22.69 ± 0.72) and its photo-product (21.31 ± 0.55) were in close alignment with the values measured in the ocean, for the classes L_1 and L_2 of Fe(III) ligands, whereas the polyphenol type ligands constant (18.75 ± 0.46) might correspond to weaker ligand classes (L_3 or L_4). The Fe(II)-PhC type ligand dominated the speciation between pH 7.9 and 8.5 when DOC levels reached 127.13 and 150.51 μmol C L^{-1} under Fe-limited and Fe-replete conditions, respectively. At those DOC concentrations, Fe(II)-Syn complex become the second most important contributor at pH values between 7.0 and 7.4 and Fe(II)-PhC exceed the 10% of contribution of k_{app} between 7.9 and 8.2 . Because of iron availability modifies the composition and nature of organic ligands excreted, the redox behaviour of Fe in the solution seem to be affected when iron fertilization events take place.

CHAPTER IV

4.1 Introduction

In seawater, organic ligands have been categorized according to their binding affinities for iron (Gledhill and Buck, 2012; Boyd and Tagliabue, 2015). Due to similarities in the conditional stability constants, the siderophores (iron chelating compounds with low molecular weight that are generated by some prokaryote microorganism in response to iron stress conditions (Hider and Kong, 2010)) probably make up an important component of the strongest organic Fe-binding ligands (L_1), which dominate the iron(III) speciation in open surface ocean waters (Mawji et al., 2008). Moreover, the Fe(III)-siderophore complexes with hydroxyl-carboxylic acid moieties are photoreactives, which leads to reduction of Fe(III) to Fe(II) and the oxidation of the ligand through the loss of a molecule of CO_2 and two protons (Barbeau et al., 2001; Ito and Butler, 2005; Kpper et al., 2006). This irreversible reaction can also involve the destruction of the siderophore and the ultimate formation of un-complexed Fe(III) (Amin et al., 2009a). Therefore the presence of the photoreactive hydroxyl-carboxylic acid moieties, in marine siderophores, has a significant influence on the redox behavior and bioavailability of iron in marine environments (Amin et al., 2009b; Grabo et al., 2014). In addition, the reduced Fe^{2+}, a soft Lewis acid, can interact with a strong chelate (i.e siderophores), facilitating its oxidation, due to the negative redox potentials observed for Fe-L_1 complexes (Harrington and Crumbliss, 2009). Likewise, the Fe(III)-siderophore complexes can undergo one electron reduction, without photolytic mediation, to give the corresponding Fe(II) complexes, since donor ligands control the redox potentials for the Fe^{2+}/Fe^{3+} couple (Dhungana and Crumbliss, 2005).

Donor-acceptor interactions are also a common phenomenon, occurring within all natural hydroxy-or polyhydroxy-aromatic substances that form appropriate acceptors upon partial oxidation through either biochemical or photochemical pathways (Jiang and Kappler, 2008). For example, catechol, a characteristic phenolic functional group, can form ferric complexes and subsequently decompose to produce Fe(II) and a semiquinone radical (Santana-Casiano et al., 2010). Polyphenols can also form complexes although their affinity for Fe(III) is noticeably lower than that

of some hexadentated siderophores, such as enterobactin or bacillibactin (Butler and Theisen, 2010). Phenolic compounds chelate iron to produce relatively stable phenolic Fe complexes, avoiding the iron precipitation in oxidative conditions (Wu et al., 2016). The polyphenols have been extensively studied for their ability to produce reactive oxygen species (such as through radical scavenging) or to prevent, by binding iron, the generation of these radicals (López-Alarcón and Denicola, 2013). Although the presence of nanomolar levels of polyphenols might decreases the Fe(II) oxidation rate (Santana-Casiano et al., 2014) and might increases the Fe uptake rate by phytoplankton (Maldonado et al., 2005), there is still scant understanding of how affect their presence to the redox behavior and bioavailability of iron in the ocean.

Inorganic Fe(II) and weakly organic complexed Fe forms are the species most easily assimilated by phytoplankton (Shaked and Lis, 2012). Iron availability can cause modifications in the structure of phytoplankton community (Trick et al., 2010), as well as, alterations in the physiology of photosynthetic microorganism (Achterberg et al., 2013; Ryan-Keogh et al., 2013) which can determine the release of organic exudates (Croot et al., 2007). Recently, in open ocean, the spatial and temporal dynamics of most of these natural organic ligands, denote they have been biosynthesized in situ (Boyd and Tagliabue, 2015; Roy and Wells, 2011). Accordingly, the presence and role of phenolic compounds and siderophores in seawater, that can simultaneously act as Fe-chelates and Fe(III)-reducing agents, should be appraised. Thereby, laboratory studies are highly recommendable, in order to elucidate the role played by the natural exudates on the redox chemistry of iron. Recently, studies with exudates obtained from cultures of eukaryote phytoplankton have evaluated their effect on the Fe(II) oxidation rates (González et al., 2014; Steigenberger et al., 2010). Nevertheless, currently, the iron redox behavior in presence of cyanobacterial exudates is poorly characterized.

Marine picophytoplankton, accounts for 25% of global ocean primary productivity (Uitz et al., 2010). The genus *Synechococcus* are the most widely distributed group of photosynthetic prokaryote across the world's (Flombaum et al., 2013),. The variation in *Synechococcus* abundance is controlled by environmental

parameters such as temperature, salinity, light and availability of inorganic nutrients (Rajaneesh and Mitbavkar, 2013). Furthermore some *Synechococcus* strains have showed the capacity to produced polyphenolic compounds and siderophores under iron deficiency conditions (Li et al., 2007; Trick and Wilhelm, 1995). In the present study we have selected the cyanobacteria *Synechococcus* (strain PCC 7002), in order to evaluate the effect of their exudates on the Fe redox cycling in seawater. The aim of this research has been to study the effect of organic exudates of *Synechococcus*, both on the Fe(II) oxidation rate and on Fe(III) reduction rate, in terms of the concentration of natural ligands, pH, temperature and salinity. The reactivity of the excreted ligands, as function of iron availability in medium, has been also analysed. A kinetic model has been developed in order to compute the Fe(II) speciation in presence of *Synechococcus* exudates. Having into account the chemical assays, carried out in a previous study and exposed in the chapter III, two specific types of ligands with redox behavior well differentiated, have been considered in the model. In addition, the kinetic modeling approach has been carried out in order to elucidate the contribution of Fe(II) species to the overall rate constant. In this contest, the Marcus theory (Marcus, 1956) has been applied to the Fe(II)-ligands oxidation rates, to evaluate if an outer-sphere electron transfer process controls the oxygenation of Fe(II) in the presence of natural cyanobacterial exudates.

4.2 Material and methods

4.2.1 Sampling and cultures

Figure 1 shows the layout of experimental method followed in order to obtain the seawater enriched with organic exudates from *Synechococcus* PCC 7002. Both UV-treatment and characteristics of sampled seawater used for this study, as well as the nutrient enrichment, to which has been subjected, are described in the point 2.2.1 of chapter II. In turn, the experimental procedure and determination of the organic ligands from exudates of *Synechococcus* PCC 7002 are reported during the chapter III.

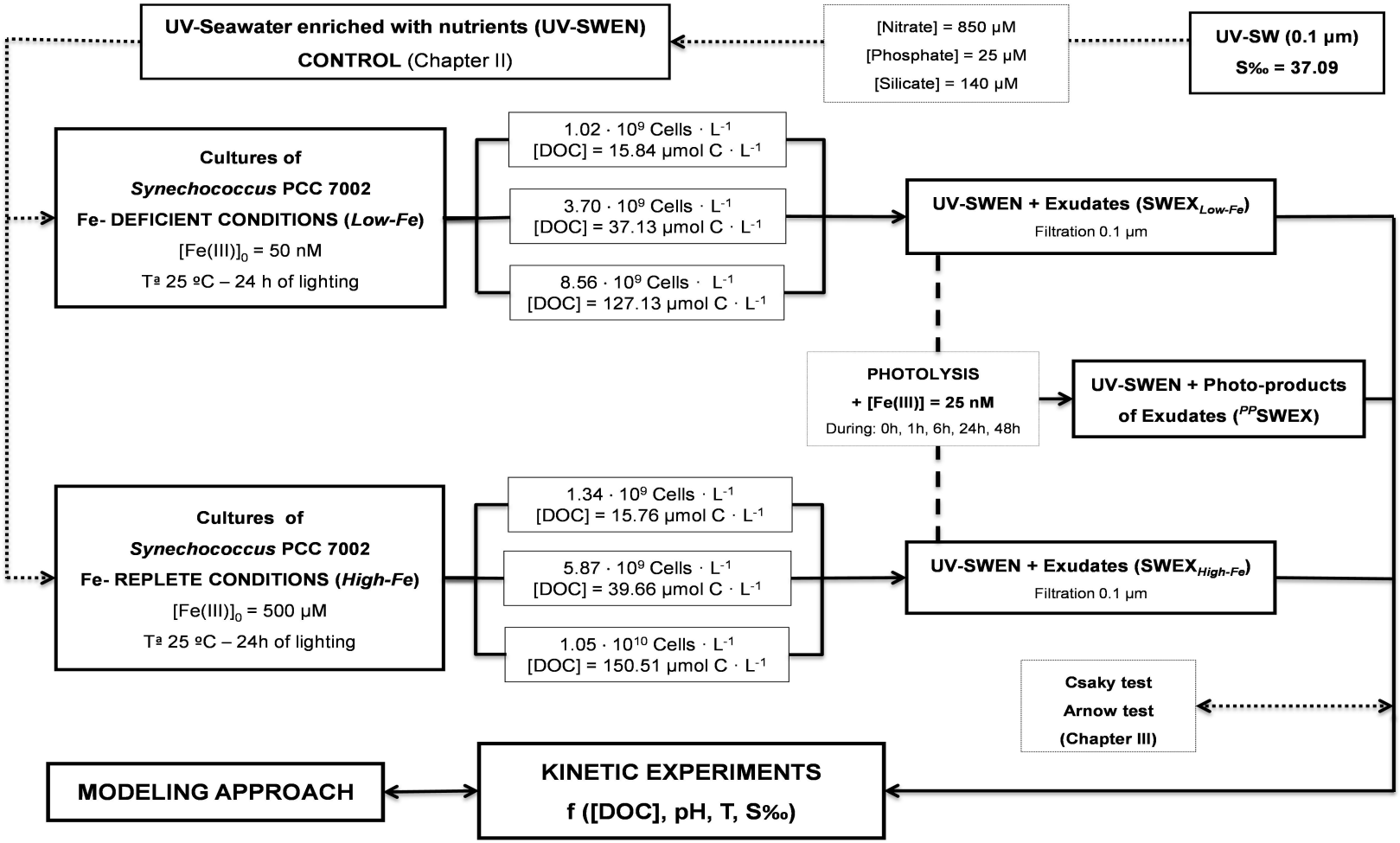

Fig. 4.1 Flowchart of method followed in order to obtain the seawater enriched with organic exudates from the *Synechococcus* PCC 7002 cultures and subsequent experimental procedure.

4.2.2 Kinetic studies and theory

The Fe(II) oxidation experiments were carried out as a function of the pH, temperature, and salinity. The Fe(III) reduction experiments were performed as a function of the pH at 25 ºC. Both studies were done in seawater control (UV treated seawater enriched with nutrients, SWEN) and for the same seawater enriched with organic exudates from *Synechococcus,* both from Fe-deficient ($SWEX_{Low\text{-}Fe}$) and Fe-replete conditions ($SWEX_{High\text{-}Fe}$).

All kinetic studies took place in a 250 ml glass thermostatic reaction vessel with saturated air conditions, by bubbling pure air through the solution for one hour and keeping a controlled bubbling in order to achieve and keep the desired pH value. Small adjustments were done by automatic additions of HCl (1 M) using a titrator system (Tritino 719S, Methrom). The pH was measured potentiometrically, on the free hydrogen ion scale (pH_F = -log[H^+]) with an Orion pH-meter. Tris-(hydroximethyl)aminomethane(tris)-artificial seawater buffer (0.005 mol kg^{-1} Tris and Tris-HCl in artificial seawater) was used to calibrate the combination electrode (Ross Combination, glass body). The temperature was set with an error of ± 0.02 ºC in a NesLab circulating bath. Over all the studies the effect of temperature and salinity was appraised on the pK* of the Tris-buffers (Millero, 1986). The [O_2] were determined from the theoretical solubility equations (Benson and Krause, 1984).

Fe(II) concentrations were measured spectrophotometrically using the ferrozine method revisited (Viollier et al., 2000). The oxidation/reduction studies were carried out taking this technique, because allowed following the full-spectra over time and detect any intermediate or interaction formed during the experiments. A blank, with UV treated seawater and reagents, was carried out for each experiment. During the oxidation/reduction experiments, the addition of Fe(II)/Fe(III) to the reaction cell corresponded to time zero. Then, at selected times, 10 ml of solution was added to the 25 ml glass flask that contained the reagents. A 5 m long waveguide capillary flow cell (World precision instrument^{TM}) connected to the UV-VIS detector S2000 (Ocean Optics^{TM}) was used to measure Fe(II) concentrations at nano-molar levels. The limit detection for the Fe(II) concentration determination was 0.7 nM.

The overall rate equation of reduction of Fe(III) with organic ligands can be represented by

$$d[Fe(III)]/dt = - k_{red} [Fe(III)]^a [L]^b \quad (30)$$

where, a and b are the order of the reactions with respect to Fe(III) and organic ligand (L) respectively. The Fe(II) reduction rate was determined by measuring the regeneration of Fe(II). The disappearance of total Fe(III) ($[Fe(III)]_D = [Fe(III)]_0 - [Fe(II)]$), where the subscript zero denotes the initial concentration, was calculated as a function of time under pseudo-first conditions, assuming an excess of L. The first-order rate constant for the reduction of Fe(III) under these conditions is given by,

$$d[Fe(III)]/dt = - k^* [Fe(III)] \quad (31)$$

where $k^* = k_{red}[L]^b$.

The oxidation kinetics of Fe(II) with O_2 can be expressed as a function of the apparent oxidation rate (k_{app}) and defined by the equation (Santana-Casiano et al., 2006).

$$d[Fe(II)]/dt = - k_{app} [Fe(II)] [O_2] \quad (18)$$

Under air saturated conditions the pseudo-first order rate constant is obtained according to the equation,

$$d[Fe(II)]/dt = - k' [Fe(II)] \quad (19)$$

where, $k' = k_{app} [O_2]$.

4.2.3 Photo-reaction

Photoproducts (*PP*) of natural organic ligands were obtained by irradiating the exudates of *Synechococcus* (filtered by 0.1 μm), with previous addition of ferric chloride hexahydrate (Sigma). The photo-reaction was performed in a clean culture chamber (Friocell FC11), at 80000 flux, with temperature-controlled (25ºC) and bubbling pure air, in acid-washed and autoclaved flasks. The initial concentration of Fe(III) added to the solution was always 25 nM. The solutions were blended during

the irradiation with a Teflon-coated magnetic stirrer. The duration of irradiations ranged from 1 h to 48 h. To evince the photolysis effect in the exudates, additions of iron in the exudates ([Fe(III)] = 25 nM), without irradiation, was also carried out

4.2.4 Numerical model

The relationship between Fe(II) oxidation rate constant and the concentration of DOC, pH, temperature and salinity was examined by regression analysis. A probability level of $\alpha = 0.05$ was considered.

A kinetic model was developed using the Gepasi software (Version 3.30). The overall and individual rate constants *ki* were obtained by adjusting experimental Fe(II) concentrations/time pairs of data to the model output as indicated elsewhere (Mendes, 1997). The kinetic model took into consideration all the experimental conditions in this study.

4.3 Results and discussion

4.3.1 Photochemical reduction experiments

The reduction of Fe(III) was studied in both UV-treated seawater enriched with nutrients (SWEN) and seawater enriched with exudates (SWEX) of *Synechococcus* PCC 7002, produced under deficient and replete conditions, ($[DOC]_{Low\text{-}Fe}$ = 127.13 ± 8.38 μmol C L^{-1} and $[DOC]_{High\text{-}Fe}$ = 150.51 ± 8.59 μmol C L^{-1}, respectively) at two different pH values (7.5 and 8.0). All Fe(III)-reduction experiments were performed under oxygen saturated conditions and constant temperature (25 ºC). The initial Fe(III) concentration (t = 0) in the reaction-cell reaction was always 250 nM. The presence of the Fe(II) chelator ferrozine in the solution acted as a sink for the regenerated Fe(II), thereby preventing any back reactions and allowing the determination of the direct reduction process. The maximum Fe(II) concentrations measured during the reaction time were 3.6 ± 0.2 nM and 5.5 ± 0.3 nM at pH 8.0 and pH 7.5 respectively (Fig. 4.2). The regeneration

of Fe(II) was only detected under light conditions. Therefore the ligand-to-metal charge transfer reaction did not appear to be a non-dissociative reduction of organically complexed iron(III), which is induced by O_2^- without photolytic mediation (Garg et al., 2007).

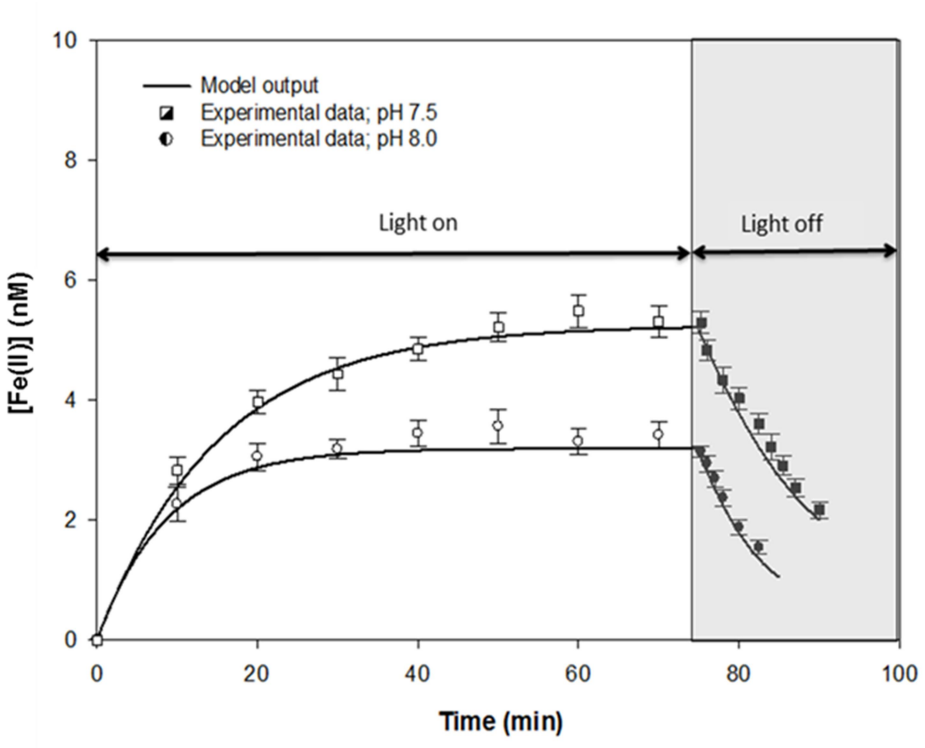

Fig. 4.2 Photo-reduction of Fe(III) to Fe(II) in presence of organic ligands ([DOC] = 127.13 ± 8.38 µmol C L^{-1}) excreted by *Synechococcus* PCC 7002, under Fe limited conditions ($SWEX_{Low\text{-}Fe}$), with irradiation of simulated sunlight, at pH 8.0 and pH 7.5. At t = 0 min, irradiation was begun and at t=75 min, the light was turned (grey box). Symbols are the average of three measurements of concentrations of Fe(II). Bars denote the error standard of data estimate and the lines are the model kinetic fit. $[Fe(III)]_0$= 250 nM. Temperature (25 ºC) and salinity (37.09) were kept constant.

Under the experimental conditions of this study, the presence of phenolic compounds in the exudates of *Synechococcus* PCC 7002 (Samperio-Ramos et al., submitted) might also favor the reduction of Fe(III) to Fe(II) (Santana-Casiano et al., 2014). Nevertheless, the interaction of the benzoquinone intermediate with divalent cations highly present in the seawater waters, such as Mg^{2+} and to a lesser extent Ca^{2+}, inhibited this process photo-independent (Santana-Casiano, et al; 2010). In addition, the photo mediated electronic reduction of Fe(III) to Fe(II) was only carried out in presence of exudates excreted under Fe-deficient conditions ($SWEX_{Low\text{-}Fe}$). One of the specific characteristics of the exudates of *Synechococcus* PCC 7002,

when those are excreted under low Fe concentrations, is la presence of hydroxamate-type siderophores (synechobactin), which are comprised of a citric acid backbone linked to two 1,3-diaminopropane units (Boiteau et al., 2013; Boiteau and Repeta, 2015; Ito and Butler, 2005). The Fe(III)-synechobactin complex undergoes a photolytic perturbation into the charge transfer band, from the α-hydroxy carboxylate moiety to Fe(III), inducing the ligand oxidation and release of CO_2 along with reduction of Fe(III) to Fe(II) (Ito and Butler, 2005). Accordingly, in the present study it was assumed that the bulk of photolytically reduced Fe(II) proceeded from the Fe(III)-siderophore complexes.

The photo-reduction of Fe(III) was pH dependent, showing higher Fe(II) regeneration rate with increasing $[H^+]$, which suggests that the photo-reduction was highly affected by the Fe(III)-organic speciation The photo-reduction of Fe(III) followed a pseudo-first order kinetic with rate constants increasing as pH decreased from $\log k^* = -3.05 \pm 0.05$ min^{-1} at pH = 8.0 to $\log k^* = -2.92 \pm 0.02$ min^{-1} at pH 7.5. Both results were comparable with the photo-reduction rate determined by Miller et al. (1995) in a solar simulation system with Narragansett Bay water. Nevertheless, they were an order of magnitude lower than those obtained for the Fe(III)-aquachelin at pH 5 (Barbeau et al., 2001). The disagreement in the results might be due to the structural differences of ligands studied, what at the same time could induce differences in the reactivity of α-hydroxy carboxylic moieties (Rijkenberg et al., 2006; Sayre et al., 2010). In addition, it should also be appraised that the photo-reduction of dissolved inorganic Fe(III), by reaction with O_2^- , is greatly significant at pH < 7.0 (King et al. 1993; Rose and Waite, 2005; Rose, 2012).

After the light source was extinguished, the Fe(II) apparent oxidation rate measured was 2.77 ±.0.03 M^{-1} min^{-1} and 2.40 ± 0.04 M^{-1} min^{-1} for pH 8.0 and pH 7.5 respectively. These values were significantly different to the results obtained with not-light treated exudates (Tables 4.1 and 4.2), which suggests the photo-reaction modified the behaviour of organic ligands-Fe(II) complexes. Citrate-containing siderophores can vary their reactivity with Fe(II), due to a change of coordination between metal and ligand, via the formation of a ketoenolate group, derived from a ketoglutarate moiety, in the decarboxylation reaction (Butler and Theisen, 2010).

Table 4.1 Log k_{app} and the half time ($t_{1/2}$) accounted for oxidation experiments in the seawater enriched both with nutrients (SWEN; control) and exudates released under Fe-deficient conditions ($SWEX_{Low\text{-}Fe}$) as a function of pH, temperature and salinity.

Media	pH	Temperature (ºC)	S	Log k_{app} ($M^{-1} \cdot min^{-1}$)	± SE	$t_{1/2}$ (min)
UV-treated Seawater (Control)	8.2	25	37.09	3.26	0.01	1.8
	8.0	25	37.09	3.03	0.01	3.1
	7.8	25	37.09	2.78	0.02	5.4
	7.5	25	37.09	2.54	0.02	9.4
	7.2	25	37.09	2.30	0.01	16.3
	8.0	35	37.09	3.61	0.01	0.9
	8.0	15	37.09	2.41	0.02	10.6
	8.0	5	37.09	1.91	0.03	27.0
	8.0	25	30.00	3.11	0.02	2.4
	8.0	25	20.00	3.22	0.01	1.8
	8.0	25	10.00	3.38	0.01	1.1
$SWEX_{Low\text{-}Fe}$ from $1.02 \cdot 10^9$ cell/L [DOC] = 15.84 ± 6.12 µmol C L^{-1}	8.2	25	37.09	3.23	0.03	1.9
	8.0	25	37.09	2.98	0.03	3.4
	7.8	25	37.09	2.80	0.02	5.2
	7.5	25	37.09	2.53	0.02	9.7
	7.2	25	37.09	2.28	0.03	17.2
	8.0	35	37.09	3.61	0.02	0.9
	8.0	15	37.09	2.38	0.03	11.4
	8.0	5	37.09	1.92	0.03	26.5
	8.0	25	30.00	3.00	0.04	3.1
	8.0	25	20.00	3.07	0.03	2.5
	8.0	25	10.00	3.17	0.02	1.9
$SWEX_{Low\text{-}Fe}$ from $3.70 \cdot 10^9$ cell/L [DOC] = 37.13 ± 4.30 µmol C L^{-1}	8.2	25	37.09	3.10	0.03	2.6
	8.0	25	37.09	2.92	0.02	3.9
	7.8	25	37.09	2.72	0.02	6.2
	7.5	25	37.09	2.52	0.01	9.9
	7.2	25	37.09	2.33	0.02	15.3
	8.0	35	37.09	3.46	0.04	1.3
	8.0	15	37.09	2.32	0.05	12.9
	8.0	5	37.09	1.81	0.04	34.3
	8.0	25	30.00	2.93	0.03	3.7
	8.0	25	20.00	3.00	0.03	3.0
	8.0	25	10.00	3.06	0.03	2.5
$SWEX_{Low\text{-}Fe}$ from $8.56 \cdot 10^9$ cell/L [DOC] = 127.13 ± 8.38 µmol C L^{-1}	8.2	25	37.09	3.02	0.03	3.1
	8.0	25	37.09	2.82	0.02	5.0
	7.8	25	37.09	2.67	0.02	6.9
	7.5	25	37.09	2.51	0.02	10.1
	7.2	25	37.09	2.37	0.02	13.9
	8.0	35	37.09	3.27	0.04	2.0
	8.0	15	37.09	2.21	0.03	16.8
	8.0	5	37.09	1.67	0.04	46.8
	8.0	25	30.00	2.82	0.03	4.8
	8.0	25	20.00	2.86	0.04	4.1
	8.0	25	10.00	2.94	0.04	3.2

Table 4.2 Oxidation rate (log k_{app}) and the half time ($t_{1/2}$) accounted for oxidation experiments in the seawater enriched with exudates produced under Fe-replete conditions ($SWEX_{High\text{-}Fe}$) as a function of pH, temperature and salinity.

Media	pH	Temperature (ºC)	S	k_{app} ($M^{-1} \cdot min^{-1}$)	± SE	$t_{1/2}$ (min)
$SWEX_{High\text{-}Fe}$ from $1.34 \cdot 10^9$ cell/L	8.0	25	37.09	2.94	0.03	3.7
[DOC] = 15.76 ± 3.52 µmol C L^{-1}	7.5	25	37.09	2.49	0.03	10.5
$SWEX_{High\text{-}Fe}$ from $5.87 \cdot 10^9$ cell/L	8.0	25	37.09	2.88	0.02	4.4
[DOC] = 39.66 ± 6.73 µmol C L^{-1}	7.5	25	37.09	2.43	0.03	12.1
$SWEX_{High\text{-}Fe}$ from $1.05 \cdot 10^{10}$ cell/L [DOC] = 150.51 ± 8.59 µmol C L^{-1}	8.2	25	37.09	2.90	0.03	4.1
	8.0	25	37.09	2.72	0.02	6.3
	7.8	25	37.09	2.55	0.02	9.2
	7.5	25	37.09	2.31	0.03	15.9
	7.2	25	37.09	2.14	0.02	23.7
	8.0	35	37.09	3.11	0.04	2.9
	8.0	15	37.09	2.12	0.03	21.0
	8.0	5	37.09	1.55	0.02	61.7
	8.0	25	30.00	2.68	0.03	6.5
	8.0	25	20.00	2.70	0.03	5.9
	8.0	25	10.00	2.76	0.02	4.9

Therefore, the next series of kinetic studies were carried out in order to determine these indirect photochemical effects in the exudates excreted under Fe-deficient conditions and their impact in the oxidation kinetics of Fe(II).

4.3.2 Photolysis effect on the oxidation rate

The Fe(II) oxidation studies were performed in seawater enriched with natural exudates released under Fe-limited conditions ([DOC] = 127.13 ± 8.38 µmol C L^{-1}) and subsequently photo-treated. Under lighting and air-saturated conditions, the photo-products were generated through the addition of the Fe(III) (25 nM) to the solution, which corresponded to the zero time. Then, the effect of the photoproducts ($^{PP}SWEX_{Low\text{-}Fe}$) on k_{app}, was evaluated as a function of light time exposure (from 0h to 48h). When the sample was maintained in darkness (48 h), the effect of adding Fe(III) on the k_{app} was negligible (Fig. 3). Accordingly, the Fe(II) oxidation rate, obtained from exudates kept in darkness after adding Fe(III), was considered as reference (blank). Moreover, the oxidation kinetic of 25 nM Fe(II) in exudates photo-treated, was studied in darkness, aerating the solution with pure air for 1 h, prior and

during the experiments, to avoid interferences, due to regeneration of Fe(II) originated from the previous Fe(III) addition.

Table 4.3 Apparent Fe(II) oxidation rate (log k_{app}) and the half time ($t_{1/2}$) accounted for Fe(II) oxidation experiments in seawater enriched with organic exudates, as a function of pH, temperature and salinity. The exudates was released under Fe-deficient conditions and was subjected to photolysis reaction for 24 h ($^{PP}SWEX_{Low\text{-}Fe}$) in presence of Fe(III) (25 nM).

Media	pH	Temperature (ºC)	S	k_{app} ($M^{-1} \cdot min^{-1}$)	± SE	$t_{1/2}$ (min)
$^{PP}SWEX_{Low\text{-}Fe}$ from $1.02 \cdot 10^9$ cell/L	8.0	25	37.09	2.97	0.02	3.5
[DOC] = 15.84 ± 6.12 µmol C L^{-1}	7.5	25	37.09	2.51	0.03	10.0
$^{PP}SWEX_{Low\text{-}Fe}$ from $3.70 \cdot 10^9$ cell/L	8.0	25	37.09	2.90	0.02	4.1
[DOC] = 37.13 ± 4.30 µmol C L^{-1}	7.5	25	37.09	2.48	0.03	10.7
$^{PP}SWEX_{Low\text{-}Fe}$ from $8.56 \cdot 10^9$ cell/L [DOC] = 127.13 ± 8.38 µmol C L^{-1}	8.2	25	37.09	2.93	0.02	3.8
	8.0	25	37.09	2.76	0.02	5.6
	7.8	25	37.09	2.61	0.03	8.1
	7.5	25	37.09	2.39	0.03	13.3
	7.2	25	37.09	2.22	0.02	19.8
	8.0	35	37.09	3.19	0.03	2.5
	8.0	15	37.09	2.16	0.04	18.8
	8.0	5	37.09	1.61	0.02	54.6
	8.0	25	30.00	2.74	0.03	5.7
	8.0	25	20.00	2.79	0.03	4.8
	8.0	25	10.00	2.83	0.03	4.1

The oxidation experiments were carried out at two different pH values (8.0 and 7.5). Figure 4.3 shows a decrease of log k_{app}, in both pH studied, as well as it happened when the photo-oxidation process was prolonged, reaching minimum values (log k_{app} = 2.76 ± 0.02 M^{-1} min^{-1} and log k_{app} = 2.39 ± 0.03 M^{-1} min^{-1} at pH 8 and pH 7.5 respectively) in the exudates that were subject to 24 h of light irradiation. When the light exposure was extended to 48h, no differences were found in the log k_{app} (Fig 4.3), indicating the photolysis could be considered complete (>95%) after the first 24 h of irradiation. The experimental data (Tables 4.1 and 4.3) indicated that, regarding Fe(II), the reactivity of exudates generated after photolysis ($^{PP}SWEX_{Low\text{-}Fe}$) was lower than to the original and non-phototreated exudates ($SWEX_{Low\text{-}Fe}$), decreasing the Fe(II) oxidation rate. During iron starvation, *Synechococcus* PCC 7002 synthesizes a citrate siderophore, synechobactin, which is stable as uncomplexed acid, but when coordinates to Fe(III) undergoes a photo-oxidation of its citrate backbone (Ito and Butler, 2005). The loss of the α-hydroxy carboxylate

moiety might play a key role in the Fe(II) oxidation rate stabilization, involving that the Fe(II) regenerated during the photolytic process, can persist in surface seawater for longer periods.

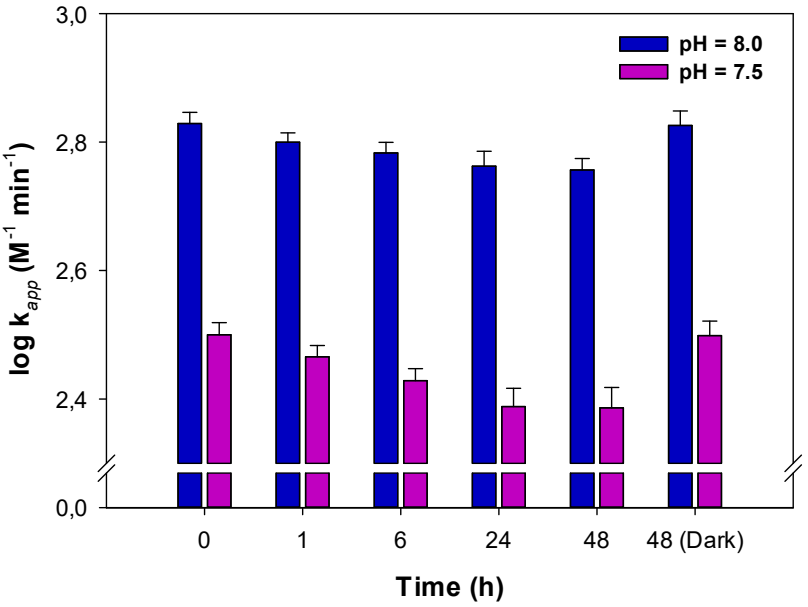

Fig. 4.3 Photolysis effect on the Fe(II) oxidation rate constant (at pH 8.0 and 7.5), as a function of irradiation time. The seawater was enriched with natural exudates of *Synechococcus* PCC 7002 excreted under Fe-deficient conditions ($SWEX_{Low\text{-}Fe}$; [DOC] = 127.13 ± 8.38 µmol C L^{-1}). The temperature (25 ºC) and salinity (37.09) were kept constant. Bars denote standard error.

The bulk of iron organic ligands excreted by *Synechococcus*, that modify the redox behavior of iron in the present study, are included in the DOC fraction. Due to the cultures of *Synechococcus* are a satisfactory source of natural organic ligands, the next series of experiments were carried out in order to determine the effect of natural organic exudates released during the cyanobacteria growth on the Fe(II) oxidation rate.

4.3.3 DOC dependence

The Fe(II) oxidation rates as a function of DOC were determined with the effect of exudates, produced during the cyanobacterial growth under the different Fe

treatments (Fig. 4 and Table 4.1-4.3). The oxidation of 25 nM Fe(II) was studied both at pH 8.0 and 7.5, at constant temperature (25 ºC) and salinity (37.09). Figure 4.4 shows the effect of DOC released under different Fe-treatments by cultures of *Synechococcus* on the Fe(II) oxidation constant rate.

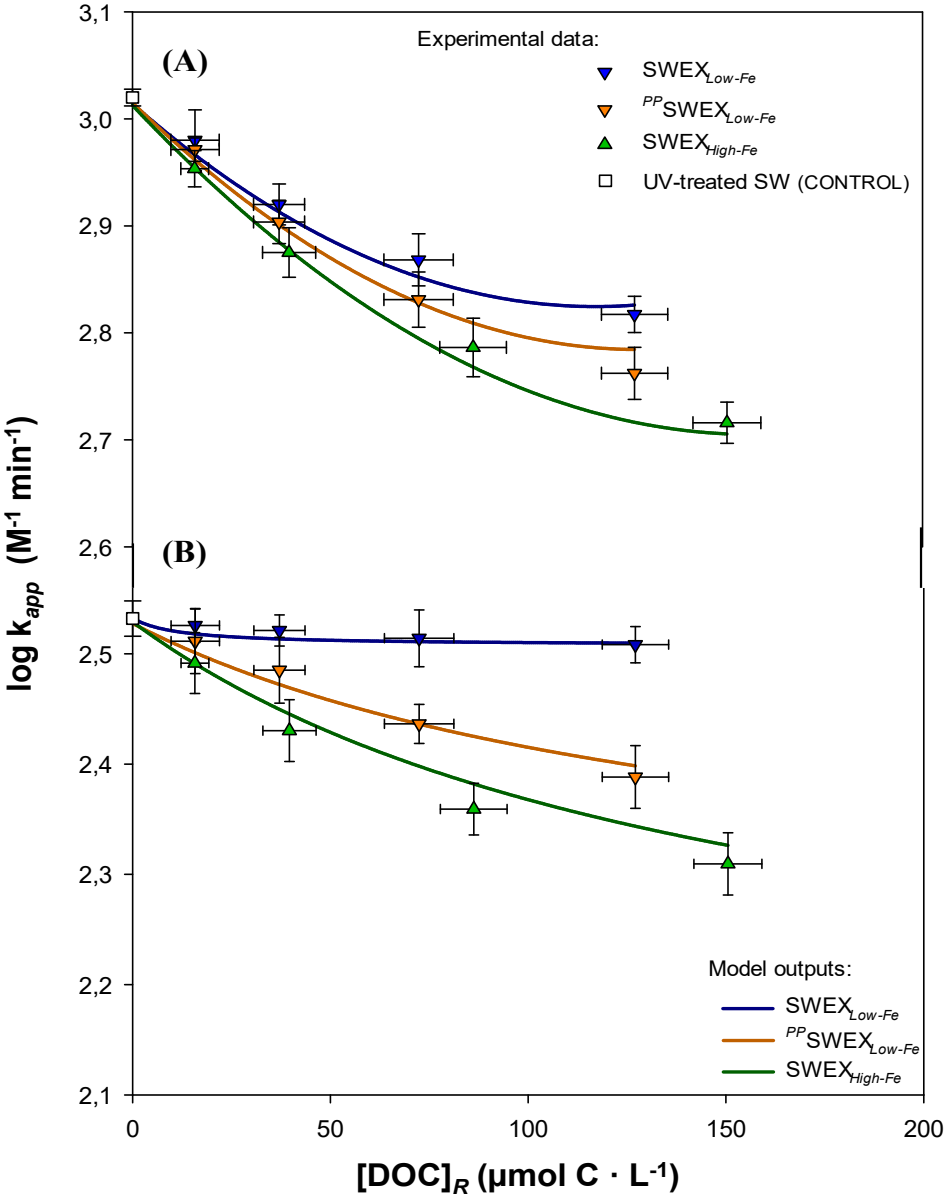

Fig 4.4 Fe(II) oxidation rates at pH = 8.00 (A) and pH 7.50 (B), as a function of dissolved organic carbon released ($[DOC]_R$) under Fe-replete ($SWEX_{High-Fe}$) and under Fe-deficient conditions, without ($SWEX_{Low-Fe}$) and with previous photolysis ($^{PP}SWEX_{Low-Fe}$), Tª = 25 ºC and S‰ = 37.09). Symbols represent the experimental data and the lines show the model outputs. Bars denote standard error.

The differences on Fe(II) oxidation rate ($\Delta \log k_{app} = \log k_{app}^{DOC} - \log k_{app}^{Control}$), between seawater control and seawater enriched with exudates excreted

under Fe-deficient conditions were more pronounced at pH 8.0 than pH 7.5. While at pH 8.0 the Δlog k_{app} increased with DOC levels reaching maximum values (0.21 M^{-1} min^{-1}) at the maximum DOC produced by cells the drop at pH 7.5 was only 0.03 (M^{-1} min^{-1}). When these exudates of *Synechococcus* were photo-treated for 24h ($^{PP}SWEX_{Low\text{-}Fe}$), the Fe(II) oxidation rate declined more intensely, in relation to the seawater control. The differences were 0.27 and 0.15 (M^{-1} min^{-1}) for pH 8.0 and pH 7.5, which supposed a drop in k_{app} of 46% and 29% respectively. In presence of exudates of *Synechococcus,* excreted under Fe-replete conditions ($SWEX_{High\text{-}Fe}$; $[DOC]_R$ = 150.51 ± 8.59 μmol C L^{-1}), Δlog k_{app} at pH 8.0 was 0.31 (M^{-1} min^{-1}), while at pH 7.5, the difference was 0.23 (M^{-1} min^{-1}). Therefore, the Fe(II) oxidation rate constant decreased by 51% and 42% for pH 8.0 and 7.5 respectively. The results presented here endorsed the observations carried out in different marine systems with variability both in rate of iron inputs and productivity (Shaked, 2008; Breitbarth et al., 2009; Roy and Wells, 2011). For example, in waters of the iron-limited eastern subarctic Pacific waters, was observed an increase on the overall Fe(II) oxidation rate, near the chlorophyll maximum, due to the high levels of strong Fe(III)-complexing organic ligands (e.g., siderophores) measured (Roy and Wells, 2011). While in the Baltic Sea during a cyanobacterial bloom, were measured Fe(II) oxidation rates (Breitbarth et al., 2009) significantly lower than those both in theoretical values (Millero et al. 1987) and in experimental results obtained with Fe-limited ocean water (Roy and Wells, 2011).

The parabolic decrease in the Fe(II) oxidation rate in each Fe-treatment (Fig. 4.4 and Table 4.4) has to be directly linked to the effect of the organic compounds, excreted by the cyanobacteria. The exudates produced under both Fe-replete and Fe-limited conditions presented half-life times (Tables 4.1 and 4.2) that raised as DOC levels increased in solution, denoting that Fe(II) could remain in surface seawater for longer periods of time due to Fe(II)−organic ligand interaction. Li et al. (2007) detected phenolic content in natural organic exudates of marine *Synechococcus* sp. The presence of dihydroxiphenol moities in exudates of *Synechococcus* might explain the drop in the Fe(II) oxidation rate here observed, since polyphenolic compounds chelate ferrous ions and can prevent the Haber-Weiss redox cycle, occupying the coordination sites in the metal (Santana-Casiano et al., 2014). In

addition, the absence of hydroxamate ligands in solution under Fe-replete conditions (Samperio-Ramos et al., submitted), correlated with the decline in the Fe(II) oxidation rate. Notwithstanding, the iron availability in *Synechococcus* cultures, might also modify the composition and nature of organic ligands excreted, that affect to the speciation and reactivity of Fe(II) in the solution.

Table 4.4 Coefficients for parabolic-decay relationship between Fe(II) oxidation rate and DOC release (log $k_{app} = y_0 + (a \cdot b) / (b + [DOC]_R)$, at pH 8.00 and 7.50. Natural organic exudates were excreted under Fe-deficient, without ($SWEX_{Low\text{-}Fe}$) and with previous photoreaction for 24 h ($^{PP}SWEX_{Low\text{-}Fe}$), and Fe-replete conditions ($SWEX_{High\text{-}Fe}$). Temperature (25 ºC) and salinity (37.09) were kept constants.

Fe-treatment	pH	y_0	a	b	r^2	±SE
$SWEX_{Low\text{-}Fe}$	8.00	2.63 (±0.08)	0.40 (±0.07)	123.12 (±45.29)	0.994	0.09
	7.50	2.48 (±0.06)	0.05 (±0.01)	133.18 (±64.51)	0.989	0.10
$^{PP}SWEX_{Low\text{-}Fe}$	8.00	2.58 (±0.04)	0.44 (±0.04)	93.08 (±18.23)	0.996	0.07
	7.50	2.23 (±0.09)	0.29 (±0.06)	129.61 (±76.66)	0.977	0.14
$SWEX_{High\text{-}Fe}$	8.00	2.56 (±0.03)	0.45 (±0.04)	79.25 (±11.88)	0.997	0.07
	7.50	2.16 (±0.03)	0.38 (±0.03)	100.67 (±17.20)	0.998	0.05

Since the oxidation process was modified by the presence of natural organic ligands, three DOC concentrations, excreted at three cyanobacterial growth stages (days 3, 6, and 12 to represent the initial, exponential and stationary phases, respectively), were selected in order to study the effect of pH, temperature, and salinity on the Fe(II) oxidation rate. These DOC concentrations, under Fe-deficient conditions, were 15.84 ± 6.12, 37.13 ± 4.30, and 127.13 ± 8.38 μmol C L^{-1}, excreted by 1.02×10^9, 3.70×10^9, and 8.56×10^9 cell L^{-1}, respectively. The DOC levels picked, for $SWEX_{High\text{-}Fe}$, were 15.76 ± 3.52, 39.66 ± 6.73, and 150.51 ± 8.59 μmol C L^{-1}, exuded by 1.34×10^9, 5.87×10^9, and 1.26×10^{10} cell L^{-1}, respectively.

4.3.4 pH dependence

The effect of pH on the k_{app}, was studied, in the range 7.2-8.2 with exudates of *Synechococcus*, produced both in Low-Fe conditions and High-Fe conditions (Fig 4.5), considering the DOC concentration in the solution. The photo-reactivity of

natural organic exudates, oozed under Low-Fe conditions, was also evaluated.

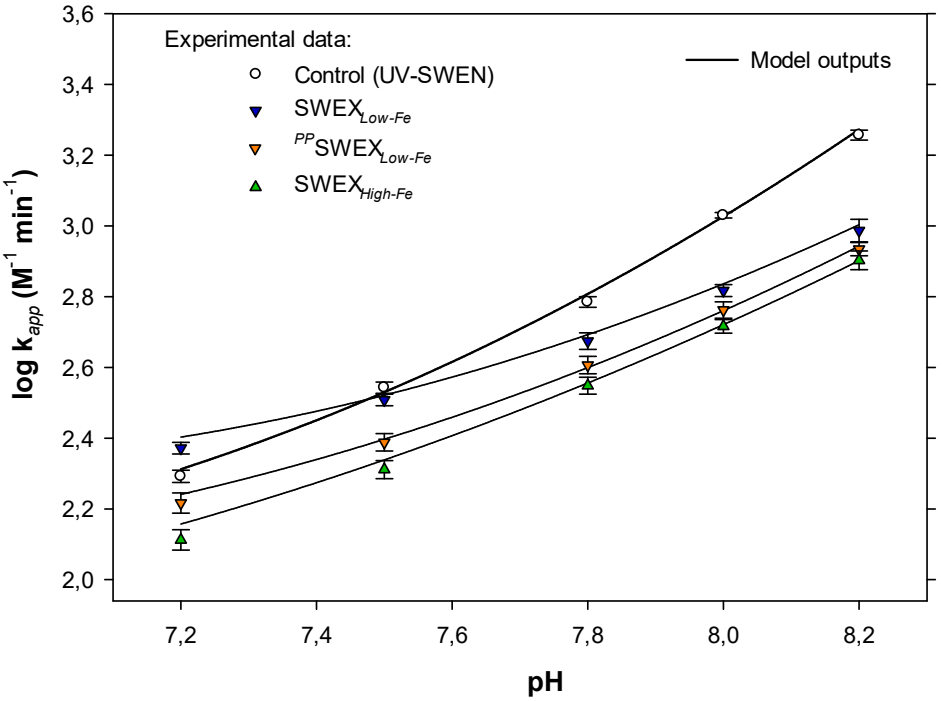

Fig 4.5 The Fe(II) oxidation rate constant as a function of the pH for the UV-treated seawater enriched with nutrients (control) and the seawater enriched with natural organic exudates, excreted by *Synechococcus* PCC 7002, under Fe-replete conditions ($SWEX_{High\text{-}Fe}$ with $[DOC]_R$ = 150.51 ± 8.59 µmol C L^{-1}) and under Fe-deficient conditions ($[DOC]_R$ = 127.13 ± 8.38 µmol C L^{-1}), without ($SWEX_{Low\text{-}Fe}$) and with previous photolysis ($^{PP}SWEX_{Low\text{-}Fe}$). Temperature (25 ºC) and salinity (37.09) were kept constant. The lines represent the output of model. Bars denote standard error.

The log k_{app} decreased as a function of the pH, giving the minimum oxidation rates at the lower values of pH studied (Fig 4.5). However, in the experiments conducted at pH lower than 7.5, in presence of $SWEX_{Low\text{-}Fe}$, the Fe(II) oxidation rate was increased compared to the UV-treated seawater (control). At pH 7.2 log k_{app} was 2.30 ± 0.01 M^{-1} min^{-1} in control seawater, while in the presence of exudates ($[DOC]_R$ = 127.13 ± 8.38 µmol C L^{-1}) the log k_{app} was 2.37 ± 0.02 M^{-1} min^{-1}. The Fe(II) oxidation rate constant increased by 17% due to its interaction with organic ligands. These results reveal that the organic ligands excreted under iron deficient conditions intensify the Fe(II) oxidation process at the lowest of pH range here studied. This increase is explained by the formation of an Fe(II)–ligand complex that has a higher oxidation rate than the inorganic Fe(II) species, since at pH ≤ 7.5, Fe^{2+} is clearly the dominant inorganic Fe(II) species in seawater (González et al., 2010; Samperio-

Ramos et al., 2016; Santana-Casiano et al., 2005) and thus readily available to form organic complexes.

Our results were comparable with other Fe(II) oxidation studies (Welch et al., 2002) carried out in Tris-buffer solution (pH 7.0), in the presence of hydroxamate siderophore, deferoxamine, Therefore, the presence of hydroxamate ligands, in exudates released under Fe-deficient conditions (Samperio-Ramos et al., submitted), would facilitate the Fe(II) oxidation, due to formation of Fe-complexes with large negative redox potential at pH < 7.5. In fact, the study carried out with water from Lake Graffen, where it was found a marked acceleration of Fe(II) oxidation rate at pH lower than 7.5, attributed to the presence of organic ligands (Emmenegger et al. 1998), corroborates the results here argued.

When the exudates of *Synechococcus*, produced in Fe-limited conditions, were photo-treated for 24 h ($^{PP}SWEX_{Low\text{-}Fe}$; $[DOC]_R$ = 127.13 ± 8.38 μmol C L^{-1}) the Fe(II) oxidation rate decreased at any pH value, regarding the studies conducted with UV-treated seawater and non-photo-treated natural exudates. It was obtained (Fig 4.5) that at pH 8.2 the log k_{app} changed from 3.26 ± 0.01 $M^{-1}min^{-1}$ (control) to 2.99 ± 0.03 $M^{-1}min^{-1}$ in $SWEX_{Low\text{-}Fe}$, and 2.93 ± 0.02 $M^{-1}min^{-1}$ in photo-treated exudates ($^{PP}SWEX_{Fe\text{-}Low}$). At pH 7.2, the log k_{app} varied from 2.30 ± 0.01 $M^{-1}min^{-1}$ (control) to 2.37 ± 0.02 $M^{-1}min^{-1}$ ($SWEX_{Low\text{-}Fe}$), and to 2.24 ± 0.02 $M^{-1}min^{-1}$ ($^{PP}SWEX_{Low\text{-}Fe}$). In relation to UV treated SWEN, the k_{app}, in presence of $^{PP}SWEX_{Low\text{-}Fe}$ decreased by 52% and 18% at pH 8.2 and 7.2, respectively, increasing the half-life time of Fe(II), as a function of pH, increase when the pH was reduced (Tables 4.1 and 4.3).

The Fe(II) oxidation rate also decreased in presence of $SWEX_{High\text{-}Fe}$ at any pH value (Fig 4.5 and Table 4.2), with the highest effect at [DOC] = 150.51 ± 8.59 μmol C L^{-1}. The same trend in the Fe(II) oxidation rates was obtained in an ocean acidification mesocosm experiments with Norwegian fjord water of high Fe-content, after phytoplankton bloom (Breitbarth et al., 2010). The authors suggested that the organic iron chelation affected the Fe(II) half-life time in the different CO_2 treatments, either because the organic complexes were the major pool of Fe(II) by photoreduction of Fe(III), or retarding the Fe(II) oxidation rate due to the direct effect of the biologically mediated Fe-ligands. Nevertheless, in our results, the

contribution to k_{app} decrease of Fe(II) photo-regenerated is negligible, because Fe(II) oxidation experiments were lead in darkness. Therefore, the natural ligands excreted by *Synechococcus* under Fe-replete conditions, played a key role in the drop of Fe(II) oxidation rate along the pH studied. Thereby, the log k_{app} decreased to 2.90 ± 0.03 $M^{-1}min^{-1}$ at pH 8.2 and to 2.11 ± 0.02 $M^{-1}min^{-1}$ at pH 7.2, which represented a drop in the oxidation rate, with respect to the control, of 56% and 35% for pH 8.2 and pH 7.2, respectively. Accordingly, ligand released under High-Fe conditions diminished the k_{app} more efficiently at high pH. The contribution to chelate Fe(II) of phenolic moieties, within the organic ligand set excreted by *Synechococcus* is pH-dependent and a rise of $[H^+]$ increase also the phenolic protonation, preventing partly the iron binding by phenolic compounds (Perron et al., 2010).

The results of these studies will provide valuable information for understanding the effect of environmental variations, such as the ocean acidification or the daily dynamics of ocean pH on the redox cycle of iron (Hofmann et al., 2011; Hutchins and Boyd, 2016). The log k_{app} as a function of pH and DOC released were fitted to a second polynomial function (Table 4.5; eqs 1-3).

Table 4.5 Equations relationship between log k_{app} and the variables considered in the study ($[DOC]_R$, pH, temperature and salinity).

Independent variables	Eq (Nº)	Fe-treatment	Log k_{app} (M^{-1} min^{-1})	r^2	±SE
pH, $[DOC]_R$	1	$SWEX_{Low\text{-}Fe}$	$10.31\ (\pm7.74) - 2.74\ (\pm2.01)pH + 0.23\ (\pm0.13)pH^2 - 0.7\ (\pm0.3)\cdot10^{-4}\ [DOC]_R$	0.981	0.05
	2	$^{PP}SWEX_{Low\text{-}Fe}$	$11.43\ (\pm5.74) - 3.03(\pm1.49)pH + 0.25\ (\pm0.10)pH^2 - 1.3\ (\pm2.0)\cdot10^{-4}\ [DOC]_R$	0.992	0.02
	3	$SWEX_{High\text{-}Fe}$	$9.88\ (\pm5.32) - 2.70\ (\pm1.38)pH + 0.23\ (\pm0.09)pH^2 - 1.4\ (\pm1.0)\cdot10^{-4}\ [DOC]_R$	0.994	0.02
T, $[DOC]_R$	4	$SWEX_{Low\text{-}Fe}$	$19.08\ (\pm0.36) - 4782.1\ (\pm105.4)/T - 2.0\cdot(\pm3.0)\cdot10^{-4})[DOC]_R$	0.994	0.06
	5	$^{PP}SWEX_{Low\text{-}Fe}$	$18.95\ (\pm0.50) - 4741.5\ (\pm145.6)/T - 2.5\cdot(\pm3.0)\cdot10^{-4})[DOC]_R$	0.996	0.05
	6	$SWEX_{High\text{-}Fe}$	$19.39\ (\pm0.42) - 4870.9\ (\pm122.8)/T - 2.4\cdot(\pm2.0)\cdot10^{-4})[DOC]_R$	0.997	0.04
S, $[DOC]_R$	7	$SWEX_{Low\text{-}Fe}$	$3.35\ (\pm0.03) - 1.7\ (\pm0.3)\cdot10^{-2}\ S + 2.0\ (\pm0.5)\cdot10^{-4}\ S^2 - 1.2\ (\pm0.1)\cdot10^{-3}\ [DOC]_R$	0.986	0.01
	8	$^{PP}SWEX_{Low\text{-}Fe}$	$3.48\ (\pm0.10) - 1.7\ (\pm1.0)\cdot10^{-2}\ S + 2.0\ (\pm0.7)\cdot10^{-4}\ S^2 - 2.8\ (\pm0.3)\cdot10^{-3}\ [DOC]_R$	0.974	0.05
	9	$SWEX_{High\text{-}Fe}$	$3.45\ (\pm0.17) - 1.7\ (\pm1.0)\cdot10^{-2}\ S + 2.0\ (\pm0.6)\cdot10^{-4}\ S^2 - 3.1\ (\pm0.4)\cdot10^{-3}\ [DOC]_R$	0.951	0.08

The effect of the organic exudates from *Synechococcus* on the Fe(II) oxidation rate was computed by subtracting the log k_{app} values in the UV-treated seawater (Table 4.6; eqs 1-3). The dependence of log k_{app}, over the whole pH range, reports changes in the Fe(II) speciation, which could represent the major process of control, considering only the effect of natural ligands. These changes are related to a variation on the type and concentration of dissolved organic carbon.

Table 4.6 Equations relationship between Fe(II) oxidation rate, subtracted the effect of SWEN (Δlog k_{app}), and the independent variables considered in the study ($[DOC]_R$, pH, temperature and salinity).

Independent variables	Eq (N°)	Fe-Treatment	Δlog k_{app} (M^{-1} min^{-1})	r^2	±SE
pH, $[DOC]_R$	1	$SWEX_{Low\text{-}Fe}$	$-0.84\ (\pm0.04)\ pH + 0.11\ (\pm4.8 \cdot 10^{-3})pH^2 + 6.0\ (\pm2.8) \cdot 10^{-4}\ [DOC]_R$	0.972	0.06
	2	$^{PP}SWEX_{Low\text{-}Fe}$	$-0.83\ (\pm0.02)\ pH + 0.10\ (\pm2.9 \cdot 10^{-3})pH^2 - 4.0(\pm1.0) \cdot 10^{-4}\ [DOC]_R$	0.993	0.02
	3	$SWEX_{High\text{-}Fe}$	$-0.90\ (\pm0.02) + 0.11\ (\pm2.3 \cdot 10^{-3})pH^2 - 2.0\ (\pm0.9) \cdot 10^{-4}[DOC]_R$	0.996	0.02
T, $[DOC]_R$	4	$SWEX_{Low\text{-}Fe}$	$16.11(\pm0.42) - 4790.1\ (\pm121.0)/T - 5.0\ (\pm1.5) \cdot 10^{-4}[DOC]_R$	0.993	0.06
	5	$^{PP}SWEX_{Low\text{-}Fe}$	$15.85(\pm0.62) - 4720.8\ (\pm180.9)/T - 5.0\ (\pm1.1) \cdot 10^{-4}[DOC]_R$	0.993	0.06
	6	$SWEX_{High\text{-}Fe}$	$16.31(\pm0.50) - 4856.1\ (\pm146.4)/T - 5.0\ (\pm1.6) \cdot 10^{-4}[DOC]_R$	0.995	0.05
S, $[DOC]_R$	7	$SWEX_{Low\text{-}Fe}$	$-0.36\ (\pm0.02) + 1.7\ (\pm0.3) \cdot 10^{-2}\ S - -2.0\ (\pm0.1) \cdot 10^{-4}\ S^2 + 0.2\ (\pm0.1) \cdot 10^{-3}[DOC]_R$	0.987	0.01
	8	$^{PP}SWEX_{Low\text{-}Fe}$	$-0.49\ (\pm0.13) + 1.9\ (\pm1.3) \cdot 10^{-2}\ S - -2.0\ (\pm0.4) \cdot 10^{-4}\ S^2 + 0.9\ (\pm0.3) \cdot 10^{-3}[DOC]_R$	0.952	0.04
	9	$SWEX_{High\text{-}Fe}$	$-0.46\ (\pm0.21) + 1.8\ (\pm2.3) \cdot 10^{-2}\ S - -2.0\ (\pm0.6) \cdot 10^{-4}\ S^2 + 1.4\ (\pm0.4) \cdot 10^{-3}[DOC]_R$	0.917	0.07

4.3.5 Temperature dependence

The effect of temperature on the Fe(II) oxidation rate, in the gradient 5−35°C, was evaluated in seawater enriched with exudates of *Synechococcus*, produced at 25°C both in Low-Fe and High-Fe conditions, and equilibrated at the selected temperatures. The effect of temperature on the reactivity of $^{PP}SWEX_{Low\text{-}Fe}$ was also examined. The log k_{app} values were the lowest in seawater enriched with the higher dissolved organic carbon levels (127.13 ± 8.38 μmol C L^{-1}). The difference on the

oxidation rate along the thermal range studied ($\Delta^T \log k_{app} = \log k_{app}^{35ºC} - \log k_{app}^{5ºC}$) was 1.70 ± 0.01 ($M^{-1}$ min^{-1}), in the UV-seawater control, decreasing in presence of $SWEX_{Low\text{-}Fe}$ to 1.69 ± 0.03, 1.65 ± 0.04, and 1.60 ± 0.04 M^{-1} min^{-1} for 15.84 ± 6.12, 37.13 ± 4.30, and 127.13 ± 8.38 µmol C L^{-1}, respectively. After photo-treating exudates during 24h ($[DOC]_R$ = 127.13 ± 8.38 µmol C L^{-1}) this difference diminished to 1.58 ± 0.02 $M^{-1}min^{-1}$. The $\Delta \log k_{app}$ was 1.68 ± 0.03 M^{-1} min^{-1} in presence of $SWEX_{High\text{-}Fe}$ ($[DOC]_R$ = 150.51 ± 8.59 µmol C L^{-1}).

At pH 8.0 and 5°C, $t_{1/2}$ was 27.0 min in the control. In seawater enriched with the highest concentrations of exudates, released under Fe-deficient conditions ($[DOC]_R$ = 127.13, ± 8.38 µmol C L^{-1}), $t_{1/2}$ became 46.8 min. When these ligands were photo-treated the half time for Fe(II) reached 54.6 min (Table 4.1). In the presence of $SWEX_{High\text{-}Fe}$ ($[DOC]_R$ = 150.51 ± 8.59 µmol C L^{-1}), $t_{1/2}$ was 61.7 min. Therefore in cold waters, compared to the UV treated seawater (control), Fe(II) remained up to 30 min longer when the exudates were produced under Fe-replete conditions, scenario that could occur in many coastal waters of high latitudes (Breitbarth et al. 2009).

Log k_{app} was linearly related with the inverse of temperature (Table 4.5; eqs 4-6). The effect of the organic ligands excreted by *Synechococcus* on the Fe(II) oxidation rate constant, as a function of temperature, compared to the values for the control seawater was also estimated (Table 4.6; eqs 4-6). The changes in the oxidation rate under different temperatures are affected by the presence of natural organic ligands. The slight differences on thermal trend of the oxidation rates, between the two Fe-scenarios analyzed, can be attributed to the absence of hydroxamic ligands in the organic exudates produce under Fe-replete conditions, since the stability constants of Fe-hydroxamate complexes decreased when the temperature is increased (Andrieoux et al. 2011), and therefore is possible to consider that the contribution of Fe(II)-hydroxamate complexes, to the overall oxidation rate, is lower at the highest temperatures studied.

Using the data from Table 4.1-4.3, the minimum energy required to carry out the chemical oxidation process, (energy of activation, E_a, Arrhenius, 1889), was similar over all iron treatments. The energy of activation slightly decreased from

93.7 ± 4.6 kJ mol^{-1} in the seawater control to 88.6 ± 2.6 kJ mol^{-1} in $SWEX_{Low\text{-}Fe}$ (127.13 ± 8.38 μmol C L^{-1}), and to 87.8 ± 3.1 kJ mol^{-1} when such exudates are light pre-exposed. The energy demanded (E_a = 92.8 ± 2.5 kJ mol^{-1}) in the oxidation process was also estimated when the exudates was excreted under Fe-replete conditions ($[DOC]_R$ = 150.51 ± 8.59 μmol C L^{-1}) These energies of activation were comparable with those reported both in natural Pacific Subartic seawater (95.8 kJ mol^{-1}; Roy and Wells, 2008) and Atlantic seawater enriched with exudates from *D. tertiolecta* (84.2 kJ mol^{-1}; González et al. 2014). These results of E_a mirrored that the mechanism of reaction was similar between SWEN and SWEX were present in solution. Albeit, the slight variations in E_a between iron treatments could be related to changes in the composition of organic Fe(II) species in solution.

4.3.6 Effect of salinity

The dependence of the salinity on the oxidation rate of Fe(II) was studied for the range of salinities from 10 to 37 (Tables 4.1-4.3). The log k_{app} of Fe(II) exhibited a different level of dependence with salinity for the three types of DOC considered in this study. The maximum difference in the oxidation rates, due to changes in salinity ($\Delta^S \log k_{app} = \log k_{app}^{S=37} - \log k_{app}^{S=10}$), was found in UV-seawater control (0.35 ± 0.01 M^{-1} min^{-1}). In the $SWEX_{Fe\text{-}Low}$, the range of variability was reduced to 0.22 ± 0.02 M^{-1} min^{-1} ($[DOC]_R$ = 127.13 ± 8.38 μmol C L^{-1}). This effect of salinity was 0.17 ± 0.03 M^{-1} min^{-1} when these exudates underwent a previous photolysis, whereas in $SWEX_{Fe\text{-}High}$ $\Delta^S \log k_{app}$ was 0.04 ± 0.02 M^{-1} min^{-1} ($[DOC]_R$ = 150.51 ± 8.59 μmol C L^{-1}). This was also reflected by observing the half-life of Fe(II), which decreased in control UV-seawater from 3.1 to 1.1 min when the salinity changed from 37 to 10. However, in presence of $SWEX_{Fe\text{-}Low}$, the difference in the $t_{1/2}$, between S = 37 and S = 10, amounted to 1.5 min ($[DOC]_R$ = 15.84 ± 6.12 μmol C L^{-1}), 1.4 min ($[DOC]_R$ = 37.13 ± 4.30 μmol C L^{-1}), and 1.8 min ($[DOC]_R$ = 127.13 ± 8.38 μmol C L^{-1}). When the organic ligands, included in the 127.13 ± 8.38 μmol C L^{-1} of DOC released, were photo-treated ($^{PP}SWEX_{Fe\text{-}Low}$), the $t_{1/2}$ was 2.3 min. Moreover, for the ligands excreted under Fe-replete conditions ($[DOC]_R$ = 150.51 ± 8.59 μmol C L^{-1}), the $t_{1/2}$ decreased from 6.3 min at S = 37, to 4.9 min at S =10. The

experimental data indicate that the organic ligands play a key role in the Fe(II) oxidation rate stabilization compared to UV treated seawater, which have a greater control over the oxidation process exerted by the interaction with the major inorganic species. Besides, organic ligands modify their role in the Fe(II) stabilization, according with the iron conditions under which they are produced or if they are undergoing photochemical modifications.

The experimental results were fitted to a second order polynomial function (Table 4.5; eqs 7-9). The change in the Fe(II) oxidation rate constants due to the presence of organic ligands, as a function of salinity, was also calculated (Table 4.6; eqs 7-9). Moreover, the apparent rate constant (M^{-1} min^{-1}) was fitted under the experimental conditions of $[DOC]_R$ (μmol C L^{-1}), pH (free scale), temperature (Kelvin) and salinity, for each scenario studied. (eqs 34-36).

$$\boldsymbol{log\ k_{app}(SWEX_{Low-F}\ ) =}$$

$$\mathbf{4.24\ (\pm 0.18)pH - 2.2\ (\pm 0.1) \cdot 10^{-1}pH^2 - 4873.3\ (\pm 200.6)/T - \ 2.2(\pm 1.5) \cdot 10^{-2}\ S + 3.0\ (\pm 3.0) \cdot 10^{-4}\ S^2 - \ 1.5\ (\pm 0.3) \cdot 10^{-3}\ [DOC]_R} \quad (32)$$

$r^2 = 0.955$; Error of estimation = 0.11

$$\boldsymbol{log\ k_{app}(^{PP}SWEX_{Low-Fe}) =}$$

$$\mathbf{4.11\ (\pm 0.17)pH - 2.2\ (\pm 0.1) \cdot 10^{-1}pH^2 - 4678.4\ (\pm 187.1)/T - \ 1.4(\pm 1.3) \cdot 10^{-2}\ S + 1.0\ (\pm 3.0) \cdot 10^{-4}\ S^2 - \ 1.3\ (\pm 0.3) \cdot 10^{-3}\ [DOC]_R} \quad (33)$$

$r^2 = 0.988$; Error of estimation = 0.05

$$\boldsymbol{log\ k_{app}(SWEX_{High-}\ ) =}$$

$$\mathbf{4.22\ (\pm 0.15)pH - 2.2\ (\pm 0.1) \cdot 10^{-1}pH^2 - 4919.4\ (\pm 170.1)/T - \ 1.4(\pm 1.3) \cdot 10^{-2}\ S + 3.0\ (\pm 3.0) \cdot 10^{-4}\ S^2 - \ 1.3\ (\pm 0.2) \cdot 10^{-3}\ [DOC]_R} \quad (34)$$

$r^2 = 0.991$; Error of estimation = 0.05

The effect in the Fe(II) oxidation process, just due to the presence of ligands produced by *Synechococcus* (log $k_{app\text{-exudates}}$), was also estimated (eqs. 37-39), which allows the determination of apparent oxidation rate in the environment, under different experimental conditions applied in the present study.

$$\Delta log\ k_{app}(SWEX_{Low-Fe}) =$$

$$4.24\ (\pm 0.18)\mathrm{pH} - 2.2\ (\pm 0.1) \cdot 10^{-1}\mathrm{pH}^2 - 4873.3\ (\pm 200.6)/\mathrm{T} - 2.2(\pm 1.5) \cdot 10^{-2}\ \mathrm{S} + 3.0\ (\pm 3.0) \cdot 10^{-4}\ \mathrm{S}^2 - 1.5\ (\pm 0.3) \cdot 10^{-3}\ [\mathrm{DOC}]_R \quad (35)$$

$r^2 = 0.955$; Error of estimation = 0.11

$$\Delta log\ k_{app}({}^{PP}SWEX_{Low-Fe}) =$$

$$4.11\ (\pm 0.17)\mathrm{pH} - 2.2\ (\pm 0.1) \cdot 10^{-1}\mathrm{pH}^2 - 4678.4\ (\pm 187.1)/\mathrm{T} - 1.4(\pm 1.3) \cdot 10^{-2}\ \mathrm{S} + 1.0\ (\pm 3.0) \cdot 10^{-4}\ \mathrm{S}^2 - 1.3\ (\pm 0.3) \cdot 10^{-3}\ [\mathrm{DOC}]_R \quad (36)$$

$r^2 = 0.988$; Error of estimation = 0.05

$$\Delta log\ k_{app}(SWEX_{High-Fe}) =$$

$$4.22\ (\pm 0.15)\mathrm{pH} - 2.2\ (\pm 0.1) \cdot 10^{-1}\mathrm{pH}^2 - 4919.4\ (\pm 170.1)/\mathrm{T} - 1.4(\pm 1.3) \cdot 10^{-2}\ \mathrm{S} + 3.0\ (\pm 3.0) \cdot 10^{-4}\ \mathrm{S}^2 - 1.3\ (\pm 0.2) \cdot 10^{-3}\ [\mathrm{DOC}] \quad (37)$$

$r^2 = ;0.991$; Error of estimation = 0.05

These equations show that the ligand effect is conditioned by physico-chemical conditions such as pH, temperature, and salinity, which modify the reactivity between iron and the organic ligands present in the natural waters. In addition, in multidimensional biogeochemical ocean models, considering organic ligand dynamics (Jiang et al., 2013; Völker and Tagliabue, 2014) these equations could be weighed as archetype of the reactivity between Fe(II) and organic natural ligands excreted by prokaryote organisms. Therefore, they may be also used to

estimate the fractional contribution of organic exudates on the Fe(II) oxidation process relative to those different iron scenarios that can be found in the ocean.

4.3.7 Kinetic modelling approach

A kinetic model was applied to the experimental data in order to describe the pH effect in both the speciation of Fe(II) and the contribution of each individual species to the Fe(II) overall rate constant. Due to the high variability of organic compounds that can regulate the kinetics of Fe(II) (Roy and Wells, 2011), two ligands with different iron affinities were included in the kinetic model. The strong ligand, related to the hydroxamic moieties detected by the Csaky assay, was produced only under iron limited conditions. In addition, the exudates produced under Fe-deficient conditions were photo-reactive, and therefore, the syderophore-type ligand was only included in the model for a Fe-limited scenario. The phenolic compounds, excreted in both Fe-treatments (Arnow test), were evaluated in the model as weaker ligands.

The model includes all aspects above indicated. Following the results presented in Figure 4.2, a Fe(III) reduction rate equation has been included and fitted in the model (Table 4.7; Eq 2). Because of spectrophotometric titrations and electrospray ionisation mass spectrometry analyses have showed that the marine citric acid-containing siderophores coordinates iron with a 1:1 stoichiometry (Kpper, et al. 2006), the model included the equilibrium formation constants of Fe(II) and Fe(III)-complexes (Table 4.6; eqs 1-4), for both synechobactin (Syn) and its photoproduct (Syn^{PP}), as well as their corresponding redox reactions (Table 4.7).

Table 4.7 The computed redox kinetic constants of ligands considered for the kinetic model. T[a] = 25 ºC, S‰ = 37.09.

N°	Reactions	Kinetic constants
1	$Fe(II) - Syn + O_2 \rightarrow Fe(III) - Syn$	$\log k_{Fe(II)-Syn} = 7.46 \pm 0.41\ (M^{-1}min^{-1})$
2	$Fe(III) - Syn + h\nu \rightarrow Fe(II) + Syn^{PP} + CO_2$	$\log k_{Red} = -4.85 \pm 0.11\ (min^{-1})$
3	$Fe(II) - Syn^{PP} + O_2 \rightarrow Fe(III) - Syn^{PP}$	$\log k_{Fe(II)-Syn^{PP}} = 6.71 \pm 0.27\ (M^{-1}min^{-1})$
4	$Fe(II) - PPH + O_2 \rightarrow Fe(III) - PPH$	$\log k_{Fe(II)-PPH} = 1.42 \pm 0.38\ (M^{-1}min^{-1})$

The Fe(III)-siderophore type-complex formation constant ($K_{Fe(III)-Syn}$), which best fits the experimental data (Table 4.8; eq 3), is similar to the stability constants for the strong iron complexes determined in the first 200 m of the upper layer of the ocean (Boye et al., 2006; Ibisanmi et al., 2011; Thuróczy et al., 2011), where the highest bacterioplanktonic activity is measured (Hunt et al., 2013). The Fe(III)-binding strength of the photo-product ($K_{Fe(III)-Syn^{PP}}$), computed in the model (Table 4.8; eq 4). is similar to the values observed for a weaker class of Fe(III)-binding ligands in sea water (Boyd and Tagliabue, 2015; Rue and Bruland, 1997, 1995), which is consistent with a partial loss of the complexing ability of the siderophores during the decarboxilation reaction (Vraspir and Butler, 2009). In agree with results obtained by Ito and Butler (2005), model results suggested the strongest ligand class L_1, include siderophores produced by *Synechococcus* PCC 7002, while its photoproduct is part of a different strong ligand class, operationally defined as L_2.

Table 4.8 The reactions and fitted equilibrium constants of ligands considered for the kinetic model. T[a] = 25 ºC, S = 37.09.

Nº	**Reactions**	**Equilibrium constants (M^{-1})**
1	$Fe(II) + Syn \leftrightarrow Fe(II) - Syn$	$\log K_{Fe(II)-Syn} = 3.45 \pm 0.29$
2	$Fe(II) + Syn^{PP} \leftrightarrow Fe(II) - Syn^{PP}$	$\log K_{Fe(II)-Syn^{PP}} = 4.16 \pm 0.34$
3	$Fe(III) + Syn \leftrightarrow Fe(III) - Syn$	$\log K_{Fe(III)-Syn} = 22.69 \pm 0.72$
4	$Fe(III) + Syn^{PP} \leftrightarrow Fe(III) - Syn^{PP}$	$\log K_{Fe(III)-Syn^{PP}} = 21.31 \pm 0.55$
5	$Fe(II) + PhC \leftrightarrow Fe(II) - PhC$	$\log K_{Fe(II)-PhC} = 9.42 \pm 0.81$
6	$Fe(III) + PhC \leftrightarrow Fe(III) - PhC$	$\log K_{Fe(III)-PhC} = 18.75 \pm 0.46$

Nevertheless, the distribution in marine environments of weaker binding ligands (L_3 and L_4) is less understood, because of their detection has not been as statistically robust, as with stronger ligand classes (Wu and Jin, 2009). Recently, Bundy et al. (2014) investigated seasonal characteristics of dissolved Fe-binding ligands in the California Current, measuring binding capacities by competitive ligand exchange–adsorptive cathodic stripping voltammetry and creating a wide range of competition strengths. This multiple analytical windows enabled them the detection of two new types of ligands, defined as L_3 and L_4, with lower Fe(III) stability constants than L_1 and L_2. During their study, L_3 and L_4 were associated to the

terrestrial organic matter degraded and transported by runoff, which is formed mainly by humic and fulvic substances, and within which, aromatic moieties are the principal reactant component (Stubbins et al., 2008). Among them, the use of UV-visible absorption spectra has shown that phenolic compounds are effective iron chelators with pH independent Fe(III) stability constant ranging from 16 to 21 (Perron and Brumaghim, 2009), and therefore could be part of L_3 and L_4 iron ligands pools in seawater. Significant levels of phenolic moieties have been measured in different fractions obtained from cultures of *Synechococcus* sp (Li et al., 2007), as well as, in the present work. Thus, a weaker ligand than siderophores (L_3 or L_4 type ligands) was included in the model approach and assumed to produce iron complexes with polyphenol-type ligands (PhC) with the corresponding oxidation processes (Table 4.7; eq 4). The value of $K_{Fe(III)-PhC}$, determined by the model output that best fit the experimental data (Table 4.8; eq 6) is in good agreement with the iron chelation constants found in literature for different phenolic compounds (Perron and Brumaghim, 2009).

Marcus theory have been applied in order to evaluate the individual oxidation rate of Fe-organic ligands fitted in the model, as well as for their Fe(II) formation constant, since the Marcus theory relates second order rate constants for outer-sphere electron-transfer reactions with the free energy of the reaction (Stumm and Morgan,1996).

$$k_i = \frac{k_d}{1+\frac{k_d}{K_d Z}\exp\left[\frac{\frac{\lambda}{4}\left(1+\frac{\Delta G^\circ}{\lambda}\right)^2}{RT}\right]} \qquad (38)$$

where k_d is the diffusion-controlled limit (10^{10} M^{-1} sec^{-1}), k_d/K_dZ has a constant value of 0.1 (King and Farlow, 2000) and λ is a fitting parameter related with the reorganization energy required to rearrange the transition state of precursor and accounted as 103 kJ mol^{-1} for organic compounds (Rose and Waite, 2003). R is the universal gas constant and T is the temperature in Kelvin units. The oxidation rate constants of individual Fe(II) species can provide the standard free energy, ΔG^0, for each reaction. The estimated free energies varied from -8.97 ± 1.08 and 56.70 ± 4.85 kJ mol^{-1}, for the siderophore and phenol type ligands, respectively.

Once the energy for the electron transfer reaction for the reduction of oxygen to superoxide is known and assuming that during the oxidation process the electronic transition happens without nuclear coordination modification (Franck-Condon principle), the free energy computed for the oxidation of one Fe−L complex by oxygen, can be defined by,

$$\Delta G° = -F(E^0_{O_{2\rightarrow O_2^-}} - E^0_{Fe(III)L\rightarrow Fe(II)L}) \quad (39)$$

where, F is the Faraday constant, $E^0_{O_{2\rightarrow O_2^-}}$ in aqueous solutions oscillate between -0.16 V and -0.20 V (Koppenol et al., 2010) and E^0_{FeL} is the half potential for reduction of the Fe−L complex. Solving the eq 12, the half potential for reduction of the Fe−siderophore complex ranged between -0.204 and -0.335 V, whilst the $E^0_{Fe-Syn^{PP}}$ varied from -0.082 to -0.226 V. These values were very similar to those obtained in hydroxamate siderophores with citrate structure, as aerobactin (Crumbliss and Harrington, 2008). The half potential for the reduction of the Fe−phenol complex (computed between +0.334 and +0.385 V), was the same order as those measured in some Fe-flavonoids complexes (Perron et al. 2008). From the Nernst equation and using the corresponding values of E^0_{FeL}, the equilibrium constant ratio ($K_{Fe(III)-L}/KFe_{(II)-L}$) can be accounted for each organic iron complexes considered in the kinetic model.

$$E^0_{FeL} = E^0_{Fe} - 0.059 \log\left(\frac{K_{Fe(III)-L}}{K_{Fe(II)-L}}\right) \quad (40)$$

If the standard half reaction potential for $E^0_{Fe} = 0.77\,V$ is used, the $K_{Fe(III)-L}/K_{Fe(II)-L}$ ratios of 10^{15}–10^{18} and 10^{14}–10^{16} are assessed for the ligands assumed as synechobactin, and its photoproduct, respectively. The $K_{Fe(III)-L}/K_{Fe(II)-L}$ ratio for the weakest ligand types were 10^5-10^8. These ratios are computed considering the Fe formation constants assumed in the kinetic model approach (Table 3). In addition, the application of Marcus theory, gives also consistency to the individual Fe(II)-L oxidation constant rates provided by the model (Table 4.8), that best fits the experimental data. The *ki* computed by the model correlate with the half potential for reduction for each type of Fe−L complex considered. The value of $\log k_{Fe(II)-Syn}$reflects that hydroxamate siderophores, such as synechobactin, are

efficient catalysts of Fe(II) oxidation, as has been demonstrated previously (Welch et al., 2002). Perron et al. (2010) have shown that the Fe(II) oxidation rate rises in presence of phenolic compounds as the number of iron-binding groups present in the aromatic ring increase. Thereby, it has been observed that gallol functional groups facility faster iron oxidation than their catechol analogues. Therefore, the $\log k_{Fe(II)-PhC}$ fitted in the model seems to be in close alignment with Fe(II) oxidation rates observed in presence of phenols with dihydroxybenzene moieties, such as (-)-epicatechin or metil-3,4-dihydroxybenzoate (Perron et al. 2010), which also have positive reduction potentials (Perron et al., 2008). The derivatives of catechins are ones of the polyphenols that more inhibit the Fe(II) oxidation (Perron et al., 2010). They have recently been identified as one of the flavanols most abundant in exudates of marine phytoplankton (Rico et al. 2013; Lopez et al., 2015).

Table 4.9 Computed acidity constants for the ligands considered for the kinetic model. T[a] = 25ºC.

Ligand proposed	Nº	Reaction	pK_a
Siderophore (Sid) (Kpper et al. 2006)	1	$LH_6 \leftrightarrow LH_5 + H^+$	3.11
	2	$LH_5 \leftrightarrow LH_4 + H^+$	3.48
	3	$LH_4 \leftrightarrow LH_3 + H^+$	4.31
	4	$LH_3 \leftrightarrow LH_2 + H^+$	8.93
	5	$LH_2 \leftrightarrow LH + H^+$	9.44
	6	$LH \leftrightarrow L^- + H^+$	11.0
Siderophore photoproduct (^{PP}Sid) (Kpper et al. 2006)	1	$LH_5 \leftrightarrow LH_4 + H^+$	2.50
	2	$LH_4 \leftrightarrow LH_3 + H^+$	3.71
	3	$LH_3 \leftrightarrow LH_2 + H^+$	8.64
	4	$LH_2 \leftrightarrow LH + H^+$	9.62
	5	$LH \leftrightarrow L^- + H^+$	10.80
Phenolic ligand (PhC) (Herrero-Martínez et al. 2005)	1	$LH_2 \leftrightarrow LH + H^+$	9.19
	2	$LH \leftrightarrow L^- + H^+$	13.09

The formation constants for the Fe-complexes considered in the model have been written in terms of the fully deprotonated ligand states. Therefore, in order to examine the pH effect on the oxidation kinetics, it is necessary to consider the

protonation equilibria of those ligands. Due to the structural similarity between the citrate-type siderophores, the hydroxamate chelating agents (Sid and Sid^{PP}) was adopted to have the ligand acidity constants (Table 4.8) of aerobactin and its photoproduct, determined by Kpper et al. (2006). Similarly, it has been considered three acidity constants of (-)-epicatechin (Herrero-Martínez et al., 2005) for the phenol type ligand (PhC) included in the model.

Taking in account both the chemical assays and the molecular structures of synechobactin and its photo-product, which comprised one citrate-based with two hydroxamate groups (Ito and Butler, 2005), the concentrations of specific ligand, siderophore-type, provided by the model which best fits the data are 34 ± 6, 139 ± 22, and 394 ± 40 nM when the total of DOC excreted was 15.84 ± 6.12, 37.13 ± 4.30, and 127.13 ± 8.38 μmol C L^{-1}, respectively. In cultures of *Synechococcus* PCC 7002 with chemostat-growth, Trick & Wilhelm (1994) detected significantly higher concentrations, of extracellular organic ligand that would react with Csaky test, than those found in this study. The differences can be explained by higher cyanobacteria density reached in the bioreactor system. The flavanols levels detected in both *P.tricornutum* and *D.tertiolecta* cultures (López et al., 2015; Rico et al., 2013) converge reasonably with the Arnow chemical assay and with the best fitting model, found for ligands with dihydroxiphenolic moieties, in both iron regimens analysed. These concentrations were 3 ± 1, 12 ± 2, and 19 ± 5 nM corresponding with the levels of DOC released of 15.84 ± 6.12, 37.13 ± 4.30, and 127.13 ± 8.38 μmol C L^{-1} respectively, for Fe-deficient conditions and 3 ± 2; 14 ± 1 and 24 ± 7 nM when the DOC levels were 15.76 ± 3.52, 39.66 ± 6.73, and 150.51 ± 8.59 μmol C L^{-1} respectively for $SWEX_{High\text{-}Fe.}$.

The modelling approach for speciation of Fe(II) is based on inorganic protonation and ion-pair formation constants referenced from Santana-Casiano et al. (2006), extended with the introduction of nutrient species (Mao et al., 2011; Samperio-Ramos et al., 2016) (Table 2.1), as well as, the organic ligands considered in this work (Tables 4.8 and 4.9).

The oxidation process of Fe(II) integrates several parallel reactions in which the individual Fe(II) species react at different rates with oxygen. The apparent Fe(II)

oxidation rate can be expressed in terms of the weighted sum of the oxidation rates of the individual Fe(II) species.

$$k_{app} = k_{Fe^{2+}}\alpha_{Fe^{2+}} + k_{FeOH^+}\alpha_{FeOH^+} + k_{Fe(OH)_2}\alpha_{Fe(OH)_2} + k_{FeHCO_3^+}\alpha_{FeHCO_3^+} +$$

$$+ k_{FeCO_3}\alpha_{FeCO_3} + k_{Fe(CO_3)_2}\alpha_{Fe(CO_3)_2} + k_{Fe(CO_3)OH^-}\alpha_{Fe(CO_3)OH^-} + k_{FeCl^+}\alpha_{FeCl^+} + k_{FeSO_4}\alpha_{FeSO_4} +$$

$$+ k_{FeH_3SiO_4^+}\alpha_{FeH_3SiO_4^+} + k_{FePO_4^-}\alpha_{FePO_4^-} + k_{FeHPO_4}\alpha_{FeHPO_4} + k_{FeH_2PO_4^+}\alpha_{FeH_2PO_4^+} +$$

$$+ \boldsymbol{k_{Fe\text{-}Sid}\,\alpha_{Fe\text{-}Sid} + k_{FeSid^{pp}}\,\alpha_{FeSid^{pp}} + k_{Fe\text{-}PhC}\,\alpha_{Fe\text{-}PhC}} \quad (41)$$

where $\alpha_i = [FeX_i] / [Fe(II)]_T$ denotes the molar fraction of each Fe(II) species in the solution, and *ki* are the individual rate constant for the Fe(II) species

The Figure 4.6 shows Fe(II) speciation for the seawater control and $SWEX_{Low\text{-}Fe}$ with 15.84 ± 6.12 µmol C L^{-1} and 37.13 ± 4.30 µmol C L^{-1} of DOC. In the seawater control, the Fe(II) speciation was controlled from pH 7 to 8.2 for Fe^{2+}, varying from 58% to 35%. At pH >8.2, $FeCO_3$ accomplishes the most important role and attains the 44% of speciation at pH 8.5. The organic ligands influence powerfully on the Fe(II) speciation and this is reflected specially when the dissolved organic carbon reaches 127.13 ± 8.38 µmol C L^{-1} (Fig 4.6). Although Fe^{2+} remains the dominant specie up to pH 7.9 (28%), Fe(II) speciation is controlled, from pH 7.9 (29%) to 8.5 (51%), phenol-Fe(II) complex (Fe-PhC), and hence, $FeCO_3$ is reduced to 18% and 23% at pH 7.9 and 8.5 respectively. Under Fe-limited conditions, the mole fraction of Fe(II)-siderophore species (Fe(II)-Sid and Fe(II)-Sid^{PP}) were minor components, compared to species that dominated the speciation. Therefore, the iron availability during harvesting does not seem to modify the Fe(II) speciation significantly.

The kinetic modelling approach, applied to the experimental results obtained in this work, has allowed discerning the contribution of the organic complexes, assessed in the model, to the overall constant. Figure 4.7 presents the fractional contribution of each individual specie to the overall Fe(II) oxidation rate in $SWEX_{Low\text{-}Fe}$, with 15.84 ± 6.12 µmol C L^{-1} and 37.13 ± 4.30 µmol C L^{-1} of DOC. When the organic ligands are considered in the model, the fractional contributions to the overall Fe(II) oxidation rate are modified with respect to control (Fig 4.8, A).

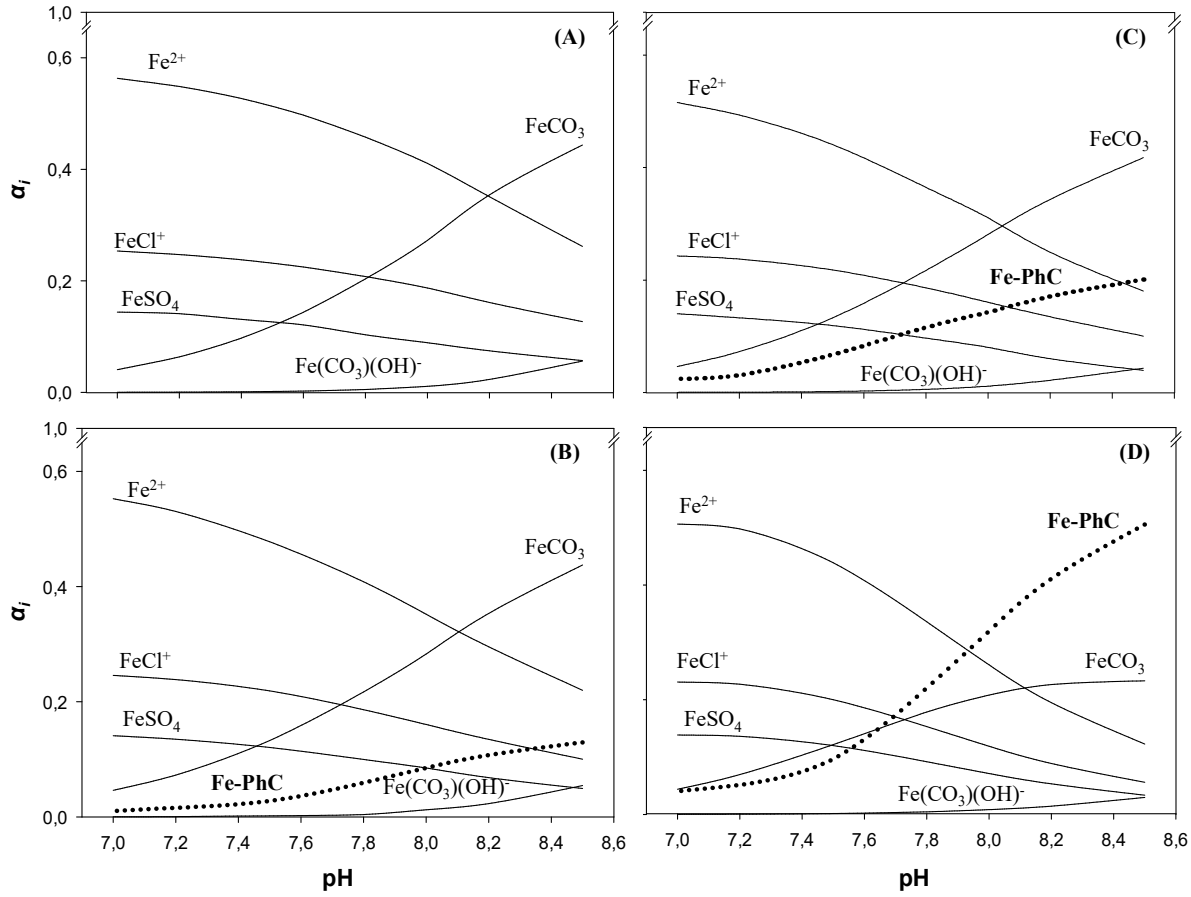

Fig 4.6 Fe(II) speciation modeled for (A) Seawater with f/2 nutrients (SWEN) and (B-D) SWEX produced from cultures of *Synechococcus* PCC 7002 during days 2, 6 and 12 of growth, respectively. Fe-treatments do not modified the principal components of the Fe(II) speciation.

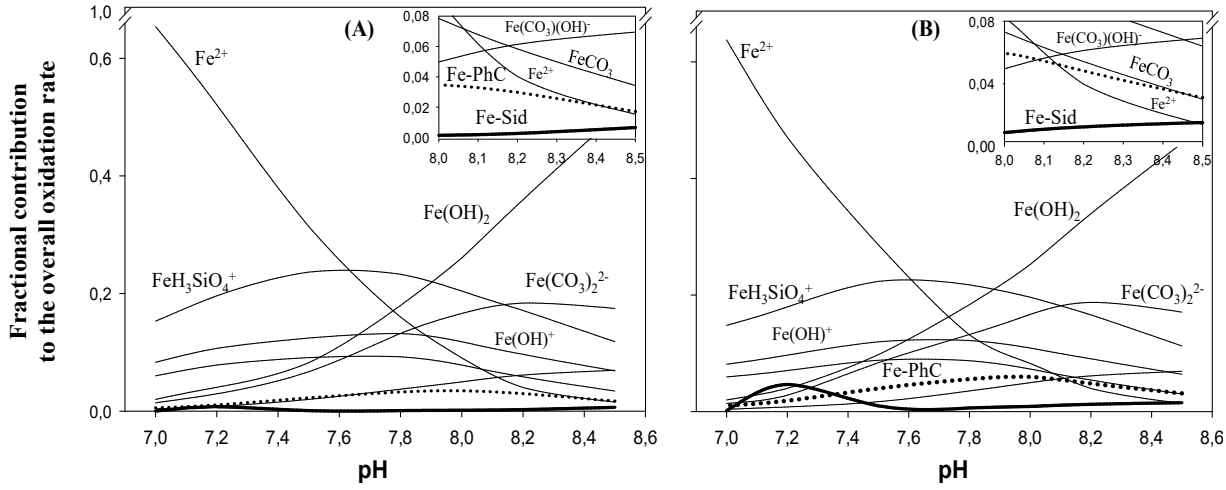

Fig 4.7 Fractional contribution to the overall oxidation rate in $SWEX_{Low\text{-}Fe}$ from cultures of *Synechococcus* PCC 7002. (A) [DOC] = 15.84 ± 6.12, and (B) 37.13 ± 4.30 µmol C L^{-1}.

When the DOC reaches 127.13 ± 8.38 μmol C L^{-1} (Fig. 4.8), the inorganic contributions diminish significantly by the presence of natural organic ligands. For example at pH 7.0, the fractional contribution of Fe^{2+} diminishes to 59% in presence of organic ligands excreted under Fe-deficient conditions. At the same time, the Fe(II)-Syn complex is converted into the second most important contributor at pH values between 7.0 and 7.4, reaching a maximum (24%) at pH 7.2. When the photolysis effect on the natural exudates ($^{PP}SWEX_{Low\text{-}Fe}$) is considered in the model, the photoproduct attains the 15% at pH 7.2 and became in the second most important contributor at pH values between 7.0 and 7.2. The maximum contribution of the Fe(II)-PhC specie took place at pH 8.0 and with exudates from 127.13 ± 8.38 μmol C L^{-1}, when it reached between 10-14% in both Fe-scenarios analysed.

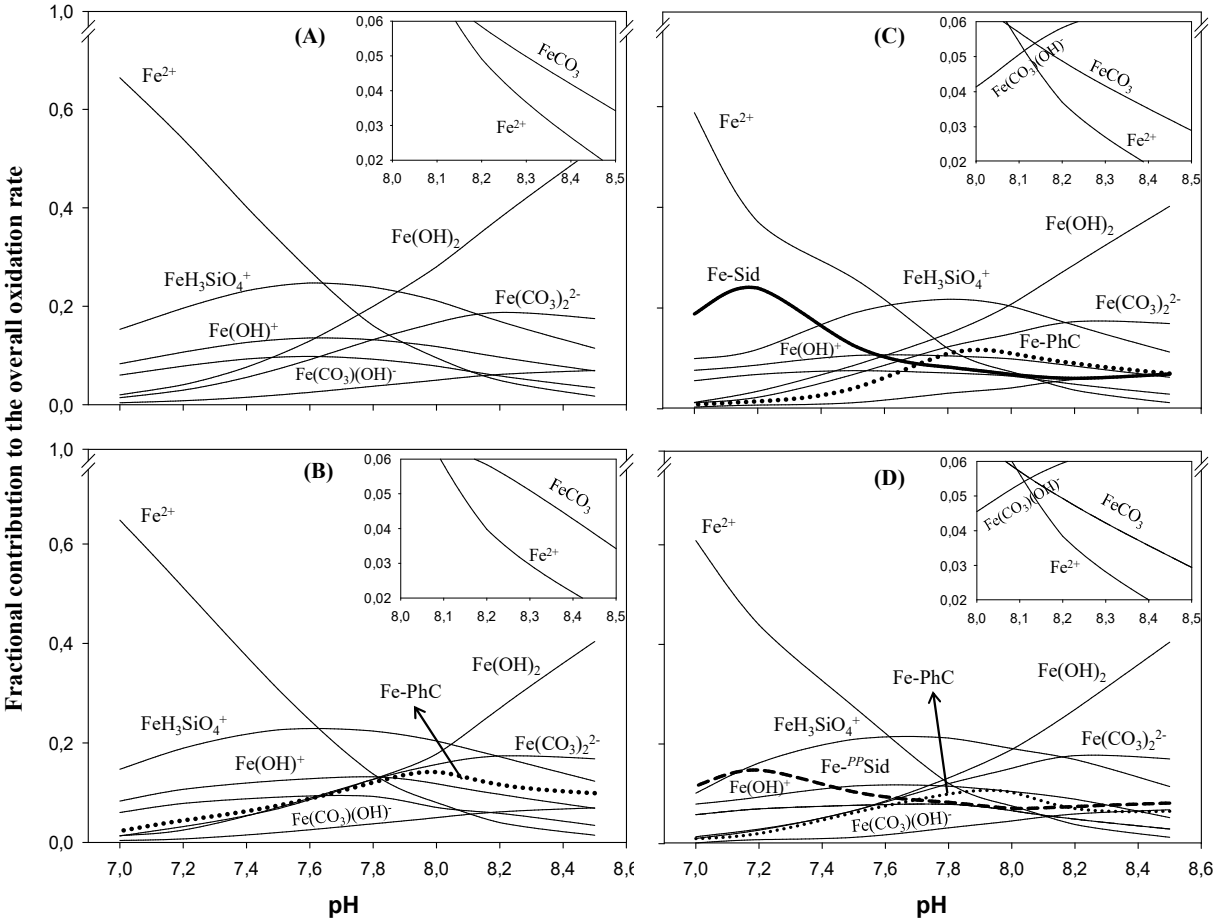

Fig. 4.8 Fractional contribution to the overall oxidation rate of Fe(II) from the kinetic model approach for (A) UV-treated seawater enriched with nutrients (Control) and seawater enriched with exudates produced under (B) Fe-replete conditions ($SWEX_{High\text{-}Fe}$) (C) Fe-deficient conditions ($SWEX_{Low\text{-}Fe}$) and (D) Fe-deficient conditions with previous photo-reaction ($^{PP}SWEX_{Low\text{-}Fe}$) for 24h.

The individual contributions to the overall Fe(II) rate constant, in presence of *Synechococcus* exudates, demonstrate that Fe(II)−siderophore complexes can play a key role in the Fe(II) oxidation rate at pH<7.5, while the oxidation process is controlled by the Fe(II)-hydroxide and Fe(II)-carbonate species at pH>8.0. In addition, the contribution of Fe(II)-phenol complexes controlled significantly the overall rate between pH 7.5 and 8.5, drawing out the half-life of Fe(II) in seawater.

As it is shown in Figures 4.2, 4.4 and 4.5, the model outputs and experimental data of log k_{app} (M^{-1} min^{-1}) versus pH agreed over the whole Fe treatments studied. The slight deviations observed at the lower pH values for $SWEX_{High\text{-}Fe}$, may be due to interaction between Fe(II) and some organic ligand not-considering in the model approach. Uronic acids have been described as the most abundant ligands, with capacity to bind cationic metals, in cyanobacteria exudates (Pereira et al., 2009) . At seawater pH, the aldonic acids, principal components of acid sugars, could retard the oxidation of Fe(II) until 9%, due to the steric hindrance for the oxygen attack on Fe(II)-aldonates complexes (Kuma et al., 1995). This mechanism should be more effective at pH < 7.5, where the hydrolysis of metals, which prevents the coordination of Fe(II) with the hydroxycarboxylic moieties, is lower (Gyurcsik and Nagy, 2000).

2.4 Environmental implications

The interaction between iron and organic ligands, released by photosynthetic microorganism, control the biogeochemistry of Fe in the Ocean. The natural ligands excreted by *Synechococcus* under Fe-replete conditions retard the Fe(II) oxidation rate in seawater and can act as an important Fe(II) supplier to other marine organisms. Nevertheless, the presence in exudates of strong chelate, produced under iron starvation, implies the formation of reactive organic-Fe(II) complexes that oxidise faster to organic-Fe(III) strong complexes. Therefore, Fe-bioavailability can modify the composition of natural exudates excreted by phytoplankton, determining the role played by the organic ligands in the iron redox chemistry. In fact, the

proteome of *Synechococcus* PCC 7002, expressed both under Fe-replete and anoxic conditions, does not included biosynthesis of siderophore and some Fe-transporter proteins associated to siderophores (Swanner et al., 2015)

Under Fe-deficient conditions the ferrisiderophores, through specific ligand exchange mechanisms developed in the plasma membrane, are highly bioavailable iron forms for bacterioplankton (Cordero et al., 2012; Kranzler et al., 2014). In addition, and because of that the reduction of the photoreactive Fe(III)-complexes occurs before Fe-uptake, iron may become in biologically more available for eukaryote phytoplankton via ligand-to-metal charge transfer reactions, which activing the passive diffusion of Fe(II) through nonspecific transmembrane channels (porins) (Morrissey and Bowler, 2012).

The physicochemical dependence on redox behavior of iron presented in this study, improve our knowledge about the environmental variables which can condition the Fe-uptake by marine microorganisms, especially in a context of ocean acidification, where an increase of the physiological stress could imply a decrease in the Fe-bioavailability (Shi, et al. 2010, 2012). The application of a kinetic model, supported by the Marcus theory, indicated the organic exudates, excreted by *Synechococcus* PCC 7002, bind organically iron, modifying its redox cycle in the upper ocean.

CHAPTER IV

CHAPTER V

Variability in the organic ligands released by Emiliania huxleyi, under simulated ocean acidification conditions

Samperio-Ramos, G., Santana-Casiano, J.M., González-Dávila, M., Ferreira, S. and Coimbra, M.A.: Variability in the organic ligands released by *Emiliania huxleyi*, under simulated ocean acidification conditions. *International Journal of Molecular Science s*. Submitted.

CHAPTER V

➢ Abstract

Acquisition mechanisms of trace metals by autotrophic microorganisms are strongly subject by the presence of organic matter biologically mediated. The variability in the extracellular release of organic ligands by *Emiliania huxleyi* under four different pCO_2 scenarios (225, 350, 600 and 900 μatm), was determined. The growth in the batch cultures was promoted enriching only with major nutrients and low iron concentrations. These conditions, without chelating agents controlling metal speciation, generated a development of cocclithophorids where iron limited their growth. During the initial (IP), exponential (EP) and steady (SP) phases, extracellular release, normalized per cell and day, of dissolved organic carbon (DOC_{ER}), phenolic compounds (PhC_{ER}), dissolved combined carbohydrates ($DCCHO_{ER}$) and dissolved uronic acids (DUA_{ER}) were determined in the exudates.

The growth rate decreased in the highest CO_2 treatment in the IP (<48 h), but it increased, when the exposure was longer (from 6 days). Although no relationship among $DCCHO_{ER}$ and the CO_2 conditions was observed, DCCHO was a substantial fraction of freshly organic material and accounted for 18% to 37%, in EP, and 14% to 23%, in SP, of DOC produced. While in EP, the PhC_{ER} was no detected and the DUA_{ER} was sustained highly similar in all CO_2 treatments, the increase of pCO_2 induced a strong response in PhC_{ER} and DUA_{ER} during SP, suggesting that acid polysaccharides and phenolic compounds were produced and excreted in response to physiological stress by the low iron availability and acidification conditions.

CHAPTER V

CHAPTER V

5.1 Introduction

Increasing atmospheric carbon dioxide levels causes rapid alterations of the physical and chemical seawater conditions, affecting the ecosystem dynamics (Gattuso et al. 2015). This last process so called ocean acidification may increase carbon fixation rates in some photosynthetic organisms (Doney et al. 2012; Riebesell and Tortell, 2011). Therefore, the contribution of primary producers, modifying the concentration of CO_2 in the surface natural water, has an important impact on global biogeochemical carbon cycle, affecting the net CO_2 flux across the air-sea interface (Behrenfeld et al. 2006).

The extracellular release of dissolved organic carbon, normalized by cell (DOC_{ER}, is an excretion rate, which indicates the discharge to medium of recently fixed inorganic carbon. In highly productive marine systems, the release of dissolved organic compounds by phytoplankton can contribute up to 45% of total primary production (Bosc et al. 2004; Morán and Estrada, 2001). Accordingly, autotrophic DOC_{ER} plays a key role in the biogeochemical balance of ocean carbon, contributing decisively to the biologically-mediated carbon cycle (Hansell, 2013; Honjo et al. 2014). In the open ocean, it represents the main input of reactive organic carbon in the photic layer (Carlson and Hansell, 2015), followed by cell lysis (Agustí and Duarte, 2013), heterotrophic organic exudation, and grazing (Ruiz-Halpern et al. 2011). The dissolved organic carbon (DOC) export by mixing processes from the surface waters to bathypelagic and mesopelagic zones and its consequent remineralization, via microbial loop, is the dominant carbon sink in the ocean (Giering et al. 2014; Legendre et al. 2015). Another important loss of DOC is carried out by the photochemical processes (Mopper et al. 2015) and by the physical mechanisms that transfer dissolved molecules into particulate size (Engel et al. 2004; Passow, 2002; Verdugo et al. 2004). An understanding of these carbon dynamics require the deciphering of factors, affecting the production, transformation and loss of DOC in marine systems.

Although only a small fraction of marine autotrophic DOC has been identified (Repeta, 2015), when biological production and DOC-loss processes are decoupled, either temporarily or spatially, combined carbohydrates (CCHO) and phenolic compounds represent an important fraction of reactive dissolved organic matter in seawater (Benner et al. 1992; Leenheer and Croué, 2003). In the last years, several distribution studies of different biochemical components in the ocean have been carried, both in the dissolved and/or particulate phases (Kaiser and Benner, 2009; Khodse et al. 2007; Velasquez et al. 2011), and the CCHO have shown to be the dominant constituent in the colloidal size fraction (Benner, 2011). CCHO are key structural components of cell walls and serve as a storage reservoir for microalgae and bacteria, in response to iron availability (Van Oijen et al. 2005). Dissolved combined carbohydrates (DCCHO) are the major component of reactive organic carbon and can reach up to 10% of DOC in open ocean, where suffers sharply concentration declining in the subsurface layers (Goldberg et al. 2009; Kaiser and Benner, 2009), whereas in margin continental and coastal systems represent between 15% and 35% of DOC (Hung et al. 2003, 2001). The molecular composition of DCCHO excreted by autotrophic organisms is mainly shaped by hexoses, deoxyhexoses, and acidic hexoses (Borchard and Engel, 2012; Nelson et al. 2013). Extracellular polymeric substances released by microorganisms during their growth contain a high proportion of dissolved uronic acids (DUA) (Galgani et al. 2016; Underwood et al. 2013), a class of sugar acids with carboxylic acid functional groups, which confer a net negative charge to form resilient linkages between the polymers chains (Hassler et al. 2011a). The coagulation of those aggregates involves the formation of the transparent exopolymeric particles, which play an important role in the sink of marine DOC (Engel et al. 2004; Verdugo et al. 2004).

Phenolic compounds (PhC) are also naturally present in marine systems, since they are considered to be one of the principal functional groups in humic substances (Stubbins et al. 2008). Phenols can be also released from polymers, during both photochemical decomposition and biodegradation of natural organic matter (Li et al. 2015; Lu et al. 2016). Therefore, river discharge and the subsequent physical mixing processes of seawater plays an important role in controlling the concentration and distribution of PhC in the ocean (Lu et al. 2016). Phenolic fractions also contribute

significantly to the fluorescence of organic matter extracted from interstitial water of marine sediments (Klapper et al. 2002). and comprise an important part of DOC pool, accounting up to 5%, accrued in the surface waters of subtropical ocean gyres (Helms et al. 2015). Moreover, PhC are excreted by a wide range of marine macroalgae as secondary metabolites (López-Alarcón and Denicola, 2013). Although the regulatory processes of exudation of phenolic compounds by phytoplankton have not been clearly established, recently there an important phenolic content in exudates of eukaryote phytoplankton have been reported (López et al. 2015; Rico et al. 2013).

Phenolic compounds and dissolved uronic acids can form complex with iron by hydroxyl and carboxylic acid groups (Elhabiri et al. 2007; Sreeram et al. 2004). Both catechol, a frequent and reactive dihydroxyphenolic moiety found in exudates of phytoplankton (Santana-Casiano et al. 2014), and uronic acids bind iron to produce relatively stable Fe-organic complexes, preventing the iron precipitation in oxidative conditions (Hassler and Schoemann, 2009; Wu et al. 2016) and increasing the iron bioavailability in seawater (Hassler et al. 2011b; Maldonado et al. 2005). The fractional contribution of phenolic substances and DUA to the pool of autotrophic DOC production is controlled by the physic-chemical parameters of the extracellular medium, such as temperature, pH, light, and bioavailability of inorganic nutrients (Celis-Plá et al. 2015; Engel et al. 2011; Gunderson et al. 2016; López et al. 2015; Mueller et al. 2016; Zondervan, 2007). Moreover, the variations projected for the marine carbonate chemistry (IPCC, 2014) might decrease the need for employing CO_2-concentrating mechanisms in autotrophic microorganisms (Wu et al. 2010), modifying the carbon fixation efficiency and, consequently, the release of organic matter by marine phytoplankton (Engel et al. 2005). Ocean acidification alters the physiologic pathways of the coccolithophorid *Emiliania.huxleyi*, afecting the Krebs cycle and mitochondrial respiration are affected by enhancing the production of PhC (Jin et al. 2015). Such elevated CO_2 conditions can also stimulate the release of DUA in eukariota community (Lidbury et al. 2012). In fact, chemostat experiments have exhibited an increase in the production of DCCHO in *E. huxleyi*, as well as magnification in the transfer of dissolved high molecular weight carbohydrates to transparent exopolymeric particles, by abiotic aggregation processes (Borchard and Engel, 2012). Nevertheless, an experimental assessment of releasing *E. huxleyi*-

derived Fe-ligands under ocean acidifcation conditions has not been conducted without continue nutrient supply, which regulate the rate of growth and, therefore, the physiological status of microorganisms. Moreover, the chemical variation of Fe-binding agents by ocean acidification, along growth curve in coccolitophorids, is not yet clear, having in account that growth phases have been shown to affect the composition of DOC released by phytoplankton (Barofsky et al. 2009).

In order to improve our understanding on extracellular release of organic ligands excreted by phytoplankton under future and pre-industrial marine carbon chemistry, we have conducted several microcosm experiments with *E. huxleyi* where the dissolved inorganic carbon and the pH have been manipulated. The coccolithophorids play a key role in the biogeochemical cycle of carbon and are particularly sensitive to ocean acidification, due to the production of calcite coccoliths (Doney et al. 2009). The high genomic plasticity of coccolithophorid *E. huxleyi* causes it thrives successfully in large-scale episodic blooms of a wide variety of habitats (Read et al. 2013; Tyrrell and Merico, 2004). Therefore, the objectives of this research are (1) to study the variation, normalized per cell and day, of DOC_{ER}, saccharides (i.e. DCCHO and DUA) and phenolic compounds in the exudates of *E. huxleyi* during the different growth stages, (2) to quantify the contribution of organic compounds excreted to DOC in each CO_2 treatment, and (3) to carry out a statistical analysis for growth rates, DOC_{ER} and organic ligands, having into account the effect of CO_2 conditions of the *E. huxleyi* batch cultures under low iron environment content

5.2 Material and methods

5.2.1 Set-up and cultures

The carbonate chemistry in the culture medium was manipulated through a system (Fig 5.1) based on bubbling a gas mixture of CO_2-free air and pure CO_2 (Riebesell et al. 2010). To ensure quasi-constant seawater carbonate chemistry (Table 1), when the seawater pH values reached the target value, a solenoid valve, connected both to gas cylinders and pH controller, modulated the CO_2 flux,

maintaining the set pH (± 0.02). The pH was measured on the free hydrogen ion scale, $pH_F = -\log [H^+]$ with a Ross Combination glass body electrode daily calibrated with TRIS buffer solutions.

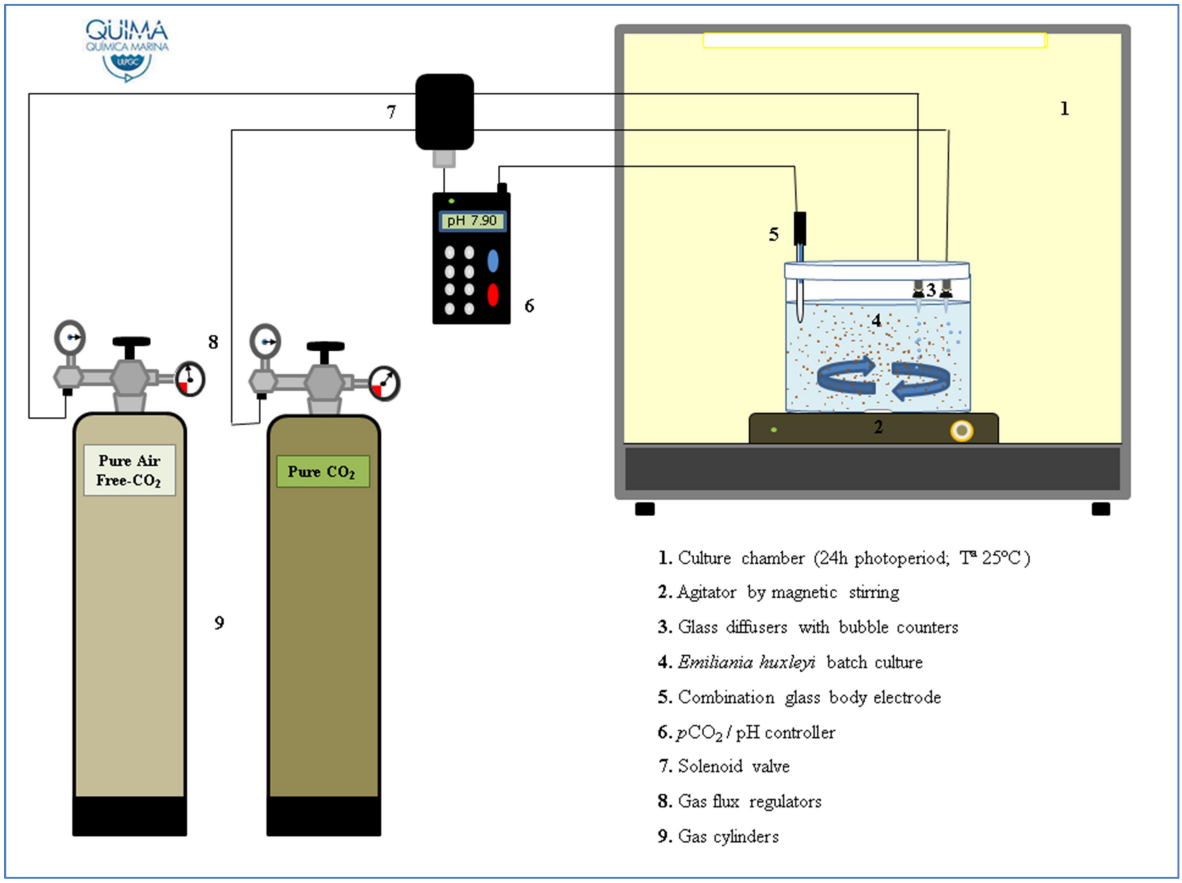

Fig 5.1 CO_2/pH perturbation experiment set-up, indicating the components

To establish the present and future CO_2 ocean conditions, four experimental scenarios, based on Intergovernmental Panel on Climate Change projections (IPCC, 2014) were fixed: preindustrial, close to contemporary and two futures ocean acidification conditions with pCO_2 225, 350, 600 and 900 µatm, respectively. Consequently, the aeration with CO_2-air-mixture generated constant pH values of 8.25, 8.10, 7.90 and 7.75 (Table 1). Microcosms were performed in autoclaved and closed 2.5 L polycarbonate cylindrical tanks to avoid both the gas exchange between the medium and the ambient atmosphere and to prevent variation in salinity by evaporation. To ensure gas homogeneity in the solution and to keep cells in suspension, the cultures were mixed at 60 rpm with a teflon-coated magnetic stirrer. Material, including cell incubators, gas inoculators and tubes connected to them,

were cleaned according to a standard protocol (Achterberg et al. 2001) and subsequently sterilized by autoclaving at 121ºC for 30 min before usage.

The axenic culture stock of E. *huxleyi* was supplied by the Spanish Bank of Algae (BEA, Taliarte) in f/2 medium (Guillard, 1975). The stock and experimental cultures were placed in an incubator clean chamber (Friocell FC111) at a constant temperature of 25 ºC, under complete photoperiod (24 h) with light intensity of 200 µmol photons m^{-2}. In order to pre-adapt to each CO_2 treatment, the stock cultures were maintained under each experimental conditions during 48 h before starting each experiment, allowing the acclimatization to CO_2 perturbation, avoiding short-term stress effects on coccolithophorid physiology. Experimental cultures grown in sterile filtered (0.1µm) North Atlantic seawater (S = 36.48) obtained at the ESTOC site (29º 10' N, 15º 30' W). When the seawater reached the pCO_2/pH desired value, the cocolitophorids were inoculated in batch cultures to a density of 10^6 cells L^{-1}.

Stock and experimental cultures were monitored for contamination and cell densities using a microscope and a hematocytometer (Microbiotest, Inc.). Immediately and in order to promote an useful development during the coccolithophorid growth, nitrate and phosphate were added at a ratio of 30:1 (Engel et al. 2004), yielding initial concentrations of ortophosphate (PO_4^{3-}) and nitrate (NO_3^-) of 28 and 850 µM, respectively. To promote coccolithophorid growth, iron was added to seawater from a stock solution (1 mM) of ferric chloride (Sigma), making an initial concentration of 2.5 nM. All nutrients used in the batch cultures were trace analytical grade. To carry out the organic assays, the seawater enriched with exudates was sampled and filtered using acid cleaned and combusted polycarbonate (Nucleopore) syringe-filters (0.45 µm), to avoid cell breakage.

5.2.2 Alkalinity and Dissolved Inorganic Carbon

Samples for total alkalinity were potentiometrically titrated with HCl to carbonic acid end point using VINDTA 3C system described in detail by González-Dávila et al. (2010). The titration of the different CRMs (provided by A. Dickson at Scripps Institution of Oceanography) was used to test the performance of the titration

system giving values with an accuracy of ± 1.5 µmol kg^{-1}. The precision (between-bottle reproducibility) as judged from regular measurements of duplicate samples was 0.5 µmol·kg^{-1}. Dissolved inorganic carbon was analyzed with coulometer determination. The accuracy was ± 1.0 µmol kg^{-1} after CRMs titration. In order to compare with other seawater values, dissolved inorganic carbon and total alkalinity (X) were normalized (X_n) to a constant salinity ($S_{ref} = 35$), $X_n = (X/S_{sample})\cdot S_{ref}$.

The package Seawater Carbonate (Seacarb version 3.0), development by Lavigne et al (2011) with R (R development Core Team), was used to corroborate the values of pCO_2, using the experimental results of the pH, DIC and AT and considering the carbonic acid dissociation constants of Millero (2010). The pH conversion from free scale to total scale was performed with the Dickson (1990) constants, how is recommended by the guide to best practices for ocean CO_2 measurements (Dickson et al. 2007).

Table 5.1 Carbonate chemistry parameters, for each CO_2 treatment: pH (total scale), total alkalinity (TA) normalized to S‰ = 35, total dissolved inorganic carbon concentration ([DIC]) and calculated pCO_2 (µatm) Temperature 25 ºC. Mean values and standard errors (in parentheses) were derived from sampling (n=3).

pCO_2 treatment (µatm)	pH_T (± 0.02)	TA (µmol· kg^{-1})	[DIC] (µmol · kg^{-1})	pCO_2 (µatm)
225	**8.25**	2355.5 (± 13.8)	1886.8 (± 19.0)	223.2 (±1.2)
350	**8.10**	2353.7 (± 15.4)	1991.6 (± 16.2)	351.4 (± 3.9)
600	**7.90**	2368.3 (± 16.2)	2106.6 (± 18.1)	607.7 (± 5.3)
900	**7.75**	2383.6 (± 11.9)	2196.3 (± 12.8)	917.8 (± 12.6)

5.2.3 Dissolved Organic Carbon

DOC concentration in samples (both in seawater and in the seawater enriched with *E .huxleyi* natural exudates) was monitored using a Total Organic Carbon analyzer (Shimadzu TOC-V) previously calibrated from standard curves (20 to 300 µmol C L^{-1}) with potassium hydrogen phthalate standard (Sigma-Aldrich) (Arístegui et al. 2014). DOC reference material (D. Hansell; University of Miami) was analyzed to check for the accuracy and precision of instrument. The method had an uncertainty

of 3% and a detection limit of 1.3 μmol C L^{-1}. The instrument blank (3–10 μmol C L^{-1}) was measured using UV-irradiated Milli-Q water and was subtracted from each sample.

5.2.4 Phenolic compounds (PhC)

The Arnow test (Arnow, 1937) enabled the selective detection of dihydroxyphenolic compounds in seawater enriched with exudates of *E. huxleyi* (5 mL, filtered by 0.45 μm) by addition of hydrochloric acid (5 mL; 0.5 M), followed by addition of 5 mL (0.5 M) of sodium molybdate (Sigma-Aldrich) and 5 mL (0.5 M) sodium nitrite (PanReac). Then, sodium hydroxide (Sigma) was added in excess (5 mL; 1 M). Maximum absorbance was read at 510 nm using UV-VIS spectrophotometer (S4000, Ocean Optics™), connected to a 5 m long waveguide capillary flow cell (World precision instruments™), which allowed to reach a detection limit of 2 10^{-8} M. The standard employed for the assay was catechol (Sigma-Aldrich) and Mili-Q water with the reagents was used as blank.

5.2.5 Total dissolved combined carbohydrates (DCCHO)

The levels of DCCHO both in seawater and seawater enriched with exudates of *E. huxleyi* were analysed by the method developed by Myklestad et al. (1997) with slightly amendments (Hung and. Santschi, 2000), which is based upon oxidizing the free reduced DCCHO with the 2,4,6-Tris(2-pyridyl)-s-triazine (TPTZ; Sigma-Aldrich). The assay involved the acid hydrolysis with HCl (0.4 mL) of the sample (4 mL), in a sealed ampoule, for 2 h at 120 ºC. When the solution was neutralised (0.4 mL of 1 M NaOH), 1 mL of the hydrolysate was added to a 1 mL of a solution 0.7 mM potassium ferricyanide (Sigma-Aldrich), prepared in 1 L of Milli-Q water containing 20 g $NaCO_3$ and 400 mg NaOH. Then, the well-mixed solution was placed in a boiling water bath for 15 min. Both 1mL of 2 mM solution of ferric chloride, prepared adding 16.4 g sodium acetate, 4.2 g citric acid and 30 g acetic acid to 1 L of Milli-Q water, and 2 mL of 2.5 mM. TPTZ solution in 3 M acetic acid were

promptly added and suitably mixed on a Vortex. After 30 min, the absorbance was measured, using UV-VIS spectrophotometer (S4000, Ocean Optics^{TM}), at 595 nm, (S4000, Ocean Optics^{TM}). The standard employed was glucose (Sigma-Aldrich) and the absorbance of reagent blank in Milli-Q water was subtracted before reading the absorbance of the monosaccharide of each sample.

5.2.6 Dissolved uronic acids (DUA)

In order to have a measurable level for DUA, the samples were concentrated by rotary evaporation, under reduced pressure at 40ºC. Then, the concentration of DUA were measured according to the method reported by Blumenkrantz and Asboe-Hansen (1973) and modified in Bastos et al. (2015). To 0.5 mL of a concentrated, 3 mL of 75 mM sodium tetraborate in concentrated sulfuric acid was added and the resulting solution was heated at 100 °C for 10 min in boiling water bath. After cooling, 100 µL 0.15% m-hydroxydiphenyl (Sigma-Aldrich) was added, and the absorbance was determined spectrophotometrically at 525 nm. The reagent blank was considered in order to compute the final concentration of the monosaccharide. Galacturonic acid (Sigma-Aldrich) was used as standard.

5.2.7 Data and statistical treatments

The growth rates (µ, day^{-1}) were calculated from the changes in the cell number over time and data were fitted to an exponential growth model ($\mu = (\ln N_{t2} - \ln N_{t1})/\Delta t$). The cell densities (N) were determined from an average 5 experimental batch cultures at each pCO_2 treatment. The goodness of the fit for each curve was estimated by the coefficient of correlation ($r^2 > 0.95$). Under the different CO_2 scenarios, the development of *E. huxleyi* happened according to a sigmoid curve (Fig 5.2) showing three significantly marked trends in the growth rates, as the culture time elapsed (Table 2). Thus, the measurements of (DOC (µmol C L^{-1}), as well as, the determination of organic extracellular release rates (µmol C cell^{-1} day^{-1}), were carried out distinguishing the three stages in the growth curves of *E. huxleyi*: initial

(IP, until 2nd day), exponential (EP, from 3rd to 5th day) and stationary (SP, from 6th to 8th day) phases (Table 2 and 3). The concentrations of, DOC, PhC, DCCHO and DUA were corrected to levels of seawater and the unit utilized were obtained by multiplying the concentrations values (µmol L^{-1}) by the number of carbon per mole of compounds used as standards during calibrations (i.e phthalate, catechol, glucose and galacturonic acid, respectively). Due to the exudation rate of freshly dissolved material is a parameter best specified when is normalized per cell and day, we followed the Borchard and Engel (2012) advices. Thus, extracellular release rates (µmol C $cell^{-1}$ day^{-1}) were derived from DOC accumulation rate (µmol C L^{-1} day^{-1}) and variation of the cell densities.

R (R Development Core Team, 2008) was used for statistical computing. Analysis of variance (ANOVA) was carried out to test for significant effects both of different pCO_2 treatments and growth stages on the production normalized of DOC, DCCHO and organic Fe-ligands (i.e. PhC and DUA) present in the *E. huxleyi* natural exudates during cultures development. A post-hoc test, Tukey's HSD, was used to do a multiple comparison procedure to find means that are significantly different. The assumptions of normality and homoscedasticity were verified using the Shapiro-Wilk and Barlett tests respectively. Regression models were used to assess the relationships between organic parameters. For all statistical procedures, a probability level of $\alpha = 0.05$ was considered.

5.3 Results and discussion

5.3.1 Growth rates

Initially, average *E. huxleyi* cell numbers were 10^6 and increased continuously during 8 days of study to $9.98 \pm 0.53 \cdot 10^7$ (pCO_2 225 µatm), $1.07 \pm 0.13 \cdot 10^8$ (pCO_2 350 µatm), $1.04 \pm 0.07 \cdot 10^8$ (pCO_2 600 µatm) and $9.15 \pm 0.41 \cdot 10^7$ (pCO_2 900 µatm) (Fig 5.2), therefore, acidification conditions did not affect significantly to final cells densities (one-way ANOVA, F-value: 1.327, p = 0.332).

Nevertheless, to evaluate in detail pCO_2/pH effect on coccolithophorids cellular division rates, we distinguished three growth stages separately: initial phase (IP), exponential phase (EP) and steady phase (SP).

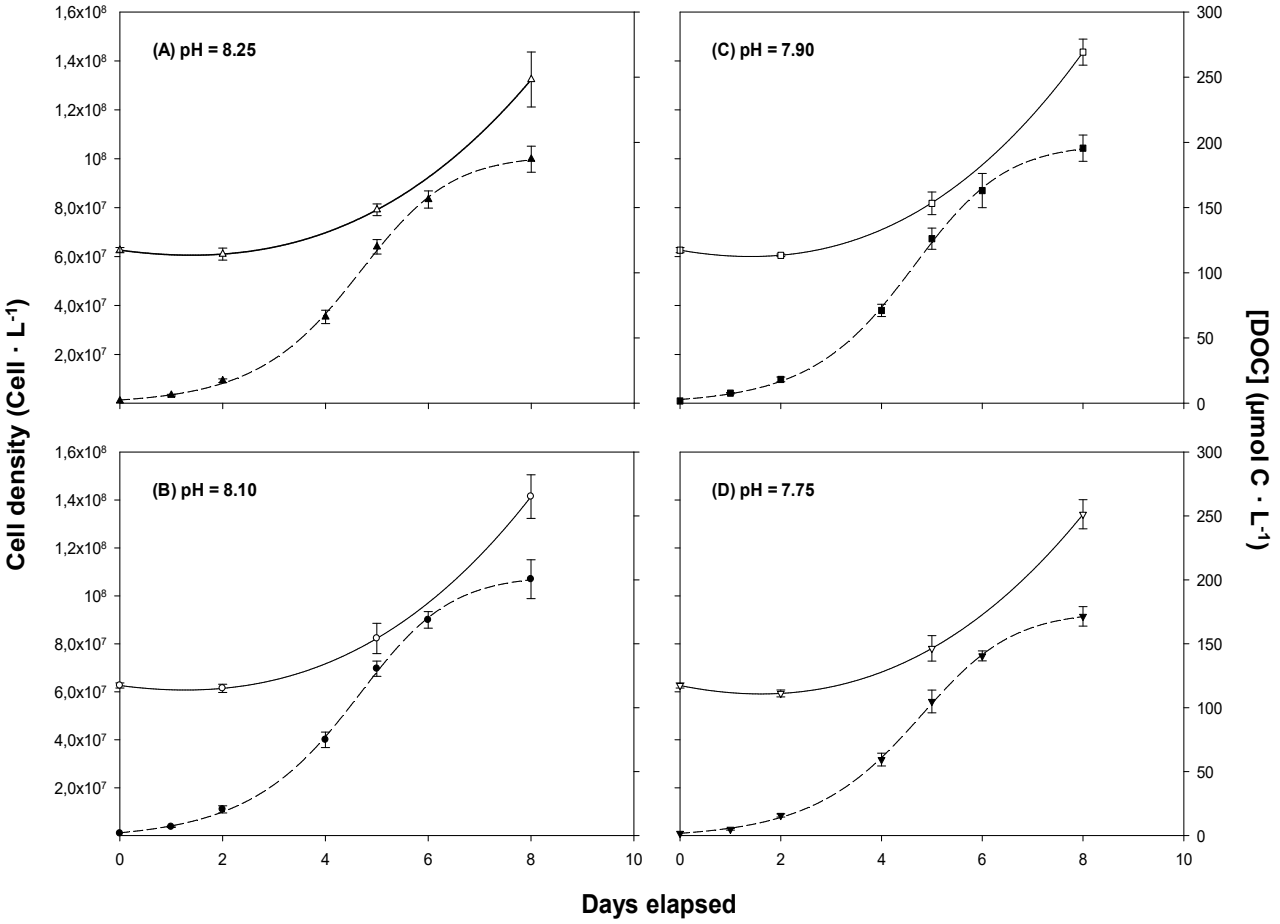

Fig 5.2 Changes in *Emiliania huxleyi* abundances (broken lines) and dissolved organic carbon (DOC) concentrations (solid lines), under different CO_2 conditions, during experimental cultures. Error bars represent ± SE of the mean (n = 5 and 3 for cell densities and DOC levels, respectively).

During the IP, the growth rate showed the lowest values when the microalgae were exposed to the highest CO_2 levels ($\mu = 1.07 \pm 0.05$ day^{-1}), while the maximum growth rates were achieved with pCO_2 350 µatm and 600 µatm ($\mu = 1.19 \pm 0.07$ and 1.15 ± 0.03 day^{-1}, respectively). In EP, the growth rates were sustained highly similar under the different CO_2 conditions evaluated and were close to the results found for *Emiliania huxleyi* (Müller et al. 2008) and other cocolitophorid species (Daniels et al. 2014) in studies conducted in batch cultures. However, during SP it was observed a growth rate rise statistically significant (one-way ANOVA, F-value: 4.228, $p < 0.05$),

in response to increasing CO_2 concentration, reaching 0.19 (± 0.01) day^{-1} at pCO_2 900 µatm, (Table 2). Our results indicate that the *E. huxleyi* populations were adapted to experimental acidification, displaying a slight increase of growth rates during SP. Nevertheless, the highest peaks of algae biomass, 1.07 (± 0.10) and 1.04 (± 0.06) × 10^8 cells L^{-1}, were recorded in the microcosms with intermediate CO_2 levels (350 and 600 µatm respectively).

During the last decade, the studies with acidification perturbation experiments, carried out with coccolitophorids in batch cultures, have exhibited variability on the specific growth response (Bach et al. 2012; Iglesias-Rodriguez et al. 2008; Langer et al. 2009; Lohbeck et al. 2012; Müller et al. 2010; Shi et al. 2009), related to intrinsic physiological parameters such as the process of calcification or cell size of the different strains (Meyer and Riebesell, 2015). Environmental conditions such as light intensity (Rokitta and Rost, 2012), temperature (Sett et al. 2014) or major nutrients availability (Borchard et al. 2011; Sciandra et al. 2003) were also pointed out as decisive co-factors to induce changes in the division rates during CO_2/pH perturbation experiments. However, in the present study, the cultures were kept under identical temperature and photon flux density. In the short term incubations here discussed, we exclude the limitation of P and N as cause of decline in growth rates, since both the initial nitrate and phosphate concentrations (850 µM and 28µM, respectively) are fairly above of half-saturation constant of N and P uptake (Riegman et al. 2000). Even though *E. huxleyi* has typically been assumed to be strong competitor under iron deficient conditions (Zondervan, 2007), incubation experiments provided evidence that iron can limit *E. huxleyi* community growth (Nielsdóttir et al. 2009). During an Fe-induced mesoscale bloom in the northeast Pacific Ocean, a correlation between photosynthetic efficiency (F_m/F_v) and dissolved iron concentrations (dFe) was also assessed inside the fertilization patch (Boyd et al. 2005). In the last stages of bloom, the authors found a marked threshold, at around 0.2 nM dFe, below which quantum yield was halved with a consequently decline on growth rates in the *E. huxleyi* populations. In addition, the initial concentration here fixed (2.5 nM) was slightly higher than those considered as iron limited control conditions (total dFe = 1.35 nM) in experiments conducted with seawater and natural populations from high-nutrient low-chlorophyll (HNLC) region of the Bering Sea

(Sugie et al. 2013). Taking in to account that in the present work the initial biomass, and therefore the biological demand of iron was considerably higher than in natural populations evaluated by Sugie et al. (2013), we suggest that the development of *E. huxleyi* might have been subjected to a continuum biological use of Fe, giving place a reversal in the iron-status levels, and so appearing Fe-depleted conditions during the last growth phase (SP), which limit the growth of *E. huxleyi*.

5.3.2 DOC dynamics

From seawater control initial DOC concentrations (117.34 ± 1.97 μmol C L^{-1}) decreased non-significantly during IP (one-way ANOVA: F-value = 2.273, P = 0.156). This decline of DOC levels was slightly affected by CO_2 conditions, since the loss of DOC varied from pCO_2 225 μatm (3.04 ± 2.32μmol C L^{-1}) to pCO_2 900 μatm (6.19 ± 2.71 μmol C L^{-1}). In spite of the microcosms were carried out in a clean culture chamber, complete no-axenic conditions were assumed in the experimental cultures. Although pre-sterilization both of seawater and bioreactors allowed to keep low density of heterotrophic bacteria (< 10^6 cell · L^{-1}) in the course of experimental period, microbial organic matter degradation might explain the heterotrophic behavior in experimental cultures during IP. In bacterial enzyme's environments, a drop of the pH modifies the ionization state of labile organic matter, exposing the actives sites of its three-dimensional structure (Alexov and Gunner, 1997), and thus accelerating its degradation (Piontek et al. 2013). Thereby, the recent publication by Endres et al. (2014) shows the efficiency of the protein degrading enzyme leucine aminopeptidase, which significantly increases its activity at the highest pCO_2 mesocosm, when is compared to the controls. DOC sinking might also be due to aggregation of high molecular weight dissolved components, which is increased at high CO_2 levels (Riebesell et al. 2007). We did not measured the transparent exopolymeric particles formation but the aggregation process is highly dependent on the physiological status of microbial community (MacGilchrist et al. 2014) and its formation occurs after exhaustion of majority nutrients (Engel et al. 2004). Therefore, in the short term incubations, conducted under N and P replete conditions, the relevance of abiotic aggregation processes can be considered negligible.

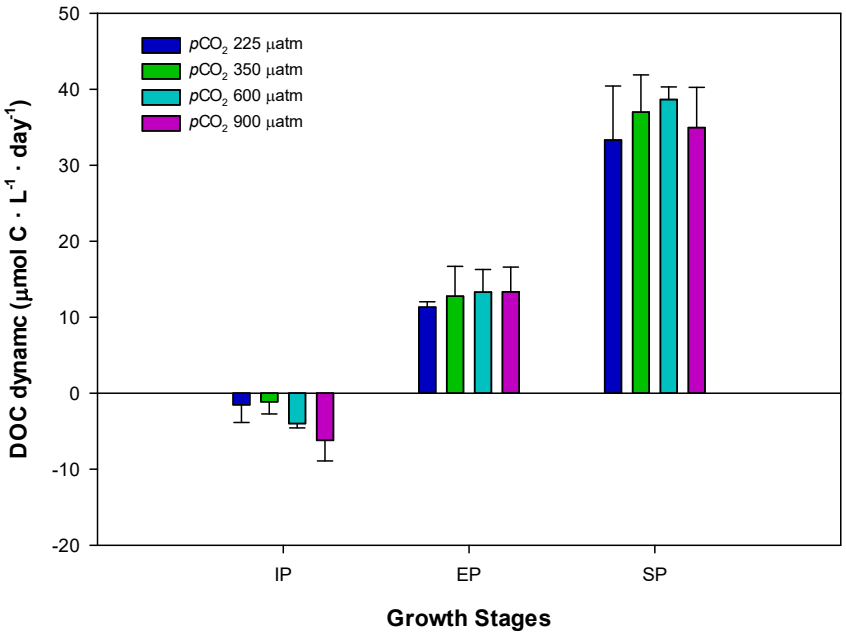

Fig 5.3 DOC dynamics of experimental *E. huxleyi* batch cultures, at initial (IP), exponential (EP) and steady growth stages, under various pCO_2 conditions. Mean values and error standard deviations were derived from three replicates.

The incubations showed changes in the productivity status, from heterotrophic conditions (Duarte et al. 2011) to highly autotrophic conditions (Williams et al. 2013). Heterotrophic consumption played a minor role in the DOC dynamics during EP and SP (Fig 5.3). The accumulation of DOC gradually increased during EP and SP, although without significant difference among the CO_2-treatments (one-way ANOVA: F-value = 0.174, P = 0.911 for EP; F-value = 0.474, P = 0.709 for SP). In the same way, Borchard and Engel (2012) found no significant effect of pCO_2 on concentrations of DOC during steady state growth in continuous cultures of *E. huxleyi.* DOC concentrations measured during shipboards bioassays experiments, with natural community from North Sea, either showed significant dependence with CO_2 levels (MacGilchrist et al. 2014). Nevertheless, the amount DOC exuded in to environment may be highly variable, in function of the dominant specie and its response to changes in the CO_2 conditions (Paul et al. 2015). For example, in mesocosms carried out in a high nutrient low chlorophyll region of Pacific Ocean, the pH-dependence in the DOC levels was only shown when diatoms increased their dominance over haptophyta algae group (i.e. coccolithophorids) (Yoshimura et al. 2013).

Unlike absolute measures, the organic production rates (i.e. extracellular release) are relatively constant parameters between the different phytoplankton species and only changing in response to physiological perturbations produced by environmental factors, such as nutrient availability or CO_2 conditions (Borchard and Engel, 2012; Thornton, 2014). Extracellular release rate of DOC (DOC_{ER}) increased as the levels of CO_2 were higher in the culture medium, from 177.06 ± 10.95 fmol C · $cell^{-1}$ · day^{-1} (pCO_2 225 µatm) to 209.74 ± 50.00 fmol C · day^{-1} · $cell^{-1}$ (pCO_2 900 µatm) in EP and from 333.68 ± 71.35 fmol C · $cell^{-1}$ · day^{-1} (pCO_2 225 µatm) to 384.19 ± 47.40 fmol C · day^{-1} · $cell^{-1}$ (pCO_2 900 µatm) in SP (Fig 5.4 and Table 5.2). Our results are comparable with the range of DOC_{ER} presented by Becker et al. (2014) with different strains of cyanobacteria and diatoms. However, the increment of pCO_2 in the experimental cultures, from 225 µatm to 900 µatm, enhanced DOC_{ER} 19% and 15% during EP and SP, respectively. As CO_2 is a key substrate for the primary production , the dependence with pCO_2 of DOC_{ER} was also in agreement with the trend obtained during the first week of a long-term mesocosm with phytoplankton pelagic community, where the assimilation of inorganic carbon was improved under acidified conditions (Spilling et al. 2016).

As bioassay time proceeded, from 5 to 8 day (EP to SP), an increase of DOC_{ER} between 83% (pCO_2 225 µatm) and 89% (pCO_2 900 µatm) was estimated. Higher DOC_{ER} in SP compared to the EP have been also noted previously in batch cultures both of diatom (Underwood et al. 2004; Wetz and Wheeler, 2007) and cocolithophorids (Biddanda and Benner, 1997; Van Oostende et al. 2013). Thereby, DOC_{ER} of *E. huxleyi* might have been stimulated by the synergic effect of Fe depleted conditions and elevated CO_2, albeit a no significant effect of pCO_2 x growth stages was determined (Table 5.2).

Experiments with chemostat bioreactors demonstrated that when *E .huxleyi* grew under nutrient replete conditions, a linear relationship between primary production and extracellular release were generated. However, the depletion of nutrients under simulated acidification conditions shifts biogenic carbon flows from particulate to dissolved forms and disengages the link between primary production and DOC_{ER}, due to an increase of percentage of extracellular release (Borchard and

Engel, 2012; Kim et al. 2011). On the other hand, during other Baltic Sea mesoscosms study (Engel et al. 2014) and also at laboratory incubations (Song et al. 2014), the rising of CO_2 levels supported the production and release of carbon-rich components by microorganisms. Therefore, in order to know how the CO_2 perturbation experiments, carried out in the present work, condition the composition of organic ligands in natural exudates of *E. huxleyi*, the release of PhC, DCCHO and DUA were monitored

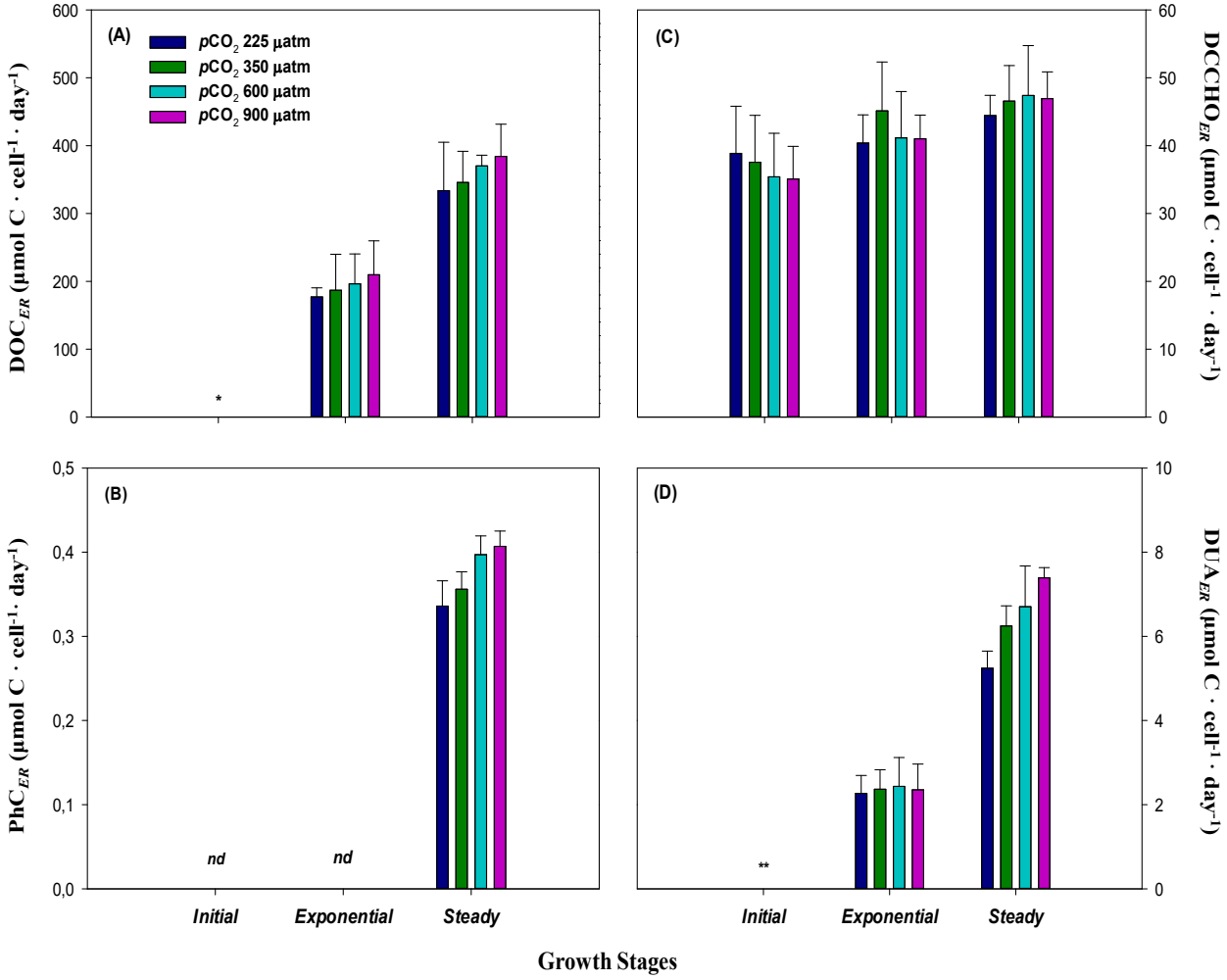

Fig 5.4 Extracellular release rates of (a) dissolved organic carbon (DOC), (b) phenolic compounds (PhC), (c) dissolved combined carbohydrates (DCCHO), and dissolved uronic acids (DUA) for each growth stage, under different CO_2 treatments. Stacked bars show the standard error (n = 3, 5, 5 and 3 for DOC, Ph, DCCHO and DUA respectively). The following indications: *nd, * and* ** denotes not detected (nd), heterotrophic conditions not allowed to compute DOC_{ER} (*) and no significate differences between seawater and seawater enriched with microalga exudates (**), respectively.

Experiments with chemostat bioreactors demonstrated that when *E .huxleyi* grew under nutrient replete conditions, a linear relationship between primary production and extracellular release were generated. However, the depletion of nutrients under simulated acidification conditions shifts biogenic carbon flows from particulate to dissolved forms and disengages the link between primary production and DOC_{ER}, due to an increase of percentage of extracellular release (Borchard and Engel, 2012; Kim et al. 2011).

Table 5.2 Parameters computed during pCO_2/pH treatments for each growth stage.

Growth Stages	pCO_2 (µatm)	µ (day^{-1})	DOC_{ER} (fmol C $cell^{-1}$ day^{-1})	PhC_{ER} (fmol C $cell^{-1}day^{-1}$)	$DCCHO_{ER}$ (fmol C $cell^{-1}$ day^{-1})	DUA_{ER} (fmol C $cell^{-1}$ day^{-1})
IP (day 2)	**225**	1.12 ± 0.03	-	-	38.86 ± 5.94	-
	350	1.18 ± 0.06	-	-	34.59 ± 6.92	-
	600	1.15 ± 0.04	-	-	35.39 ± 6.42	-
	900	1.07 ± 0.06	-	-	35.08 ± 4.82	-
EP (day 5)	**225**	0.59 ± 0.05	177.06 ± 10.95	-	40.38 ± 4.16	2.27 ± 0.42
	350	0.60 ± 0.04	186.84 ± 52.96	-	45.43 ± 7.20	2.36 ± 0.46
	600	0.62 ± 0.02	196.33 ± 44.01	-	41.14 ± 6.82	2.64 ± 0.90
	900	0.60 ± 0.05	209.74 ± 50.00	-	41.00 ± 3.49	2.35 ± 0.61
SP (day 8)	**225**	0.13 ± 0.03	333.68 ± 71.35	0.34 ± 0.03	44.43 ± 2.98	5.24 ± 0.41
	350	0.15 ± 0.01	345.75 ± 45.86	0.36 ± 0.02	45.74 ± 4.93	6.25 ± 0.48
	600	0.16 ± 0.02	370.14 ± 15.79	0.40 ± 0.02	47.39 ± 7.36	6.70 ± 0.97
	900	0.19 ± 0.01	384.19 ± 47.40	0.41 ± 0.02	46.95 ± 3.92	7.39 ± 0.30
Factors of variation						
Growth Stages	*F value*	-	**25.8422**	-	**3.4735**	**80.9422**
	p	-	**< 0.001**	-	**< 0.05**	**< 0.001**
G. Stages x pCO_2	*F value*	-	0.0212	-	0.162	0.9084
	p	-	0.9956	-	0.9855	0.4787
pCO_2 - (IP)	*F value*	1.257	-	-	0.095	-
	p	0.324	-	-	0.962	-
pCO_2 - (EP)	*F value*	0.113	0.3161	-	0.168	0.208
	p	0.949	0.8136	-	0.916	0.888
pCO_2 - (SP)	*F value*	**4.228**	0.0212	**3.765**	0.086	**6.227**
	p	**< 0.05**	0.9956	**< 0.05**	0.967	**<0.05**

On the other hand, during other Baltic Sea mesoscosms study (Engel et al. 2014) and also at laboratory incubations (Song et al. 2014), the rising of CO_2 levels

supported the production and release of carbon-rich components by microorganisms. Therefore, in order to know how the CO_2 perturbation experiments, carried out in the present work, condition the composition of organic ligands in natural exudates of *E. huxleyi*, the release of PhC, DCCHO and DUA were monitored.

5.3.3 Production of Phenolic Compounds

Figure 5.5 shows the strong correlations between the concentrations of freshly PhC with DOC, indicating that phenolic compound made up a relatively constant fraction of the organic material excreted by *E. huxleyi*. However, the dissolved phenolic compounds were only detected in SP and their release rate was affected by CO_2 conditions (Fig 5.4).

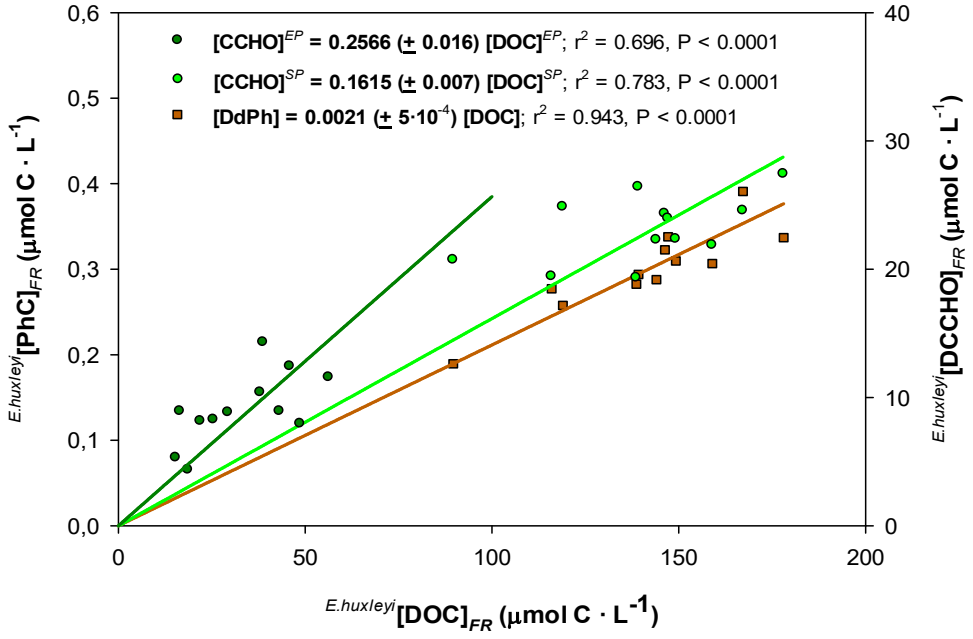

Fig 5.5 Linear correlations between fresh release concentrations of phenolic compounds ($[PhC]_{FR}$) and dissolved combined carbohydrates ($[DCCHO]_{FR}$) with dissolved organic carbon ($[DOC]_{FR}$). The relationship with fresh DCCHO released in *E. huxleyi* cultures was distinguishing the growth stages (Exponential as EP, Steady as SP).

Extracellular release of phenolic compounds (PhC_{ER}) was statistically higher (Table 5.2) at pCO_2 900 µatm (0.41 ± 0.02 fmol C $cell^{-1}$ day^{-1}) than at pCO_2 225µatm

(0.34 ± 0.03 fmol C $cell^{-1}$ · $day^{-}1$; Tukey contrast: t value = 2.898; $p<0.05$) and 350µatm (0.36 ± 0.02 µmol C · $cell^{-1}$ · day^{-1}; Tukey contrast: t value = 2.495; $p<0.1$). The biosynthesis of PhC has implications for grazers, pathogens (Zubia et al. 2008), for preventing photo-damage (Celis-Plá et al. 2016) and free radical scavenging activity (Huang et al. 2016). Phytoplankton can also regulate the bioavailability of trace metals through the production and release of phenolic compounds (Santana-Casiano et al. 2014), because hydroxyl groups can form weak complexes with iron (Perron and Brumaghim, 2009), modifying its chemical speciation and reactivity in seawater (Santana-Casiano et al. 2010). Phenolic moieties from humic substances play a key role in iron complexation in coastal system (Laglera et al. 2011; Yang and Van Den Berg, 2009). In this sense, *E. huxleyi* exudates have also shown high content of Fe-binding humic substance-like material (i.e phenolic moieties), enhancing both the solubility and bioavailability of iron in Fe-limited Sub-Antarctic seawater (Hassler et al. 2015) and therefore, in some oceanic regions phytoplankton could be a significant source of phenolic compounds (Heller et al. 2016). Additionally, an increase of phenolic content in exudates of diatoms (*Phaeodactylum tricornutum*) and green algae (*Dunaliella tertiolecta*), were measured when those microorganisms grow under iron deficient scenario or copper stress conditions (López et al. 2015; Rico et al. 2013), suggesting that phenolic release might be a response to unfavorable growth iron limited conditions. Similarly, under iron starvation state, autotrophic prokaryote microorganisms synthesize and secretion ferric chelators (i.e siderophores) (Butler and Theisen, 2010; Gledhill et al. 2004), which are capable of solubilizing, capturing, and delivering iron to the cell through protein-specific transport systems (Kranzler et al. 2014; Morrissey and Bowler, 2012). In addition, marine siderophore production seems to be optimum in buffer acidified media (Manwar et al. 2004), although in natural seawater the pH-dependence on siderophore release is yet unknown.

The mechanism by which autotrophic organisms regulate their phenolic exudation in response to increased pCO_2 is also not clear. Jin et al. (2015) have reported that the high CO_2-induced changes in seawater carbonate chemistry enhanced the intracellular production of phenolic compounds in *E. huxleyi*. Recently, another study has also determined how a natural acidification event regulates the

phenolic compounds biosynthesis in calcified macroalgae communities, although the magnitude of their response depends on nutrient and light levels (Celis-Plá et al. 2015). In contrast, a previous work has shown seagrass meadows exposed to high environmental CO_2 conditions decreased the production of phenolic compounds (Arnold et al. 2012). Our data (Fig 5.4) suggest that ocean acidification might intensify significantly the PhC_{ER}, when *E. huxleyi* grows under Fe-deplete situations. Thereby, an increase of the phenolic fractions in the exudates of *E. huxleyi* might improve its capacity for iron acquisition (Hassler and Schoemann, 2009; Maldonado et al. 2005) under an ocean acidification scenario, in which the bioavailability of strongest Fe-ligands (i.e siderophores) for eukaryote phytoplankton seem to decline (Shi et al. 2010).

5.3.4 DCCH production

The initial concentration of DCCHO in the cultures was 24.14 ± 0.88 μmol C L^{-1}. DCCHO was continuously accumulating in solution during *E. huxleyi* growth, representing a substantial fraction of freshly produced DOC during all growth stages. The levels of freshly DCCHO produced were highly similar between the different CO_2 treatments (data not shown). The autotrophic DCCHO is a robust indicator of the diagenetic state of organic matter since most of DCCHO produced by phytoplankton are a carbon active reservoir for bacterioplankton (Bourgoin and Tremblay, 2010), especially in an ocean acidification context (Jørgensen et al. 2014; Piontek et al. 2010, 2013). However, through degradation experiments using DOM from axenic *E. huxleyi* cultures, it was shown that the high C:N ratio of those exudates decreased bacterial assimilation efficiency, possibly due to the recalcitrant nature of DCCHO excreted by the coccolithophorids (Van Oostende et al. 2013).

Figure 5.4 shows the significant linear relationships between the concentrations of freshly DCCHO and DOC yielded, where the contribution of DCCHO to fresh DOC excreted was higher during EP (18-37%) than during SP (14-23%). Our data are comparable with that obtained by Hung et al. (2003) in high productivity Gulf of Mexico waters, where the authors linked the increase in DCCHO levels to the different peaks of chlorophyll *a* found in that region.

Extracellular release of dissolved combined carbohydrates ($DCCHO_{ER}$) during initial-state of *E. huxleyi* growth were 38.9 ± 6.9 fmol · C · $cell^{-1}$ · day^{-1}, 34.6 ± 7.7 fmol · C · $cell^{-1}$ · day^{-1}, 35.4 ± 6.4 fmol · C · $cell^{-1}$ · day^{-1} and 35.1 ± 4.8 fmol · C · $cell^{-1}$ · day^{-1} for pCO_2 225, 350, 600 and 900 μatm respectively (Fig 3), increasing significantly as time elapsed from EP until the cultures reached the SP (Table 5.2). Quantitatively, extracellular release rates of DOC and DCCHO slightly differ than those determined by Borchard and Engel (2012) during steady-state growth exposed under CO_2 simulated condition in phosphorus controlled chemostats. Those differences might be attributed both to different cocolithophorid strains evaluated and experimental drawing, as well as physic-chemical parameters fixed during the growth of *E. huxleyi*, such as light:dark cycle, photon intensity, and nutrient status (i.e P and Fe). Although in agreement with our results, these previous results did not reflect the relationship among $DCCHO_{ER}$ and CO_2 conditions. For the batch cultures here presented the $DCCHO_{ER}$ was statistically lower in IP than EP and SP (Table 5.2) in accordance with previous observations with several phytoplankton species (Alderkamp, 2006; Van Oostende et al. 2013; Smith and Underwood, 2000).

The effect of nutrient availability on the amount of DCCHO produced and excreted by phytoplankton are often highly species-specific. Different laboratory studies performed with marine diatoms found that P-depletion determined an increase the $DCCHO_{R,}$ compared to nutrient-replete conditions, but the magnitude of those increases was different for each species examined (Obernosterer and Herndl, 1995; Urbani et al. 2005). The specific iron dependence on biosynthesis and extracellular release of DCCHO by *E. huxleyi* is largely unknown, although indirect findings provide important information. On the one hand, the effect of iron starvation on the photosynthetic process in *E. huxleyi,* decrease Chl *a* : C ratios, (Hiscock et al. 2008; Schulz et al. 2007) and increase the C:N ratio in the compounds (i.e. DCCHO) yielded (Muggli and Harrison, 1996). Simultaneously to reduce the overflow metabolism the gross intracellular production of DCCHO seem to be hampered under Fe-deficient conditions (Van Oijen et al. 2004).

5.3.5 DUA production

Initial DUA concentrations of 3.43 ± 0.12 µmol C L^{-1} were determined in the natural seawater used in the *E. huxleyi* cultures. During IP, no-significant differences (one-way ANOVA, F=0.13, p = 0.891) were found in the levels of DUA between seawater and seawater enriched with exudates of *E. huxleyi*, released in the different pCO_2 treatments, where the average DUA concentration was 3.49 ± 0.10 µmol C L^{-1}. The levels of newly fixed DUA increased along EP and SP. The quantification of DUA in the cultures, corrected to seawater, reveled highest concentrations in treatments with pCO_2 350 µatm (0.56 ± 0.13 µmol C L^{-1} and 2.57 ± 0.16 µmol C L^{-1} for IP and SP respectively) and pCO_2 600 µatm (0.60 ± 0.26 µmol C L^{-1} and 2.69 ± 0.12 µmol C L^{-1} for IP and SP respectively). The concentrations of DUA show a strong correlation in the different pCO_2 treatments with the freshly production of DOC (Fig 5.6), indicating that the contribution of DUA to DOC was fairly constant between EP and SP, although slightly varied due to CO_2 conditions during SP, enhancing from 1.4 % (pCO_2 225 µatm) to 1.9% (pCO_2 900 µatm).

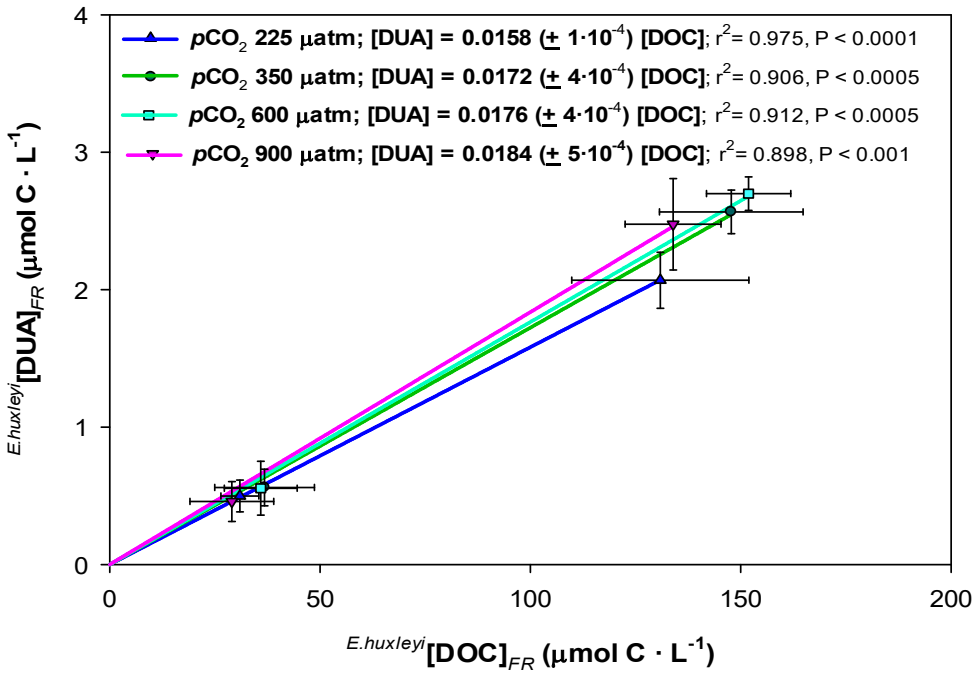

Fig 5.6 Linear correlations between concentrations of freshly dissolved uronic acids (DUA) and dissolved organic carbon (DOC), released in *E. huxleyi* cultures during different CO_2 treatments. Stacked bars show the standard error of replicate samplings (n = 3).

The fraction of DUA to DCCHO shows a more drastic pH/pCO_2 pattern, increasing importantly during SP from 12.2% to 19.1% when the partial pressure of CO_2 enhanced from 225 µatm to 900 µatm (Fig 5.7). Similarly, the DUA fractions computed are in agreement with the values obtained by other authors in different natural systems with high primary production conditions, where the concentrations of DUA accounted for about 0.7% to 5.3% of DOC and 4.2 to 17.2% of DCCHO (Hung et al. 2001; Khodse et al. 2010). In laboratory studies with continuous cultures of *E .huxleyi*, DUA ranged between 5% and 25% of high molecular weight combined carbohydrates (Borchard and Engel, 2015).

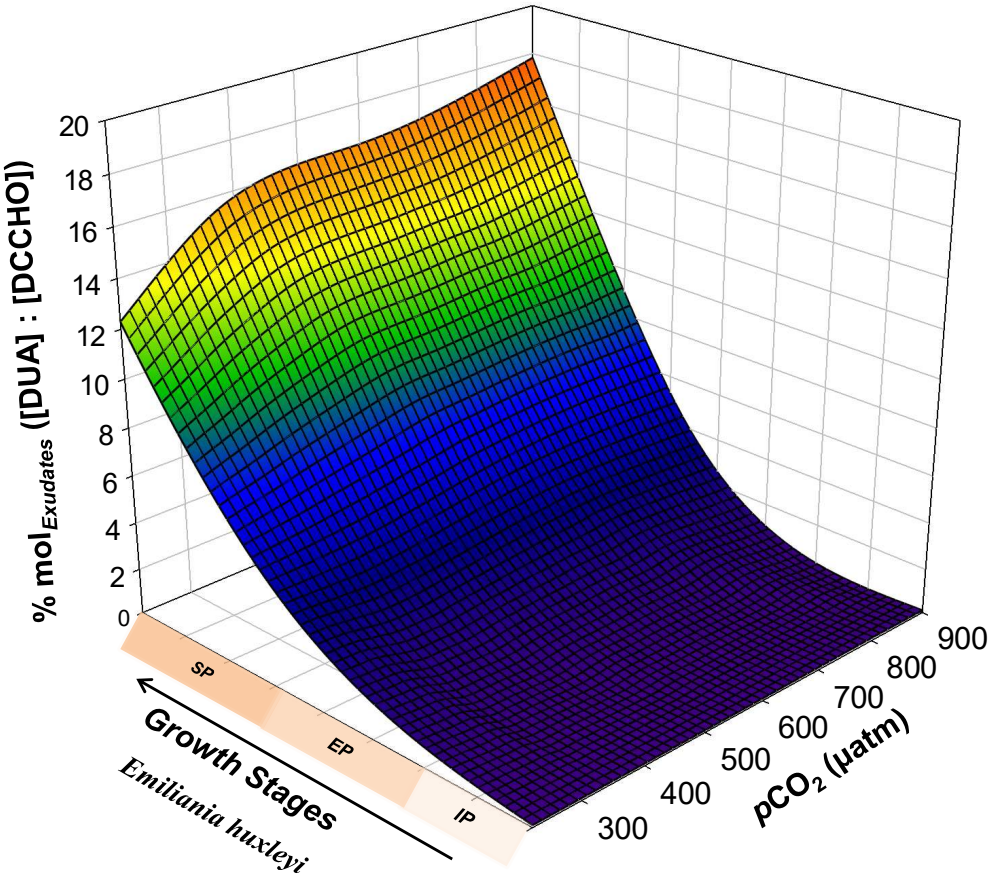

Fig. 5. 3D-model contribution of freshly dissolved uronic acids (DUA) to dissolved carbohydrates (CCH) released by *E. huxleyi* cultures during the different growth stages (IP: Initial phase; EP: exponential phase and SP: steady phase) under different ocean acidification and major nutrient replete conditions. Tª 25 ºC.

Table 5.2 shows that DUA_{ER} concurrently increased with the raise of DOC_{ER}. In all CO_2 treatments DUA_{ER} was maximal in the SP. During the period of exponential growth (EP) no-statistically differences in DUA_{ER} between treatments were observed. However, in SP, DUA_{ER} significantly varied due to changes in the CO_2 conditions and was higher at pCO_2 900 µatm (7.39 ± 0.30 µmol C $cell^{-1}$ day^{-1}) than pCO_2 225 µatm (5.24 ± 0.30 µmol C $cell^{-1}$ day^{-1}; Tukey contrast: t value = 4.206; $p<0.05$) and pCO_2 350 µatm (6.25 ± 0.48 µmol C $cell^{-1}$ day^{-1}; Tukey contrast: t value = 2.834; $p<0.1$), whereas at pCO_2 600 (6.70 ± 0.97 µmol C $cell^{-1}$ day^{-1}) was higher than pCO_2 225 µatm (Tukey contrast: t value = 2.864; $p<0.1$) (Table 2). DUA are a major constituent of the carbohydrates found in *E. huxleyi* exudates during exponential and steady growth phases (Fig 5.2). They have been recognize as a dominant surface-active fraction of extracellular polymeric substances produced by both eukaryotic phytoplankton, and heterotrophic and autotrophic bacteria (Galgani et al. 2016; Nichols et al. 2005b; Ozturk et al. 2014). The carboxylic groups of uronic acids can bind cations with valence ≥ 2 (Chow et al. 2015; Zhang et al. 2008), including Fe(II)and Fe(III) (Gyurcsik and Nagy, 2000), affecting both chemical speciation of dissolved iron and its redox behavior, as well as the Fe-uptake kinetics (Hassler et al. 2015; Norman et al. 2015; Steigenberger et al. 2010). *In vitro* experiments carried out with seawater from Southern Ocean, one of the largest region where the low concentration of trace metals, notably iron, limits microalgae development (de Baar et al. 1990; Boyd, 2004; Lancelot et al. 2009), have shown that the addition of DUA and uronic acids-rich extracellular polymeric substances enhanced iron bioavailability, yielding an increase of growth in autochthonous populations of eukaryotic phytoplankton (Hassler and Schoemann, 2009). The enhancement of Fe bioavailability in presence of DUA is due to both the stabilisation of Fe within the dissolved phase and the formation of chemically labile organic forms of Fe (Hassler et al. 2011b). *E. huxleyi* adaptation to low-iron bioavailability includes strategies that diminish the intracellular iron requirements (Shi et al. 2010) and excretion of specific iron ligands to alter Fe-bioavailability (Boye and Van Den Berg, 2000). Shi et al. (2010) proved that pH variations, in a range similar to the one here studied, decreased the Fe-uptake capabilities of *E. huxleyi*, and hence its growth, in EDTA-buffered culture medium. Nevertheless, it should be note that conditional

stability constants with Fe of the organic ligands usually used in laboratory experiments largely determine the residence time and potential bioavailability of iron in seawater (Tagliabue et al. 2009), and in turn ocean acidification can change these organic-trace metal interactions (Gledhill et al. 2015). Such is that during a mesocosm performed in Southern Ocean, without adding any external metal chelator, the Fe-uptake capacities of phytoplankton slightly enhanced with increasing pCO_2 (Hoppe et al. 2013). In addition, the chemical composition of extracellular polymeric substances excreted by these natural microbial communities have shown high content of DUA (Hassler et al. 2011a; Nichols et al. 2005a; Norman et al. 2015).

5.4 Environmental implications

The results presented in our study allowed concluding that carbonate chemistry conditions regulated the relative growth rates of *Emiliania huxleyi*. Under acidification conditions, decreasing intracellular iron requirements as strategy to low iron supply (Shi et al. 2010), and increasing extracellular release, by excess of CO_2 fixed during photosynthesis (Thorton, 2014), potentially represented physiological responses, which allowing sustained the growth during IP and SP and increase the growth rate during SP. These findings cannot be simply extrapolated to the natural systems, because our results were derived microcosms and might introduce experimental artifacts (i.e. bottle effects) (Geider and La Roche, 1994), nevertheless, they revealed new information on how the extracellular organic release in *E. huxleyi* is influenced by Fe-bioavailability and acidification conditions

Ocean acidification is a crucial driver to change the speciation of iron in the marine systems, with consequent implications on Fe-bioavailability (Hutchins and Boyd, 2016; Lis et al. 2015). Although inorganic iron is more bioavailable than the organically bound iron forms (Morel et al. 2008), the Fe-complexes with phenolic compounds and uronic acids have shown to be highly available to eukaryotic phytoplankton assemblages (Hassler et al. 2011b; Maldonado et al. 2005). In the present work, the variation of pH/pCO_2 conditions in the cultures changed the

chemical composition of *E. huxleyi* exudates and the release rates of ligands with highly capacity to bind trace metals, such as iron. Possible effects of rising oceanic CO_2 concentrations on organic ligands excretion will therefore play a major role in Fe-bioavailability in the future ocean (Hoffmann et al. 2012). Accordingly, the CO_2-dependence for PhC_{ER} and DUA_{ER} could also have direct effects in Fe-bioavailability. However, in order to discover if the CO_2-estimulated extracellular release, of phenolic compounds and uronic acids, increase the Fe-bioavailability, additional Fe-uptake experiments need to be conducted under ocean acidification conditions.

CHAPTER VI

Effect of organic Fe-ligands, released by Emiliania huxleyi on Fe(II) oxidation rate, under simulated Ocean Acidification conditions. Modelling approach

Samperio-Ramos, G., Santana-Casiano, J.M. and González-Dávila, M.: Effect of organic Fe-ligands released by *Emiliania huxleyi* on Fe(II) oxidation rate, under simulated Ocean Acidification conditions. Modelling approach. *Marine Chemistry*. Submitted.

CHAPTER VI

➢ Abstract

The organic complexation of iron with compounds excreted by phytoplankton is the primary factor that regulates Fe reactivity and its bioavailability in the open ocean. Additionally, our understanding of the specific effects of ocean acidification on organic exudation and the interactions of these compounds biologically mediated with iron is limited. Thus, *Emiliania huxleyi* was exposed in controlled batch cultures, under low-Fe conditions, to investigate the role played by the organic ligands, released in the different pCO_2 treatments, on the Fe(II) oxidation rate at different stages of growth. In order to elucidate the role played by dissolved uronic acids (DUA) excreted by *E. huxleyi*, on the Fe(II) oxidation kinetics, the oxidation of Fe(II) in artificial seawater (S = 35) was investigated at nanomolar levels over a range of pH (7.75 – 8.25) at 25 ºC in presence of different glucuronic acid concentrations. The oxidation kinetics of Fe(II) were studied in presence of exudates of *E. huxleyi* under different pCO_2 conditions (225-900 µatm) and dissolved organic carbon levels (0-141.11 µmol C L^{-1}) produced by coccolithophorids.

DUA slightly increased the experimental rate compared to control artificial seawater and might be ascribed to the stabilization of the oxidized form by chelation. This behavior was a function of the Fe(II):DUA ratio and obeyed to a pH dependence. A first model was applied to the experimental results with DUA to fit both the Fe(II) equilibrium constant ($K_{Fe(II)\text{-}DUA}$ = 3.68 ± 0.81) and individual oxidation rate (log $k_{Fe(II)\text{-}DUA}$ = 3.28 ± 0.41 M^{-1} min^{-1}) of Fe(II)-DUA complex considering the Marcus theory. The half potential for reduction (E^0_{FeL}) and the standard free energy (ΔG^0) of Fe−DUA complex ranged between 0.214-0.242 V and 35.87-39.13 kJ mol^{-1}, respectively. The best fit model for the Fe(II) complexing constant was limited between 13-16.

The Fe(II) oxidation rate always decreased in the presence of organic exudates with respect to that in the exudates-free seawater. The organic ligands present in the coccolithophorid exudates was responsible for decreasing the Fe(II) oxidation process. For the seawater enriched with exudates of *E. huxleyi* a second kinetic

modelling approach was applied for computing the Fe(II) speciation, and the contribution of each Fe(II) species to the overall oxidation rate as a function of pH. Fe(II) complexing constant and oxidation rate of a phenolic-type ligand (Fe(II)-PhC) was also included in the context of Marcus theory where E^0_{Fe-Ph} and ΔG° varied between 0.304-0.378 V and 48.79-52.15 kJ mol^{-1}. The Fe complexing constants were log $K_{Fe(II)\text{-}PhC}$ = 11.46 ± 1.58 and $K_{Fe(III)\text{-}PhC}$ = 20.05 ± 1.80, and the corresponding computed oxidation rates was log $k_{Fe(II)\text{-}PhC}$ = 1.84 ± 0.25 M^{-1} min^{-1}. The Fe(III)-PhC complex was in close alignment with the values measured in the ocean, for the classes L_2 of Fe(III)-ligands, whereas the DUA-type ligands constant might correspond to weaker ligand classes (L_3 or L_4). The influence of Fe(II)-PhC type ligand in the speciation decreased as pCO_2 increased in solution and it was the most important contributing specie to the overall oxidation rate from 385 µatm (23%) to 528 µatm when DOC levels reached 141.11 µmol C L^{-1}. At those DOC concentrations, Fe(II)-DUA complex become the most important contributor between pCO_2 530 µatm (24%) to 900 µatm (34%). Because CO_2 levels modify the composition of organic ligands excreted, the redox behaviour of Fe in the solution seems to be affected when acidification conditions take place.

CHAPTER VI

6.1 Introduction

Redox transformations play a central role in determining the physical and chemical form of iron and its subsequent bioavailability for the microorganisms (Fujii et al. 2010; Shaked and Lis, 2012). In order to explain the persistent and unusual measured concentrations of Fe(II) in sea surface waters (Croot et al. 2008; Roy et al. 2008), both the continuous Fe(II) production and/or the Fe(II) stabilization by organic ligands must be heeded. Direct photolysis mechanisms, that include both of inorganic and organically complexed Fe(III), are considered the dominant pathways to regenerate Fe(II) in ocean upper layers (Barbeau et al. 2001; King et al. 1993; Miller et al. 1995; Roy and Wells, 2011). Nevertheless, relatively little is known about the reactivity of the organic compounds present in seawater and their effects on the iron redox chemistry

Phenolic compounds have been widely studied by prevent the generation of reactive oxygen species through their binding to ferrous ions (Perron and Brumaghim, 2009) and recently they have also been identified in exudates of eukaryote phytoplankton (López et al. 2015; Rico et al. 2013) in which the Fe(II) oxidation rate decreased as a function of DOC concentration (González et al. 2014). Contrary, extracellular polymeric substances released by phytoplankton and bacteria may accelerate Fe(II) oxidation and thus Fe(II) removal from solution (Norman et al. 2015). These natural polymers of high molecular weight are mostly compose by proteins and polysaccharides. Ozturk et al. (2014), using Fourier transform infrared spectrum analysis in extracellular polymers isolated from cyanobacteria, have shown that the presence of uronic acids confer a negative net charge on the polymer that serves to bind metallic trace elements. Thereby, the presence of uronic acids on cell wall of microorganisms also prevents a direct contact between the cells and toxic heavy metals that may be present in the environment (Gonzalez et al. 2010).

Although inorganic iron is higher available than the most organically chelated iron forms (Morel et al. 2008), an increase in bioavailability of organically binding-Fe, due to redox speciation changes have been determinedin laboratory studies with

diatom cultures and natural populations (Barbeau et al. 2001; Rijkenberg et al. 2008). Nevertheless, Shi et al. (2010) proved that a pH decrease in the culture medium declines the uptake capabilities, both of inorganic iron and iron bound to organic ligands, in eukaryotic phytoplankton. The authors suggest that the observed decrease in Fe assimilation rate is presumably due to a change in the chemical speciation of iron. The inorganic iron complexation in seawater has a strong dependence on pH, because of that hydrolysis of Fe(II) and Fe(III) is enhanced strongly with increasing pH (Gledhill et al. 1998; Millero, 2009; Santana-Casiano et al. 2005). Likewise, Haber–Weiss mechanism is affected by pH, since the rates both of O_2^- dismutation and HO_2 protonation, to form H_2O_2, are pH-dependents (Rose and Waite, 2005). Because much of the organic ligands possess –OH and –COOH functional groups, the organic speciation of iron are also affected by variation in the pH (Millero, 2009). Thereby, Gledhill et al. (2015), using non-ideal competitive adsorption–Donnan model, suggest that organic complexation of Fe(III) would wane as pH decreased.

Additionally, a drop of seawater pH conditions, seem increase the production and release of Fe organic ligands, such as uronic acids and phenolic compounds by bacteria and eukaryote phytoplankton (Jin et al. 2015; Lidbury et al. 2012) Accordingly, due to the rising anthropogenic atmospheric CO_2 and the consequent CO_2-uptake by the oceans, is expected a shift in the carbonate chemistry system, as well as, an important decrease in sea surface water pH from its current value of 8.1 to 7.8 (IPCC 2014) and therefore this process may have a strong impact on the redox behavior and bioavailability of iron in seawater (Hoffmann et al.2012; Hutchins and Boyd, 2016).

The pH-dependence of Fe redox kinetics in seawater has been the goal for a number of studies during three last decades (Catrouillet et al. 2014; Emmenegger et al. 2001; González-Davila et al. 2005; González et al. 2010; King et al. 1995; King and Farlow, 2000; Mao et al. 2011; Miller et al. 1995; Millero et al. 1987; Pullin and Cabaniss, 2003; Samperio-Ramos et al. 2016; Santana-Casiano et al. 2006, 2004). Nevertheless few studies have addressed this research (i.e pH-dependence), taking account the role played by the natural exudates produced by phytoplankton on the iron chemistry (González et al. 2014; Santana-Casiano et al. 2014). The experimental

and modelled data obtained by these studies have explained the pH effect on the Fe redox kinetics in the presence of organic ligands released by the diatom *Dunaliella tertiolecta* and *Phaedactylum tricornutum*. Nevertheless, those exudates were always produced and excreted at natural seawater pH and then exposed under the different physicochemical conditions applied during the study (González et al. 2014). However, the variation of pH/pCO_2 seawater conditions might change the type and amount of dissolved organic material released by phytoplankton (Paul et al. 2015; Spilling et al. 2016), including Fe-ligands (Borchard et al. 2012), since ocean acidification regulates the inorganic carbon concentrating mechanisms and the photosynthetic carbon fixation rates in autotrophic microorganism (Riebesell et al. 2007; Wu et al. 2010), especially in calcifying microorganisms (Reinfelder, 2011).

Due to an adaptive widely capacity, the calcite forming coccolithophorid *Emiliania huxleyi* is globally distributed, ranging from the equator ocean to the subarctic zones (Iglesias-Rodriguez et al. 2002; Read et al. 2013). *E. huxleyi* represents an essential component in the cycle of oceanic carbon, since they are currently responsible for a large part of carbonate production in the surface ocean (Beaufort et al. 2011) and because of that, they are especially sensitive to ocean acidification (Doney et al. 2009). Thus, we study, for the first time, the oxidation of Fe(II) at nanomolar levels in seawater enriched with exudates of *E. huxleyi*, produced under different CO_2 concentrations. The Fe(II) speciation as a function of the pH have been modeled, having into account the detection of Fe-ligands (i.e phenols and uronic acids), exposed in the chapter V. In addition, a kinetic modeling approach has been carried out to elucidate the fractional contribution of most kinetically active Fe(II) species to the overall oxidation rate to elucidate the Fe(II) redox behavior over a wide range of scenarios of acidification of the upper ocean, as well as, changes due to natural ambient fluctuations of pH (i.e upwelling systems or volcano events). In this contest, the Marcus theory (Marcus, 1956) has been applied to the Fe(II)-ligands oxidation rates, to evaluate if an outer-sphere electron transfer process controls the oxygenation of Fe(II) in the presence of specific type *E. huxleyi* ligands.

6.2 Material and methods

6.2.1 Chemicals

According to standard operating procedure, the reagents of Winkler method (Dickson and Goyet, 1994) were manganous sulphate solution (3 M), alkaline-iodide solution (NaOH 8 M, NaI 4 M) and sulphuric acid solution (10 M), sodium thiosulfate (0.055 M) and potassium iodate (1.67 mM). For the oxidation experiments, the stock Fe(II) solution (4×10^{-4}M) was prepared in a saline matrix (NaCl, 0.7 M), using ammonium iron(II) sulfate hexahydrate (Sigma). The working Fe(II) solutions were prepared in 2 mM HCl (Sigma) to prevent Fe(II) oxidation yet low enough to avoid significant pH change that might alter the kinetic experiments when iron was added. The solutions of disodium salt of 3-(2-pyridyl)-5,6-bis(4-phenylsulfonic acid)-1,2,4-triazine (Ferrozine, 0.01 M), sodium fluoride (0.001 M) were weekly prepared and kept in fridge until their use in the kinetic experiments. Glucuronic acid standard was purchased from Sigma-Aldrich. Experiments with glucuronic acid were performed in an artificial solution (S = 35) that containing the main inorganic species present in natural seawater, as described by Millero (1986). All dilutions were prepared with Milli-Q water (18 MΩ) and the chemicals used for the Fe(II) determination were trace analytical grade. Equipment in contact with culturing solutions and ASW was cleaned according to a standard protocol (Achterberg et al. 2001).

6.2.2 Organic exudate enrichment

The stock of axenic cultures of *E. huxleyi* was supplied by the Spanish Bank of Algae (BEA, Taliarte) in f/2 medium (Guillard, 1975). In the experimental batch cultures, the coccolithophorids were grown in filtered and sterile (Nucleopore, 0.1 μm) North Atlantic seawater obtained at the ESTOC site (29º 10’ N, 15º 30’ W). The seawater salinity (S = 36.48) was determined by a salinometer (Portasal, 8410A) with error of determination ± 0.001. The selected aliquots from *E. huxleyi* stock cultures were centrifuged (1200 rpm) 3 times with autoclaved natural seawater, to avoid introducing chemical buffers from f/2 medium, which might produce

interferences in the chemical assays, interactions with iron during the kinetic experiments or changes in the metal trace bioavailability during batch cultures (Shi et al. 2009). A more detailed description of the experimental medium conditions and the set-up to manipulate the carbonate chemistry system, as well as, the results and proceeding of organic assays during experimental cultures are given in the chapter V.

6.2.3 Oxidation experiments

The Fe(II) oxidation experiments were carried out under dark conditions in a double-jacketed thermostatic vessel (250 mL) at constant temperature of 25 ± 0.02 ºC using an AG-2^{TM} bath. The pH was adjusted to the desired value and in order to keep the pH constant during the experiment to ± 0.01, small additions of suprapur HCl 0.1 M were done using an automatic titration system (Titrino 719S, Metrohm). The pH was measured on the free hydrogen ion scale, $pH_F = -\log[H^+]$, at 25 ºC with an Orion pHmeter and calibrating the combination electrode (Ross Combination, glass body) with tris(hydroximethyl)-aminomethane (Tris)−artificial seawater buffers (Millero 1986). The studies were done in triplicate and the average results were denoted. The addition of a fixed concentration (25 nM) of Fe(II) to the sample corresponded to the zero time of the reaction. The samples were mixed at 120 rpm with a teflon-coated magnetic stirrer.

To investigate the effect of DUA model ligand in the Fe(II) oxidation, glucuronic acid was added to 200 ml of artificial seawater. The solutions containing at Fe:L ratios from 1:1 to 1:100 were prepared and equilibrated for 24 h at 4 °C in darkness. After equilibration the samples were brought to experimental temperature in air saturated conditions, by bubbling the solution with pure air for 1h, prior to and end the oxidation studies. The Fe(II) oxidation rate was also studied in the control artificial seawater (control) without ligand addition.

To study the behavior of Fe(II) in presence of ligands released by *E. huxleyi* under different CO_2 scenarios, oxidation experiments were carried out with 200 ml of seawater enriched with exudates (SWEX) and seawater enriched with nutrients (SWEN, as control). SWEX was obtained from the experimental batch cultures in

two consecutive steps (gravity and vacuum for 0.45 μm) in order to prevent cell rupture. Once the seawater enriched with organic exudates culture was filtered, the Fe(II) oxidation kinetic studies was immediately to carried out as described previously, although, both SWEN and SWEX were not bubbled with pure air in order to avoid alterations of carbonate chemistry generated in the experimental batch cultures and because of that, the oxygen concentrations were measured before the kinetic studies.

Iron concentrations in the samples were determined UV–vis spectroscopy using a colorimetric method described by Viollier et al. (2000) and modified by Santana-Casiano et al. (2005) in order to work at nanomolar levels of Fe(II). Ferrozine reacts extremely rapidly with Fe(II), forming a water soluble complex with ferrous ion, which forms a stable peak at 652 nm during 30 minutes in a pH range 4–9. Although FZ has been shown to slowly promote the reduction of Fe(III) to Fe(II) (Hudson et al. 1992), it does not bind Fe(III) to a significant degree (Pullin and Cabaniss, 2003), especially in presence of inorganic complex NaF (Gonzalez-Davila et al 2005). In addition, the oxidation experiments were carried out following the ferrozine technique because it allows us to follow the full-spectra over time and if any intermediate or interaction is formed, it can be taken into account during the experiment.

At each selected time, 10 mL of sample was withdrawn from reaction vessels to a 25 mL glass flask containing ferrozine (50 μL), NaF (50 μL) and acetate buffer (2 mL, pH 5.5). The absorbance was read with a 5 m long waveguide capillary flow cell (World Precision Instruments™) connected to the UV–vis detector USB2000 (Ocean Optics™). The detection limit of the instrument at both 22 °C and 4 °C was 0.8 nM Fe(II) calculated as three times the standard deviation of the lowest calibration value (n = 3; 10 nM Fe(II)). The light used was a halogen light source (HL-2000-FHSAfrom Mikropack). The capillary flow cell and the detector were connected using optical fiber. The spectra were recorded using the OOIBase32 software by Ocean Optics. The samples were introduced in to the column using a peristaltic pump (EXPETEC Perimax 12) with a flux of 1 mL/min.

6.2.4 Oxygen measurements

The dissolved oxygen content in the experimental cultures was determined during 2^{nd}, 5^{th} and 8^{th} day, by the modified Winkler's method (Dickson and Goyet, 1994) and expressed as μmol L^{-1}. To the sample, carefully taken in a 125 ml Winkler oxygen bottle, 2ml solutions of manganous sulphate and alkaline iodide were added, one after the other. The temperature of the water at the time of sampling was recorded and was used to correct the bottle volume in the calculation of the oxygen concentration after the titration. After placing the stopper the bottle was shaken, and the manganic hydroxide formed was allowed to settle down. Prior to analysis, the sample is acidified (2mL, H_2SO_4) to dissolve the precipitate and the amount of iodine generated is determined by potentiometric titration with thiosulfate. The thiosulphate solution used in the titration was standardized against an iodate pattern solution (10 ml) before use. The detection of end point of titration is carried out using a programmed Metrohm Titrino.

6.2.5 Data treatment and numerical model

R (R Development Core Team, 2008) was used for statistical computing. Between CO_2 scenarios, statistical differences in the dissolved organic carbon concentration and in the levels of oxygen in the seawater enriched with exudates of *E. huxleyi* were evaluated using a one-way analysis of variance (ANOVA). The assumptions of normality and homoscedasticity were verified using the Shapiro-Wilk and Barlett tests respectively. The relationship between Fe(II) oxidation rate and the concentration of DOC and pH. was examined by regression analysis. For all statistical analyses, a probability level of $\alpha = 0.05$ was considered.

The Gepasi Version 3.30 software system was used to model the chemical kinetics for all reagents. The overall and individual rate constants ki were obtained by adjusting experimental Fe(II) concentrations/time pairs of data to the model output as indicated elsewhere (Mendes 1997). In accordance with the experimental data obtained in this article, the kinetic model (Santana-Casiano et al.2006) was broadened to include both Fe(II)-phosphate, Fe(II)-silicate species and organic

ligands considered, and it was applied as a function of pH and temperature for both seawater enriched with nutrients (SWEN) and seawater enriched withnatural organic exudates, considering all dissociation and equilibrium constants for the reaction of Fe(II) species with the major inorganic species in seawater under different experimental conditions.

6.3 Results and discussion

6.3.1 Fe(II) oxidation rate in presence of exudates of *E. huxleyi*

The kinetic studies were performed in seawater and seawater enriched with natural exudates of *Emiliania huxleyi* excreted under different pCO_2 scenarios. Fourth experimental scenarios, based on Intergovernmental Panel on Climate Change projections (IPCC, 2014) were fixed: preindustrial, close to contemporary and two futures ocean acidification conditions with pCO_2 225, 350, 600 and 900 µatm respectively. Consequently, the aeration with CO_2-air-mixture generated constant pH values of 8.25, 8.10, 7.90 and 7.75 in the seawater enriched with exudates of *E. huxleyi.*

The effect of natural organic exudates on the Fe(II) oxidation rate was carried out as a function of the dissolved organic carbon (DOC) at constant temperature (25 ºC). The log k_{app} decreased when the DOC levels enhanced in the solution, indicating that the presence of organic compounds excreted by the coccolithophorids affected the rate of oxidation of Fe(II). The organic material present during initial phase (IP) of growth did not modify significantly the k_{app} respect different of control seawater (Fig 6.1). However, when the production of DOC was detected, the k_{app} decreased, reaching minimum values at maximum DOC released (141.1± 10.27 µmol C L^{-1}). At this concentration of DOC, the Δlog k_{app} (log k_{app}^{SW} – log k_{app}^{SWEX}) enhanced as the pCO_2 condition increased, from 0.14 M^{-1} min^{-1} (pCO_2 225 µatm) to 0.22 M^{-1} min^{-1} (pCO_2 900 µatm). This is equivalent to a decrease between 27% and 40% in k_{app}, respectively. This reduction in the rate of oxidation of

Fe(II) in the presence of exudates of *E. huxleyi* is due to the interaction of these organic compounds with iron.

Table 6.1 Fe(II) oxidation rate (k_{app}) and half-life ($t_{1/2}$) as a function of the CO_2 treatment for SWEN and SWEX excreted by *Emiliania huxleyi* during the different growth stages (IP = initial phase; EP: exponential phase and SP: steady phase). The temperature (25ºC) and salinity (36.48) were kept constant (25ºC). [O_2] was 194.41 ± 13.78 µmol L^{-1}. ±SE represents the standard error (n=3).

Medía	pCO_2 treatment (µatm)	log k_{app} (M^{-1} min^{-1})	±SE	$t_{1/2}$ (min)
SWEN (Control)	225	3.36	0.03	1.5
	350	3.18	0.02	2.4
	600	2.99	0.03	3.7
	900	2.86	0.02	4.9
SWEX from IP [DOC] = [a]	225	3.35	0.03	1.6
	350	3.19	0.02	2.3
	600	2.97	0.04	3.9
	900	2.88	0.03	4.7
SWEX from EP [DOC] = 33.18 ± 3.78 µmol C L^{-1}	225	3.29	0.02	1.8
	350	3.08	0.03	3.0
	600	2.91	0.03	4.4
	900	2.77	0.05	6.0
SWEX from SP [DOC] = 141.11 ± 10.27 µmol C L^{-1}	225	3.23	0.03	2.1
	350	3.00	0.04	3.6
	600	2.81	0.02	5.5
	900	2.64	0.03	8.1

Table 6.1 shows the Fe(II) oxidation rate (k_{app}) and half-life ($t_{1/2}$) as a function of the CO_2 treatment for the seawater enriched with nutrints and seawater enriched with natural exudates excreted by *E. huxleyi* during the different growth stages. The half-lifetime ($t_{1/2}$) increased 0.6 min (pCO_2 225 µatm), 1.2 min (pCO_2 350 µatm), 1.8 min (pCO_2 600 µatm) and 3.2 min (pCO_2 900 µatm) from SWEN to SWEX obtained during the steady phase due to the decrease in pH (Table 6.1).

Recently, Gonzalez et al. (2014) studied the effect of pH on the Fe(II) oxidation rate in presence of natural exudates of diatom *Dunaliella tertiolecta*. Nevertheless, the authors obtained the exudates at natural seawater pH, which were exposed then to the different pH conditions applied in their research. In the present

study, the exudates of *E. huxleyi* were excreted under different pH/pCO_2 conditions. As soon as the cells were carefully removed by filtration from solution, the kinetic experiments were carried out, to avoid variations in the carbonate chemistry reached during the incubations. Figure 6.1 shows as the $\underline{k_{app}}$ decreased as a function of the pH/pCO_2, under different DOC levels, giving the minimum oxidation rates at the lower/higher values of pH/pCO_2 studied. The log k_{app} also decreased in the presence of natural exudates at any pH value when the accumulation of DOC in solution was detected, with greater effect at [DOC] = 141.11± 10.27 µmol C L^{-1}. The log k_{app} varied from 3.36 ± 0.03 M^{-1} min^{-1} and 3.23 ± 0.03 M^{-1} min^{-1} (pCO_2 225 µatm) to 2.86 ± 0.02 M^{-1} min^{-1} and 2.64 M^{-1} min^{-1} (pCO_2 900 µatm) in seawater control and seawater enriched with exudates (141.11 ± 10.27 µmol C L^{-1}) respectively. Due to changing pH/pCO_2 conditions, the k_{app} decreased by 68% and 75% in seawater control and seawater enriched with natural organic exudates (141.11 ± 10.27 µmol C L^{-1}), respectively.

The experimental results of Fe(II) oxidation rates were fitted to a second order equation as a function of pH and DOC concentrations (eq 42), where r^2 was 0.987 and the standard error of the estimation in log k_{app} was 0.03.

$$\log k_{app} = 24.87\ (\pm 1.68) - 6.48\ (\pm 0.42)\ pH\ +\ 0.48\ (\pm\ 0.03) pH^2 - 1.2 \cdot 10^{-3}\ (\pm\ 10^{-4})\ [DOC]^{E.huxle} \quad (42)$$

The difference between SWEN and SWEX was not constant over the entire pH range studied, therefore the effect of the organic exudates from *E. huxleyi* on the Fe(II) oxidation rate was computed by subtracting the log k_{app} values in the control seawater and those in equation 43 for the growth phases, where the DOC was accumulated in the present study. r^2 was 0.952, and standard error of estimate was 0.03.

$$\Delta\log k_{app} = 3.9 \cdot 10^{-2}\ (\pm\ 3.4 \cdot 10^{-3})\ pH -\ 5 \cdot 10^{-3}\ (\pm\ 4 \cdot 10^{-3}) pH^2 + 10^{-3}\ (\pm\ 10^{-4})\ [DOC]^{E.huxleyi} \quad (43)$$

This equation allows computing the changes in the apparent oxidation rate in a context of ocean acidification, under the presence of ligands excreted by the *E. huxleyi*. The observed dependence over the whole pH range, showed that the organic

ligands present in phytoplankton exudates determine the kinetic behavior of iron due to variations in the Fe(II) speciation, and therefore the decrease in the Fe(II) oxidation rate was directly linked to the production of organic compounds during the growth of coccolithophorid in each pCO_2 treatment.

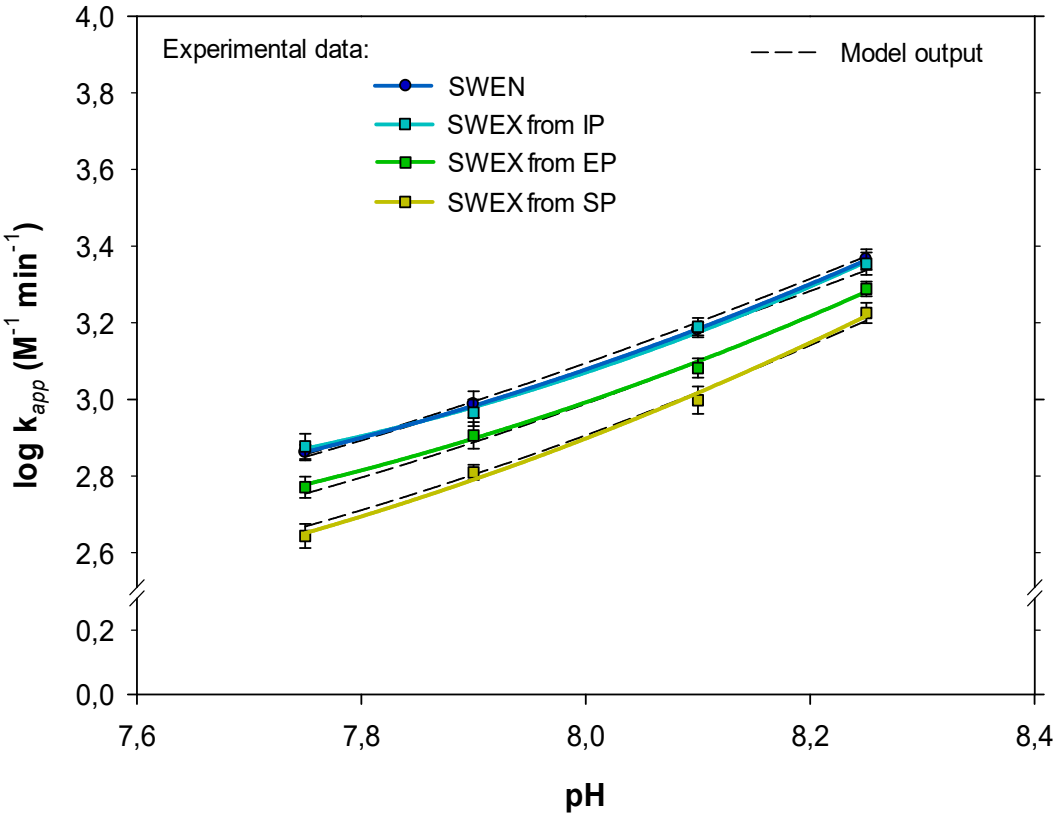

Fig 6.1 Fe(II) oxidation rate constant as a function of pH for the seawater and the seawater enriched with the organic exudates excreted by *E. huxleyi* during the different growth stages (IP initial phase; EP: exponential phase and SP: steady phase). Temperature (25 ºC) and salinity (36.48) were kept constant. Error bar denoted standard error of esteem (n=3).

The changes in the levels of uronic acids and phenolic moieties in the cultures of *E. huxleyi,* due to variations in the CO_2 conditions (chapter V), might modify the interactions between Fe(II) and the exudates. Albeit the $t_{1/2}$ (Table 6.1) of Fe(II) increased in response to CO_2 enrichment both in seawater control (3.4 min) and seawater enriched with exudates (4.2 min and 6.0 min for 33.18 ± 3.78 µmol C L^{-1} and 141.11 ± 10.27 µmol C L^{-1}, respectively). Our results indicated that Fe(II) might persist in surface seawater for longer periods of time as a result of the Fe(II)−organic exudate interactions under ocean acidification conditions. Our data are comparable with the obtained by Breitbarth et al. (2010) during a coastal seawater mesocosm

experiment, where the authors linked the significant increase of Fe(II) half-lifes to Fe(II) complexation by biologically mediated organic ligands, especially in the lower pH treatments.

6.3.2 Oxidation rate in presence of uronic acids

To explain the role played by DUA in the natural exudates of *E. huxleyi*, a series of studies has been performed using a simplified model with glucuronic acid in artificial seawater (ASW), in order to avoid that the presence of other organic ligands interference in the interaction of Fe(II) with DUA, and therefore in redox behavior of Fe(II)-DUA complex. In order to determine the effects of a model ligand, type DUA, on the Fe(II) oxidation rate, concentrations of glucuronic acid (0 – 1000 nM) and H^+ (pH 7.75 and 8.25) were independently varied. The oxidation rate, as well as, the half time of Fe(II) in DUA-ASW solution (25 ºC) were determined and presented in Table 6.2. The results of Fe(II) oxidation rate vary depending on L:Fe ratios, increasing oxidation rate and decreasing the half-life as the concentration of DUA enhanced, from 25 nM to 1000 nM. Similar findings were recently observed in the natural sea surface water from Tasman Sea (Norman, 2015). Contrarily to this type of behavior, Kuma et al. (1995) determined that the addition of glucuronic acid to seawater from Funka Bay, slightly slowed Fe(II) oxidation at micromolar levels.

Table 6.2 Pseudo-first order rate (k' s^{-1}) and half-life ($t_{1/2}$) for Fe(II) (25 nM) oxidation at pH 8.25 and 7.75 in artificial seawater (ASW, S = 35) only and in the presence of glucuronic acid in concentrations from 25 to 1000 nM (ligand to Fe ratio, L:Fe 1 to 40). Temperature fitted at 25 ºC. ±SE denotes the standard error of the estimate in triplicate samples for all experiments.

[DURA] (nM)	L:Fe ratio	pH 8.25			pH 7.75		
		Log k_{app} (M^{-1} min^{-1})	± SE	$t_{1/2}$ (min)	*Log* k_{app} (M^{-1} min^{-1})	± SE	$t_{1/2}$ (min)
0 (Control)	**0**	3.30	0.01	1.62	2.51	0.01	10.12
25	**1**	3.30	0.02	1.61	2.52	0.02	9.71
100	**4**	3.31	0.01	1.60	2.55	0.01	9.13
250	**10**	3.31	0.01	1.59	2.59	0.03	8.35
500	**20**	3.32	0.01	1.57	2.64	0.02	7.35
1000	**40**	3.32	0.03	1.54	1.953	0.03	5.92

Organic ligands can accelerate, retard or produce no effect on the oxidation rate of Fe(II), depending on reactivity of the complex formed (Santana-Casiano et al 2000; Rose and Waite 2002). The specific interaction–ion-pairing model for Fe(II) speciation and oxidation by molecular oxygen are a function of pH, temperature and medium composition. In fact, organic ligands can form complexes with Fe(II) in function of ligand stabilization capacity of other organic compounds presents in solution. Therefore, it is difficult to make direct comparison of our results with other studies carried out in natural seawater due to both different physicochemical parameters fixed for experiments, such as temperature and pH, as well as, the lack of details of natural iron-ligands present in solution, since the presence of organic material in the medium modifies the influence of DUA in the oxidation rate of Fe(II) due to the competitive effects produced between the redox and the complexing processes. In our experiments in ASW, iron oxidation rates varied linearly with increasing molar ratio of DUA to Fe(II), implying that the reaction is first order with respect to ligand concentration for both pH tested. It is often expected that a decrease in half pH unit might results in a decrease in the percentage of ionized uronic specie (Kohn and Kovác, 1978). However at pH 7.75 the presence of DUA might cause stronger changes in the overall mechanism of the oxidation. The pH dependence can be related to uncomplexed inorganic Fe(II) form, the more labile specie to form organic complexes, which dominates the fractional contribution to the overall oxidation rate at pH lower than 7.8 (Gonzalez et al. 2010; Samperio-Ramos et al. 2016). Thereby, organic ferrous complexes can behave differently depending on the pH conditions to which they are exposed. Similarly, at pH 6.0 citrate has been shown to enhance Fe(II) oxidation, but at pH 8.0 the Fe(II) oxidation decreased (Pham and Waite, 2008).

Binding capacities and kinetic reactivity between iron and dissolved uronic acids (DUA) are key factors for a greater understanding of the biogeochemical behavior of iron in ocean, since DUA regulate the uptake of iron to phytoplankton by more readily disassociating and releasing unchelated Fe(III), which it can be reduced to Fe(II), the form of Fe that may be highly bioavailable (Morel 2008; Hassler 2015). The regenerated Fe(II) can reoxidized through Fenton type reactions (eq 1-4), although it has been observed that the presence of organic ligands can regulate

oxidation process (Rose and Waite, 2002, 2003; Catrouillet et al. 2014; Santana-Casiano et al. 2014)

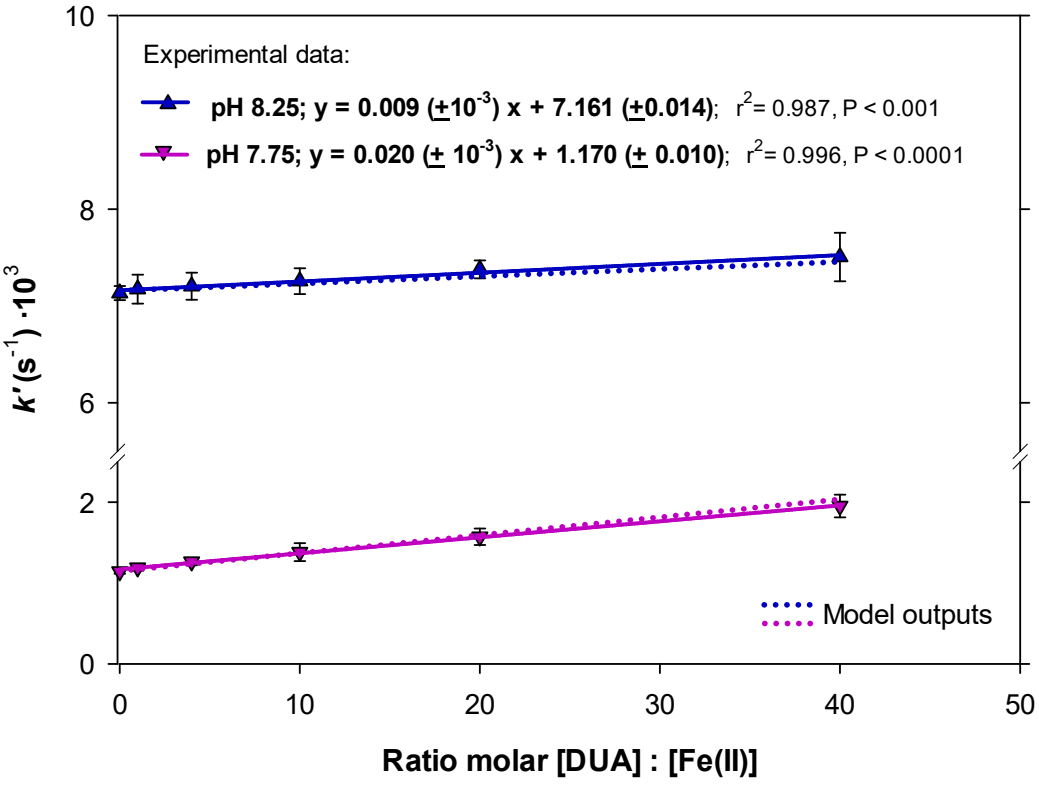

Fig 6.2 Fe(II) oxidation shows pseudo-first-order kinetics in artificial seawater (ASW) in the presence of glucuronic acid under different [DUA]:[Fe(II)] ratios. T^a = 25ºC, $[Fe\ II]_0$ = 25 nM

6.3.3 Modelling approach for Fe(II)-DUA

In order to elucidate the role played by uronic acids excreted by *E. huxleyi*, on the speciation and oxidation rate of Fe(II), we used the experimental results from section 6.3.2 and applied the modelling approach describe by Santana Casiano et al. (2005). We fitted the complexing constant between glucuronic acid (denoted as DUA) and Fe(II), as well as the individual oxidation rate of Fe(II)-DUA complex (Tables 6.3 and 6.5). The modelling approach also included the equilibrium constants (Table 2.1) for the inorganic species considered, making it valid and appropriate for the results of this study with ASW.

Table 6.3. The computed stability constants for Fe(II) and Fe(III) by the ligands fitted for the kinetic model. Tª = 25 ºC.

Ligand proposed	Iron Specie	Reaction	*Log K ± SE* (M^{-1})
Uronic Acid	Fe(II)	$Fe^{2+} + L^{-} \leftrightarrow Fe - L^{+}$	3.68 ± 0.81
	Fe(III)	$Fe^{3+} + L^{-} \leftrightarrow Fe - L^{2+}$	14.22 ± 1.26
Polyphenol	Fe(II)	$Fe^{2+} + L^{2-} \leftrightarrow Fe - L$	11.46 ± 1.58
	Fe(III)	$Fe^{3+} + L^{2-} \leftrightarrow Fe - L^{+}$	20.05 ± 1.80

The model explains the reaction formation Fe(II)-UA complex in terms of the fully deprotonated ligand state (Table 6.3). In order to describe the experimental pH range considered (7.75-8.25), it is necessary to include in the model approach the protonation equilibria of glucuronic acid. Potentiometric measurements supported the conclusion that bindings in complexes between DUA and divalent cations involve the carboxylate moiety (Papargeogiou et al. 2010; Jastrzab et al. 2016) and therefore, the value of the protonation constant of the carboxyl group of glucuronic acid computed (Table 6.4) was obtained from Kohn and Kovác (1978).

Table 6.4 Acidity constants for the ligands considered for the kinetic model. Tª = 25 ºC.

Ligand proposed	Reaction	pK_a
Uronic Acids (Kohn and Kovác, 1978)	$LH \leftrightarrow L^{-} + H^{+}$	3.26
Phenolic Compounds (Herrero-Martínez et al. 2005)	$LH_2 \leftrightarrow LH^{-} + H^{+}$	9.19
	$LH \leftrightarrow L^{2-} + H^{+}$	13.09

Table 6.5. The oxidation rates for the ligands considered for the kinetic model. Tª = 25 ºC.

Ligand proposed	Reaction	*Log* k_i ± *SE* (M^{-1} min^{-1})
Uronic Acids	$Fe - L^{+} + O_2 \rightarrow Fe - L^{2+}$	3.28 ± 0.41
Phenolic Compounds	$Fe - L + O_2 \rightarrow Fe - L^{+}$	1.84 ± 0.25

The equilibrium and oxidation rate between glucuronic acid and Fe(II) (Tables 6.3 and 6.5), that produce the best agreement between experimental and the

model output computed by Gepasi software, included all the experimental conditions fixed for the different concentrations of glucuronic acid concentrations (Fig 6.2).

The electron transfer in the oxidation of organic Fe(II) complexes by oxygen, is accomplished by an outer-sphere mechanism, through the precursor complex, without any change in the inner sphere of the molecule (Gonzalez et al. 2014). Marcus theory connects these outer-sphere electron-transfer mechanisms with the free energy of the oxidation reaction (Stumm & Morgan, 1996). Additionally, it is possible delimit the free energy from Fe(II)-UA oxidation rate allowing the form described by Tratnyek and Hoigné (1993).

$$k_i = \frac{k_d}{1+\frac{k_d}{K_d Z}\exp\left[\frac{\frac{\lambda}{4}\left(1+\frac{\Delta G^\circ}{\lambda}\right)^2}{RT}\right]} \qquad (38)$$

where k_d is the diffusion-controlled limit (10^{10} M^{-1} sec^{-1}), R is the universal gas constant and T is the temperature in Kelvin units. The term k_d/K_dZ has a constant value of 0.1 (King and Farlow, 2000) and λ is a fitting parameter related with the reorganization energy required to rearrange the transition state of precursor and accounted as 103 kJ mol^{-1} for organic complexes (Rose and Waite, 2003). The oxidation rate constants of individual Fe(II)-DUA specie provide a standard free energy, ΔG^0 of 37.45 ± 1.58 kJ mol^{-1}. The reduction of oxygen to superoxide considers the Franck-Condon principle, which defines the oxidation process as an electronic transition without nuclear coordination modification. From the ΔG^0 computed, is possible determine the half potential for reduction between Fe-DUA complexes (E^0_{FeL})

$$\Delta G^\circ = -F\left(E^0_{O_{2\rightarrow O_2^-}} - E^0_{Fe(III)L\rightarrow Fe(II)L}\right) \qquad (39)$$

where, F is the Faraday constant, $E^0_{O_{2\rightarrow O_2^-}}$ in aqueous solutions oscillate between -.16 V and -0.20 V (Koppenol et al. 2010). Solving the eq 39, the half potential for reduction of the Fe−DUA complexes ranged between 0.214 and 0.242 V. From the Nernst equation and using the corresponding value of E^0_{FeL}, the equilibrium constant ratio ($K_{Fe(III)-L}/KFe_{(II)-L}$) can be accounted.

$$E^0_{FeL} = E^0_{Fe} - 0.059 \log\left(\frac{K_{Fe(III)-L}}{K_{Fe(II)-L}}\right) \quad (40)$$

Considering the standard half reaction potential for $E^0_{Fe} = 0.77\,V$, a $K_{Fe(III)-L}/K_{Fe(II)-L}$ ratio between 10^9–10^{11} is computed. To date, gluconic acid is the only mono-saccharide presents in seawater, in which have been reported the stability constant for (10^{19} L mol^{-1}) for Fe^{3+} (Croot and Johansson, 2000), due to the analytical overlapping range, which complicates the detection of weaker ligand classes (Gledhill and Buck, 2012). Thus, the acid saccharides are considered a class part of ligands with weakest affinity (L_3 and L_4) for Fe(III) (Bundy et al. 2014). In addition, Baldi et al. (2009) determined that the stability constant, log K, between Fe(III) and binding groups of bacterial exopolysaccharides substances ranged from 12 to 14. Different authors suggested that iron complexing capacities by extracellular polymeric substances are due to the presence of DUA as union sites (Baldi et al. 2009; Nichols et al. 2005; Norman et al. 2015; Strmečki et al. 2010). Resolving the ration $K_{Fe(III)-L}/K_{Fe(II)-L}$ computed from Marcus theory with the equilibrium constant between DUA and Fe(II), which best fitting in the model (log K = 3.68 ± 0.81), the log $K_{(FeIII)-L}$ would limit between 13-16. This range is slightly higher than the considered by Baldi et al. (2009). Nevertheless, the ability to chelate iron in extracellular polymeric substances is related not only to the amount of anionic groups but also to the three-dimensional distribution of binding groups and their accessibility (Micheletti et al. 2008). These polymers are characterized by a significant level of hydrophobicity, which is due to the presence of no charged groups, such as ester-linked acetyl fractions, peptidic moieties and deoxysugars, which might decreased the effective binding capacity of uronic fractions (Rossi and De Philippis, 2015). The value of equilibrium constant of Fe(II)-DUA complex fixed in the model is close to that obtained through the potentiometric titration between glucuronic acid and divalent cations, such as Mg^{2+} or Cu^{2+} (Jastrzab et al. 2016).

6.3.4 Kinetic model for exudates of *E. huxleyi*

In order to explained the key role played by Fe(II)−organic complexes on speciation and oxidation rate of Fe(II), a kinetic model (Santana-Casiano et al. 2005)

was carried out. The kinetic model included the contributions of others (King, 1998; King et al. 1995; King and Farlow, 2000; Mao et al. 2011; Rose and Waite, 2003) and took into consideration that the variation of pH/pCO_2 conditions used. In addition it was assumed two dominant processes: formation and oxidation of inorganic and organic complexes of Fe(II) with DUA and PhC. The exudates of *E. huxleyi* discussed in the present work result from a mixture of saccharides, phenolic compounds and other organic ligands undetermined and uncharacterized (L_x). Therefore, the model included ligands with hydroxyl (PhC) and carboxyl (DUA) fractions, which are the most metal-active functional groups present in the phytoplankton exudates (Taylor et al. 1994; Gonzalez-Dávila et al. 1995; Strmecki et al. 2010; Norman et al. 2015; Gledhill et al. 2015) and therefore the contribution of the complexes L_x-Fe(II), with hydroxyl and carboxyl moieties to the overall Fe(II) oxidation rate is assumed within the two ligands considered in the model (i.e PhC and DUA). Additionally, the absence in the modelling approach of different Fe-binding moieties with less presence in exudates, such as pyrrole or thiols groups, should be also taken into account when evaluating the outputs of model.

While the parameters for PhC were fixed during this modelling approach, the complexing constant and the oxidation rates of Fe(II)-DUA complex, as well as, the protonation constant of carboxyl group of DUA, were obtained from section 6.3.3. The acidify constant considered in the modelling approach for PhC are also shown in the Table 6.4. The oxidation reaction of Fe(II) is composed of several parallel reactions in which the individual Fe(II) species react at different rates with oxygen. The Fe(II) oxidation rate for each equation can be determined as a function of the weighted sum of the oxidation rates of the individual Fe(II) species

$$\boldsymbol{k_{app}} = k_{Fe^{2+}}\alpha_{Fe^{2+}} + k_{FeOH^+}\alpha_{FeOH^+} + k_{Fe(OH)_2}\,\alpha_{Fe(OH)_2} + k_{FeHCO_3^+}\,\alpha_{FeHCO_3^+} + k_{FeCO_3}\,\alpha_{FeCO_3} +$$

$$+ k_{Fe(CO_3)_2}\alpha_{Fe(CO_3)_2} + k_{Fe(CO_3)OH^-}\,\alpha_{Fe(CO_3)OH^-} + k_{FeCl^+}\alpha_{FeCl^+} + k_{FeSO_4}\alpha_{FeSO_4} + k_{FePO_4^-}\,\alpha_{FePO_4^-} +$$

$$+ k_{FeHPO_4}\alpha_{FeHPO_4} + k_{FeH_2PO_4^+}\,\alpha_{FeH_2PO_4^+} + k_{FeH_3SiO_4^+}\,\alpha_{FeH_3SiO_4^+} + k_{FeH_3SiO_4^+}\,\alpha_{FeH_3SiO_4^+} +$$

$$+ \boldsymbol{k_{Fe\text{-}DUA}\,\alpha_{Fe\text{-}DUA}} + \boldsymbol{k_{Fe\text{-}PhC}\,\alpha_{Fe\text{-}PhC}} \qquad (44)$$

where $\alpha_i = [FeX_i] / [Fe(II)]_T$ denotes the molar fraction of each Fe(II) species in the solution, and *ki* are the individual rate constant for the Fe(II) species.

The reactivity of Fe-PhC complexes is highly variable, due to different chemical structure and spatial layout of functional groups. Phenols can bind Fe(II) by carboxylic and hydroxyl functional groups (Andjelkovićet al. 2006), however the complexes formed by dihydroxyl moieties seem be ligands more relevant in the biogeochemical behaviour of Fe(II) in natural waters, since they bind Fe(II) more efficiently (Perron and Brumaghim, 2009). In addition, phenolic compounds with catechol functional groups, such as catechin, inhibit the Fe(II) oxidation and prolong the half-life of Fe(II) more efficiently than their analogues with galloyl or carboxylate structure (Perron et al. 2010). Thereby, oxidation rate fixed in the model represents an average values from the sum of individual rates weighted by the fraction of each phenolic compound in solution with catechol functional group.

$$k_{Fe-PhC} = \Sigma_{all\ n}\, \alpha_n\, k_n \qquad (45)$$

The oxidation kinetic rate for PhC-Fe(II) complexes that produces the best agreement between the experimental distribution and the model output presented value log k = 1.82 ± 0.25 M^{-1} min^{-1}. This oxidation rate was studied in the context Marcus theory providing a standard free energy, ΔG^0 of 50.47 ± 1.68 kJ mol^{-1} and a range of half potential for reduction between 0.304 and 0.378 V, so that a $K_{Fe(III)-L}/K_{Fe(II)-L}$ ratio between 10^6–10^8 is obtained. The best fit in the model (Table 6.3) for the apparent binding constants for Fe(II)-PhC (log K = 11.46 ± 1.58) and Fe(III)-PhC (log K = 20.05 ± 1.80) were close alignment with the bibliographic values, which are estimated a range of 6 to 13 and 17 to 21 for the phenolic stability constants for complexes with Fe(II) and Fe(III) respectively (Guo et al. 2007; Perron and Brumaghim, 2009). In addition, there is a very reasonable agreement between the log K for Fe(III) estimated by Boye and van der Berg (2000) in exudates obtained from *E. huxleyi* cultures and the value fitted in our model. Therefore, PhC excreted by *E. huxleyi* could be part of iron ligands pools in seawater with lower affinity than those are operationally defined as L_1 (Gledhill and Buck, 2012; Heller et al. 2016).

Phenolic fractions were detected in the exudates of *E. huxleyi* under different experimental CO_2 scenarios, indicating that phenols made up a relatively constant fraction of the organic material excreted during coccolithophorid growth. The best fitting concentrations were set for PhC type-ligand during the EP with 16 ± 3 nM (pCO_2 225 µatm), 21 ± 2 nM (pCO_2 350 µatm), 22 ± 6 nM (pCO_2 600 µatm) and 18 ± 2 nM (pCO_2 900 µatm). During the SP, the concentrations included in the model (49 ± 6, 56 ± 11, 62 ± 8 and 55 ± 8 nM for pCO_2 conditions of 225, 350, 600 and 900 µatm, respectively) were in agreement with the levels measured during the cultures in the different CO_2 treatments (Chapter V). In both cases, these concentrations are within range (5-114 nM) of specific ligands accounted by other authors in exudates of *E. huxleyi,* with binding capacities similar to the fitted in the model for PhC (Boye and Van Den Berg, 2000; Vasconcelos et al. 2002; Vasconcelos and Leal, 2008). Additionally Borchard et al. (2012) determined during the steady state growth, in continuous cultures of *E. huxleyi* under acidification simulated conditions, similar levels of DUA (180-400 nM) than measured (345 ± 34, 428 ± 10, 450 ± 20 and 413 ± 39 nM for pCO_2 conditions of 225, 350, 600 and 900 µatm, respectively) and fitted in this modelling approach. DUA concentrations of 83 ± 14, 94 ± 16, 100 ± 30 and 76 ± 17 nM corresponded with pCO_2 225, 350, 600 and 900 µatm, during the EP. Because no significant differences were found in the production of DOC, PhC and DUA between the control seawater and the seawater enriched with organic exudates (SWEX) released during the IP (Chapter V), the speciation and individual contribution of each Fe(II) species, including Fe(II)−UA and Fe(II)−PhC species, are only shown for the EP and the SP (Figs 6.3 and 6.4). Therefore the speciation and fractional contribution of the IP can be considered inside of SWEN.

In SWEN and during the IP, the speciation under the different CO_2 conditions was controlled by Fe^{2+} (Fig 6.3), changing from 37% (pCO_2 225 µatm) to 47% (pCO_2 900 µatm. The second most important specie at pCO_2 225 µatm, $FeCO_3$ (33%), decreased its fraction molar under simulated acidification conditions, reaching 19% at pCO_2 900 µatm. Fe(II) speciation was strongly affected when the levels organic ligands were significantly different to control seawater (i.e EP and SP). The EP showed that the influence of Fe-PhC decreased as the CO_2 levels increased in the cultures. During the SP, the speciation was controlled by Fe^{2+} and

Fe(II)−PhC, which was the most important species between pCO_2 225 µatm and pCO_2 300 µatm, reaching 33% and 28%, respectively.

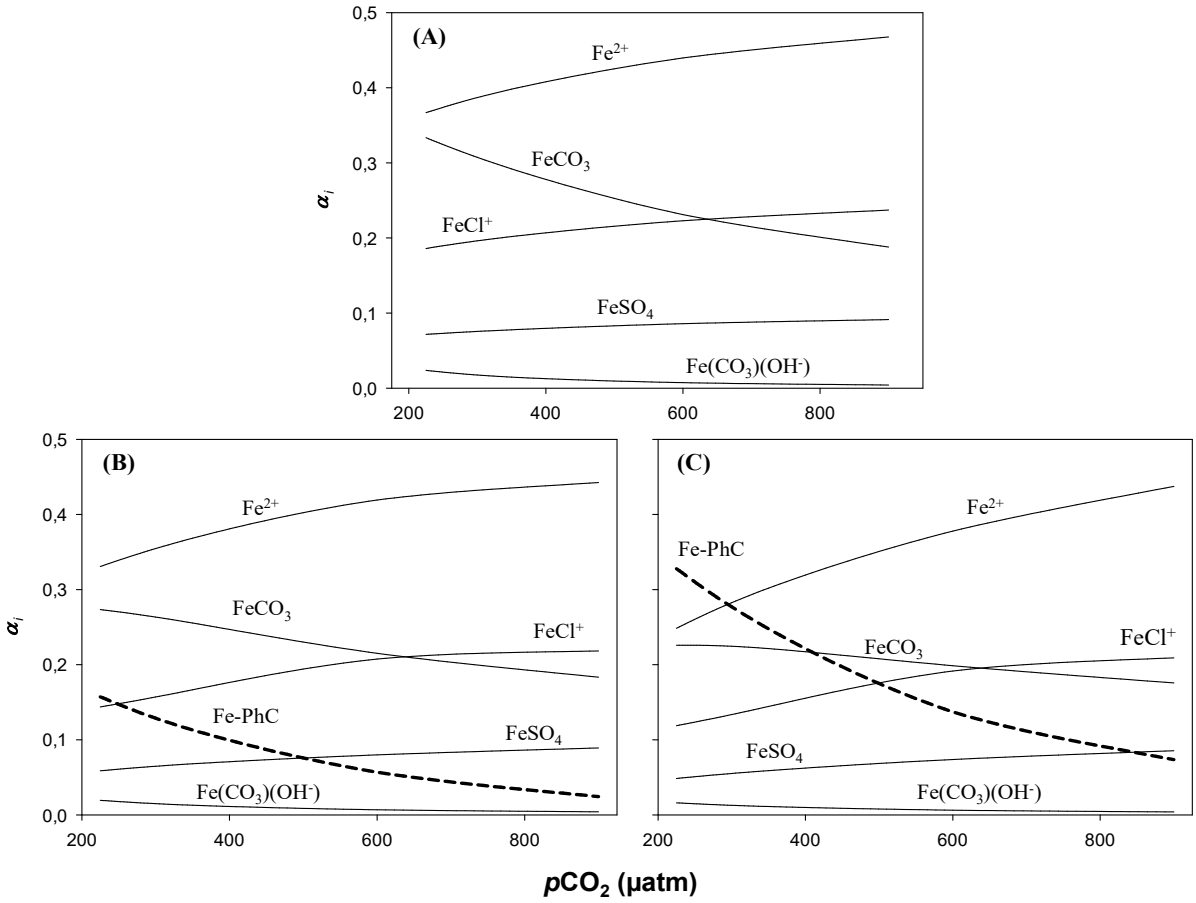

Fig 6.3 Fe(II) speciation from the kinetic modelling approach in cultures of *E. huxleyi* under different CO_2 scenarios. (A) SWEN including the IP (0-2 days), (B) SWEX from the EP ([DOC] = 33.18 ± 3.78 µmol $C \cdot L^{-1}$), and (C) and SWEX from the SP ([DOC] = 141.11 ± 10.27 µmol $C \cdot L^{-1}$). T^a = 25 ºC and S = 36.48.

Contrarily the role played by Fe(II)-UA complexes in the speciation was secondary (0.1-0.5%) although it became more important as the ligand concentration and CO_2 levels enhanced. In line with our work, recently Gledhill et al (2015) carried out a non-ideal competitive adsorption model, using phenolic and carboxylic moieties as binding modelling components, to determine the chemical speciation of Fe(III) in seawater under different pH conditions. As in our case with Fe(II), their results indicated that a decrease in iron binding by phenolic fractions and an increase in the Fe-carboxylate complexes at low pH is produced.

Figure 6.4 shows the contributions of the different Fe(II) species to the Fe(II) oxidation rate with O_2. The oxidation processes in SWEN and SWEX during the IP, were controlled by the $Fe(OH)_2$, from 225 µatm (42%) to 665 µatm (21%), and by $FeH_3SiO_4^+$, from 670 µatm (22%) to 900 µatm (23%). The presence of organic ligands changed the contribution of each individual species to the overall Fe(II) oxidation rate along the pCO_2 conditions exposed during the cultures (Fig 6.4).

The $Fe(OH)_2$ continue to be the most important contributor from 225 µatm (34%) to 780 µatm (15%) during the EP and from 225 µatm (32%) to 384 µatm (23%) during the SP, while the Fe-DUA complex began to be the most important specie between 780 µatm (15%) and 900 µatm (18%) during the EP and between 530 µatm (22%) and 900 µatm (34%) during the SP. Additionally, Fe-PhC was the most important contributing specie from 385 µatm (23%) to 528 µatm (22%) during the SP. During the EP the maximum contribution for the Fe-PhC complex was 10% (pCO_2 430 µatm).

The individual contributions to the overall Fe(II) rate demonstrated that Fe(II).organic complexes played a key role in the Fe(II) oxidation process, especially when the natural ligands were produced under acidified conditions (> 380 µatm). In addition, when the CO_2 concentrations in the cultures were lower than the current averaged levels measured in the ocean (IPCC, 2014), the Fe(II) oxidation rate was controlled by the Fe(II) hydroxide species.

6.4 Environmental implications

When the levels of DOC increased in the cultures, the Fe(II) oxidation rate was always lower in the presence of organic exudates from *E. huxleyi* than in seawater without ligands, under different acidification scenarios. Therefore, Fe(II) oxidation process was a function of the organic ligands released by *E. huxleyi* at different pCO_2 conditions. The experimental results confirm that Fe(II) can be present for a longer time in the presence of natural ligands produced under simulated acidification conditions. The overall equation (eq 43) allows determining the fraction

of the Fe(II) oxidation rate that corresponds to the organic exudates released from coccolithophorids in a seawater under ocean acidification conditions

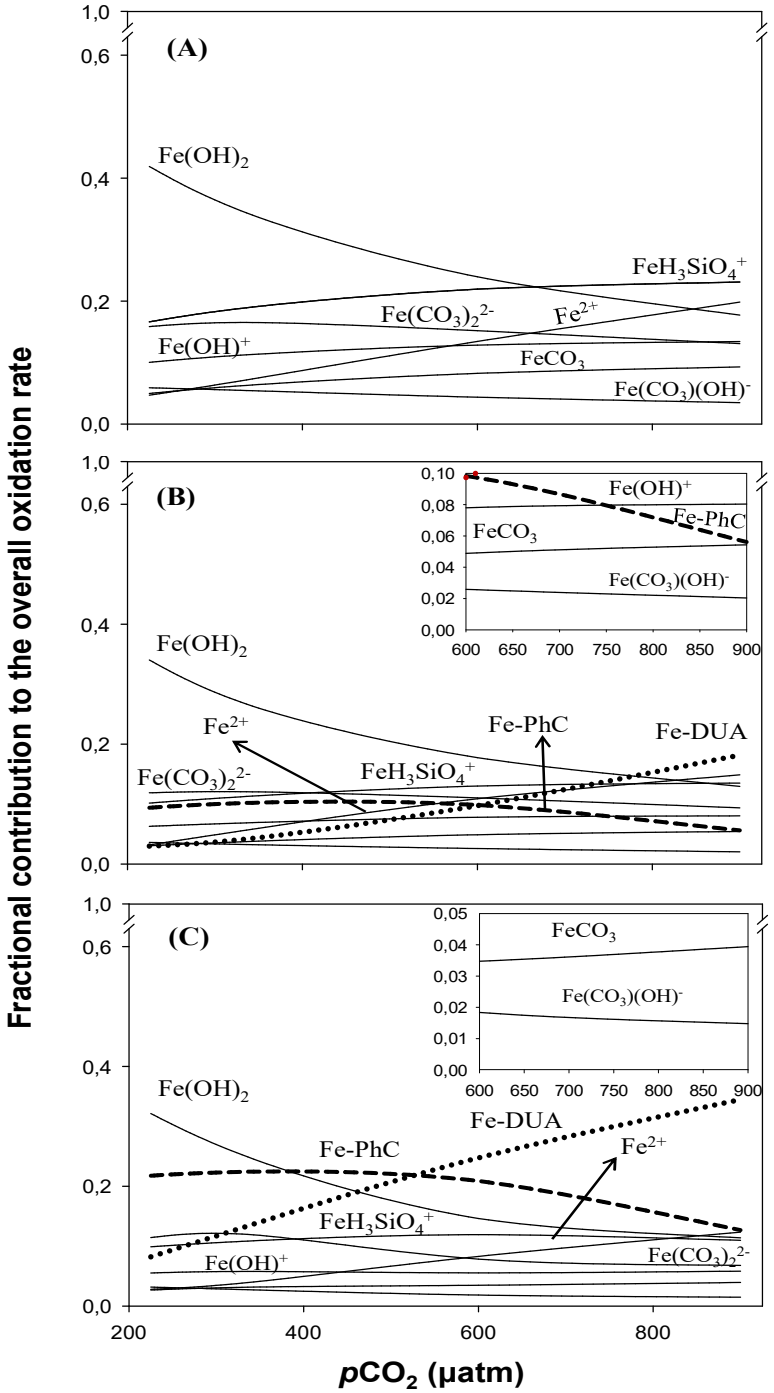

Fig 6.4 Contribution of each Fe(II) species to the overall rate constant from the kinetic model in cultures of *E. huxleyi* under different CO_2 scenarios: (A) SWEN including the IP (0-2 days), (B) SWEX from the EP ([DOC] = 33.18 ± 3.78 µmol C·L^{-1}), and (C) SWEX from the SP ([DOC] = 141.11 ± 10.27 µmol C·L^{-1}) T^a = 25 ºC ans S = 36.48.

CHAPTER VI

.

Elevated CO_2 will increase exudation by phytoplankton in the ocean (Borchard and Engel, 2012; Spilling et al. 2016) and therefore the key role played by organic ligands produced by eukaryote microalgae on the Fe(II) oxidation rate can be highly affected under acidification conditions. The kinetic model shows that the presence of phenolic moieties and uronic acids in exudates from *E. huxleyi* significantly interact with Fe(II), affecting both the speciation and the contribution of each species of Fe(II) in seawater to the overall rate. The effect of ocean acidification on the biosynthesis of ligands by phytoplankton species controls the speciation and redox behaviour Fe(II) in seawater and therefore the phytoplankton uptake.

CHAPTER VII

General conclusions

Conclusiones generales

CHAPTER VII

- ## General Conclusions

This Thesis has been carried out to improve our understanding on the redox behavior of iron in presence of nutrients and phytoplanktonic exudates released under different environmental conditions. The findings of this project can be delimited into five sections:

1. Eutrophication effect on the Fe(II) oxidation rate

- The oxidation of Fe(II) was faster by the presence of nutrients (phosphate and silicate, mainly).
- The increase in the Fe(II) oxidation rate is more intensive at higher temperatures due to role played by the Fe(II)-silicate reactive specie ($FeH_3SiO_4^+$).
- The individual oxidation rates by oxygen, for the Fe(II) most kinetically active species is fitted as a function of the temperature.
- Kinetic model revealed that the fractional contribution of $FeH_3SiO_4^+$ to the Fe(II) overall oxidation rate will be increased under ocean acidification conditions.
- Equilibrium formation constant for the $FeH_3SiO_4^+$ has been determined as a function of temperature

2. Effect of iron bioavailability on the exudation of Synechococcus PCC 7002

- *Synechococcus* PCC 7002 compensates growth-limiting levels of iron availability by decreasing its maximum growth rate.
- The type of organic ligand excreted by *Synechococcus* is a function of Fe-bioavailability.
- Extracellular release rate of phenolic and hydroxamic ligands increase under low-Fe conditions.

3. Effect of Synechococcus PCC 7002 exudates on iron redox behaviour

- A pH-dependence in the Fe(III) photo-reduction process has been determined in presence of *Synechococcus* exudates released under low-Fe conditions.
- The Fe(II) oxidation rate shows a dependence with dissolved organic carbon, pH, temperature and salinity.
- Photolytic reaction modify the reactivity of organic ligands with respect to Fe(II), when are excreted under iron deficient scenario.
- The exudates of *Synechococcus* released under low iron conditions intensified the Fe(II) oxidation at low pH < 7.5.
- The presence of organic exudates produced under Fe-replete conditions decreased the Fe(II) oxidation process respect to control seawater along pH gradient studied.
- Two equations to compute the changes in the apparent oxidation rate by the presence of prokaryote exudates, produced under high and low Fe-biovailabilty scenarios have been determined. The effect of photolysis has been also included.
- The kinetic model developed, considering phenolic and hydroxamic type ligands, suggest that the speciation and the fractional contribution of Fe(II) species are affected by the presence of both organic ligands.

4. Effect of ocean acidification on the organic exudation of Emiliania huxleyi

- The development of *E. huxleyi* is dependent of experimental acidification, during the later stages of growth.
- Dissolved combined carbohydrates and phenolic compounds are a substantial fraction of organic material excreted by *E. huxleyi* under the different CO_2 conditions.
- The contribution of dissolved uronic acids to dissolved carbohydrates released by *E. huxleyi* is conditioned by the acidification conditions during the stationary phase of growth.
- The different CO_2 conditions induce a strong response to extracellular release rate of uronic acids and phenolic compounds.

5. *Effect of exudate of E. huxleyi on the Fe(II) oxidation rate under different CO_2 conditions*

- The exudates excreted by *E.huxleyi* under different CO_2 conditions retard the oxidation process of Fe(II).

- The pH dependence of the Fe(II) oxidation rate in the presence of dissolved organic material released by *E. huxleyi,* indicating that the organic ligands, produced under different pCO_2 conditions, modify the speciation and fractional contribution of each Fe(II) species in solution.

- An equation to compute the changes in the apparent oxidation rate by the presence of *E. huxleyi* exudates, in a context of ocean acidification, has been elucidated.

- The kinetic reactivity between Fe(II) and uronic acids is determine in artificial seawater, to elucidate the role played by these ligands, present in the exudates of *E.huxleyi*, on the Fe(II) oxidation rate.

- The kinetic model approach indicates that the ligand models used (uronic acids and phenolic compounds) are significant controlling the oxidation process and the speciation in the different CO_2 conditions studied.

- The application of Marcus theory and a kinetic model support the Fe(II) complexation with ligands released by the phytoplankton in seawater under oxic conditions, when the direct measurements are not available.

CHAPTER VII

• Conclusiones generales

Esta tesis se ha llevado a cabo con el objetivo de mejorar nuestro nuestra comprensión y conocimiento sobre el comportamiento redox del hierro en presencia de nutrientes y exudados fitoplanctónicos liberados bajo diferentes condiciones ambientales. Las conclusiones de este proyecto pueden ser delimitadas en cinco secciones

1. Efecto de la eutrofización en la velocidad de oxidación de Fe(II)

- La oxidación de Fe(II) es acelerada por la presencia de nutrientes (fosfato y silicato, principalmente).
- El incremento de la velocidad de oxidación de Fe(II) es más acusada a altas temperaturas debido al rol desempeñado por la especie reactiva Fe(II)-silicato ($FeH_3SiO_4^+$).
- Las velocidades de oxidación individuales, para las especies cinéticamente más activas han sido determinadas en función de la temperatura.
- El modelo cinético ha demostrado que la contribución a la velocidad global de oxidación del Fe(II) de la especie $FeH_3SiO_4^+$ se verá incrementada por la acidificación oceánica.
- La constante de formación para la especie $FeH_3SiO_4^+$ ha sido determina en función de la temperatura.

2. Efecto de la biodisponibilidad de hierro en la exudación por parte Synechococcus PCC 7002

- *Synechococcus* PCC 7002 compensa lo niveles limitantes de hierro reduciendo su tasa de crecimiento.
- El tipo de ligando excretado por *Synechococcus* es función de la biodisponibilidad de hierro.
- La tasa de liberación extracelular para los ligandos fenólicos e hidroxámicos incrementa bajo condiciones limitantes de hierro.

3. Efecto de los exudados de Synechococcus PCC 7002 sobre el comportamiento redox del hierro

- Se ha determinado una dependencia respecto al pH en el proceso de foto-reducción de Fe(III) por presencia de exudados de *Synechococcus* liberados en condiciones deficientes de hierro.
- La velocidad de oxidación de Fe(II) muestra una dependencia con los niveles de carbono orgánico disuelto, pH, temperatura y salinidad.
- La reacción fotolítica modifica la reactividad de los ligandos orgánicos con respecto al Fe(II), cuando éstos son excretados bajo un escenario deficiente de hierro.
- Los exudados de *Synechococcus* liberados con bajos niveles de hierro intensifican la oxidación de Fe(II) a pH < 7.5.
- La presencia de exudados orgánicos producidos bajo condiciones saturadas de Fe reducen el proceso de oxidación de Fe(II) respecto al control a lo largo del gradiente de pH estudiado.
- Han sido determinadas dos ecuaciones para calcular los cambios en la velocidad aparente de oxidación de Fe(II) por la presencia de exudados procariotas producidos con altos y bajos niveles de hierro El efecto fotolítico también ha sido incluido en una ecuación .
- El modelo cinético desarrollado, considerando los ligados de tipo fenólico e hidroxámico, sugiere que la especiación y la oxidación de Fe(II) son afectadas por la presencia de ambos tipos de ligandos.

4. Efecto de la acidificación oceánica en la producción orgánica de Emiliania huxleyi

- El desarrollo de *E. huxleyi* es dependiente de la acidificación experimental durante las última etapa de crecimiento.
- Los carbohidratos combinados disueltos y compuestos fenólicos son una sustancial fracción del material orgánico excretado por *E. huxleyi* bajo las diferentes condiciones de CO_2.
- La contribución de los ácidos urónicos a los carbohidratos disueltos liberados por *E. huxleyi* es condicionada por las condiciones de acidificación durante la fase estacionaria del crecimiento.

- Las condiciones de CO_2 inducen una fuerte respuesta de la tasa de liberación extracelular de ácidos urónicos y compuestos fenólicos.

5. Efecto de los exudados de E. huxleyi en la tasa de oxidación de Fe(II) bajo diferentes condiciones de CO_2

- El conjunto de los exudados excretados por *E.huxleyi* bajo diferentes condiciones de CO_2 retardan el proceso de oxidación de Fe(II).

- La dependencia con el pH de la velocidad de oxidación de Fe(II) en presencia del material orgánico liberado por *E. huxleyi,* indica que los ligandos orgánicos producidos bajo diferentes condiciones de pCO_2 modifican la contribución parcial de cada especie de Fe(II).

- Una ecuación para calcular los cambios en la velocidad de oxidación aparente de Fe(II) debido a la presencia de exudados de *E. huxleyi*, en un contexto de acidificación oceánica, ha sido determinada.

- La reactividad cinética entre Fe(II) y ácidos urónicos se determina en agua de mar artificial para posteriormente dilucidar el rol desempeñado por este tipo de ligandos, presente en los exudados de *E.huxleyi*, en la velocidad de oxidación de Fe(II).

- El modelo cinético indica que los ligandos modelados (ácidos urónicos y compuestos fenólicos) controlan la oxidación y la especiación bajo las diferente condiciones de CO_2 estudiadas.

- La aplicación de la Teoría de Marcus junto al modelo cinético apoya la complejación de Fe(II) con ligandos liberados porel fitoplancton en agua de mar bajo condiciones óxicas, cuando las medidas directas no son viables.

CHAPTER VIII

Future research

Investigaciones futuras

CHAPTER VIII

- **Future research**

The exudates of phytoplankton result from a wide mixture of organic ligands, and the reactivity with trace metals in the most of these compounds is still poorly characterized. In order to know the most significant ligands for the trace metal redox behavior in the ocean, studies in artificial seawater, with a simplified ligand model, should be performed in the future.

In order to better estimate the real effects and potential consequences of ocean warming and acidification on the phytoplanktonic ligands exudation, it is necessary to carry out mesocosms with natural oceanic communities and laboratory incubations with individual species, changing the natural environmental factors (i.e. nutrient availability or light conditions). In addition to reach a better understanding of individual and combined effects of CO_2 and temperature on Fe requirements and bioavailability by phytoplankton, uptake experiments become fundamental. Therefore, the study of how iron is assimilated by microorganisms should be performed both with individual ligands and natural exudates released under controlled conditions (Hutchins and Boyd, 2016).

Concurrently with kinetic experiments, methodologies for isolation and identification of the organic compounds present in phytoplantonic exudates, such as achieve by high-performance liquid chromatography (Boiteau and Repeta, 2015; Lopez et al. 2015), should continue to be development.

On the other hand, the chemical interactions and competitive mechanisms of iron with other trace metals, reactive oxygen species or major components present in seawater should be thoroughly studied.

Finally and with the purpose to improve the knowledge about the complexation between Fe(II) and organic compounds present in oceanic waters the develop of an accurate analytical technique, as it happened with Fe(III) and the Competitive Ligand Exchange Adsorptive Cathodic Stripping Voltammetry two decades ago (Gledhill and van der Berg, 1994), will be required. This would produce a breakthrough in the biogeochemical study of iron in the ocean.

- # Estudios futuros

Los exudados de fitoplancton son resultado de una amplia mezcla de ligandos orgánicos y la reactividad de los metales traza con la mayoría de estos compuestos está todavía pobremente caracterizada Con el fin de conocer los ligandos más significativos para el comportamiento redox de los metales traza en el océano, un mayor número de estudios en agua de mar artificial, mediante un modelo de ligando simplificado, deben ser realizados en el futuro.

Para estimar de forma más eficiente los efectos y consecuencias potenciales del calentamiento del océano y su acidificación sobre la exudación de ligandos fitoplanctónicos, es necesario llevar a cabo mesocosmos con comunidades naturales del océano e incubaciones en el laboratorio con especies aisladas, incluyendo otros factores ambientales (como pueden ser la disponibilidad de nutrientes o la luz). Además para alcanzar un mayor entendimiento de los efectos y co-efectos producidos por los altos niveles de CO_2 y la temperatura sobre la biodisponibilidad y requerimientos de Fe por el fitoplancton, la realización de experimentos de asimilación es fundamental. Por lo tanto, los estudios de como el hierro es asimilado por los microorganismos debe ser llevado a cabo tanto con ligandos individuales como exudados naturales producidos bajo condiciones controladas.

Paralelamente a los experimentos cinéticos, deberían seguir desarrollándose metodologías para el aislamiento y la identificación de compuestos organicos presentes en exudados fitoplantónicos, como los obtenidos por cromatografía líquida de alta resolución (Boiteau y Repeta, 2015; López et al., 2015).

Por otro lado, las interacciones ymecanismos competitivos del hierro con otros metals traza, con especies reactivas del oxígeno o con otros componentes mayoritarios presentes en el agua de mar deben seguir estudiándose en profundidad.

Por último y con el fin de mejorar el conocimiento sobre la complejación del Fe(II) con ligandos orgánicos presentes en el océano, es requerido el desarrollo de una técnica analítica precisa, como ocurrió hace dos décadas para el Fe(III) con la Voltamperometría de Desprendimiento Catódico Adsorbente (Gledhill y van der

Berg, 1994). Esto produciría un gran avance en el estudio biogeoquímico del hierro en el océano.

CHAPTER VIII

REFERENCES

REFERENCES

Achterberg E. P., Holland T. W., Bowie A. R., et al.: Determination of iron in seawater. Anal Chim Acta 442:1–14. doi: 10.1016/S0003-2670(01)01091-1. 2001.

Achterberg, E. P., Moore, C. M., Henson, S. A., Steigenberger, S., Stohl, A., Eckhardt, S., Avendano, L. C., Cassidy, M., Hembury, D., Klar, J. K., Lucas, M. I., MacEy, A. I., Marsay, C. M. and Ryan-Keogh, T. J.: Natural iron fertilization by the Eyjafjallajkull volcanic eruption. Geophysical Research Letters 40, 921–926. doi:10.1002/grl.50221. 2013

Adly, C. L., Tremblay, J.-E., Powell, R. T., Armstrong, E., Peers, G. and Price, N. M.: Response of heterotrophic bacteria in a mesoscale iron enrichment in the northeast subarctic Pacific Ocean. Limnology and Oceanography 60, 136–148. doi:10.1002/lno.10013, 2015

Aeschbacher, M., Graf, C., Schwarzenbach, R. P. and Sander, M.: Antioxidant Properties of Humic Substances Antioxidant Properties of Humic Substances. Environmental Science & Technology 46, 4916–4925. doi:10.1021/es300039h, 2012.

Agustí, S. and Duarte, C. M.: Phytoplankton lysis predicts dissolved organic carbon release in marine plankton communities, Biogeosciences, 10(3), 1259–1264, 2013.

Alderkamp, A.-C.: Carbohydrate production by phytoplankton and degradation in the marine microbial food web., 2006.

Amin, S., Green, D. H., Hart, M. C., Küpper, F. C., Sunda, W. G. and Carrano, C. J.: Photolysis of iron, siderophore chelates promotes bacterial, algal mutualism. Proceedings of the National Academy of Sciences 106, 17071–17076. 2009a.

Amin, S., Green, D. H., Küpper, F. C. and Carrano, C. J.:. Vibrioferrin , an Unusual Marine Siderophore : Iron Binding, Photochemistry, and Biological Implications. Inorganic Chemistry 48, 11451–11458. doi:10.1021/ic9016883. 2009b.

Arnold, T., Mealey, C., Leahey, H., Miller, a. W., Hall-Spencer, J. M., Milazzo, M. and Maers, K.: Ocean Acidification and the Loss of Phenolic Substances in Marine Plants, PLoS ONE, 7(4), e35107, doi:10.1371/journal.pone.0035107, 2012.

Arístegui J., Duarte C. M., Reche I., Gómez-Pinchetti J. L.: Krill excretion boosts microbial activity in the Southern Ocean. PLoS One 9: 389-391. 2014.

Armbrecht, L. H., Thompson, P. A., Wright, S. W., Schaeffer, A., Roughan, M., Henderiks, J. and Armand, L.K.: Comparison of the cross-shelf phytoplankton distribution of two oceanographically distinct regions off Australia. Journal of Marine Systems 148, 26–38. doi:http://dx.doi.org/10.1016/j.jmarsys.2015.02.002, 2015.

Armstrong, J. E. and Van Baalen, C.: Iron transport in microalgae: the isolation and biological activity of a hydroxamate siderophore from the blue-green alga Agmenellum quadruplicatum. Journal of General Microbiology 111, 253–262. doi:10.1099/00221287-111-2-253, 1979.

Arnow, L. E.: Colorimetric determination of the components of 3,4-dihydroxyphenylalaninetyrosine mixtures. The Journal of Biological Chemistry 118, 531–537, 1937.

Arrhenius S.A.: Über die Dissociationswärme und den Einflusß der Temperatur auf den Dissociationsgrad der Elektrolyte". Z. Physik. Chem. 4: 96–116. 1889.

de Baar, H. J. W.: Synthesis of iron fertilization experiments: From the Iron Age in the Age of Enlightenment, Journal of Geophysical Research, 110(C9), C09S16, doi:10.1029/2004JC002601, 2005.

de Baar, H. J. W., Buma, A. G. J., Nolting, R. F., Cadee, G. C., Jacques, G. and Treguer, P. J.: On iron limitation of the Southern Ocean : experimental observations in the Weddell and Scotia Seas, Marine Ecology Progress Series, 65(2), 105–122, 1990.

de Baar, H. J. W., de Jong, J. T. M., Bakker, D. C. E., Loscher, B. M., Veth, C., Bathmann, U. and Smetacek, V.: Importance of iron for plankton blooms and carbon dioxide drawdown in the Southern Ocean, Nature, 373(6513), 412–415, 1995.

De Baar, H. J. W., Gerringa, L. J. A., Laan, P. and Timmermans, K. R.: Efficiency of carbon removal per added iron in ocean iron fertilization, Marine Ecology Progress Series, 364, 269–282, doi:10.3354/meps07548, 2008. de Baar, H. J. W., Buma, A. G. J., Nolting, R. F., Cadee, G. C., Jacques, G. and Treguer, P. J.: On iron limitation of the Southern Ocean : experimental observations in the Weddell and Scotia Seas, Marine Ecology Progress Series, 65(2), 105–122, doi:10.3354/meps065105, 1990.

Bach, L. T., Bauke, C., Meier, K. J. S., Riebesell, U. and Schulz, K. G.: Influence of changing carbonate chemistry on morphology and weight of coccoliths formed by *Emiliania huxleyi*, Biogeosciences, 9(8), 3449–3463, doi:10.5194/bg-9-3449-2012. 2012.

Baker, A. R. and Croot, P. L.: Atmospheric and marine controls on aerosol iron solubility in seawater. Marine Chemistry 120, 4–13. doi:10.1016/j.marchem.2008.09.003. 2010.

Baldi, F., Marchetto, D., Battistel, D., Daniele, S., Faleri, C., De Castro, C. and Lanzetta, R.:. Iron-binding characterization and polysaccharide production by *Klebsiella oxytoca* strain isolated from mine acid drainage. Journal of Applied Microbiology 107, 1241–1250. doi:10.1111/j.1365-2672.2009.04302.x. 2009.

Barbeau, K.: Photochemistry of organic iron(III) complexing ligands in oceanic systems., Photochemistry and photobiology, 82(6), 1505–1516, 2006.

Barbeau, K., Moffett, J. W., Caron, D. A., Croot, P. L. and Erdner, D. L.: Role of protozoan grazing in relieving iron limitation of phytoplankton, Nature, 380(6569), 61–64 [online] Available from: http://dx.doi.org/10.1038/380061a0, 1996.

Barbeau, K., Rue, E. L., Bruland, K. W. and Butler, A: Photochemical cycling of iron in the surface ocean mediated by microbial iron(III)-binding ligands., Nature, 413(6854), 409–413, doi:10.1038/35096545, 2001.

Barofsky, A., Vidoudez, C. and Pohnert, G.: Metabolic profiling reveals growth stage variability in diatom exudates. Limnology and Oceanography: Methods 7, 382–390. doi:10.4319/lom.2009.7.382, 2009.

Baron, J. S., Hall, E. K. , Nolan, B. T., et al.: The interactive effects of excess reactive nitrogen and climate change on aquatic ecosystems and water resources of the United States. Biogeochemistry 114:71–92. doi: 10.1007/s10533-012-9788-y. 2013.

Bastos, R., Coelho, E. and Coimbra, M. A.: Modifications of Saccharomyces pastorianus cell wall polysaccharides with brewing process, Carbohydrate Polymers, 124, 322–330, doi:https://doi.org/10.1016/j.carbpol.2015.02.031, 2015.

Batchelli, S., Muller, F. L. L., Chang, K. C. and Lee, C. L.: Evidence for Strong but Dynamic Iron−Humic Colloidal Associations in Humic-Rich Coastal Waters, Environmental Science & Technology, 44(22), 8485–8490, doi:10.1021/es101081c, 2010.

Beaufort, L., Probert, I., de Garidel-Thoron, T., Bendif, E. M., Ruiz-Pino, D., Metzl, N., Goyet, C., Buchet, N., Coupel, P., Grelaud, M., Rost, B., Rickaby, R. E. M., de Vargas, C.: Sensitivity of coccolithophores to carbonate chemistry and ocean acidification. Nature 476, 80–83. doi:10.1038/nature10295. 2011.

Becker, J. W., Berube, P. M., Follett, C. L., Waterbury, J. B., Chisholm, S. W., DeLong, E. F. and Repeta, D.J.: Closely related phytoplankton species produce similar suites of dissolved organic matter. Frontiers in Microbiology 5, 1–14. doi:10.3389/fmicb.2014.00111, 2014.

Behrenfeld, M. J. and Milligan, A. J.: Photophysiological Expressions of Iron Stress in Phytoplankton, Annual Review of Marine Science, 5(1), 120717164858000, doi:10.1146/annurev-marine-121211-172356, 2011.

Behrenfeld, M. J., O'Malley, R. T., Siegel, D. a, McClain, C. R., Sarmiento, J. L., Feldman, G. C., Milligan, A. J., Falkowski, P. G., Letelier, R. M. and Boss, E. S.: Climate-driven trends in contemporary ocean productivity., Nature, 444(7120), 752–755, doi:10.1038/nature05317, 2006.

Benner, R.: Loose ligands and available iron in the ocean, Proceedings of the National Academy of Sciences of the United States of America, 108(3), 893–894, doi:10.1073/pnas.1018163108, 2011.

Benner, R., Pakulski, J. D., McCarthy, M., Hedges, J. I. and Hatcher, P. G.: Bulk Chemiccal Characteristics of Dissolved Organic Matter in the Ocean, Science, 255(5051), 1561–1564, 1992.

Benson, B. B. and Krause, D.: The concentration and isotopic fractionation of oxygen dissolved in freshwater and seawater in equilibrium with the atmosphere. Limnol Oceanogr 29:620–632. doi: 10.4319/lo.1984.29.3.0620. 1984.

Bergquist, B. A., Wu, J. and Boyle, E. A.: Variability in oceanic dissolved iron is dominated by the colloidal fraction>, Geochimica et Cosmochimica Acta, 71(12), 2960–2974, doi:10.1016/j.gca.2007.03.013, 2007.

Biddanda, B. and Benner, R.: Carbon, nitrogen, and carbohydrate fluxes during the production of particulate and dissolved organic matter by marine phytoplankton. Limnology and Oceanography 42, 506–518. doi:10.4319/lo.1997.42.3.0506, 1997.

Blumenkrantz, N. and Asboe-Hansen, G.: New method for quantitative determination of uronic acids, Analytical Biochemistry, 54(2), 484–489, doi:http://dx.doi.org/10.1016/0003-2697(73)90377-1, 1973.

Boiteau, R. M., Fitzsimmons, J. N., Repeta, D. J. and Boyle, E.A.: Detection of Iron Ligands in Seawater and Marine Cyanobacteria Cultures by High-Performance Liquid Chromatography − Inductively Coupled Plasma-Mass Spectrometry. Analytical Chemistry 85, 4357–4362, 2013.

Boiteau, R. M. and Repeta, D. J.: An extended siderophore suite from *Synechococcus* sp. PCC 7002 revealed by LC-ICPMS-ESIMS. Metallomics 7, 877–884, 2015.

Borchard, C., Borges, A. V., Händel, N. and Engel, A.: Biogeochemical response of *Emiliania huxleyi* (PML B92/11) to elevated CO_2 and temperature under phosphorous limitation: A chemostat study, Journal of Experimental Marine Biology and Ecology, 410, 61–71, doi:10.1016/j.jembe.2011.10.004, 2011.

Borchard, C. and Engel, A.: Organic matter exudation by *Emiliania huxleyi* under simulated future ocean conditions, Biogeosciences, 9(8), 3405–3423, doi:10.5194/bg-9-3405-2012, 2012.

Borchard, C. and Engel, A.: Size-fractionated dissolved primary production and carbohydrate composition of the coccolithophore *Emiliania huxleyi*, Biogeosciences, 12(4), 1271–1284, doi:10.5194/bg-12-1271-2015, 2015.

Borer, P., Sulzberger, B., Hug, S. J, et al.: Photoreductive dissolution of iron(III) (hydr)oxides in the absence and presence of organic ligands: experimental studies and kinetic modeling. Environ Science Technolology 43:1864–70, 2009.

Bosc, E., Bricaud, A. and Antoine, D.: Seasonal and interannual variability in algal biomass and primary production in the Mediterranean Sea, as derived from 4 years of SeaWiFS observations, Global Biogeochemical Cycles, 18, 1–17, doi:10.1029/2003GB002034, 2004.

Bourgoin, L.-H. and Tremblay, L.: Bacterial reworking of terrigenous and marine organic matter in estuarine water columns and sediments, Geochimica et Cosmochimica Acta, 74(19), 5593–5609, doi:http://dx.doi.org/10.1016/j.gca.2010.06.037, 2010.

Bowie, A. R., Whitworth, D. J., Achterberg, E. P., Mantoura, R. F. C. and Worsfold, P. J.: Biogeochemistry of Fe and other trace elements (Al, Co, Ni) in the upper Atlantic Ocean, Deep Sea Research Part I: Oceanographic Research Papers, 49(4), 605–636, doi:https://doi.org/10.1016/S0967-0637(01)00061-9, 2002.

Boyd, P.: Ocean science. Ironing out algal issues in the Southern Ocean., Science (New York, N.Y.), 304(5669), 396–397, doi:10.1126/science.1092677, 2004.

Boyd, P. W., Doney, S. C.: The impact of climate change and feedback processes on the ocean carbon cycle. In: Fasham MJR (ed) Ocean biogeochemistry. SpringerVerlag, Berlin, p 157−193. 2003.

Boyd, P. W. and Ellwood, M. J.: The biogeochemical cycle of iron in the ocean, Nature Geoscience, 3(10), 675–682, doi:10.1038/ngeo964, 2010.

Boyd, P. W. and Tagliabue, A.: Using the L* concept to explore controls on the relationship between paired ligand and dissolved iron concentrations in the ocean, Marine Chemistry, 173, 52–66, doi:10.1016/j.marchem.2014.12.003, 2015.

Boyd, P. W., Jickells, T., Law, C. S., Blain, S., Boyle, E. a, Buesseler, K. O., Coale, K. H., Cullen, J. J., de Baar, H. J. W., Follows, M., Harvey, M., Lancelot, C., Levasseur, M., Owens, N. P. J., Pollard, R., Rivkin, R. B., Sarmiento, J., Schoemann, V., Smetacek, V., Takeda, S., Tsuda, a, Turner, S. and Watson, a J.: Mesoscale iron enrichment experiments 1993-2005: synthesis and future directions., Science (New York, N.Y.), 315(5812), 612–7, doi:10.1126/science.1131669, 2007.

Boyd, P. W., Dillingham, P. W., McGraw, C. M., Armstrong, E. A., Cornwall, C. E., Feng, Y. -y., Hurd, C. L., Gault-Ringold, M., Roleda, M. Y., Timmins-Schiffman, E. and Nunn, B. L.: Physiological responses of a Southern Ocean diatom to complex future ocean conditions, Nature Climate Change, (October), doi:10.1038/nclimate2811, 2015.

Boye, M., Aldrich, A., van den Berg, C. M. G., de Jong, J. T. M., Nirmaier, H., Veldhuis, M., Timmermans, K. R. and de Baar, H. J. W.: The chemical speciation of iron in the north-east Atlantic Ocean, Deep Sea Research Part I: Oceanographic Research Papers, 53(4), 667–683, doi:10.1016/j.dsr.2005.12.015, 2006.

Boye, M. and van Den Berg, C. M. G.: Iron availability and the release of iron-complexing ligands by *Emiliania huxleyi*, Marine Chemistry, 70(4), 277–287, doi:10.1016/S0304-4203(00)00032-3, 2000.

Boye, M., van den Berg, C. M. G., de Jong, J. T. M., Leach, H., Croot, P. and de Baar, H. J. W.: Organic complexation of iron in the Southern Ocean, Deep Sea Research Part I: Oceanographic Research Papers, 48(6), 1477–1497, doi:10.1016/S0967-0637(00)00099-6, 2001.

Boye, M., Nishioka, J., Croot, P. L., Laan, P., Timmermans, K. R. and de Baar, H.J.W.: Major deviations of iron complexation during 22 days of a mesoscale iron enrichment in the open Southern Ocean. Marine Chemistry 96, 257–271. doi:10.1016/j.marchem.2005.02.002, 2005.

Boye, M., Nishioka, J., Croot, P., Laan, P., Timmermans, K. R., Strass, V. H., Takeda, S. and de Baar, H. J. W.: Significant portion of dissolved organic Fe complexes in fact is Fe colloids, Marine Chemistry, 122(1–4), 20–27, doi:10.1016/j.marchem.2010.09.001, 2010.

Breitbarth, E., Gelting, J., Walve, J., Hoffmann, L. J., Turner, D. R., Hassellöv, M. and Ingri, J.: Dissolved iron (II) in the Baltic Sea surface water and implications for cyanobacterial

bloom development, Biogeosciences Discussions, 6(2), 3803–3850, doi:10.5194/bgd-6-3803-2009, 2009.

Breitbarth, E., Achterberg, E. P., Ardelan, M. V., Baker, a. R., Bucciarelli, E., Chever, F., Croot, P. L., Duggen, S., Gledhill, M., Hassellöv, M., Hassler, C., Hoffmann, L. J., Hunter, K. a., Hutchins, D. a., Ingri, J., Jickells, T., Lohan, M. C., Nielsdóttir, M. C., Sarthou, G., Schoemann, V., Trapp, J. M., Turner, D. R. and Ye, Y.: Iron biogeochemistry across marine systems – progress from the past decade, Biogeosciences, 7(3), 1075–1097, doi:10.5194/bg-7-1075-2010, 2010a.

Breitbarth, E., Bellerby, R. J., Neill, C. C., Ardelan, M. V, Meyerhöfer, M., Zöllner, E., Croot, P. L. and Riebesell, U.: Ocean acidification affects iron speciation in seawater, Biogeosciences Discussions, 7(4), 1065–1073, doi:10.5194/bgd-6-6781-2009, 2010b.

Buma, A. G. J., De Baar, H. J. W., Nolting, R. F. and Van Bennekom, A. J.: Metal enrichment experiments in the Weddell-Scotia Seas: Effects of iron and manganese on various plankton communities, Limnology and Oceanography, 36(8), 1865–1878, doi:10.4319/lo.1991.36.8.1865, 1991.

Bundy, R. M., Biller, D. V, Buck, K. N., Bruland, K. W. and Barbeau, K. A.: Distinct pools of dissolved iron-binding ligands in the surface and benthic boundary layer of the California Current, Limnology and Oceanography, 59(3), 769–787, doi:10.4319/lo.2014.59.3.0769, 2014.

Butler, A. and Theisen, R. M.: Iron(III)-siderophore coordination chemistry: Reactivity of marine siderophores, Coordination Chemistry Reviews, 254(3–4), 288–296, doi:10.1016/j.ccr.2009.09.010, 2010.

Byrne, R. H.: Inorganic speciation of dissolved elements in seawater: the influence of pH on concentration ratios, Geochemical Transactions, 2(2), 11, doi:10.1039/b109732f, 2002.

Byrne, R. H., Kump, L. R. and Cantrell K. J.: The influence of temperature and pH on trace metal speciation in seawater. Marine Chemistry 25:163–181. doi: 10.1016/0304-4203(88)90062-X. 1988.

Byrne, R. H., Mecking, S., Feely, R. A. and Liu, X.: Direct observations of basin-wide acidification of the North Pacific Ocean. Geophys Res Lett 37:1–5. doi: 10.1029/2009GL040999. 2010.

Cadier, M., Gorgues, T., Sourisseau, M., Edwards, C. A., Aumont, O., Mari, L. and Memery, L.: Assessing spatial and temporal variability of phytoplankton communities' composition in the Iroise Sea ecosystem (Brittany, France): A 3D modeling approach. Part 1: Biophysical control over plankton functional types succession and distribution. Journal of Marine Systems 165, 47–68. doi:10.1016/j.jmarsys.2016.09.009, 2017.

Cai, W-J., Hu, X., Huang, W-J., et al. Acidification of subsurface coastal waters enhanced by eutrophication. Nature Geoscience 4:766–770. 2011.

Caldeira, K. and Wickett, M. E.: Oceanography: Anthropogenic carbon and ocean pH, Nature, 425(6956), 365 [online] Available from: http://dx.doi.org/10.1038/425365a, 2003.

Carlson, C. A. and Hansell, D. A.: Chapter 3 - {DOM} Sources, Sinks, Reactivity, and Budgets, in Biogeochemistry of Marine Dissolved Organic Matter (Second Edition), edited by D. A. Hansell and C. A. Carlson, pp. 65–126, Academic Press, Boston., 2015.

Catrouillet, C., Davranche, M., Dia, A., Bouhnik-Le Coz, M., Marsac, R., Pourret, O. and Gruau, G.: Geochemical modeling of Fe(II) binding to humic and fulvic acids, Chemical Geology, 372(Ii), 109–118, doi:10.1016/j.chemgeo.2014.02.019, 2014.

Celis-Plá, P. S., Hall-spencer, J. M., Horta, P. A., Milazzo, M., Korbee, N., Cornwall, C. E. and Figueroa, F. L.: Macroalgal responses to ocean acidification depend on nutrient and light levels, Frontiers in Marine Science, 2(May), 1–12, doi:10.3389/fmars.2015.00026, 2015.

Celis-Plá, P. S. M., Bouzon, Z. L., Hall-Spencer, J. M., Schmidt, E. C., Korbee, N. and Figueroa, F. L.: Seasonal biochemical and photophysiological responses in the intertidal macroalga Cystoseira tamariscifolia (Ochrophyta). Marine Environmental Research 115, 89–97. doi:http://dx.doi.org/10.1016/j.marenvres.2015.11.014, 2016.

Chen, M. and Wang, W. X: Accelerated uptake by phytoplankton of iron bound to humic acids. Aquat Biol 3:155–166. doi: 10.3354/ab00064. 2008.

Chester, R.: Marine Geochemistry, Wiley & Sons., 2009.

Chever, F., Sarthou, G., Bucciarelli, E., Blain, S. and Bowie, A. R.: An iron budget during the natural iron fertilisation experiment KEOPS (Kerguelen Islands, Southern Ocean), Biogeosciences, 7, 455–468, doi:10.5194/bgd-6-6803-2009, 2010.

Chow, J. S., Lee, C. and Engel, A.: The influence of extracellular polysaccharides, growth rate, and free coccoliths on the coagulation efficiency of *Emiliania huxleyi*, Marine Chemistry, 175, 5–17, doi:10.1016/j.marchem.2015.04.010, 2015.

Cloern, J. E.: Our evolving conceptual model of the coastal\reutrophication problem. Mar Ecol Prog Ser 210:223–253. doi: 10.3354/meps210223. 2001.

Conley, D. J., Paerl, H. W., Howarth, R. W., et al.: Controlling eutrophication: nitrogen and phosphorus. Science 323:1014–1015. doi: 10.1126/science.1167755. 2009.

Cooper, W. J. and Zika, R. G.: Photochemical Formation of Hydrogen Peroxide in Surface and Ground Waters Exposed to Sunlight, Science, 220(4598), 711–712, doi:10.1126/science.220.4598.711, 1983.

Croot, P. L. and Heller, M. I.: The importance of kinetics and redox in the biogeochemical cycling of iron in the surface ocean., Frontiers in microbiology, 3(June), 219, doi:10.3389/fmicb.2012.00219, 2012.

Croot, P. L. and Johansson, M.: Determination of iron speciation by cathodic stripping voltammetry in seawater using the competing ligand 2-(2- thiazolylazo)-p-cresol (TAC), Electroanalysis, 12(8), 565–576, 2000.

Croot, P. L., Laan, P., Nishioka, J., Strass, V., Cisewski, B., Boye, M., Timmermans, K. R., Bellerby, R. G., Goldson, L., Nightingale, P. and de Baar, H. J. W.: Spatial and temporal distribution of Fe(II) and H_2O_2 during EisenEx, an open ocean mescoscale iron enrichment. Marine Chemistry 95, 65–88. doi:10.1016/j.marchem.2004.06.041. 2005.

Croot, P. L., Passow, U., Assmy, P., Jansen, S. and Strass, V. H.: Surface active substances in the upper water column during a Southern Ocean Iron Fertilization Experiment (EIFEX). Geophysical Research Letters 34, 1–5. doi:10.1029/2006GL028080. 2007.

Cunningham, K. M., Goldberg, M. C. and Weiner, E. R.: Mechanisms for aqueous photolysis of adsorbed benzoate, oxalate, and succinate on iron oxyhydroxide (goethite) surfaces, Environmental Science & Technology, 22(9), 1090–1097, 1988.

Daniels, C. J., Sheward, R. M. and Poulton, A. J.: Biogeochemical implications of comparative growth rates of *Emiliania huxleyi* and Coccolithus species, Biogeosciences, 11(23), 6915–6925, doi:10.5194/bg-11-6915-2014, 2014.

Desboeufs, K. V, Losno, R. and Colin, J. L.: Factors influencing aerosol solubility during cloud processes, Atmospheric Environment, 35(20), 3529–3537, 2001.

Dhungana, S. and Crumbliss, A. L.: Coordination Chemistry and Redox Processes in Siderophore-Mediated Iron Transport. Geomicrobiology Journal 22, 87–98. 2005.

Doney, S. C.: The dangers of ocean acidification. Scientific American 294(3): 58-65. 2006.

Doney, S. C., Fabry, V. J., Feely, R. A. and Kleypas, J. A.: Ocean Acidification: The Other CO_2 Problem, Annual Review of Marine Science, 1(1), 169–192, doi:10.1146/annurev.marine.010908.163834, 2009.

Doney, S. C., Ruckelshaus, M., Emmett Duffy, J., Barry, J. P., Chan, F., English, C. A., Galindo, H. M., Grebmeier, J. M., Hollowed, A. B., Knowlton, N., Polovina, J., Rabalais, N. N., Sydeman, W. J. and Talley, L. D.: Climate Change Impacts on Marine Ecosystems, Annual Review of Marine Science, 4(1), 11–37, doi:10.1146/annurev-marine-041911-111611, 2012.

Dore, J. E., Lukas, R., Sadler, D. W., et al.: Physical and biogeochemical modulation of ocean acidification in the central North Pacific. Proc Natl Acad Sci 106:12235–12240. 2009.

Duarte, C. M., Regaudie-de-Gioux, A., Arrieta, J. M., Delgado-Huertas, A. and Agustí, S.: The Oligotrophic Ocean Is Heterotrophic, Annual Review of Marine Science, 5(1), 120913145809009, doi:10.1146/annurev-marine-121211-172337, 2011.

Duce, R. A. and Tindale, N. W.: Atmospheric transport of iron and its deposition in the ocean, Limnology and Oceanography, 36(8), 1715–1726, doi:10.4319/lo.1991.36.8.1715, 1991.

Dutkiewicz, S., Follows, M. J. and Parekh, P.: Interactions of the iron and phosphorus cycles: A three-dimensional model study. Global Biogeochem Cycles 19:n/a–n/a. doi: 10.1029/2004GB002342. 2005.

Elhabiri, M., Carrër, C., Marmolle, F. and Traboulsi, H.: Complexation of iron(III) by catecholate-type polyphenols, Inorganica Chimica Acta, 360(1), 353–359, doi:10.1016/j.ica.2006.07.110, 2007.

Elrod, V. A., Berelson, W. M., Coale, K. H. and Johnson, K. S.: The flux of iron from continental shelf sediments: A missing source for global budgets, Geophysical Research Letters, 31(12), 2–5, doi:10.1029/2004GL020216, 2004.

Emmenegger, L., King, D. W., Sigg, L. and Sulzberger, B.: Oxidation Kinetics of Fe (II) in a Eutrophic Swiss Lake. Environmental science & technology 32, 2990–2996. 1998.

Emmenegger, L., Schönenberger, R., Sigg, L. and Sulzberger, B.: Light-induced redox cycling of iron in circumneutral lakes. Limnology and Oceanography. doi:10.4319/lo.2001.46.1.0049. 2001.

Fujii, M., Rose, A.L., Omura, T., Waite, T.D., 2010. Effect of Fe (II) and Fe (III) Transformation Kinetics on Iron Acquisition by a Toxic Strain of *Microcystis aeruginosa* 44, 1980–1986.

Engel, A., Thoms, S., Riebesell, U., Rochelle-Newall, E. and Zondervan, I.: Polysaccharide aggregation as a potential sink of marine dissolved organic carbon, Nature, 428(6986), 929–932. http://dx.doi.org/10.1038/nature02453, 2004.

Engel, A., Händel, N., Wohlers, J., Lunau, M., Grossart, H. P., Sommer, U. and Riebesell, U.: Effects of sea surface warming on the production and composition of dissolved organic matter during phytoplankton blooms: Results from a mesocosm study, Journal of Plankton Research, 33(3), 357–372, doi:10.1093/plankt/fbq122, 2011.

Engel, A., Piontek, J., Grossart, H. P., Riebesell, U., Schulz, K. G. and Sperling, M.: Impact of CO_2 enrichment on organic matter dynamics during nutrient induced coastal phytoplankton blooms, Journal of Plankton Research, 36(3), 641–657, doi:10.1093/plankt/fbt125, 2014.

Engel, a., Zondervan, I., Aerts, K., Beaufort, L., Benthien, a., Chou, L., Delille, B., Gattuso, J.-P., Harlay, J. and Heemann, C.: Testing the direct effect of CO_2 concentration on a bloom of the coccolithophorid *Emiliania huxleyi* in mesocosm experiments, Limnology and Oceanography, 50(2), 493–507, doi:10.4319/lo.2005.50.2.0493, 2005.

Eyring, H.: The Activated Complex in Chemical Reactions. J Chem Phys 3:107–115. doi: 10.1063/1.1749604. 1935.

Fabry, V., Seibel, B., Feely, R. A. and Orr, J. C.: Impacts of ocean acidification on marine fauna and ecosystem processes, ICES Journal, (Dic), 414–432 [online] Available from: http://icesjms.oxfordjournals.org/content/65/3/414.short, 2008.

Fan, S. M.: Photochemical and biochemical controls on reactive oxygen and iron speciation in the pelagic surface ocean. Marine Chemistry 109, 152–164, 2008.

Fan, S. M., Moxim, W. J. and Levy, H.: Aeolian input of bioavailable iron to the ocean, Geophysical Research Letters, 33(7), 2–5, doi:10.1029/2005GL024852, 2006.

Feely, R. A., Alin, S. R, Newton, J., et al.: The combined effects of ocean acidification, mixing, and respiration on pH and carbonate saturation in an urbanized estuary. Estuar Coast Shelf Sci 88:442–449. doi: 10.1016/j.ecss.2010.05.004. 2010.

Feely, R. A., Doney, S. C. and Cooley, S. R.: Ocean Acidification: Present Conditions and Future Changes in High CO_2 World, Oceanography, 22(4), 36–47, doi:http://dx.doi.org/10.5670/oceanog.2009.95, 2009.

Flombaum, P., Gallegos, J. L., Gordillo, R. A., Rincón, J., Zabala, L. L., Jiao, N., Karl, D., Li, W., Lomas, M., Veneziano, D., Vera, C., Vrugt, J. A and Martiny, A. C.: Present and future global distributions of the marine Cyanobacteria *Prochlrococcus* and *Synechococcus*. Proceedings of the National Academy of Sciences 110, 9824–9829. 2013.

Flynn, K. J., Clark, D. R. and Xue, Y.: Modeling the release of dissolved organic matter by phytoplankton. Journal of Phycology 44, 1171–1187, 2008.

Galgani, L., Piontek, J. and Engel, A.: Biopolymers form a gelatinous microlayer at the air-sea interface when Arctic sea ice melts, Scientific Reports, 6(April), 29465, doi:10.1038/srep29465, 2016.

Garg, S., Rose, A. L. and Waite, T. D.: Superoxide-mediated reduction of organically complexed iron(III): Impact of pH and competing cations (Ca^{2+}), Geochimica et Cosmochimica Acta, 71(23), 5620–5634, doi:10.1016/j.gca.2007.08.002, 2007a.

Garg, S., Rose, A. L. and Waite, T. D.: Superoxide mediated reduction of organically complexed iron(III): comparison of non-dissociative and dissociative reduction pathways., Environmental science & technology, 41(9), 3205–12 [online] Available from: http://www.ncbi.nlm.nih.gov/pubmed/17539527, 2007b.

Garg, S., Rose, A. L. and Waite, T. D.: Photochemical production of superoxide and hydrogen peroxide from natural organic matter. Geochim Cosmochim Acta 75:4310–4320. doi: 10.1016/j.gca.2011.05.014. 2011.

Garmendia, M., Revilla, M., Bald, J., et al.: Phytoplankton communities and biomass size structure (fractionated chlorophyll “a”), along trophic gradients of the Basque coast (northern Spain). Biogeochemistry 106:243–263. doi: 10.1007/s10533-010-9445-2. 2011.

Gattuso, J.-P., Magnan, A., Billé, R., Cheung, W. W. L., Howes, E. L., Joos, F., Allemand, D., Bopp, L., Cooley, S. R., Eakin, C. M., Hoegh-Guldberg, O., Kelly, R. P., Pörtner, H.-O., Rogers, A. D., Baxter, J. M., Laffoley, D., Osborn, D., Rankovic, A., Rochette, J., Sumaila, U. R., Treyer, S. and Turley, C.: Contrasting futures for ocean and society from different anthropogenic CO_2 emissions scenarios, Science, 349(6243), doi:10.1126/science.aac4722, 2015.

Gerringa, L. J. A., Alderkamp, A.-C., Laan, P., Thuróczy, C.-E., De Baar, H. J. W., Mills, M. M., van Dijken, G. L., Haren, H. van and Arrigo, K. R.: Iron from melting glaciers fuels the phytoplankton blooms in Amundsen Sea (Southern Ocean): Iron biogeochemistry, Deep Sea Research Part II: Topical Studies in Oceanography, 71–76, 16–31, doi:https://doi.org/10.1016/j.dsr2.2012.03.007, 2012.

Giering, S. L. C., Sanders, R., Lampitt, R. S., Anderson, T. R., Tamburini, C., Boutrif, M., Zubkov, M. V, Marsay, C. M., Henson, S. A., Saw, K., Cook, K. and Mayor, D. J.: Reconciliation of the carbon budget in the ocean/'s twilight zone, Nature, 507(7493), 480–483 [online] Available from: http://dx.doi.org/10.1038/nature13123, 2014.

Gillam, A. H., Lewis, A. G. and Andersen, R. J.: Quantitative determination of hydroxamic acids. Analytical Chemistry 53, 841–844. doi:10.1021/ac00229a023, 1981.

Gledhill, M., Achterberg, E. P., Li, K., Mohamed, K. N. and Rijkenberg, M. J. A.: Influence of ocean acidification on the complexation of iron and copper by organic ligands in estuarine waters, Marine Chemistry, 177, 421–433, doi:10.1016/j.marchem.2015.03.016, 2015.

Gledhill, M. and Van den Berg, C. M. G.: Determination of complexation of iron (III) with natural organic complexing ligands in seawater using cathodic stripping voltammetry, Marine Chemistry, 47, 41–54, doi:10.1016/0304-4203(94)90012-4, 1994.

Gledhill, M., Van Den Berg, C. M. G., Nolting, R. F. and Timmermans, K.R.: Variability in the speciation of iron in the northern North Sea. Marine Chemistry 59, 283–300. doi:10.1016/S0304-4203(97)00097-2. 1998.

Gledhill, M., McCormack, P., Ussher, S., Achterberg, E. P., Mantoura, R. F. C. and Worsfold, P. J.: Production of siderophore type chelates by mixed bacterioplankton populations in nutrient enriched seawater incubations. Marine Chemistry 88, 75–83. doi:10.1016/j.marchem.2004.03.003, 2004.

Gledhill, M. and Buck, K. N.: The organic complexation of iron in the marine environment: a review., Frontiers in microbiology, 3(February), 69, doi:10.3389/fmicb.2012.00069, 2012.

Goldberg, S. J., Carlson, C. A., Hansell, D. A., Nelson, N. B. and Siegel, D. A.: Temporal dynamics of dissolved combined neutral sugars and the quality of dissolved organic matter in the Northwestern Sargasso Sea, Deep Sea Research Part I: Oceanographic Research Papers, 56(5), 672–685, doi:http://dx.doi.org/10.1016/j.dsr.2008.12.013, 2009.

González, A. G., Santana-Casiano, J. M., Pérez, N. and González-Dávila, M.: Oxidation of Fe(II) in natural waters at high nutrient concentrations., Environmental science & technology, 44(21), 8095–101, doi:10.1021/es1009218, 2010.

González, A. G., Santana-Casiano, J. M., González-Dávila, M. and Pérez-Almeida, N.: Effect of organic exudates of *Phaeodactylum tricornutum* on the Fe(II) oxidation rate constant, Ciencias Marinas, 38(1B), 245–261, 2012.

González, A. G., Santana-Casiano, J. M., González-Dávila, M., Pérez-Almeida, N. and Suárez De Tangil, M.: Effect of *Dunaliella tertiolecta* organic exudates on the Fe(II) oxidation kinetics in seawater, Environmental Science and Technology, 48(14), 7933–7941, doi:10.1021/es5013092, 2014.

González, A. G., Pérez-Almeida, N., Magdalena Santana-Casiano, J., Millero, F. J. and González-Dávila, M.: Redox interactions of Fe and Cu in seawater, Marine Chemistry, 179(February), 12–22, doi:10.1016/j.marchem.2016.01.004, 2016.

González-Davila, M., Santana-Casiano, J. M. and Millero, F. J.: Oxidation of iron(II) nanomolar with H_2O_2 in seawater, Geochimica et Cosmochimica Acta, 69(1), 83–93, doi:10.1016/j.gca.2004.05.043, 2005.

González-Dávila, M., Santana-Casiano, J. M. and Millero, F. J.: Competition Between O_2 and H_2O_2 in the Oxidation of Fe(II) in Natural Waters, Journal of Solution Chemistry, 35(1), 95–111, doi:10.1007/s10953-006-8942-3, 2006.

González-Dávila, M., Santana-Casiano, J. M., de Armas, D., et al.: The influence of island generated eddies on the carbon dioxide system, south of the Canary Islands. Marine Chemistry 99:177–190. doi: DOI 10.1016/j.marchem.2005.11.004. 2006b.

González-Dávila, M., Santana-Casiano, J. M., González, A. G., Pérez, N. and Millero, F. J.: Oxidation of copper(I) in seawater at nanomolar levels, Marine Chemistry, 115(1–2), 118–124, doi:10.1016/j.marchem.2009.07.004, 2009.

González-Dávila, M., Santana-Casiano, J. M., Rueda, M-J., et al.: Seasonal and interannual variability of sea-surface carbon dioxide species at the European Station for Time Series in the Ocean at the Canary Islands (ESTOC) between 1996 and 2000. Global Biogeochem Cycles. doi: 10.1029/2002GB001993. 2003.

González-Dávila, M., Santana-Casiano, J. M., Rueda, M. J. and Llinás, O.: The water column distribution of carbonate system variables at the ESTOC site from 1995 to 2004, Biogeosciences, 7(10), 3067–3081, doi:10.5194/bg-7-3067-2010, 2010.

Gordon, R. M., Martin, J. H. and Knauer, G. A.: Iron in north-east Pacific waters, Nature, 299(5884), 611–612 [online] Available from: http://dx.doi.org/10.1038/299611a0, 1982.

Grabo, J. E., Chrisman, M. A., Webb, L. M. and Baldwin, M.J.: Photochemical reactivity of the iron(III) complex of a mixed-donor, α-hydroxy acid-containing chelate and its biological relevance to photoactive marine siderophores. Inorganic Chemistry 53, 5781–5787. doi:10.1021/ic500635q. 2014.

Gruber, N.: Warming up, turning sour, losing breath: ocean biogeochemistry under global change, Philosophical Transactions of the Royal Society A: Mathematical, Physical and Engineering Sciences, 369(1943), 1980–1996, doi:10.1098/rsta.2011.0003, 2011.

Guenther, M., Araújo, M., Flores-Montes, M., et al.: Eutrophication effects on phytoplankton size-fractioned biomass and production at a tropical estuary. Marine Pollution Bulletin 91:537–547. doi: 10.1016/j.marpolbul.2014.09.048, 2015.

Gunderson, A. R., Armstrong, E. J. and Stillman, J. H.: Multiple Stressors in a Changing World: The Need for an Improved Perspective on Physiological Responses to the Dynamic Marine Environment, Annual Review of Marine Science, 8(1), 357–378, doi:10.1146/annurev-marine-122414-033953, 2016.

Guo, M., Perez, C., Wei, Y., Rapoza, E., Su, G., Bou-Abdallah, F. and Chasteen, N. D.: Iron-binding properties of plant phenolics and cranberry's bio-effects. Dalton Trans. 4951–4961. doi:10.1039/B705136K. 2007.

Gyurcsik, B. and Nagy, L.: Carbohydrates as ligands: coordination equilibria and structure of the metal complexes, Coordination Chemistry Reviews, 203(1), 81–149, doi:10.1016/S0010-8545(99)00183-6, 2000.

Haber, F. and Weiss, J.: Über die Katalyse des Hydroperoxydes, Naturwissenschaften, 20(51), 948–950, doi:10.1007/BF01504715, 1932.

Hansard, S. P., Landing, W. M., Measures, C. I. and Voelker, B. M.: Deep-Sea Research I Dissolved iron (II) in the Pacific Ocean : Measurements from the PO_2 and P16N CLIVAR / CO_2 repeat hydrography expeditions, Deep-Sea Research Part I, 56(7), 1117–1129, doi:10.1016/j.dsr.2009.03.006, 2009.

Hansell, D. A., Carlson, C. A., Repeta, D. J. and Schlitzer, R.: Dissolved Organic Matter in the Ocean. A controversy stimulates new insights. Oceanography 22:202–211, 2009.

Hansell, D. A.: Recalcitrant dissolved organic carbon fractions, Ann Rev Mar Sci, 5, 421–445, doi:10.1146/annurev-marine-120710-100757, 2013.

Haroun, R. J.: Environmental description of an artificial reef site in Gran Canaria (Canary Islands, Spain) prior to reef placement. Bull Mar Sci 55:932–938, 1994.

Harrington, J. M. and Crumbliss, A. L.: The redox hypothesis in siderophore-mediated iron uptake, BioMetals, 22(4), 679–689, doi:10.1007/s10534-009-9233-4, 2009.

Hassler, C. S. and Schoemann, V.: Article Bioavailability of organically bound Fe to model phytoplankton of the Southern Ocean Biogeosciences Bioavailability of organically bound Fe to model phytoplankton of the Southern Ocean, Biogeosciences, 6(10), 2281–2296, doi:10.5194/bg-6-2281-2009, 2009.

Hassler, C. S., Alasonati, E., Mancuso Nichols, C. a. and Slaveykova, V. I.: Exopolysaccharides produced by bacteria isolated from the pelagic Southern Ocean - Role in Fe binding, chemical reactivity, and bioavailability, Marine Chemistry, 123(1–4), 88–98, doi:10.1016/j.marchem.2010.10.003, 2011a.

Hassler, C. S., Schoemann, V., Boye, M., Tagliabue, A., Rozmarynowycz, M., McKay, R. M.: Iron bioavailability in the Southern Ocean. Oceanogr. Mar. Biol. 50, 1–64. 2012.

Hassler, C. S., Schoemann, V., Nichols, C. M., Butler, E. C. V and Boyd, P. W.: Saccharides enhance iron bioavailability to Southern Ocean phytoplankton., Proceedings of the National Academy of Sciences of the United States of America, 108(3), 1076–81, doi:10.1073/pnas.1010963108, 2011b.

Hassler, C. S., Norman, L., Mancuso Nichols, C. A., Clementson, L. A., Robinson, C., Schoemann, V., Watson, R. J. and Doblin, M. A.: Iron associated with exopolymeric substances is highly bioavailable to oceanic phytoplankton, Marine Chemistry, 173, 136–147, doi:10.1016/j.marchem.2014.10.002, 2015.

Heller, M. I., Wuttig, K. and Croot, P. L.: Identifying the Sources and Sinks of CDOM/FDOM across the Mauritanian Shelf and Their Potential Role in the Decomposition of Superoxide (O_2^-), Frontiers in Marine Science, 3(August), 132, 2016.

Helms, J. R., Mao, J., Chen, H., Perdue, E. M., Green, N. W., Hatcher, P. G., Mopper, K. and Stubbins, A.: Spectroscopic characterization of oceanic dissolved organic matter isolated by reverse osmosis coupled with electrodialysis, Marine Chemistry, 177, 278–287, doi:10.1016/j.marchem.2015.07.007, 2015.

Herrero-Martínez, J. M., Sanmartin, M., Rosés, M., Bosch, E. and Ràfols, C.: Determination of dissociation constants of flavonoids by capillary electrophoresis. Electrophoresis 26, 1886–1895. doi:10.1002/elps.200410258. 2005.

Hider, R. C. and Kong, X.: Chemistry and biology of siderophores. Nat. Prod. Rep. 27, 637–657. doi:10.1039/B906679A, 2010.

Hiscock, M. R., Lance, V. P., Apprill, A. M., Bidigare, R. R., Johnson, Z. I., Mitchell, B. G., Smith, W. O. and Barber, R. T.: Photosynthetic maximum quantum yield increases are an essential component of the Southern Ocean phytoplankton response to iron., Proceedings of the National Academy of Sciences of the United States of America, 105(12), 4775–4780, doi:10.1073/pnas.0705006105, 2008.

Hoegh-Guldberg, O. and Bruno, J. F.: The Impact of Climate Change on the World's Marine Ecosystems, Science, 328(5985), 1523–1528, doi:10.1126/science.1189930, 2010.

Hoffmann, L. J., Breitbarth, E., Boyd, P. W. and Hunter, K. a.: Influence of ocean warming and acidification on trace metal biogeochemistry, Marine Ecology Progress Series, 470, 191–205, doi:10.3354/meps10082, 2012.

Hofmann, G. E., Smith, J. E., Johnson, K. S., et al.: High-Frequency Dynamics of Ocean pH: A Multi-Ecosystem Comparison. PLoS One 6:e28983. doi: 10.1371/journal.pone.0028983, 2011.

Hofmann, M. and Schellnhuber, H.-J.: Oceanic acidification affects marine carbon pump and triggers extended marine oxygen holes, Proceedings of the National Academy of Sciences, 106(9), 3017–3022, doi:10.1073/pnas.0813384106, 2009.

Hong, H. and Kester, D. R.: Redox state of iron in the offshore waters of Peru, Limnology and Oceanography, 31(3), 512–524, do Honjo, S., Eglinton, T. ., Taylor, C. ., Ulmer, K. M., Sievert, S. ., Bracher, A., German, C. ., Edgcomb, V., Francois, R., Iglesias-Rodriguez, M. ., Van Mooy, B. and Repeta, D. .: Understanding the role of the biological pump in the global carbon cycle. An imperative for Ocean Science, Oceanography, 27(3), 10–16, 2014.

Hoppe, C. J. M., Hassler, C. S., Payne, C. D., Tortell, P. D., Rost, B. R. and Trimborn, S.: Iron limitation modulates ocean acidification effects on Southern Ocean phytoplankton communities, PLoS ONE, 8(11), doi:10.1371/journal.pone.0079890, 2013.

Hu, C., Muller-Karger, F. E. and Swarzenski, P. W.: Hurricanes, submarine groundwater discharge, and Florida's red tides. Geophys Res Lett 33:L11601. doi: 10.1029/2005GL025449. 2006.

Huang, J. J.-H., Xu, W.-W., Lin, S.-L. and Cheung, P. C.-K.: Phytochemical profiles of marine phytoplanktons: an evaluation of their in vitro antioxidant and anti-proliferative activities, Food Funct., 7(12), 5002–5017, doi:10.1039/C6FO01033D, 2016.

Hung, C. C., Tang, D., Warnken, K. W. and Santschi, P. H.: Distributions of carbohydrates, including uronic acids, in estuarine waters of Galveston Bay, Marine Chemistry, 73(3–4), 305–318, doi:10.1016/S0304-4203(00)00114-6, 2001.

Hung, C.-C., Guo, L., Santschi, P. H., Alvarado-Quiroz, N. and Haye, J. M.: Distributions of carbohydrate species in the Gulf of Mexico, Marine Chemistry, 81(3–4), 119–135, doi:10.1016/S0304-4203(03)00012-4, 2003.

Hunt, D. E., Lin, Y., Church, M. J., Karl, D. M., Tringe, S. G., Izzo, L. K. and Johnson, Z. I.: Relationship between abundance and specific activity of bacterioplankton in open ocean surface waters. Applied and Environmental Microbiology 79, 177–184. doi:10.1128/AEM.02155-12. 2013

Hutchins, D. A. and Boyd, P. W.: Marine phytoplankton and the changing ocean iron cycle, Nature Clim. Change, 6(12), 1072–1079, 2016.

Hutchins, D. A., Witter, A. E., Butler, A. and Luther, G. W.: Competition among marine phytoplankton for different chelated iron species, Nature, 400(6747), 858–861, doi:Doi 10.1038/23680, 1999.

Hutchins, D. A., Hare, C. E., Weaver, R. S., Zhang, Y., Firme, G. F., DiTullio, G. R., Alm, M. B., Riseman, S. F., Maucher, J. M., Geesey, M. E., Trick, C. G., Smith, G. J., Rue, E. L., Conn, J. and Bruland, K. W.: Phytoplankton iron limitation in the Humboldt Current and Peru Upwelling, Limnology and Oceanography, 47(4), 997–1011, doi:10.4319/lo.2002.47.4.0997, 2002.

Ibisanmi, E., Sander, S. G., Boyd, P. W., Bowie, A. R. and Hunter, K. A.: Vertical distributions of iron-(III) complexing ligands in the Southern Ocean. Deep Sea Research Part II: Topical Studies in Oceanography 58, 2113–2125. doi:10.1016/j.dsr2.2011.05.028. 2011.

Iglesias-Rodriguez, M. D., Brown, C. W., Doney, S. C., Kleypas, J. A., Kolber, D., Kolber, Z., Hayes, P. K., Falkowski, P. G.: Representing key phytoplankton functional groups in ocean carbon cycle models: Coccolithophorids. Global Biogeochemical Cycles 16, 47-1-47–20. doi:10.1029/2001GB001454. 2002.

Iglesias-Rodriguez, M. D., Halloran, P. R., Rickaby, R. E. M., Hall, I. R., Colmenero-Hidalgo, E., Gittins, J. R., Green, D. R. H., Tyrrell, T., Gibbs, S. J., von Dassow, P., Rehm, E., Armbrust, E. V. and Boessenkool, K. P.: Phytoplankton Calcification in a High-CO_2 World, Science, 320(5874), 336–340, doi:10.1126/science.1154122, 2008.

IPCC: Climate Change 2014: Synthesis Report. Contribution of Working Groups I, II and III to the Fifth Assessment Report of the Intergovernmental Panel on Climate Change, edited by R.K. Pachauri and L.A. Meyer, p. 151 pp, IPCC, Geneva, Switzerland., 2014.

Ito, Y. and Butler, A.: Structure of synechobactins, new siderophores of the marine cyanobacterium *Synechococcus* sp. PCC 7002. Limnology and Oceanography 50, 1918–1923. doi:10.4319/lo.2005.50.6.1918, 2005.

Jiang, H.-B., Lou, W.-J., Ke, W.-T., Song, W.-Y., Price, N. M. and Qiu, B.-S.: New insights into iron acquisition by cyanobacteria: an essential role for ExbB-ExbD complex in inorganic iron uptake. The ISME journal 9, 1–13. doi:10.1038/ismej.2014.123, 2014.

Jiang, J. and Kappler, A.: Kinetics of Microbial and Chemical Reduction of Humic Substances : Implications for Electron Shuttling. Environmental Science & Technology 42, 3563–3569. doi:10.1021/es7023803. 2008.

Jiang, M., Barbeau, K. A., Selph, K. E., Measures, C. I., Buck, K. N., Azam, F., Greg Mitchell, B. and Zhou, M.: The role of organic ligands in iron cycling and primary productivity in the Antarctic Peninsula: A modeling study. Deep Sea Research Part II: Topical Studies in Oceanography 90, 112–133. doi:10.1016/j.dsr2.2013.01.029. 2013.

Jickells, T. D.: Global Iron Connections Between Desert Dust, Ocean Biogeochemistry, and Climate, Science, 308(5718), 67–71, doi:10.1126/science.1105959, 2005.

Jin, P., Wang, T., Liu, N., Dupont, S., Beardall, J., Boyd, P. W., Riebesell, U. and Gao, K.: Ocean acidification increases the accumulation of toxic phenolic compounds across trophic levels., Nature communications, 6, 8714, doi:10.1038/ncomms9714, 2015.

De Jong, J. T. M., Den Das, J., Bathmann, U., Stoll, M. H. C., Kattner, G., Nolting, R. F. and De Baar, H. J. W.: Dissolved iron at subnanomolar levels in the Southern Ocean as determined by ship-board analysis, Analytica Chimica Acta, 377(2–3), 113–124, doi:10.1016/S0003-2670(98)00427-9, 1998.

Jørgensen, L., Lechtenfeld, O. J., Benner, R., Middelboe, M. and Stedmon, C. A.: Production and transformation of dissolved neutral sugars and amino acids by bacteria in seawater, Biogeosciences, 11(19), 5349–5363, doi:10.5194/bg-11-5349-2014, 2014.

Kaiser, K. and Benner, R.: Biochemical composition and size distribution of organic matter at the Pacific and Atlantic time-series stations, Marine Chemistry, 113(1–2), 63–77, doi:10.1016/j.marchem.2008.12.004, 2009.

Khodse, V. B., Fernandes, L., Gopalkrishna, V. V., Bhosle, N. B., Fernandes, V., Matondkar, S. G. P. and Bhushan, R.: Distribution and seasonal variation of concentrations of particulate carbohydrates and uronic acids in the northern Indian Ocean, Marine Chemistry, 103(3–4), 327–346, doi:10.1016/j.marchem.2006.10.003, 2007.

Khodse, V. B., Bhosle, N. B. and Matondkar, S. G. P.: Distribution of dissolved carbohydrates and uronic acids in a tropical estuary, India, Journal of Earth System Science, 119(4), 519–530, doi:10.1007/s12040-010-0029-2, 2010.

Kieber, D. J., Miller, G. W., Neale, P. J. and Mopper, K.: Wavelength and temperature-dependent apparent quantum yields for photochemical formation of hydrogen peroxide in seawater. Environ Sci Process Impacts 16:777–791. doi: 10.1039/C4EM00036F, 2014.

Kieber, R. J., Skrabal, S. a., Smith, B. J. and Willey, J. D.: Organic complexation of Fe(II) and its impact on the redox cycling of iron in rain, Environmental Science and Technology, 39(6), 1576–1583, doi:10.1021/es040439h, 2005.

Kim, J. M., Lee, K., Shin, K., Yang, E. J., Engel, A., Karl, D. M. and Kim, H. C.: Shifts in biogenic carbon flow from particulate to dissolved forms under high carbon dioxide and warm ocean conditions, Geophysical Research Letters, 38(8), doi:10.1029/2011GL047346, 2011.

Klapper, L., McKnight, D. M., Fulton, J. R., Blunt-Harris, E. L., Nevin, K. P., Lovley, D. R. and Hatcher, P. G.: Fulvic Acid Oxidation State Detection Using Fluorescence Spectroscopy, Environmental Science & Technology, 36(14), 3170–3175, doi:10.1021/es0109702, 2002.

King, W. D., Aldrich, R. A. and Charnecki, S.E.: Photochemical redox cycling of iron in NaCl solutions. Marine Chemistry 44, 105–120. doi:http://dx.doi.org/10.1016/0304-4203(93)90196-U. 1993.

King, D. W.: Role of Carbonate Speciation on the Oxidation Rate of Fe(II) in Aquatic Systems, Environmental Science & Technology, 32(19), 2997–3003, 1998.

King, D. W. and Farlow, R.: Role of carbonate speciation on the oxidation of Fe(II) by H_2O_2, Marine Chemistry, 70, 201–209, 2000.

King, D. W., Aldrich, R. A. and Charnecki, S. E.: Photochemical redox cycling of iron in NaCl solutions, Marine Chemistry, 44(2), 105–120, doi:http://dx.doi.org/10.1016/0304-4203(93)90196-U, 1993.

King, D. W., Lounsbury, H. A. and Millero, F. J.: Rates and Mechanism of Fe(II) Oxidation at Nanomolar Total Iron Concentrations, Environmental Science & Technology, 29(3), 818–824, doi:10.1021/es00003a033, 1995.

Kitayama, S., Kuma, K., Manabe, E., Sugie, K., Takata, H., Isoda, Y., Toya, K., Saitoh, S. I., Takagi, S., Kamei, Y. and Sakaoka, K.: Controls on iron distributions in the deep water column of the North Pacific Ocean: Iron(III) hydroxide solubility and marine humic-type dissolved organic matter, Journal of Geophysical Research: Oceans, 114(8), 1–13, doi:10.1029/2008JC004754., 2009.

Kleypas, J. A.: Geochemical Consequences of Increased Atmospheric Carbon Dioxide on Coral Reefs, Science, 284(5411), 118–120, doi:10.1126/science.284.5411.118, 1999.

Kohn, R. and Kovác, P.: Dissociation constants of D-galacturonic and D-glucuronic acid and their O-methyl derivatives. Chem. Zvesti 32, 478–485, 1978.

Koppenol, W. H., Stanbury, D. M. and Bounds, P.L.: Electrode potentials of partially reduced oxygen species, from dioxygen to water. Free Radical Biology and Medicine 49, 317–322. doi:10.1016/j.freeradbiomed.2010.04.011. 2010.

Kpper, F. C., Carrano, C. J., Kuhn, J. U. and Butler, A.: Photoreactivity of iron(III)-aerobactin: Photoproduct structure and iron(III) coordination. Inorganic Chemistry 45, 6028–6033. doi:10.1021/ic0604967. 2006.

Kranzler, C., Lis, H., Finkel, O. M., Schmetterer, G., Shaked, Y. and Keren, N.: Coordinated transporter activity shapes high-affinity iron acquisition in cyanobacteria., The ISME journal, 8(2), 409–17, doi:10.1038/ismej.2013.161, 2014.

Krishnamurthy, A., Moore, J. K., Mahowald, N., Luo, C., Doney, S. C., Lindsay, K. and Zender, C. S.: Impacts of increasing anthropogenic soluble iron and nitrogen deposition on ocean biogeochemistry, Global Biogeochemical Cycles, 23(3), 1–15, doi:10.1029/2008GB003440, 2009.

Kritzberg, E. S., Villanueva, A. B., Jung, M. and Reader, H. E.: Importance of boreal rivers in providing iron to marine waters, PLoS ONE, 9(9), doi:10.1371/journal.pone.0107500, 2014.

Kucuksezgin, F., Kontas, A., Altay, O., et al.: Assessment of marine pollution in Izmir Bay: Nutrient, heavy metal and total hydrocarbon concentrations. Environ Int 32:41–51. doi: 10.1016/j.envint.2005.04.007, 2006.

Kuma, K., Nakabayashi, S. and Matsunaga, K.: Photoreduction of Fe(III) by hydroxycarboxylic acids in seawater, Water Research, 29(6), 1559–1569, doi:10.1016/0043-1354(94)00289-J, 1995.

Kuma, K., Nishioka, J. and Matsunaga, K.: Controls on iron(III) hydroxide solubility in seawater: The influence of pH and natural organic chelators, Limnology and Oceanography, 41(3), 396–407, doi:10.4319/lo.1996.41.3.0396, 1996.

Kuma K. Y. Suzuki, I. Kudo, and K. Matsunaga, S. N.: Photo-reduction of Fe (III) by dissolved organic substances and existence of Fe(II) in seawater during spring blooms, Marine Chemistry, 37, 15–27, doi:10.1016/0304-4203(92)90054-e, 1992.

Kustka, A. B., Jones, B. M., Hatta, M., Field, M. P., Milligan, A. J.: The influence of iron and siderophores on eukaryotic phytoplankton growth rates and community composition in the Ross Sea. Marine Chemistry 173, 195–207. doi:10.1016/j.marchem.2014.12.002, 2015.

Laglera, L. M., Battaglia, G., van den Berg, C. M. G.: Determination of humic substances in natural waters by cathodic stripping voltammetry of their complexes with iron. Analytica Chimica Acta 599, 58–66. doi:10.1016/j.aca.2007.07.059, 2007.

Laglera, L. M., Battaglia, G. and van den Berg, C. M. G.: Effect of humic substances on the iron speciation in natural waters by CLE/CSV, Marine Chemistry, 127(1–4), 134–143, doi:10.1016/j.marchem.2011.09.003, 2011.

Lam, P. J. and Bishop, J. K. B.: The continental margin is a key source of iron to the HNLC North Pacific Ocean, Geophysical Research Letters, 35(7), 1–5, doi:10.1029/2008GL033294, 2008.

Lam, P. J., Ohnemus, D. C. and Marcus, M. A.: The speciation of marine particulate iron adjacent to active and passive continental margins, Geochimica et Cosmochimica Acta, 80, 108–124, doi:https://doi.org/10.1016/j.gca.2011.11.044, 2012.

Lannuzel, D., Schoemann, V., de Jong, J., Chou, L., Delille, B., Becquevort, S. and Tison, J.-L.: Iron study during a time series in the western Weddell pack ice, Marine Chemistry, 108(1–2), 85–95, doi:https://doi.org/10.1016/j.marchem.2007.10.006, 2008.

Lannuzel, D., Bowie, A. R., Remenyi, T., Lam, P., Townsend, A., Ibisanmi, E., Butler, E., Wagener, T. and Schoemann, V.: Distributions of dissolved and particulate iron in the sub-Antarctic and Polar Frontal Southern Ocean (Australian sector), Deep Sea Research Part II: Topical Studies in Oceanography, 58(21–22), 2094–2112, doi:10.1016/j.dsr2.2011.05.027, 2011.

Laruelle, G. G., Roubeix, V., Sferratore, A. et al.: Anthropogenic perturbations of the silicon cycle at the global scale: Key role of the land-ocean transition. Global Biogeochem Cycles 23:n/a–n/a. doi: 10.1029/2008GB003267, 2009

Lee, Y-W., Kim, G., Lim, W-A. and Hwang, D-W.: A relationship between submarine groundwater borne nutrients traced by Ra isotopes and the intensity of dinoflagellate red-tides occurring in the southern sea of Korea. Limnology and Oceanography 55:1–10. doi: 10.4319/lo.2010.55.1.0001, 2010.

Li, H., Cheng, K., Wong, C., Fan, K., Chen, F. and Jiang, Y.: Evaluation of antioxidant capacity and total phenolic content of different fractions of selected microalgae. Food Chemistry 102, 771–776. doi:10.1016/j.foodchem.2006.06.022, 2007.

Liu, S., Juneau, P., Qiu, B., 2012. Effects of iron on the growth and minimal fluorescence yield of three marine *Synechococcus* strains (Cyanophyceae). Phycological Research 60, 61–69. doi:10.1111/j.1440-1835.2011.00636.x

Liu, S.W., Qiu, B.S., 2012. Different responses of photosynthesis and flow cytometric signals to iron limitation and nitrogen source in coastal and oceanic *Synechococcus* strains (Cyanophyceae). Marine Biology 159, 519–532. doi:10.1007/s00227-011-1832-2

Lidbury, I., Johnson, V., Hall-Spencer, J. M., Munn, C. B. and Cunliffe, M.: Community-level response of coastal microbial biofilms to ocean acidification in a natural carbon dioxide vent ecosystem, Marine Pollution Bulletin, 64(5), 1063–1066, doi:10.1016/j.marpolbul.2012.02.011, 2012.

Lis, H., Shaked, Y., Kranzler, C., Keren, N. and Morel, F. M. M.: Iron bioavailability to phytoplankton: an empirical approach, Isme Journal, 9(4), 1003–1013, doi:10.1038/ismej.2014.199, 2015.

Liu, S., Juneau, P. and Qiu, B.: Effects of iron on the growth and minimal fluorescence yield of three marine *Synechococcus* strains (Cyanophyceae). Phycological Research 60, 61–69. doi:10.1111/j.1440-1835.2011.00636.x, 2012.

Liu, S and Qiu, B: Different responses of photosynthesis and flow cytometric signals to iron limitation and nitrogen source in coastal and oceanic *Synechococcus* strains (Cyanophyceae). Marine Biology 159, 519–532. doi:10.1007/s00227-011-1832-2, 2012.

Liu, X. and Millero, F. J.: The solubility of iron in seawater, Marine Chemistry, 77(1), 43–54, doi:10.1016/S0304-4203(01)00074-3, 2002.

Laglera, L. M., Battaglia, G. and van den Berg, C. M. G.: Effect of humic substances on the iron speciation in natural waters by CLE/CSV, Marine Chemistry, 127(1–4), 134–143, doi:10.1016/j.marchem.2011.09.003, 2011.

Lancelot, C., de Montety, A., Goosse, H., Becquevort, S., Schoemann, V., Pasquer, B. and Vancoppenolle, M.: Spatial distribution of the iron supply to phytoplankton in the Southern Ocean: a model study, Biogeosciences, 6(3), 4919–4962, doi:10.5194/bgd-6-4919-2009, 2009.

Langer, G., Nehrke, G., Probert, I., Ly, J. and Ziveri, P.: Strain-specific responses of *Emiliania huxleyi* to changing seawater carbonate chemistry, Biogeosciences Discussions, 6(2), 4361–4383, doi:10.5194/bgd-6-4361-2009, 2009.

Leenheer, J. J. a. and Croué, J. J.-P.: Characterizing aquatic dissolved organic matter, Environmental Science & Technology, 37(1), 18A–26A, doi:10.1021/es032333c, 2003.

Legendre, L., Rivkin, R. B., Weinbauer, M. G., Guidi, L. and Uitz, J.: The microbial carbon pump concept: Potential biogeochemical significance in the globally changing ocean, Progress in Oceanography, 134, 432–450, 2015.

Li, F., Pan, B., Zhang, D., Yang, X., Li, H., Liao, S., Ghaffar, A., Peng, H. and Xing, B.: Organic matter source and degradation as revealed by molecular biomarkers in agricultural soils of Yuanyang terrace., Scientific reports, 5(April), 11074, doi:10.1038/srep11074, 2015.

Lidbury, I., Johnson, V., Hall-Spencer, J. M., Munn, C. B. and Cunliffe, M.: Community-level response of coastal microbial biofilms to ocean acidification in a natural carbon dioxide vent ecosystem, Marine Pollution Bulletin, 64(5), 1063–1066, 2012.

Lohbeck, K. T., Riebesell, U. and Reusch, T. B. H.: Adaptive evolution of a key phytoplankton species to ocean acidification, Nature Geoscience, 5(5), 346–351, doi:10.1038/ngeo1441, 2012.

López, A., Rico, M., Santana-Casiano, J. M., González, A. G. and González-Dávila, M.: Phenolic profile of Dunaliella tertiolecta growing under high levels of copper and iron, Environmental Science and Pollution Research, 22(19), 14820–14828, doi:10.1007/s11356-015-4717-y, 2015.

López-Alarcón, C. and Denicola, A.: Evaluating the antioxidant capacity of natural products: A review on chemical and cellular-based assays, Analytica Chimica Acta, 763, 1–10, doi:10.1016/j.aca.2012.11.051, 2013.

Lu, C.-J., Benner, R., Fichot, C. G., Fukuda, H., Yamashita, Y. and Ogawa, H.: Sources and Transformations of Dissolved Lignin Phenols and Chromophoric Dissolved Organic Matter in Otsuchi Bay, Japan, Frontiers in Marine Science, 3(June), 1–12, 2016.

MacGilchrist, G. A., Shi, T., Tyrrell, T., Richier, S., Moore, C. M., Dumousseaud, C. and Achterberg, E. P.: Effect of enhanced pCO_2 levels on the production of dissolved organic carbon and transparent exopolymer particles in short-term bioassay experiments, Biogeosciences, 11(13), 3695–3706, doi:10.5194/bg-11-3695-2014, 2014.

Mahmood, A., Abualhaija, M. M., van den Berg, C. M. G. and Sander, S. G.: Organic speciation of dissolved iron in estuarine and coastal waters at multiple analytical windows, Marine Chemistry, 177, Part 5, 706–719, 2015.

Maier, G., Glegg, G. A., Tappin, A. D. and Worsfold, P. J.: The use of monitoring data for identifying factors influencing phytoplankton bloom dynamics in the eutrophic Taw Estuary, SW England. Marine Pollution Bulletin 58:1007–1015, 2009.

Maldonado, M. T. and Price, N. M.: Reduction and transport of organically bound iron by *Thalassiosira oceanica* (Bacillariophyceae), Journal of Phycology, 37(2), 298–309, doi:10.1046/j.1529-8817.2001.037002298.x, 2001.

Maldonado, M. T., Strzepek, R. F., Sander, S. and Boyd, P. W.: Acquisition of iron bound to strong organic complexes, with different Fe binding groups and photochemical reactivities, by plankton communities in Fe-limited subantarctic waters, Global Biogeochemical Cycles, 19(4), doi:10.1029/2005GB002481, 2005.

Manwar, A. V, Khandelwal, S. R., Chaudhari, B. L., Meyer, J. M. and Chincholkar, S. B.: Siderophore production by a marine Pseudomonas aeruginosa and its antagonistic action against phytopathogenic fungi, Applied Biochemistry and Biotechnology, 118(1), 243–251, doi:10.1385/ABAB:118:1-3:243, 2004.

Mao, Y., Pham, A. N., Rose, A. L. and Waite, T. D.: Influence of phosphate on the oxidation kinetics of nanomolar Fe(II) in aqueous solution at circumneutral pH. Geochim Cosmochim Acta 75:4601–4610. doi: 10.1016/j.gca.2011.05.031, 2011.

Marchetti, A., Schruth, D. M., Durkin, C. A., Parker, M. S., Kodner, R. B., Berthiaume, C. T., Morales, R., Allen, A. E., Armbrust, E. V.: Comparative metatranscriptomics identifies molecular bases for the physiological responses of phytoplankton to varying iron availability. Proceedings of the National Academy of Sciences 109, E317–E325. doi:10.1073/pnas.1118408109. 2012.

Marcus, R.A.: On the Theory of Oxidation-Reduction Reactions Involving Electron Transfer. I. The Journal of Chemical Physics 24, 966. doi:10.1063/1.1742723. 1956.

Martin, H., Gordon, R. M. and Fitzwater, S. E.: Iron limitation?, Limnology and Oceanography, 36(8), 1793–1802, 1991.

Martin, J. H.: Glacial-interglacial CO_2 change: The Iron Hypothesis, Paleoceanography, 5(1), 1–13, doi:10.1029/PA005i001p00001, 1990.

Martin, J. H. and Fitzwater, S. E.: Iron deficiency limits phytoplankton growth in the north-east Pacific subarctic, Nature, 331(6154), 341–343 [online] Available from: http://dx.doi.org/10.1038/331341a0, 1988.

Martin, J. H. and Michael Gordon, R.: Northeast Pacific iron distributions in relation to phytoplankton productivity, Deep Sea Research Part A. Oceanographic Research Papers, 35(2), 177–196, doi:http://dx.doi.org/10.1016/0198-0149(88)90035-0, 1988.

Martin, J. H., Gordon, R. M., Fitzwater, S. and Broenkow, W. W.: Vertex: phytoplankton/iron studies in the Gulf of Alaska, Deep Sea Research Part A. Oceanographic Research Papers, 36(5), 649–680, doi:http://dx.doi.org/10.1016/0198-0149(89)90144-1, 1989.

Mawji, E., Gledhill, M., Milton, J. A, Tarran, G. A, Ussher, S. and Thompson, A.: Hydroxamate siderophores: Ocurrence and importance in the Atlantic Ocean. Environmental Science & Technology 42, 8675–8680. 2008.

Meehl, G. A., Arblaster, J. M. and Tebaldi, C.: Understanding future patterns of increased precipitation intensity in climate model simulations, Geophysical Research Letters, 32(18), 1–4, doi:10.1029/2005GL023680, 2005.

Meiburg, E. and Kneller, B.: Turbidity Currents and Their Deposits, Annual Review of Fluid Mechanics, 42(1), 135–156, doi:10.1146/annurev-fluid-121108-145618, 2010.

Mendes, P.: Biochemistry by numbers: Simulation of biochemical pathways with Gepasi 3. Trends Biochem Sci 22:361–363. doi: 10.1016/S0968-0004(97)01103-1, 1997.

Meon, B. and Kirchman, D. L.: Dynamics and molecular composition of dissolved organic material during experimental phytoplankton blooms. Marine Chemistry 75, 185–199. doi:10.1016/S0304-4203(01)00036-6, 2001.

Meyer, J. and Riebesell, U.: Reviews and syntheses: Responses of coccolithophores to ocean acidification: A meta-analysis, Biogeosciences, 12(6), 1671–1682, doi:10.5194/bg-12-1671-2015, 2015.

Miller, C. J., Vincent Lee, S. M., Rose, A. L. and Waite, T. D.: Impact of Natural Organic Matter on H_2O_2-Mediated Oxidation of Fe(II) in Coastal Seawaters., Environmental science & technology, 46(20), 11078–85, doi:10.1021/es3022792, 2012.

Miller, W. L., King, D. W., Lin, J. and Kester, D. R.: Photochemical redox cycling of iron in coastal seawater, Marine Chemistry, 50(1–4), 63–77, doi:10.1016/0304-4203(95)00027-O, 1995.

Millero, F. J.: The pH of estuarine waters. Limnol Oceanogr 31:839–847. doi: 10.4319/lo.1986.31.4.0839, 1986.

Millero, F. J.: Estimate of the life time of superoxide in seawater. Geochim Cosmochim Acta 51:351–353. doi: 10.1016/0016-7037(87)90246-8, 1987.

Millero, F. J., Woosley, R., Ditrolio, B. and Waters, J.: Effect of Ocean Acidification on the Speciation of Metals in Seawater, Oceanography, 22(4), 72–85, 2009.

Millero, F. and Pierrot, D.: A chemical equilibrium model for natural waters. Aquat Geochemistry 4:153–199. doi: 10.1023/A:1009656023546, 1998.

Millero, F. J. and Sotolongo, S.: The oxidation of Fe(II) with H_2O_2 in seawater, Geochimica et Cosmochimica Acta, 53(8), 1867–1873, doi:http://dx.doi.org/10.1016/0016-7037(89)90307-4, 1989.

Millero, F. J., Sotolongo, S. and Izaguirre, M.: The oxidation kinetics of Fe(II) in seawater, Geochimica et Cosmochimica Acta, 51(4), 793–801, doi:10.1016/0016-7037(87)90093-7, 1987.

Moore, J. K., Doney, S. C. and Lindsay, K.: Upper ocean ecosystem dynamics and iron cycling in a global three-dimensional model, Global Biogeochemical Cycles, 18(4), 1–21, doi:10.1029/2004GB002220, 2004.

Moore, W. S.: The Effect of Submarine Groundwater Discharge on the Ocean. Ann Rev Mar Sci 2:59–88. doi: 10.1146/annurev-marine-120308-081019, 2010.

Mopper, K., Kieber, D. J. and Stubbins, A.: Chapter 8 - Marine Photochemistry of Organic Matter: Processes and Impacts, in Biogeochemistry of Marine Dissolved Organic Matter (Second Edition), edited by D. A. Hansell and C. A. Carlson, pp. 389–450, Academic Press, Boston., 2015.

Morán, X. A. G. and Estrada, M.: Short-term variability of photosynthetic parameters and particulate and dissolved primary production in the Alboran sea (SW Mediterranean), Marine Ecology Progress Series, 212, 53–67, doi:10.3354/meps212053, 2001.

Moran, M. A., Kujawinski, E. B., Stubbins, A., Fatland, R., Aluwihare, L. I., Buchan, A., Crump, B. C., Dorrestein, P. C., Dyhrman, S. T., Hess, N. J., Howe, B. et al.: Deciphering ocean carbon in a changing world. Proceedings of the National Academy of Sciences 113, 3143–3151. doi:10.1073/pnas.1514645113, 2016.

Morel, F. M. M. and Price, N. M.: The biogeochemical cycles of trace metals in the oceans, Science, 300(5621), 944–947, doi:10.1126/science.1083545, 2003.

Morel, F. M. M., Kustka, A. B. and Shaked, Y.: The role of unchelated Fe in the iron nutrition of phytoplankton, Limnology and Oceanography, 53(1), 400–404, doi:10.4319/lo.2008.53.1.0400, 2008.

Morrissey, J. and Bowler, C.: Iron utilization in marine cyanobacteria and eukaryotic algae, Frontiers in Microbiology, 3(MAR), 1–13, doi:10.3389/fmicb.2012.00043, 2012.

Mueller, B., den Haan, J., Visser, P. M., Vermeij, M. J. A. and van Duyl, F. C.: Effect of light and nutrient availability on the release of dissolved organic carbon (DOC) by Caribbean turf algae., Scientific reports, 6(September 2015), 23248, doi:10.1038/srep23248, 2016.

Muggli, D. L. and Harrison, P. J.: Effects of nitrogen source on the physiology and metal nutrition of *Emiliania huxleyi* grown under different iron and light conditions. Marine ecology Progress Series, 130, 255–267, doi:10.3354/meps130255, 1996.

Müller, M., Antia, A. and LaRoche, J.: Influence of cell cycle phase on calcification in the coccolithophore *Emiliania huxleyi*, Limnology and Oceanography, 53(2), 506–512, doi:10.4319/lo.2008.53.2.0506, 2008.

Müller, M. N., Schulz, K. G. and Riebesell, U.: Effects of long-term high CO_2 exposure on two species of coccolithophores, Biogeosciences Discussions, 6(6), 10963–10982, doi:10.5194/bgd-6-10963-2009, 2010.

Nelson, C. E., Goldberg, S. J., Wegley Kelly, L., Haas, A. F., Smith, J. E., Rohwer, F. and Carlson, C. a: Coral and macroalgal exudates vary in neutral sugar composition and differentially enrich reef bacterioplankton lineages., The ISME journal, 7(5), 962–79, doi:10.1038/ismej.2012.161, 2013.

Newton, A. and Mudge S. M.: Lagoon-sea exchanges, nutrient dynamics and water quality management of the Ria Formosa (Portugal). Estuar Coast Shelf Sci 62:405–414. doi: 10.1016/j.ecss.2004.09.005, 2005.

Nichols, C. M., Lardiere, S. G., Bowman, J. P., Nichols, P. D., A E Gibson, J. and Guezennec, J.: Chemical characterization of exopolysaccharides from Antarctic marine bacteria., 2005a.

Nichols, C. M., Bowman, J. P. and Guezennec, J.: Effects of ncubation temperature on growth and production of exopolysaccharides by an Antarctic Sea ice bacterium grown in batch culture, Applied and environmental microbiology, 71(7), 3519–3523, doi:10.1128/AEM.71.7.3519, 2005b.

Nielsdóttir, M. C., Moore, C. M., Sanders, R., Hinz, D. J. and Achterberg, E. P.: Iron limitation of the postbloom phytoplankton communities in the Iceland Basin, Global Biogeochemical Cycles, 23(3), 1–13, doi:10.1029/2008GB003410, 2009.

Nishioka, J. and Obata, H.: Dissolved iron distribution in the western and central subarctic Pacific: HNLC water formation and biogeochemical processes, Limnology and Oceanography, n/a--n/a, doi:10.1002/lno.10548, 2017.

Norman, L., Worms, I. A. M., Angles, E., Bowie, A. R., Nichols, C. M., Ninh Pham, A., Slaveykova, V. I., Townsend, A. T., David Waite, T. and Hassler, C. S.: The role of bacterial and algal exopolymeric substances in iron chemistry, Marine Chemistry, 173, 148–161, doi:10.1016/j.marchem.2015.03.015, 2015.

Obernosterer, I. and Herndl, G. J.: Phytoplankton extracellular release and bacterial growth: Dependence on the inorganic N:P ratio, Marine Ecology Progress Series, 116(1–3), 247–258, doi:10.3354/meps116247, 1995.

Van Oijen, T., Van Leeuwe, M. A., Granum, E., Weissing, F. J., Bellerby, R. G. J., Gieskes, W. W. C. and De Baar, H. J. W.: Light rather than iron controls photosynthate production and allocation in Southern Ocean phytoplankton populations during austral autumn, Journal of Plankton Research, 26(8), 885–900, doi:10.1093/plankt/fbh088, 2004.

Van Oijen, T., Veldhuis, M. J. W., Gorbunov, M. Y., Nishioka, J., Van Leeuwe, M. A. and De Baar, H. J. W.: Enhanced carbohydrate production by Southern Ocean phytoplankton in response to in situ iron fertilization, Marine Chemistry, 93(1), 33–52, doi:10.1016/j.marchem.2004.06.039, 2005.

Van Oostende, N., Moerdijk-Poortvliet, T. C. W., Boschker, H. T. S., Vyverman, W. and Sabbe, K.: Release of dissolved carbohydrates by *Emiliania huxleyi* and formation of transparent exopolymer particles depend on algal life cycle and bacterial activity, Environmental Microbiology, 15(5), 1514–1531, doi:10.1111/j.1462-2920.2012.02873.x, 2013.

O'Sullivan, D. W., Hanson, A. K., Miller, W. L. and Kester, D. R.: Measurement of Fe(II) in surface water of the equatorial Pacific, Limnology and Oceanography, 36(8), 1727–1741, 1991.

Orr, J. C., Fabry, V. J., Aumont, O., Bopp, L., Doney, S. C., Feely, R. A., Gnanadesikan, A., Gruber, N., Ishida, A., Joos, F., Key, R. M., Lindsay, K., Maier-Reimer, E., Matear, R., Monfray, P., Mouchet, A., Najjar, R. G., Plattner, G.-K., Rodgers, K. B., Sabine, C. L., Sarmiento, J. L., Schlitzer, R., Slater, R. D., Totterdell, I. J., Weirig, M.-F., Yamanaka, Y. and Yool, A.: Anthropogenic ocean acidification over the twenty-first century and its impact on calcifying organisms, Nature, 437(7059), 681–686 [online] Available from: http://dx.doi.org/10.1038/nature04095, 2005.

Öztürk, M., Bizsel, N. and Steinnes, E.: Iron speciation in eutrophic and oligotrophic Mediterranean coastal waters; impact of phytoplankton and protozoan blooms on iron distribution. Mar Chem 81:19–36. doi: 10.1016/S0304-4203(02)00137-8, 2003.

Ozturk, S., Aslim, B., Suludere, Z. and Tan, S.: Metal removal of cyanobacterial exopolysaccharides by uronic acid content and monosaccharide composition, Carbohydrate Polymers, 101(1), 265–271, doi:10.1016/j.carbpol.2013.09.040, 2014.

Paerl, H. W. and Paul, V. J.: Climate change: links to global expansion of harmful cyanobacteria. Water Res 46:1349–63. doi: 10.1016/j.watres.2011.08.002. 2012.

Passow, U.: Transparent Exopolymer Particles in Aquatic Environments, Progress in Oceanography, 55(3–4), 287–333, doi:10.1016/S0079-6611(02)00138-6, 2002.

Paul, A. J., Bach, L. T., Schulz, K. G., Boxhammer, T., Czerny, J., Achterberg, E. P., Hellemann, D., Trense, Y., Nausch, M., Sswat, M. and Riebesell, U.: Effect of elevated CO_2 on organic matter pools and fluxes in a summer Baltic Sea plankton community, Biogeosciences, 12(20), 6181–6203, doi:10.5194/bg-12-6181-2015, 2015.

Paytan, A. and McLaughlin, K.: The oceanic phosphorus cycle. Chem Rev 107:563–576. doi: 10.1021/cr0503613, 2007.

Payne, S. M.: Bacterial Pathogenesis Part A: Identification and Regulation of Virulence Factors, Methods in Enzymology, Methods in Enzymology. Elsevier. doi:10.1016/0076-6879(94)35151-1, 1994.

Pereira, M., Tala, F., Fernández, M. and Subida, M. D.: Effects of kelp phenolic compounds on the feeding-associated mobility of the herbivore snail *Tegula tridentata*. Marine Environmental Research 112, Part, 40–47, 2015.

Pereira, S., Zille, A., Micheletti, E., Moradas-Ferreira, P., De Philippis, R. and Tamagnini, P.: Complexity of cyanobacterial exopolysaccharides: Composition, structures, inducing factors and putative genes involved in their biosynthesis and assembly. FEMS Microbiology Reviews 33, 917–941. doi:10.1111/j.1574-6976.2009.00183.x. 2009.

Pérez, F. F., Mintrop, L., Llinás, O., et al.: Mixing analysis of nutrients, oxygen and inorganic carbon in the Canary Islands region. J Mar Syst 28:183–201, 2001.

Perron, N. R. and Brumaghim, J. L.: A review of the antioxidant mechanisms of polyphenol compounds related to iron binding. Cell Biochemistry and Biophysics 53, 75–100. doi:10.1007/s12013-009-9043-x. 2009.

Perron, N. R., Hodges, J. N., Jenkins, M. and Brumaghim, J. L.: Predicting how polyphenol antioxidants prevent DNA damage by binding to iron. Inorganic Chemistry 47, 6153–6161. doi:10.1021/ic7022727. 2008.

Perron, N. R., Wang, H. C., Deguire, S. N., Jenkins, M., Lawson, M. and Brumaghim, J. L.: Kinetics of iron oxidation upon polyphenol binding. Dalton transactions (Cambridge, England : 2003) 39, 9982–9987. doi:10.1039/c0dt00752h. 2010.

Piontek, J., Lunau, M., Händel, N., Borchard, C., Wurst, M. and Engel, A.: Acidification increases microbial polysaccharide degradation in the ocean, Biogeosciences, 7(5), 1615–1624, doi:10.5194/bg-7-1615-2010, 2010.

Piontek, J., Borchard, C., Sperling, M., Schulz, K. G., Riebesell, U. and Engel, A.: Response of bacterioplankton activity in an Arctic fjord system to elevated pCO_2: Results from a mesocosm perturbation study, Biogeosciences, 10(1), 297–314, doi:10.5194/bg-10-297-2013, 2013.

Poorvin, L., Sander, S. G., Velasquez, I., Ibisanmi, E., LeCleir, G. R. and Wilhelm, S. W.: A comparison of Fe bioavailability and binding of a catecholate siderophore with virus-mediated lysates from the marine bacterium Vibrio alginolyticus PWH3a, Journal of Experimental Marine Biology and Ecology, 399(1), 43–47, doi:10.1016/j.jembe.2011.01.016, 2011.

Pullin, M. J. and Cabaniss, S. E.: The effects of pH, ionic strength, and iron–fulvic acid interactions on the kinetics of non-photochemical iron transformations. I. Iron(II) oxidation and iron(III) colloid formation. Geochimica et Cosmochimica Acta 67, 4067–4077. doi:10.1016/S0016-7037(03)00366-1. 2003.

Rabalais, N. N., Turner, R. E., Díaz, R. J. and Justić, D.: Global change and eutrophication of coastal waters. ICES J Mar Sci 66:1528–1537. doi: 10.1093/icesjms/fsp047, 2009.

Ragueneau, O., Schultes, S., Bidle, K., et al.: Si and C interactions in the world ocean: Importance of ecological processes and implications for the role of diatoms in the biological pump. Global Biogeochem Cycles 20:n/a–n/a. doi: 10.1029/2006GB002688, 2006.

Rahmstorf, S. and Ganopolski, A.: Long-term global warming scenarios computed with an efficient coupled climate model, Climatic Change, 43(2), 353–367, doi:10.1023/A:1005474526406, 1999.

Rajaneesh, K. M. and Mitbavkar, S.: Factors controlling the temporal and spatial variations in *Synechococcus* abundance in a monsoonal estuary. Marine Environmental Research 92, 133–143. doi:http://dx.doi.org/10.1016/j.marenvres.2013.09.010. 2013.

Raven, J., Caldeira, K., Elderfield, H., Hoegh-Guldberg, O., Liss, P., Riebesell, U., Shepherd, J., Turley, C. and Watson, A.: Ocean acidification due to increasing atmospheric carbon dioxide, The Royal Society, Policy doc(June), 60, doi:10.1080/02688690801911598, 2005.

Read, B. a, Kegel, J., Klute, M. J., Kuo, A., Lefebvre, S. C., Maumus, F., Mayer, C., Miller, J., Monier, A., Salamov, A., Young, J., Aguilar, M., Claverie, J.-M., Frickenhaus, S., Gonzalez, K., Herman, E. K., Lin, Y.-C., Napier, J., Ogata, H., Sarno, A. F., Shmutz, J., Schroeder, D., de Vargas, C., Verret, F., von Dassow, P., Valentin, K., Van de Peer, Y., Wheeler, G., Dacks, J. B., Delwiche, C. F., Dyhrman, S. T., Glöckner, G., John, U., Richards, T., Worden, A. Z., Zhang, X. and Grigoriev, I. V: Pan genome of the phytoplankton *Emiliania huxleyi* underpins its global distribution., Nature, 499(7457), 209–13, doi:10.1038/nature12221, 2013.

Reinfelder, J. R.: Carbon concentrating mechanisms in eukaryotic marine phytoplankton. Annual review of marine science 3, 291–315, 2011.

Riebesell, U. and Tortell, P. D.: Effects of Ocean Acidification on Pelagic Organism and Ecosystems, in Ocean Acidification, edited by J.-P. Gattuso and L. Hansson, pp. 99–121, Oxford, UK., 2011.

Riebesell, U., Fabry, V. J., Hansson, L. and Gattuso, J.-P.: Guide to Best Practices in Ocean Acidification Research and Data Reporting., 2010.

Riebesell, U., Schulz, K. G., Bellerby, R. G. J., Botros, M., Fritsche, P., Meyerhöfer, M., Neill, C., Nondal, G., Oschlies, A, Wohlers, J. and Zöllner, E.: Enhanced biological carbon consumption in a high CO_2 ocean. Nature 450, 545–548. 2007.

Riebesell, U., Zondervan, I., Rost, B., Tortell, P. D., Zeebe, R. E. and Morel, F. M. M.: Reduced calcification of marine plankton in response to increased atmospheric CO_2, Nature, 407(6802), 364–367 [online] Available from: http://dx.doi.org/10.1038/35030078, 2000.

Riegman, R., Stolte, W., Noordeloos, A. A. M. and Slezak, D.: Nutrient uptake and alkaline phosphatase (ec 3:1:3:1) activity of *Emiliania huxleyi* (*PRYMNESIOPHYCEAE*) during growth under n and p limitation in continuous cultures, Journal of Phycology, 36(1), 87–96, doi:10.1046/j.1529-8817.2000.99023.x, 2000.

Rijkenberg, M. J. A., Gerringa, L. J. A., Carolus, V. E., Velzeboer, I. and de Baar, H. J. W.: Enhancement and inhibition of iron photoreduction by individual ligands in open ocean seawater. Geochimica et Cosmochimica Acta 70, 2790–2805. doi:10.1016/j.gca.2006.03.004. 2006.

Rijkenberg, M. J. A., Gerringa, L. J. A., Timmermans, K. R., Fischer, A. C., Kroon, K. J., Buma, A. G. J., Wolterbeek, B. T. and de Baar, H. J. W.: Enhancement of the reactive iron pool by marine diatoms, Marine Chemistry, 109(1–2), 29–44, doi:10.1016/j.marchem.2007.12.001, 2008.

Rogelj, J., Meinshausen, M. and Knutti, R.: Global warming under old and new scenarios using IPCC climate sensitivity range estimates. Nat Clim Chang 2:248–253. doi: 10.1038/nclimate1385, 2012.

Rokitta, S. D. and Rost, B.: Effects of CO_2 and their modulation by light in the life-cycle stages of the coccolithophore *Emiliania huxleyi*, Limnology and Oceanography, 2012(57 (2)), 607–618, doi:10.4319/lo.2012.57.2.0607, 2012.

Rose, A. L.: The influence of extracellular superoxide on iron redox chemistry and bioavailability to aquatic microorganisms. Frontiers in microbiology, 3(April), 124, doi:10.3389/fmicb.2012.00124, 2012.

Rose, A. L. and Waite, T. D.: Kinetic model for Fe(II) oxidation in seawater in the absence and presence of natural organic matter., Environmental science & technology, 36(3), 433–44 [online] Available from: http://www.ncbi.nlm.nih.gov/pubmed/11871559, 2002.

Rose, A. L. and Waite, T. D.: Effect of dissolved natural organic matter on the kinetics of ferrous iron oxygenation in seawater., Environmental science & technology, 37(21), 4877–86 [online] Available from: http://www.ncbi.nlm.nih.gov/pubmed/14620813, 2003.

Rose, A.L. and Waite, T. D.: Reduction of organically complexed ferric iron by superoxide in simulated natural water. Environmental science & technology 39, 2645–50. 2005.

Rose, J. M., Feng, Y., Di Tullio, G. R., Dunbar, R. B., Hare, C. E., Lee, P. A., Lohan, M., Long, M., W. O. Smith Jr., Sohst, B., Tozzi, S., Zhang, Y. and Hutchins, D. A.: Synergistic effects of iron and temperature on Antarctic phytoplankton and microzooplankton assemblages, Biogeosciences, 6(12), 3131–3147, doi:10.5194/bg-6-3131-2009, 2009.

Rossi, F. and De Philippis, R.: Role of Cyanobacterial Exopolysaccharides in Phototrophic Biofilms and in Complex Microbial Mats. Life 5, 1218–1238, 2015.

Roy, E. G. and Wells, M. L.: Evidence for regulation of Fe(II) oxidation by organic complexing ligands in the Eastern Subarctic Pacific, Marine Chemistry, 127(1–4), 115–122, doi:10.1016/j.marchem.2011.08.006, 2011.

Roy, E. G., Wells, M. L. and King, D. W.: Persistence of iron(II) in surface waters of the western subarctic Pacific, Limnology and Oceanography, 53(1), 89–98, doi:10.4319/lo.2008.53.1.0089, 2008.

Rozan, T. F., Taillefert, M., Trouwborst, R. E., Glazer, B. T., Ma, S., Herszage, J., Valdes, L. M., Price, K. S. and Iii, G. W. L.: Iron-sulfur-phosphorus cycling in the sediments of a shallow coastal bay: Implications for sediment nutrient release and benthic macroalgal blooms, Limnology and Oceanography, 47(5), 1346–1354, doi:10.4319/lo.2002.47.5.1346, 2002.

Rue, E. L. and Bruland, K. W.: Complexation of iron(III) by natural organic ligands in the Central North Pacific as determined by a new competitive ligand equilibration/adsorptive cathodic stripping voltammetric method. Marine Chemistry 50, 117–138. doi:10.1016/0304-4203(95)00031-L. 1995.

Rue, E. L. and Bruland, K. W.: The role of organic complexation on ambient iron chemistry in the equatorial Pacific Ocean and the response of a mesoscale iron addition experiment. Limnology and Ocea Ruiz-Halpern, S., Duarte, C. M., Tovar-Sanchez, A., Pastor, M., Horstkotte, B., Lasternas, S. and Agusti, S.: Antarctic krill as a source of dissolved organic carbon to the Antarctic ecosystem, Limnology and Oceanography, 56(2), 521–528, doi:http://dx.doi.org/10.4319/lo.2011.56.2.0521, 2011.

Ryan-Keogh, T. J., Macey, A. I., Nielsdóttir, M. C., Lucas, M. I., Steigenberger, S. S., Stinchcombe, M. C., Achterberg, E. P., Bibby, T. S. and Mark Moore, C.: Spatial and temporal development of phytoplankton iron stress in relation to bloom dynamics in the high-latitude North Atlantic Ocean. Limnology and Oceanography 58, 533–545. doi:10.4319/lo.2013.58.2.0533. 2013.

Sabine, C. L., Feely, R. A., Gruber, N., Key, R. M., Lee, K., Bullister, J. L., Wanninkhof, R., Wong, C. S., Wallace, D. W. R., Tilbrook, B., Millero, F. J., Peng, T.-H., Kozyr, A., Ono, T. and Rios, A. F.: The oceanic sink for anthropogenic CO_2., Science (New York, N.Y.), 305(5682), 367–71, doi:10.1126/science.1097403, 2004.nography 42, 901–910. doi:10.4319/lo.1997.42.5.0901. 1997.

Salmon, T. P., Rose, A. L., Neilan, B. a. and Waite, T. D.: The FeL model of iron acquisition: Nondissociative reduction of ferric complexes in the marine environment, Limnology and Oceanography, 51(4), 1744–1754, doi:10.4319/lo.2006.51.4.1744, 2006

Samperio-Ramos, G., Santana Casiano, J. M. and González Dávila, M.: Effect of ocean warming and acidification on the Fe(II) oxidation rate in oligotrophic and eutrophic natural waters. Biogeochemistry 128, 19–34. doi:10.1007/s10533-016-0192-x. 2016.

Sandy, M. and Butler, A.: Microbial iron acquisition: Marine and terrestrial siderophores. Chemical Reviews 109, 4580–4595. doi:10.1021/cr9002787, 2009.

Santana-Casiano, J. M., González-Dávila, M., González, A. G., Millero, F. J.: Fe(III) Reduction in the Presence of Catechol in Seawater. Aquatic Geochemistry 16, 467–482. doi:10.1007/s10498-009-9088-x. 2010.

Santana-Casiano, J. M., González-Dávila, M., Rodríguez, M. J. and Millero, F. J.: The effect of organic compounds in the oxidation kinetics of Fe(II), Marine Chemistry, 70(1–3), 211–222, doi:10.1016/S0304-4203(00)00027-X, 2000.

Santana-Casiano, J. M., González-Dávila, M. and Millero, F. J.: Oxidation of nanomolar levels of Fe(II) with oxygen in natural waters., Environmental science & technology, 39(7), 2073–9 [online] Available from: http://www.ncbi.nlm.nih.gov/pubmed/15871239, 2005.

Santana-Casiano, J. M., González-Dávila, M. and Millero, F. J.: The role of Fe(II) species on the oxidation of Fe(II) in natural waters in the presence of O_2 and H_2O_2, Marine Chemistry, 99(1–4), 70–82, doi:10.1016/j.marchem.2005.03.010, 2006.

Santana-Casiano, J. M., González-Dávila, M., González, A. G. and Millero, F. J.: Fe(III) Reduction in the Presence of Catechol in Seawater, Aquatic Geochemistry, 16(3), 467–482, doi:10.1007/s10498-009-9088-x, 2010.

Santana-Casiano, J. M., González-Dávila, M., Fraile-Nuez, E., de Armas, D., González, A. G., Domínguez-Yanes, J. F. and Escánez, J.: The natural ocean acidification and fertilization event caused by the submarine eruption of El Hierro, Scientific Reports, 3, 5–12, doi:10.1038/srep01140, 2013.

Santana-Casiano, J. M., González-Dávila, M., González, a. G., Rico, M., López, a. and Martel, a.: Characterization of phenolic exudates from *Phaeodactylum tricornutum* and their effects on the chemistry of Fe(II)-Fe(III), Marine Chemistry, 158, 10–16, doi:10.1016/j.marchem.2013.11.001, 2014.

Santos, I. R., Burnett, W. C., Chanton, J., et al.: Nutrient biogeochemistry in a Gulf of Mexico subterranean estuary and groundwater-derived fluxes to the coastal ocean. Limnol Oceanogr 53:705–718. doi: 10.4319/lo.2008.53.2.0705, 2008.

Sarthou, G., Vincent, D., Christaki, U., Obernosterer, I., Timmermans, K. R. and Brussaard, C. P. D.: The fate of biogenic iron during a phytoplankton bloom induced by natural fertilisation: Impact of copepod grazing, Deep Sea Research Part II: Topical Studies in Oceanography, 55(5–7), 734–751, doi:https://doi.org/10.1016/j.dsr2.2007.12.033, 2008.

Sayre, H., Milos, K., Goldcamp, M. J., Schroll, C. A., Krause, J. A. and Baldwin, M. J.: Mixed-Donor, α-Hydroxy Acid-Containing Chelates for Binding and Light-Triggered Release of Iron. Inorganic Chemistry 49, 4433–4439. doi:10.1021/ic9018629. 2010.

Schaum, E., Rost, B., Millar, A. J. and Collins, S.: Variation in plastic responses of a globally distributed picoplankton species to ocean acidification. Nature Climate Change 3, 298–302, 2013.

Schulz, K. G., Rost, B., Burkhardt, S., Riebesell, U., Thoms, S. and Wolf-Gladrow, D. A.: The effect of iron availability on the regulation of inorganic carbon acquisition in the coccolithophore *Emiliania huxleyi* and the significance of cellular compartmentation for stable carbon isotope fractionation, Geochimica et Cosmochimica Acta, 71(22), 5301–5312, doi:10.1016/j.gca.2007.09.012, 2007.

Schwyn, B. and Neilands, J. B.: Universal chemical assay for the detection and determination of siderophores. Analytical biochemistry 160, 47–56. doi:10.1016/0003-2697(87)90612-9, 1987.

Sciandra, A., Harlay, J., Lefèvre, D., Lemée, R., Rimmelin, P., Denis, M. and Gattuso, J. P.: Response of coccolithophorid *Emiliania huxleyi* to elevated partial pressure of CO_2 under nitrogen limitation, Marine Ecology Progress Series, 261, 111–122, doi:10.3354/meps261111, 2003.

Sett, S., Bach, L. T., Schulz, K. G., Koch-Klavsen, S., Lebrato, M. and Riebesell, U.: Temperature modulates coccolithophorid sensitivity of growth, photosynthesis and calcification to increasing seawater pCO_2, PLoS ONE, 9(2), doi:10.1371/journal.pone.0088308, 2014.

Shaked, Y.: Iron redox dynamics in the surface waters of the Gulf of Aqaba, Red Sea, Geochimica et Cosmochimica Acta, 72(6), 1540–1554, doi:10.1016/j.gca.2008.01.005, 2008.

Shaked, Y. and Lis, H.: Disassembling iron availability to phytoplankton, Frontiers in Microbiology, 3(APR), 1–26, doi:10.3389/fmicb.2012.00123, 2012.

Shaked, Y., Kustka, A. B. and Morel, F. M. M.: A general kinetic model for iron acquisition by eukaryotic phytoplankton, Limnology and Oceanography, 50(3), 872–882, doi:10.4319/lo.2005.50.3.0872, 2005.

Sharp, J. H., Carlson, C. A., Peltzer, E. T., Castle-Ward, D. M., Savidge, K. B. and Rinker, K. R.: Final dissolved organic carbon broad community intercalibration and preliminary use of DOC reference materials. Marine Chemistry 77, 239–253. doi:10.1016/S0304-4203(02)00002-6, 2002.

Shi, D., Xu, Y. and Morel, F. M. M.: Effects of the pH / pCO_2 control method on medium chemistry and phytoplankton growth, Biogeosciences, 6(7), 1199–1207, doi:10.5194/bg-6-1199-2009, 2009.

Shi, D., Xu, Y., Hopkinson, B. M. and Morel, F. M. M.: Effect of ocean acidification on iron availability to marine phytoplankton., Science (New York, N.Y.), 327(5966), 676–9, doi:10.1126/science.1183517, 2010.

Simpson, F. B. and Neilands, J.B.: Siderochromes in *Cyanophyceae*. Isolation and characterization of schizokinen from A*nabaena Sp.1*. Journal of Phycology 12, 44–48. doi:10.1111/j.1529-8817.1976.tb02824.x, 1976.

Smith, D. J. and Underwood, G. J. C.: The production of extracellular carbohydrates by estuarine benthic diatoms: the effects of growth phase and light and dark treatment, Journal of Phycology, 36(2), 321–333, doi:10.1046/j.1529-8817.2000.99148.x, 2000.

Song, C., Ballantyne IV, F. and Smith, V. H.: Enhanced dissolved organic carbon production in aquatic ecosystems in response to elevated atmospheric CO_2, Biogeochemistry, 118(1–3), 49–60, doi:10.1007/s10533-013-9904-7, 2014.

Spilling, K., Schulz, K. G., Paul, A. J., Boxhammer, T., Achterberg, E. P., Hornick, T., Lischka, S., Stuhr, A., Bermúdez, R., Czerny, J., Crawfurd, K., Brussaard, C. P. D., Grossart, H. P. and Riebesell, U.: Effects of ocean acidification on pelagic carbon fluxes in a mesocosm experiment, Biogeosciences, 13(21), 6081–6093, doi:10.5194/bg-13-6081-2016, 2016.

Sreeram, K. J., Yamini Shrivastava, H. and Nair, B. U.: Studies on the nature of interaction of iron(III) with alginates, Biochimica et Biophysica Acta (BBA) - General Subjects, 1670(2), 121–125, doi:http://dx.doi.org/10.1016/j.bbagen.2003.11.001, 2004.

Statham, P. J., Skidmore, M. and Tranter, M.: Inputs of glacially derived dissolved and colloidal iron to the coastal ocean and implications for primary productivity, Global Biogeochemical Cycles, 22(3), 1–11, doi:10.1029/2007GB003106, 2008.

Steigenberger, S., Statham, P. J., Volker, C. and Passow, U.: The role of polysaccharides and diatom exudates in the redox cycling of Fe and the photoproduction of hydrogen peroxide in coastal seawaters, 109–119, doi:10.5194/bgd-6-7789-2009, 2010.

Stengel, D. B., Connan, S. and Popper, Z. A.: Algal chemodiversity and bioactivity: Sources of natural variability and implications for commercial application. Biotechnology Advances 29, 483–501. doi:http://dx.doi.org/10.1016/j.biotechadv.2011.05.016, 2011.

Strmečki, S. A., Plavšićc, M., Steigenberger, S. and Passow, U.: Characterization of phytoplankton exudates and carbohydrates in relation to their complexation of copper, cadmium and iron. Marine Ecology Progress Series 408, 33–46. 2010

Struyf, E. and Conley, D. J.: Emerging understanding of the ecosystem silica filter. Biogeochemistry 107:9–18. doi: 10.1007/s10533-011-9590-2, 2012.

Stubbins, A., Hubbard, V., Uher, G., Law, C. S., Upstill-Goddard, R. C., Aiken, G. R. and Kenneth, M.: Relating carbon monoxide photoproduction to dissolved organic matter functionality. Environmental Science and Technology 42, 3271–3276, 2008.

Stumm, W. and Morgan, J. J.: Aquatic Chemistry: Chemical Equilibria and Rates in Natural Waters, edited by Environmental Science and Technology, Wiley., 1996.

Sunda, W. and Huntsman, S.: Effect of pH, light, and temperature on Fe–EDTA chelation and Fe hydrolysis in seawater, Marine Chemistry, 84(1–2), 35–47, 2003.

Sunda, W. G.: Iron and the Carbon Pump, Science, 327(5966), 654–655, doi:10.1126/science.1186151, 2010.

Sunda, W. G.: Feedback interactions between trace metal nutrients and phytoplankton in the ocean, Frontiers in Microbiology, 3(June), 1–22, doi:10.3389/fmicb.2012.00204, 2012.

Swanner, E. D., Wu, W., Hao, L., Wüstner, M. L., Obst, M., Moran, D. M., McIlvin, M. R., Saito, M. A. and Kappler, A.: Physiology, Fe(II) oxidation, and Fe mineral formation by a marine planktonic cyanobacterium grown under ferruginous conditions. Frontiers in Earth Science 3, 1–21. doi:10.3389/feart.2015.00060. 2015.

Tagliabue, A., Mtshali, T., Aumont, O., Bowie, A. R., Klunder, M. B., Roychoudhury, A. N. and Swart, S.: A global compilation of dissolved iron measurements: Focus on distributions and processes in the Southern Ocean, Biogeosciences, 9(6), 2333–2349, doi:10.5194/bg-9-2333-2012, 2012.

Tagliabue, A., Bowie, A. R., Boyd, P. W., Buck, K. N., Johnson, K. S. and Saito, M. A.: The integral role of iron in ocean biogeochemistry, Nature, 543(7643), 51–59 [online] Available from: http://dx.doi.org/10.1038/nature21058, 2017.

Thornton, D. C. O.: Dissolved organic matter (DOM) release by phytoplankton in the contemporary and future ocean. European Journal of Phycology, 49(1), 20–46, doi:10.1080/09670262.2013.875596, 2014.

Thuróczy, C.-E., Gerringa, L. J. A., Klunder, M. B., Laan, P., de Baar, H. J. W.: Observation of consistent trends in the organic complexation of dissolved iron in the Atlantic sector of the Southern Ocean. Deep Sea Research Part II: Topical Studies in Oceanography 58, 2695–2706. doi:10.1016/j.dsr2.2011.01.002. 2011.

Tokinaga, H., Xie, S. P., Timmermann, A., McGregor, S., Ogata, T., Kubota, H. and Okumura, Y. M.: Regional patterns of tropical indo-pacific climate change: Evidence of the walker circulation weakening, Journal of Climate, 25(5), 1689–1710, doi:10.1175/JCLI-D-11-00263.1, 2012.

Tovar-Sanchez, A., Duarte, C. M., Hernández-León, S. and Sañudo-Wilhelmy, S. A.: Krill as a central node for iron cycling in the Southern Ocean, Geophysical Research Letters, 34(11), 1–4, doi:10.1029/2006GL029096, 2007.

Tréguer, P. J. and De La Rocha, C. L.: The World Ocean Silica Cycle. Ann Rev Mar Sci 5:477–501. doi: 10.1146/annurev-marine-121211-172346, 2013.

Trick, C. G., Bill, B. D., Cochlan, W. P., Wells, M. L., Trainer, V. L. and Pickell, L.D.: Iron enrichment stimulates toxic diatom production in high-nitrate, low-chlorophyll areas\r. Proceedings of the National Academy of Sciences of the United States of America 107, 5887–92. doi:10.1073/pnas.0910579107. 2010.

Trick, C. G. and Wilhelm, S.W.: Physiological changes in the coastal marine cyanobacterium *Synechococcus* sp. PCC 7002 exposed to low ferric ion levels. Marine Chemistry 50, 207–217. doi:10.1016/0304-4203(95)00036-Q, 1995.

Tyrrell, T. and Merico, A.: *Emiliania huxleyi*: bloom observations and the conditions that induce them, in Coccolithophores: From Molecular Processes to Global Impact, edited by H. R. Thierstein and J. R. Young, pp. 75–97, Springer Berlin Heidelberg, Berlin, Heidelberg., 2004.

-Underwood, G. J. C., Boulcott, M., Raines, C. A. and Waldron, K.: Environmental effects on exopolymer production by marine benthic diatoms: Dynamics, changes in composition and pathways of production, Journal of Phycology, 40(2), 293–304, doi:10.1111/j.1529-8817.2004.03076.x, 2004.

Underwood, G. J. C., Aslam, S. N., Michel, C., Niemi, A., Norman, L., Meiners, K. M., Laybourn-Parry, J., Paterson, H. and Thomas, D. N.: Broad-scale predictability of carbohydrates and exopolymers in Antarctic and Arctic sea ice, Proceedings of the National Academy of Sciences of the United States of America, 110(39), 15734–9, doi:10.1073/pnas.1302870110, 2013.

Urbani, R., Magaletti, E., Sist, P. and Cicero, A. M.: Extracellular carbohydrates released by the marine diatoms *Cylindrotheca closterium*, Thalassiosira pseudonana and Skeletonema

costatum: Effect of P-depletion and growth status, Science of the Total Environment, 353(1–3), 300–306, doi:10.1016/j.scitotenv.2005.09.026, 2005.

Uitz, J., Claustre, H., Gentili, B. and Stramski, D.: Phytoplankton class-specific primary production in the world's oceans: Seasonal and interannual variability from satellite observations. Global Biogeochemical Cycles 24, 1–19. doi:10.1029/2009GB003680, 2010.

Vasconcelos, M. T. S. D. and Leal, M. F. C.: Exudates of different marine algae promote growth and mediate trace metal binding in *Phaeodactylum tricornutum*. Marine Environmental Research 66, 499–507, 2008.

Vasconcelos, M. T. S. D., Leal, M. F. C. and Van Den Berg, C. M. G.: Influence of the nature of the exudates released by different marine algae on the growth, trace metal uptake and exudation of *Emiliania huxleyi* in natural seawater. Marine Chemistry 77, 187–210. doi:10.1016/S0304-4203(01)00087-1. 2002.

Velasquez, I., Nunn, B. L., Ibisanmi, E., Goodlett, D. R., Hunter, K. a. and Sander, S. G.: Detection of hydroxamate siderophores in coastal and Sub-Antarctic waters off the South Eastern Coast of New Zealand, Marine Chemistry, 126(1–4), 97–107, doi:10.1016/j.marchem.2011.04.003, 2011.

Verdugo, P., Alldredge, A. L., Azam, F., Kirchman, D. L., Passow, U. and Santschi, P. H.: The oceanic gel phase: A bridge in the DOM-POM continuum, Marine Chemistry, 92(1–4 SPEC. ISS.), 67–85, doi:10.1029/2002GL016046, 2004.

Viollier, E., Inglett, P. W., Hunter, K., et al.: The ferrozine method revisited: Fe(II)/Fe(III) determination in natural waters. Appl Geochemistry 15:785–790. doi: 10.1016/S0883-2927(99)00097-9, 2000.

Völker, C. and Tagliabue, A.: Modeling organic iron-binding ligands in a three-dimensional biogeochemical ocean model. Marine Chemistry. doi:10.1016/j.marchem.2014.11.008. 2014.

Voelker, B. M. and Sedlak, D. L.: Iron reduction by photoproduced superoxide in seawater, Marine Chemistry, 50(1–4), 93–102, doi:10.1016/0304-4203(95)00029-Q, 1995.

Vraspir, J. M. and Butler, A.: Chemistry of marine ligands and siderophores., Annual review of marine science, 1, 43–63, doi:10.1146/annurev.marine.010908.163712, 2009.

Wadham, J. L., De'ath, R., Monteiro, F. M., Tranter, M., Ridgwell, A., Raiswell, R. and Tulaczyk, S.: The potential role of the Antarctic Ice Sheet in global biogeochemical cycles, Earth and Environmental Science Transactions of the Royal Society of Edinburgh, 104(1), 55–67, doi:DOI: 10.1017/S1755691013000108, 2013.

Wallace, R. B., Baumann, H., Grear, J. S., et al.: Coastal ocean acidification: The other eutrophication problem. Estuar Coast Shelf Sci 148:1–13. doi: 10.1016/j.ecss.2014.05.027. 2014.

Wang, H., Yang, Q., Ji, F., et al.: The geochemical characteristics and Fe(II) oxidation kinetics of hydrothermal plumes at the Southwest Indian Ridge. Mar Chem 134-135:29–35. doi: 10.1016/j.marchem.2012.02.009, 2012.

Waterbury, R. D., Yao W., Byrne, R. H.: Long pathlength absorbance spectroscopy: trace analysis of Fe(II) using a 4.5 m liquid core waveguide. Anal Chim Acta 357:99–102, 1997.

Welch, K. D., Davis, T. Z. and Aust, S. D.: Iron autoxidation and free radical generation: effects of buffers, ligands, and chelators. Archives of biochemistry and biophysics 397, 360–369. doi:10.1006/abbi.2001.2694. 2002.

Weller, C., Horn, S. and Herrmann, H.: Photolysis of Fe(III) carboxylato complexes: Fe(II) quantum yields andreaction mechanisms, Journal of Photochemistry and Photobiology A: Chemistry, 268, 24–36, doi:10.1016/j.jphotochem.2013.06.022, 2013.

Wetz, M. S. and Wheeler, P. a.: Release of dissolved organic matter by coastal diatoms, Limnology and Oceanography, 52(2), 798–807, doi:10.4319/lo.2007.52.2.0798, 2007.

Wilhelm, S. W., Maxwell, D. P. and Trick, C. G.: Growth, iron requirements, and siderophore production in iron-limited *Synechococcus* PCC 7002. Limnology and Oceanography 41, 89–97. doi:10.4319/lo.1996.41.1.0089, 1996.

Williams, P. J. le B., Quay, P. D., Westberry, T. K. and Behrenfeld, M. J.: The Oligotrophic Ocean Is Autotrophic, Annual Review of Marine Science, 5(1), 535–549, doi:10.1146/annurev-marine-121211-172335, 2013.

Wu, J., Iii, G. W. L. and Luther III, G. W.: Size-fractionated iron concentrations in the water column of the western North Atlantic Ocean, Limnology and Oceanography, 39(5), 1119–1129, doi:10.4319/lo.1994.39.5.1119, 1994.

Wu, J. and Jin, M.:. Competitive ligand exchange voltammetric determination of iron organic complexation in seawater in two-ligand case: Examination of accuracy using computer simulation and elimination of artifacts using iterative non-linear multiple regression. Marine Chemistry 114, 1–10. doi:10.1016/j.marchem.2009.03.001. 2009.

Wu, Y., Gao, K. and Riebesell, U.: CO_2-induced seawater acidification affects physiological performance of the marine diatom *Phaeodactylum tricornutum*, Biogeosciences, 7(9), 2915–2923, doi:10.5194/bg-7-2915-2010, 2010.

Wu, Y., Xiang, W., Fu, X., Yan, S., Su, J., Liu, J. and Bao, Z.: Geochemical interactions between iron and phenolics originated from peatland in Hani, China: implications for effective transport of iron from terrestrial systems to marine, Environmental Earth Sciences, 75(4), 336, doi:10.1007/s12665-015-5189-6, 2016.

Xu, K., Fu, F.-X. and Hutchins, D. A.: Comparative responses of two dominant Antarctic phytoplankton taxa to interactions between ocean acidification, warming, irradiance, and iron availability, Limnology and Oceanography, 59(6), 1919–1931, 2014.

Young, J. R., Poulton, A. J. and Tyrrell, T.: Morphology of *Emiliania huxleyi* coccoliths on the northwestern European shelf - Is there an influence of carbonate chemistry?, Biogeosciences, 11(17), 4771–4782, doi:10.5194/bg-11-4771-2014, 2014.

Yang, R. and Van Den Berg, C. M. G.: Metal complexation by humic substances in seawater, Environmental Science and Technology, 43(19), 7192–7197, 2009.

Yoshimura, T., Suzuki, K., Kiyosawa, H., Ono, T., Hattori, H., Kuma, K. and Nishioka, J.: Impacts of elevated CO_2 on particulate and dissolved organic matter production: Microcosm experiments using iron-deficient plankton communities in open subarctic waters, Journal of Oceanography, 69(5), 601–618, doi:10.1007/s10872-013-0196-2, 2013.

Zeebe, E.: History of Seawater Carbonate Chemistry, Atmospheric CO_2, and Ocean Acidification, Annual Review of Earth and Planetary Sciences, 40, 141–165, doi:DOI: 10.1146/annurev-earth-042711-105521, 2012.

Zhang, S., Xu, C. and Santschi, P. H.: Chemical composition and ^{234}Th(IV) binding of extracellular polymeric substances (EPS) produced by the marine diatom Amphora sp., Marine Chemistry, 112(1–2), 81–92, doi:10.1016/j.marchem.2008.05.009, 2008.

Zhu, Z., Xu, K., Fu, F., JL, S., DA, B. and Hutchins D A: A comparative study of iron and temperature interactive effects on diatoms and *Phaeocystis antarctica* from the Ross Sea, Antarctica , Marine Ecology Progress Series, 550, 39–51 [online] Available from: http://www.int-res.com/abstracts/meps/v550/p39-51/, 2016.

Zondervan, I.: The effects of light, macronutrients, trace metals and CO_2 on the production of calcium carbonate and organic carbon in coccolithophores-A review, Deep-Sea Research Part II: Topical Studies in Oceanography, 54(5–7), 521–537, 2007.

Zubia, M., Payri, C. and Deslandes, E.: Alginate, mannitol, phenolic compounds and biological activities of two range-extending brown algae, *Sargassum mangarevense* and *Turbinaria ornata* (*Phaeophyta: Fucales*), from Tahiti (French Polynesia), Journal of Applied Phycology, 20(6), 1033–1043, doi:10.1007/s10811-007-9303-3, 2008.